



In silico development of a bioelectronic islet-based artificial pancreas

Loïc Olcomendy

► To cite this version:

Loïc Olcomendy. In silico development of a bioelectronic islet-based artificial pancreas. Electronics. Université de Bordeaux, 2021. English. NNT : 2021BORD0196 . tel-03875843

HAL Id: tel-03875843

<https://theses.hal.science/tel-03875843>

Submitted on 28 Nov 2022

HAL is a multi-disciplinary open access archive for the deposit and dissemination of scientific research documents, whether they are published or not. The documents may come from teaching and research institutions in France or abroad, or from public or private research centers.

L'archive ouverte pluridisciplinaire **HAL**, est destinée au dépôt et à la diffusion de documents scientifiques de niveau recherche, publiés ou non, émanant des établissements d'enseignement et de recherche français ou étrangers, des laboratoires publics ou privés.

Thèse présentée pour obtenir le grade de

**Docteur de
l'Université de Bordeaux**

École doctorale des Sciences Physiques et de l'Ingénieur

Spécialité Électronique

Préparée au Laboratoire IMS

Par Loïc Olçomendy

***In silico* development of a bioelectronic
islet-based artificial pancreas**

Sous la direction de : Sylvie Renaud et de Yannick Bornat

Après l'avis de Thierry Bastogne et Benoît Charlot

Soutenue le 20 juillet 2021

Devant le comité d'examen formé de :

M. CHARLOT, Benoît	Directeur de recherche	CNRS, IES	Rapporteur, Président
M. BASTOGNE, Thierry	Professeur des universités	Université de Lorraine	Rapporteur
M. VISENTIN, Roberto	Assistant Professor	University of Padova	Examineur
M. NICOLESCU-CATARGI Bogdan	Professeur des universités /Praticien hospitalier	CHU de Bordeaux	Examineur
Mme RENAUD, Sylvie	Professeur des universités	Bordeaux INP	Directrice de Thèse
M. BORNAT, Yannick	Maître de conférences	Bordeaux INP	Co-encadrant
M. CIESLAK, Jérôme	Maître de conférences	Université de Bordeaux	Invité
M. RAOUX, Matthieu	Maître de conférences	Université de Bordeaux	Invité

Thèse réalisée
dans le laboratoire **IMS**
au sein de l'équipe **Elbio**.
Université de Bordeaux Laboratoire IMS
CNRS UMR-5218 – Bordeaux INP
351 cours de la Libération
33405 TALENCE Cedex
France

*Seguruenik ez zinuen zer
daukan ainitz ulertuko, baina
hala ere eskuizkribu hau zuri
eskaini nahi izan dizut.
Ez adiorik Aita.*

Abstract

The development of new therapeutic pathways for the treatment of diabetes requires highly interdisciplinary research. For the last fifty years, the need for interdisciplinarity in translational research projects has been further strengthened by the digital revolution. The Artificial Pancreas (AP) is a prime example of medical device developed thanks to the contribution of scientists, engineers, and mathematicians. APs, as “all-in-one” diabetes management systems now appear as a standard of care to restore the glucose homeostasis of type 1 diabetic patients. These semi-automated closed-loop devices successfully replace the defective endogenous insulin secretion by the continuous infusion of finely-tuned exogenous insulin boluses.

Our research consortium developed a biosensor enabling the real-time characterisation of pancreatic islet algorithms via non-invasive electrophysiological measurements. We hypothesize that, in contact with T1D patient interstitial fluids, healthy islets embedded in this wearable biosensor could provide an indication on the patient’s need in insulin and thus constitute a valuable physiological input for the AP. This thesis work investigates the contribution of numerical simulation to the development of an AP system involving this innovative sensor.

The introductory chapter of the manuscript provides the scientific context of this work, which lies at the intersection of biology, electrophysiology, electronics, control theory and diabetology. The second chapter then presents the necessary material and the methods developed to achieve the results described and discussed thereafter.

Our research approach was divided into two separate simulation pathways. A first pathway, described in Chapter 3, intended to validate the biosensor’s working principle by exploiting the advantages of numerical simulation. This approach is however not realistic from a clinical standpoint as it uses intravenous routes. In particular, we achieved excellent glucose control using a regulation scheme based on electrically-characterised endogenous islets algorithms. Integrating the islet models in an AP architecture, we then developed a second simulation pathway to assess the potential contribution of our biosensor to type 1 diabetes treatment. This pathway, described in Chapter 4, uses a more clinically realistic configuration of the virtual patient simulator which enables a comparison between our biosensor-based AP and standard treatment approaches. These preliminary results are promising: the biosensor-based AP permitted a satisfactory glucose control, even in challenging conditions (meals containing high glycaemic loads). The identification of the benefits and limitations of our simulation campaign gives rise to a discussion on the contribution of numerical simulation to the development of new solutions for the treatment of diabetes. As a conclusion, we define general guidelines in an attempt to lay the groundwork for a future real-world implementation of a biosensor-based AP system.

Key words

Diabetes, Bioelectronics, Artificial Pancreas, Sensors, Closed-loop control, Modelling.

Résumé

Le développement de nouvelles voies thérapeutiques pour le traitement du diabète nécessite une approche pluridisciplinaire de la recherche médicale. Au cours des dernières décennies, le besoin de pluridisciplinarité dans les projets de recherche translationnelle s'est considérablement accru du fait de l'utilisation croissante des technologies numériques. Le pancréas artificiel (*Artificial Pancreas* en anglais) est un exemple type de dispositif médical développé grâce à la collaboration de médecins, de scientifiques, d'ingénieurs et de mathématiciens. Les pancréas artificiels sont des dispositifs tout-en-un facilitant la gestion des différents aspects du traitement du diabète. Ils font désormais partie intégrante de l'offre thérapeutique permettant aux patients diabétiques de type 1 de rétablir une homéostasie du glucose normale. Ces dispositifs de contrôle en boucle fermée remplacent de manière efficace la sécrétion endogène d'insuline, défaillante dans le cas du diabète de type 1, par une administration continue et semi-automatique d'insuline exogène.

Notre consortium de recherche a développé un biocapteur permettant la caractérisation en temps réel des algorithmes endogènes des îlots pancréatiques par le biais de mesures électrophysiologiques non invasives. Nous formulons l'hypothèse que, mis en contact avec le liquide interstitiel de patients diabétiques de type 1, des îlots pancréatiques sains intégrés dans une version portable du biocapteur, permettraient l'estimation en temps réel du besoin en insuline des patients. Ils fourniraient ainsi une information précieuse au pancréas artificiel. Cette thèse a pour objectif d'évaluer le rôle que peut jouer la simulation numérique dans le développement d'un pancréas artificiel développé autour de ce nouveau biocapteur.

Le chapitre d'introduction de ce manuscrit permet au lecteur de découvrir le contexte scientifique de ce travail qui se trouve à l'intersection de la biologie, de l'électrophysiologie, de l'électronique embarquée, de l'automatique et de la diabétologie. Le second chapitre présente quant à lui le matériel et les différentes méthodes ayant permis l'obtention des résultats présentés et discutés dans la suite du manuscrit.

Au cours de notre travail en simulation, nous avons développé deux axes de recherche distincts. Un premier axe, décrit dans le chapitre 3, profite des possibilités offertes par la simulation numérique pour valider le principe de mesure du biocapteur. Cette approche est peu réaliste d'un point de vue clinique notamment par son recours aux voies de mesures intraveineuses. Il a permis de montrer que la régulation de la glycémie à partir de la caractérisation électrique des algorithmes endogènes des îlots pancréatiques est non seulement possible, mais permet en outre d'obtenir d'excellentes performances. L'intégration des modèles d'îlots pancréatiques, via notre biocapteur, au sein d'une architecture de pancréas artificiel a ensuite permis d'évaluer le potentiel de cette solution innovante pour le traitement du diabète de type 1. Ce second axe de recherche, décrit dans le chapitre 4, repose sur une configuration plus réaliste du simulateur de patient virtuel et permet donc une comparaison plus juste avec les options thérapeutiques de référence. Les résultats préliminaires obtenus sont encourageants : le pancréas artificiel intégrant notre biocapteur permet un contrôle glycémique satisfaisant, et ce même dans des conditions difficiles (repas riches en glucides). La discussion des qualités et défauts de notre approche *in silico* a notamment permis de décrire de manière objective le potentiel de la simulation numérique pour faciliter le développement de nouveaux traitements pour le diabète. A partir des enseignements de ce travail en simulation, la conclusion de ce

manuscrit formule un ensemble de directives ayant pour objectif de poser des fondations solides en vue de l'intégration future de notre biocapteur dans un pancréas artificiel réel.

Mots clés

Diabète, Bioélectronique, Pancréas artificiel, Capteurs, Contrôle en boucle fermée, Modélisation.

Remerciements

Ce manuscrit de thèse reflète trois années de travail qui ont nécessité une certaine autonomie. Pour autant, je n'aurai jamais pu accomplir tout cela sans l'aide et le soutien de nombreuses personnes que je me dois donc de remercier maintenant.

Merci à M. Thierry Bastogne et M. Benoît Charlot d'avoir accepté de relire mon manuscrit de thèse. J'ai apprécié vos retours constructifs tant sur le plan de la structure du manuscrit que sur le plan scientifique. Nos échanges à propos du manuscrit laissaient présager une discussion scientifique très intéressante lors de la soutenance, cela s'est vérifié par la suite. Pour cela, je tenais aussi à remercier M. Roberto Visentin qui, par sa connaissance du simulateur UVA/Padova et des systèmes pancréas artificiels, a pu répondre à nombre de mes interrogations, valider certains choix fondamentaux que j'ai dû faire au cours de ma thèse et poser de nombreuses questions pertinentes et intéressantes. Je souhaite aussi remercier MM. Bogdan Nicolescu-Catargi, Matthieu Raoux et Jérôme Cieslak, dont les questions m'étaient forcément plus familières, mais qui ont tout de même su me surprendre et jeter une lumière nouvelle sur mon travail à travers le prisme de leurs spécialités respectives. Ils ont ainsi rendu cette soutenance de thèse réellement pluridisciplinaire, point qui me tenait particulièrement à cœur. Merci enfin à Mme. Sylvie Renaud et M. Yannick Bornat, mes encadrants, pour les mots touchants qu'ils ont eu à l'égard de mon travail et de moi-même en fin de soutenance.

Je souhaiterais remercier maintenant le professeur Yann Deval, directeur de l'IMS, de m'avoir accueilli au sein de ce laboratoire de l'Université de Bordeaux, mais aussi Noëlle Lewis et Yannick Bornat de m'avoir accueilli respectivement dans le groupe Bioélectronique et dans l'équipe ELIBIO. J'ai trouvé dans cet environnement de travail, où j'ai évolué durant deux stages et une thèse, une « deuxième maison » qu'il me sera difficile de quitter le moment venu. Cet environnement ne serait pas ce qu'il est sans les personnes qui y évoluent actuellement et celles qui l'ont traversé. La deuxième partie de ces remerciements s'adresse donc à toutes les personnes que j'ai pu croiser durant mon parcours à l'IMS.

Tout naturellement, je me dois de remercier en premier lieu Sylvie Renaud et Yannick Bornat pour m'avoir offert l'opportunité de faire cette thèse sous leur direction. Je n'envisageais pas de poursuivre en thèse après mes études d'ingénieur mais découvrir la vie et le travail d'un doctorant au sein de l'équipe ELIBIO m'a donné envie de tenter l'expérience. J'ai été flatté que vous me le proposiez un an plus tard, et heureux d'accepter. Sylvie, je tenais à te remercier pour les attentions quasi maternelles qui ont permis au jeune doctorant que j'étais de se sentir bien dans cette équipe dès le départ. Par la suite, tu as su me guider et m'encadrer, toujours avec justesse, à travers les différentes étapes de la thèse (j'ai conscience que cela n'a pas toujours été facile) de telle sorte que je puisse envisager sereinement de franchir l'une des portes que m'ouvre à présent ce diplôme de docteur. Je ne sais si je serais amené à diriger une équipe ou détenir des responsabilités un jour mais tu es assurément devenue un de mes modèles à ce niveau-là tant tu sais allier efficacité, humanité et disponibilité dans ton travail quotidien, le tout en dégageant une impression de facilité souvent déconcertante. Yannick, bien que nous ayons moins collaboré que prévu à cause de l'orientation prise par ma thèse, je tenais à te remercier pour ta disponibilité et pour tes conseils toujours avisés. J'ai toujours apprécié la manière saine avec laquelle tu gères cette équipe et tout le soin que tu prends à faciliter notre

passage du statut d'élève à collègue. Dans la grande famille ELIBIO, il me faut aussi remercier le grand-frère : merci Antoine pour tout ce que tu m'as apporté, tu as mis la barre très haute avec ta thèse et n'a eu de cesse de la relever à mesure que j'en approchais. Cette émulation m'a permis de toujours essayer de me surpasser et de progresser. J'ai adoré collaborer avec toi car tu as un esprit vif, ouvert et redoutablement efficace. Nous avons une vision des choses et une manière de travailler assez différentes mais que je trouve très complémentaires. J'espère avoir la chance de travailler avec toi à nouveau. Merci aussi à Amélie qui en son temps a su égayer mes journées par sa bonne humeur ou simplement me soutenir et m'aider à prendre du recul, ton départ du bureau a laissé un grand vide. Tu m'as toujours impressionné par ton sérieux, et comme celle d'Antoine, ta soutenance m'a mis un bon coup de pression tant elle était réussie. Merci aussi à tous les autres membres d'ELIBIO, présents et passés, merci à Noëlle, Gilles, Jonathan, Donnie, Alexia, Marie pour l'excellente ambiance qui perdure dans cette équipe et nous permet de nous y épanouir malgré les difficultés rencontrées durant la thèse. Merci aussi à Chia-Hsin, Hsin-Jou, Caroline et Jieyun, mes différentes stagiaires pour le travail qu'elles ont accompli.

Si j'ai accepté cette thèse, c'est pour essayer d'obtenir un diplôme réellement pluridisciplinaire qui me permette, par la suite, de poursuivre une carrière dans le domaine des dispositifs médicaux. Je voudrais donc remercier maintenant tous les membres de notre consortium de recherche pour tout le travail accompli et sans lesquels je n'aurais pu mener cette thèse à son terme. Je voudrais aussi remercier Jochen, Matthieu, Manon, Myriam, Emilie et les autres membres du CBMN pour tout ce qu'ils m'ont appris sur la biologie et l'électrophysiologie. David H., Jérôme, David G.D. et Louis, merci pour tous nos échanges au sujet de la boucle fermée et pour ce que vous m'avez appris sur votre domaine. Enfin je voudrais remercier Bogdan de m'avoir permis de mieux comprendre les difficultés que peuvent rencontrer les patients diabétiques et leur staff médical au quotidien, me permettant ainsi de mieux cerner les problématiques réelles que nous devons nous employer à résoudre par notre travail de recherche scientifique. Mon objectif était d'être capable, une fois arrivé à la fin de ma thèse, de comprendre le langage de chacune des disciplines que je viens de citer pour être un ingénieur-chercheur réellement pluridisciplinaire. Grâce à vous j'ai l'impression de l'avoir atteint.

Je souhaiterais maintenant remercier les autres membres de l'IMS que j'ai pu croiser. Merci à Valérie, Fabienne, Nicole et à tout le reste du personnel administratif pour votre patience face à ma phobie administrative notoire et pour le travail de l'ombre que vous accomplissez au quotidien pour faciliter le nôtre. Merci à l'équipe MDA pour ce que vous m'avez appris durant mon stage et pour la formidable opportunité que vous m'avez offerte avec ce stage à Singapour. J'apprécie tout particulièrement les liens que nous avons su garder, notamment grâce à Jean-Luc, sur fond de trafic de produits du terroir. Merci Adrien pour nos discussions toujours très intéressantes, tu es un puits de connaissances et tu m'as souvent impressionné à ce titre. Merci pour tout ce que tu m'as appris lorsque nous donnions des cours ensemble et pour tous les repas très agréables que nous avons partagés. Tu es une des belles rencontres de cette thèse et tes conseils m'ont été particulièrement utiles dans la dernière ligne droite. Merci Clémence pour la confiance que tu m'as accordée jusqu'à maintenant et pour ton soutien durant les différentes épreuves de ces derniers mois, j'ai souvent eu besoin de parler et tu as su me fournir l'oreille attentive dont j'avais besoin. Merci aussi à Romain, troisième occupant de ce bureau où j'ai aimé travailler ces derniers mois. Je voudrais aussi remercier l'équipe Bio-EM et tous ses

membres pour la convivialité de nos différentes pauses, pour nos échanges scientifiques, et pour nos discussions quasi quotidiennes à refaire le monde, vous savez que j'adore ça. Merci à Florence, Melody, Charly, Alex, Anne, Clémence, Alexia et les autres pour les *afterworks* et les repas qui participent aussi à la bonne ambiance régnant dans cet étage, elle m'a donné envie de rester un peu plus longtemps parmi vous. Enfin, encore merci à tous pour vos attentions lors du décès de mon père, j'ai été très touché et nos échanges quotidiens n'ont jamais été aussi importants à mes yeux que dans les semaines qui suivirent.

La thèse représente une énorme charge de travail bien évidemment mais aussi une énorme charge psychologique qui n'est supportable que par une vie équilibrée entre travail et loisirs. Je voudrais donc remercier maintenant toutes les personnes qui ont su rendre ma vie bordelaise plus douce et m'ont permis de me changer les idées. Merci tout d'abord à tous les membres de l'US Talence Volleyball. Ces quatre saisons à vos côtés furent très agréables et m'ont souvent fourni un véritable sas de décompression après une longue journée de travail. J'étais d'ailleurs bien triste que la situation sanitaire écourte cette dernière saison tant l'ambiance dans ce nouveau groupe semblait bonne. Merci à Valentin et Justine pour les innombrables soirées à la Parcelle, vous savez à quel point je les apprécie. Pêle-mêle, merci à Mégane, Vincent, Julie, Benoît, Rémicia, Louis, Maylis pour nos différentes sorties bordelaises, vous avez toujours su me faire oublier les tracasseries quotidiennes. Merci à la Coloc à fi*** pour ces incroyables *road trips* et autres séjours à l'étranger, merci pour ces soirées du Nouvel An, j'espère avoir l'occasion d'en vivre à nouveau. Merci à Camille, Mélissa, Vincent, Maxime, Margot et à tous les autres pour nos week-ends dans le Sud-Ouest et nos sorties sur Toulouse, vous savez à quel point j'y tiens. Merci à Luigi, Katrin, Nadia, Amélie, Sergio, Davide, à tout le gang italien et leurs amis venus coloniser Bordeaux pour notre plus grand bonheur. Nos soirées sont autant de bons souvenirs de mes premières années de thèse que je conserverai encore longtemps dans ma mémoire.

Je souhaiterais aussi remercier tous mes amis d'enfance restés sur la côte basque mais qui, lors de mes retours au pays, ont su me soutenir, m'accompagner et m'offrir l'environnement et les moments dont j'avais besoin pour réellement me ressourcer. Pierre et Laure, vous avez su être là quand j'en ai eu besoin. J'aime retrouver intacte cette amitié qui nous lie, même après quelques mois ou semaines séparés. Malgré notre relation parfois chaotique ces dernières années, merci Léa d'avoir été là aux moments importants, tu n'imagines pas l'importance qu'ont eu pour moi certaines de nos discussions, merci pour les leçons et pour tout le reste. Merci Matthieu et Nicolas, malgré nos parcours assez différents après le lycée, j'apprécie tout particulièrement de pouvoir encore vous compter parmi mes amis et prends toujours autant de plaisir à vous revoir et passer du temps ensemble (si c'est à Contis c'est encore mieux ;-)). Merci Fanny, tu es devenue quelqu'un de particulièrement important pour moi ces dernières années et mérite chaque année un peu plus la confiance que je t'ai accordée jusqu'à présent.

Enfin, je souhaiterais remercier toute ma grande famille, pour son soutien au cours de cette thèse mais aussi au cours des épreuves qui ont jalonné cette curieuse année 2021, merci pour tous vos messages, vos attentions et vos encouragements. J'ai aussi été touché par votre présence en nombre à ma soutenance de thèse. J'ai ressenti une réelle pression à cause de cela lorsque j'ai prononcé mes premiers mots mais celle-ci a vite fait place à la fierté de pouvoir vous montrer ce que j'ai appris au sein de ce laboratoire et ce dont je suis capable maintenant.

Au même titre, Patxi, Xavier et Benoît, je voudrais vous remercier pour votre présence ce jour-là, je sais que Papa aurait beaucoup apprécié que ses amis de l'amicale Saint-Léon soient là pour soutenir son fils lors de ce jour si spécial. Je termine ces remerciements par les plus importants qui soient. Merci à mes parents, mon frère et ma sœur pour le foyer chaleureux qui m'attend toujours lorsque je rentre dans ma ville natale. J'apprécie plus que jamais ces moments passés en famille. Merci pour votre soutien lors de tous les moments difficiles de cette thèse. J'aurais beaucoup aimé que Papa ait pu être avec nous jusqu'au jour de la soutenance.

Pour terminer sur une note plus positive, je voudrais ajouter que ces années de thèse ont été riches et intenses à tous les niveaux, et que je ressens maintenant le besoin d'une période de transition un peu plus calme. Cependant, je sais d'ores et déjà que, quelle que soit la direction que prendra ma vie dans les prochaines années, je ne regretterai jamais d'avoir fait cette thèse, ni de l'avoir faites au laboratoire IMS. Si je peux dire cela de manière si catégorique aujourd'hui, c'est grâce à vous tous et à ce que vous m'avez transmis. Merci.

Contents

Abstract.....	7
Résumé	9
List of Figures.....	19
List of Tables.....	23
Scientific context.....	27
1.1. Understand the physiology, biology and chemistry of glucose homeostasis.....	28
1.1.1. Glucose metabolism and body cells energy supply	28
1.1.2. Glucose homeostasis.....	33
1.1.3. Endocrine regulation with glucagon and insulin.....	34
1.1.4. Anatomy and physiology of the human pancreas.....	35
1.1.5. Other regulatory circuits of insulin secretion.....	37
1.2. Diabetes mellitus.....	38
1.2.1. Pathogenesis of type 1 diabetes.....	38
1.2.2. Diagnosis and pathophysiology	39
1.2.3. Epidemiology	41
1.3. Current and future therapies for type 1 diabetes.....	43
1.3.1. Preventive treatments.....	43
1.3.2. Cures for type 1 diabetes	44
1.3.3. Insulin therapy as the mainstay of treatment	44
1.4. The Artificial Pancreas	48
1.4.1. Sensor	48
1.4.2. Insulin Pump	49
1.4.3. Closing the loop.....	51
1.4.4. Control algorithms.....	52
1.4.5. Benefits and limitations	52
1.5. An islet-based biosensor for the Artificial Pancreas.....	54
1.5.1. Electrophysiology of the endocrine pancreas	55
1.5.2. The islet-based biosensor	57
1.5.3. Towards a wearable medical device.....	58
1.5.4. <i>In silico</i> preclinical validation	58

1.5.5.	Contribution of this thesis work.....	59
	Conclusion.....	61
	Material and methods	65
2.1	A biosensor based on pancreatic islet's activity recording.....	66
2.1.1	Extracellular recording using a MicroElectrode Array.....	66
2.1.2	Signal conditioning front-end	68
2.1.3	Biosignal processing with the Multimed system	68
2.1.4	System for Acquisition with Microfluidics (SYAM).....	69
2.2	Biosensor modelling approach	71
2.3	Data-based modelling.....	74
2.3.1	Contextualised model of the pancreatic islet	74
2.3.2	<i>In vitro</i> characterisation of islet endogenous algorithms.....	75
2.3.3	Experimental protocols	76
2.3.4	A mathematical model of islet electrical activity.....	78
2.3.5	Model parameters identification.....	79
2.4	Simulation environment	80
2.4.1	UVA/Padova T1DM Simulator testing environment	80
2.4.2	Closing the loop <i>in silico</i>	82
2.4.3	Glucose intake scenarios	85
2.4.4	A framework to improve research work robustness	85
2.5	Glucose control assessment	87
2.5.1	A criteria to assess glycaemic profiles.....	87
2.5.2	Systematic performance assessment with reference metrics	89
	<i>In silico</i> validation of the biosensor's working principle	91
3.1.	Preliminary results.....	93
3.1.1.	A custom implementation of the S2008 T1DM Simulator	93
3.1.2.	Implementation of the biosensor models in the MATLAB/Simulink environment.....	96
3.1.3.	A consistent research strategy.....	100
3.2.	Islet algorithm models.....	101
3.3.	Adaptation to patient needs.....	103
3.3.1.	Description of the problematic	103
3.3.2.	Parametric analyses	104

3.4.	<i>In silico</i> results under realistic scenario.....	109
3.5.	Discussion.....	110
	Integration of the biosensor in an <i>in silico</i> Artificial Pancreas	115
4.1.	Design of an individualised controller to handle the subcutaneous delays	117
4.1.1.	Controller tuning	117
4.1.2.	PID controller architectures.....	120
4.1.3.	Is there a “best architecture”?	121
4.1.4.	Correcting an unfair disadvantage for the CGM-AP	123
4.2.	Comparison of the Bios-AP with two reference treatments.....	125
4.2.1.	Controllers’ validation with multi-meal scenarios.....	125
4.2.2.	Discussion on this first comparison	128
4.2.3.	Controller tuning with individualised meal scenarios	130
4.3.	The role of simulation in the Bios-AP design flow	134
4.3.1.	How to enhance the UVA/Padova T1DM Simulator?.....	134
4.3.2.	Contribution of simulation to the design of AP systems	136
4.4.	Real world implementation of the Bios-AP	139
4.4.1.	Management of variability in Type 1 Diabetes.....	139
4.4.2.	Integration of a CGM sensor in the Bios-AP	140
4.4.3.	Realistic real-world implementation of our biosensor	141
	Appendices.....	143
	Appendix 1 - Worldwide prevalence of diabetes and forecasts (IDF Atlas 2019).....	143
	Appendix 2 - European prevalence of diabetes and forecasts (IDF Atlas 2019).....	144
	Appendix 3 – UVA/Padova T1DMS metabolic model equations.....	145
	Appendix 4 –UVA/Padova T1DMS virtual patients’ characteristics and therapy parameters.....	147
	Appendix 5 – Performance metrics corresponding to IV/IV results of adolescents.....	148
	Appendix 6 – Performance metrics corresponding to IV/IV results of adults.....	149
	Appendix 7 – Performance metrics corresponding to IV/IV results of children.....	150
	Appendix 8 – Performance metrics corresponding to SQ/SQ results of adolescents	151
	Appendix 9 – Performance metrics corresponding to SQ/SQ results of adults	152
	Appendix 10 – Performance metrics corresponding to SQ/SQ results of children	153
	List of publications	155
	Bibliography	157

List of Figures

Figure 1: Simplified schematic of the mitochondrial metabolism.....	29
Figure 2: Carbohydrates classification	30
Figure 3: Two metrics to characterise carbohydrate content of meals.....	32
Figure 4: Insulin synthesis process in the β cells	34
Figure 5: Anatomy of the pancreas.....	36
Figure 6: Eisenbarth model of type 1 diabetes pathogenesis	39
Figure 7: Frederick Banting (right) and Charles Best (left) in 1924	45
Figure 8: The Guardian Connect CGM system (Medtronic).....	49
Figure 9: Tandem t:slim X2 insulin pump	50
Figure 10: 6-step development plan of the Artificial Pancreas Project.....	52
Figure 11: Electrophysiology of the β cell.....	56
Figure 12: Biosensor description and working principle.....	57
Figure 13 : Alternative medical device validation process using computer-aided simulation: the example of the validation of a new drug or implantable drug infusion pump in the US..	59
Figure 14: The Biomimetic Artificial Pancreas.....	62
Figure 15: Complete measurement setup scheme.....	66
Figure 16: Application-specific micro-fluidic MEA	67
Figure 17: Multimed biosignal acquisition and processing system.....	69
Figure 18: Scheme of the microfluidic measurement setup integrating SYAM.	70
Figure 19: Simplified model of the pancreatic islet:	72
Figure 20: Simplified model of the pancreatic islet adapted for the biosensor context	72
Figure 21: Simplified model of the whole biosensor	72
Figure 22: Reduced model of the biosensor used in this work.....	73
Figure 23: Contextualised model of the islet of Langerhans.....	75
Figure 24: Summary of the main islet endogenous algorithms	77
Figure 25: Working principle of the Preisach model.	79
Figure 26: UVA/Padova T1DM Simulator testing environment.....	83
Figure 27: Genetic algorithm working principle.....	84
Figure 28: Principle of operation of the GA-based controller tuning method.....	84
Figure 29: Illustrative scheme of the custom simulation framework mode of operation.....	86
Figure 30: Many faces of 6.5% A1C and 100% TIR.....	88

Figure 31: Definition of a target area (in green) based on meal scenario	88
Figure 32: Blood Glucose Index risk function	89
Figure 33: <i>In silico</i> blood glucose regulation closed loop implemented using a Python implementation of Dalla Man's meal simulation model.....	94
Figure 34: Blood glucose profiles of a healthy individual and a virtual T1D patient submitted to a realistic 24-h glucose intake scenario	95
Figure 35: Initial 100 minutes of a T1DMS simulation: modification of the initial blood glucose level setting	98
Figure 36: Impact of the low-pass filter cut-off frequency.....	99
Figure 37: Two separate <i>in silico</i> research axes.....	100
Figure 38: Comparison of former and updated versions of the Static and Hysteretic models.	102
Figure 39: BG profiles selected by the ranking algorithm.....	105
Figure 40: Evolution of the closed-loop regulation performance assessed with Time In Range (TIR), Time In Target Area (TITA) and mean Blood glucose (BG) level, as a function of K.	107
Figure 41: Parametric analysis characterising the response of adolescent#001 to different glucose intakes (10g to 160g single meal scenarios).....	108
Figure 42: Simulation results for a 48-hour, 5-meal scenario (last 24 hours are displayed) in adults, adolescents, and children, for two regulation schemes (Static model 2020, Hysteretic model 2020) using IV glucose measurement and insulin infusion routes.....	109
Figure 43: Evolution of the closed-loop regulation performance assessed with Time In Range (TIR), Time In Target Area (TITA), mean Blood glucose (BG) level, and mean Blood Glucose Index (BGI) as a function K.....	112
Figure 44: Results of the K tuning process for all the patients of the T1DMS's virtual T1D cohort for two criteria: TITA (green triangles) and Mean BGI (red circles).	113
Figure 45: Comparison of BG level figures with intravenous (IV) and subcutaneous (SQ) insulin delivery routes.....	116
Figure 46: GA-based tuning of a PID controller parameters.....	119
Figure 47: Four variants of the PID control architecture.	122
Figure 48: Comparison of 3 methods to select the optimal PID parameters for the CGM-AP controllers.....	124
Figure 49: Assessment of the 3 selection methods in the case of the Bios-AP controllers. “mean”, “best” and “fmincon”.	124
Figure 50: Closed-loop regulation scheme of the Bios-AP connected to the virtual patient through subcutaneous (SQ) glucose measurement and insulin infusion routes	125

Figure 51: Simulation results for the three case studies for the 11 adults of the T1DMS (last 24 hours are displayed), for three regulation schemes (Multiple Daily Injections (MDI), CGM-AP, Bios-AP) using SC glucose measurement and insulin delivery routes.....	126
Figure 52: Comparison of the Bios-AP with two reference therapies for the 11 adolescents and 11 children of the T1DMS virtual cohort.....	128
Figure 53: Body weight-dependent definition of the glucose intake scenarios.....	130
Figure 54: Comparison of mean BG profiles for the three virtual patient categories equipped with the Bios-AP and following different scenario definition strategies.....	131
Figure 55: Influence of meal scenario individualisation on closed-loop performance.....	132
Figure 56: Comparison of the daily glucose intake and Total Daily Insulin (TDI) of each patient for the two scenario definition methods.....	133
Figure 57: Boxplots of daily energy intakes corresponding to the individualised scenarios of each patient category.....	134
Figure 58: Evolution of the simulated blood glucose profile of adult#005 submitted to a 3-meals/2-snacks scenario for 10 values of the microfluidic delay	137
Figure 59: Model of a practical biosensor incorporating five islets whose electrical activity is monitored and processed to compute an estimation of the insulin need of a T1D patient...	138
Figure 60: Practical real-world implementation of the Biomimetic Artificial Pancreas.....	141

List of Tables

Table 1: Average GI of common food products compiled in atkinson et al. (2008).....	32
Table 2: Comparison of clinical features of type 1 and type 2 diabetes.....	38
Table 3: Model parameters for Static and Hysteretic models, and corresponding coefficient of determination R^2	102
Table 4: Comparison of three criteria to select the optimal value of K: mean Blood Glucose (BG) level, Time In Range (TIR), and Time In Target Area (TITA)	106
Table 5: Performance metrics for two regulation schemes in all three patient categories. .	110
Table 6: Comparison of TITA and BGI as two objective criteria to assess blood glucose profiles.....	112
Table 7: Comparison of closed-loop regulation performance of four PID architectures.....	121
Table 8: Performance metrics for three blood glucose level regulation schemes in the three case studies, for all adults.....	127
Table 9: Performance metrics for three blood glucose level regulation schemes in case study 2, for all adolescents and children.....	129
Table 10: Evolution of the TIR and mean BGI as a function of the microfluidic delay.....	137

List of Abbreviations:

ADA: American Diabetes Association

AP: Artificial Pancreas

APP: Artificial Pancreas Project

ATP: Adenosine Triphosphate

ATTD: Advanced Technologies & Treatment for Diabetes

BG: Blood Glucose

BGI: Blood Glucose Index

CBMN: (Laboratoire de) Chimie et Biologie des Membranes et Nano-objets

CCK: Cholecystokinin

CF: Correction Factor

CGM: Continuous Glucose Monitoring

CR: Carbohydrates Ratio

CSII: Continuous Subcutaneous Insulin Infusion

DCCT: Diabetes Control and Complications Trial

EASD: European Association Study of Diabetes

EDIC: Epidemiology of Diabetes Interventions and Complications (study)

FDA: Food and Drug Administration

FGM: Flash Glucose Monitoring

FPGA: Field Programmable Gate Array

GA: Genetic Algorithm

GI: Glycaemic Index

GIP: Gastric Inhibitory Polypeptide

GL: Glycaemic Load

GLP-1: Glucagon-Like Peptide-1

GUI: Graphical User Interface

HbA1c: Hemoglobin A1c (glycated haemoglobin)

HBGI: High Blood Glucose Index

IFB: Insulin Feedback

IIR: Insulin Infusion Rate

IMS: (Laboratoire de l') Intégration du Matériau au Système

IV: Intravenous

JDRF: Juvenile Diabetes Research Foundation

LBGI: Low Blood Glucose Index

LGS: Low Glucose Suspend

MCS: Multi Channel Systems (company)

MDI: Multiple Daily Injections (therapy)

MEA: Multi-Electrode Array

MPC: Model Predictive Control (algorithm)

NFC: Near-Field Communication

OGTT: Oral Glucose Tolerance Test

PDMS: Polydiméthylsiloxane

PID: Proportional Integral Derivative (algorithm)

PLGS: Predictive Low Glucose Suspend

SAP: Sensor-Augmented Pump (therapy)

SMBG: Self-Monitoring of Blood Glucose

SP: Slow Potentials

SQ: Subcutaneous

SSB: Subject Specific Basal

SYAM: System for Acquisition with Microfluidics

T1D: Type 1 Diabetes mellitus

T1DMS: Type 1 Diabetes Mellitus Simulator

T2D: Type 2 Diabetes mellitus

TAR: Time Above Range

TBR: Time Below Range

TCA: Tricarboxylic Acid Cycle

TDI: Total Daily Insulin

TIR: Time In Range

TITA: Time In Target Area

UVA: University of Virginia

VHDL: VHSIC Hardware Description Language

WHO: World Health Organization

Chapter 1

Scientific context

Trying to find a cure or a treatment for diabetes requires highly interdisciplinary research, particularly in translational research project investigating innovative solutions for patient treatment. For the last fifty years, the need for interdisciplinarity has been further strengthened by the digital revolution. The increasing use of computer science and high-technology devices in medicine led to the involvement of computer scientists, engineers or mathematicians in medical research. The development of the Artificial Pancreas (AP) to treat diabetes mellitus is a prime example. The regulation of blood glucose (BG) with automated closed-loop systems requires expertise in control theory; methods to measure blood glucose with higher time resolution were also developed and data scientists, with expertise in mathematics and statistics, are now necessary to analyse these data and develop powerful algorithms (e.g., adaptive algorithms, learning algorithms). In addition, a variety of engineers (e.g., electronics, computer, science, and mechanical science to name a few) is necessary to design wearable medical devices for glucose monitoring and insulin infusion.

This work is at the intersection of biology, electronics, control theory and diabetology. The development of our biosensor, integrating more inputs than traditional glucose sensors, raises the hope of a much finer tuning of diabetic patient's treatment. This biosensor is the result of ten years of research implying an interdisciplinary consortium of French research teams. In an attempt to provide the reader with the basic knowledges to understand the contribution of this work, this first chapter will define the most important concepts and key-elements from each discipline, as well as the state of the art of diabetes therapy. This thesis work is included in a broader research project, which objectives will be described.

The first chapter is organised as followed: the first subsection provides some basics about the chemistry and physiology of glucose homeostasis¹, then the diabetes disease is described with a focus on its pathophysiology. In the third subsection, the different therapeutic options are presented together with the most promising research approaches. The fourth subsection shows how the digital revolution impacted diabetes treatment by giving rise to new hopes with the development of a fully automated biomechanical pancreas. To conclude, the current technological limitations will be highlighted to define the problem that this work aims to address, thus emphasizing its relevance.

¹ Glucose homeostasis: glucose, as many other molecules (such as ions), have to be kept within a narrow range in the bloodstream and interstitial fluid to ascertain physiological function. Maintenance of this narrow range is named homeostasis.

1.1. Understand the physiology, biology and chemistry of glucose homeostasis

Even though this work is focused on computer-aided simulation and medical devices for the treatment of diabetes, some concepts of physiology and biochemistry are necessary to better understand the context of diabetes mellitus and its impact on patients. The British Physiological and Biochemical Chemistry societies define physiology and biochemistry as follows:

“Physiology is the science of life. It is the branch of biology that aims to understand the mechanisms of living things, from the basis of cell function at the ionic and molecular level to the integrated behaviour of the whole body and the influence of the external environment. Research in physiology helps us to understand how the body works in health and how it responds and adapts to the challenges of everyday life; it also helps us to determine what goes wrong in disease, facilitating the development of new treatments and guidelines for maintaining human and animal health. The emphasis on integrating molecular, cellular, systems and whole-body function is what distinguishes physiology from the other life sciences.”

(Physiological Society – United Kingdom)

“Biochemistry is the branch of science that explores the chemical processes within and related to living organisms. It is a laboratory-based science that brings together biology and chemistry. By using chemical knowledge and techniques, biochemists can understand and solve biological problems.”

(Biochemical Chemistry Society - United Kingdom)

The study of diabetes mellitus is at the crossroad of these disciplines due to the characteristics of the disease which mainly affects insulin secretion at cellular and organ levels, while having major consequences on nutrient homeostasis – i.e., at whole-body level. To better understand diabetes, the known symptoms and the currently available treatments, we will at first describe the glucose metabolism², its role in the energy supply of human body cells, and the endocrine regulation achieved by the pancreas to maintain glucose homeostasis. Then the characteristics of the disease and the available therapeutic interventions will be detailed. To conclude, the anatomy, the cellular composition and the function of the human pancreas will be described together with the other regulatory circuits involved in glucose homeostasis.

1.1.1. Glucose metabolism and body cells energy supply

In the physical world, every motion is a matter of **energy**. This rule also applies to living beings. Most of their movements require them to burn energy, released when chemical bounds in stable natural compounds are broken. The role of **nutrition** is therefore to supply the natural compounds and energy which enable them to move, grow, and reproduce. With few exceptions, animals are heterotrophic which means that they cannot produce their own food

² Metabolism: the sum of the chemical reactions that take place within each cell of a living organism and that provide energy for vital processes and for synthesizing new organic material. (Encyclopædia Britannica)

and therefore need to eat other living beings to fill their elementary needs. In so doing, and after digestion, they get the nutrients their cells need to grow and replicate.

Human beings mainly get their **energy** from the catabolism³ of **macronutrients** such as proteins, lipids and carbohydrates. These macronutrients are digested in the gastrointestinal tract and appear in the blood as smaller molecules which are easier to use by body cells: respectively **amino acids**, **fatty acids** and **glucose**. Absorbed by the cells, these molecules then converge into the TriCarboxylic Acid cycle (TCA or **Krebs cycle**), a series of chemical reactions leading to the formation of Adenosine TriPhosphate (**ATP**) (see **Figure 1**). ATP is a high potential energy molecule used to store energy directly in the cell for future use or to enable various processes (e.g., expression of genetic information, protein synthesis, hormone synthesis and secretion, nervous communication, muscle contraction). Amino acids, fatty acids and glucose are also involved in other metabolic processes as precursors for the biosynthesis of various essential molecules.

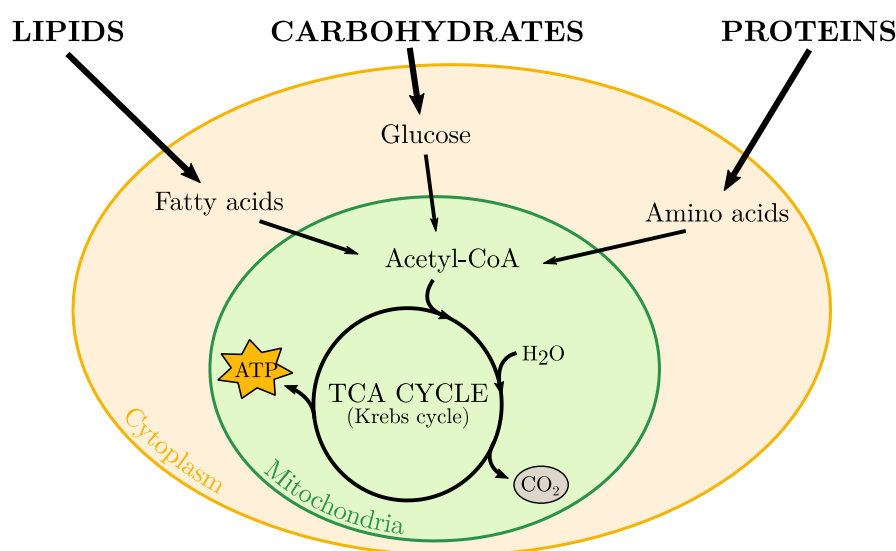


Figure 1: Simplified schematic of the mitochondrial metabolism

All body cells are capable of **absorbing glucose**. However, depending on the physiological state of the body (e.g., physical activity, nutritional status) and on the cell type, the repartition of energy supplied through the three above-cited pathways varies. For example, during rest and mild-intensity exercise, cardiac cells mainly get their energy from fatty acids but energy supply based on glucose oxidation increases with exercise intensity. Similarly, skeletal muscle and adipose cells mainly get their energy from fatty acids or endogenous stores; however, right after a meal, these cells increase their consumption of glucose in order to reduce the high blood glucose concentration resulting from food intake. In contrast, some specific cells rely exclusively on glucose to get their energy. The most common of them are the red blood cells. As they lack mitochondria, these cells cannot oxidize fatty acids and therefore ensure a continuous consumption of glucose in the body. Glucose is also the preferred energy source of brain cells, although this can change in specific physiological situations.

³ **Catabolism**: a metabolic process in which complex molecules are broken down into simple ones with the release of energy. (Collins dictionary)

As diabetes mellitus mainly affects the metabolism of glucose, we will now focus on this molecule and its blood level also referred to as glycaemia.

Glucose is a simple **sugar** – or monosaccharide – existing under two isomer forms, the L-glucose and D-glucose, the latter one being the molecule that can be found in nature also named dextrose. Monosaccharides are the simplest sugars and cannot be hydrolysed⁴ into smaller molecules. They are the basic unit of more complex molecules such as disaccharides, also referred to as complex sugars. The most common disaccharides are lactose (composed of glucose and galactose) that can be found in dairy products, sucrose (composed of glucose and fructose) which is more known under the name “table sugar” and maltose (a combination of two molecules of glucose). Polysaccharides are a combination of more than ten monosaccharides (**Figure 2**). As glucose is polar, it requires a solvent, such as water, for storage. Living beings thus favour long chain of monosaccharides, i.e., polysaccharides, to store energy on the long term in a condensed form requiring less solvent molecules. The main energy-storing polysaccharides are starch in plants and glycogen in animals. They are both polymers⁵ of glucose but glycogen is easier to metabolize and therefore better suits the lifestyle of animals which need quicker access to the energy they have stored than plants. From a dietary point of

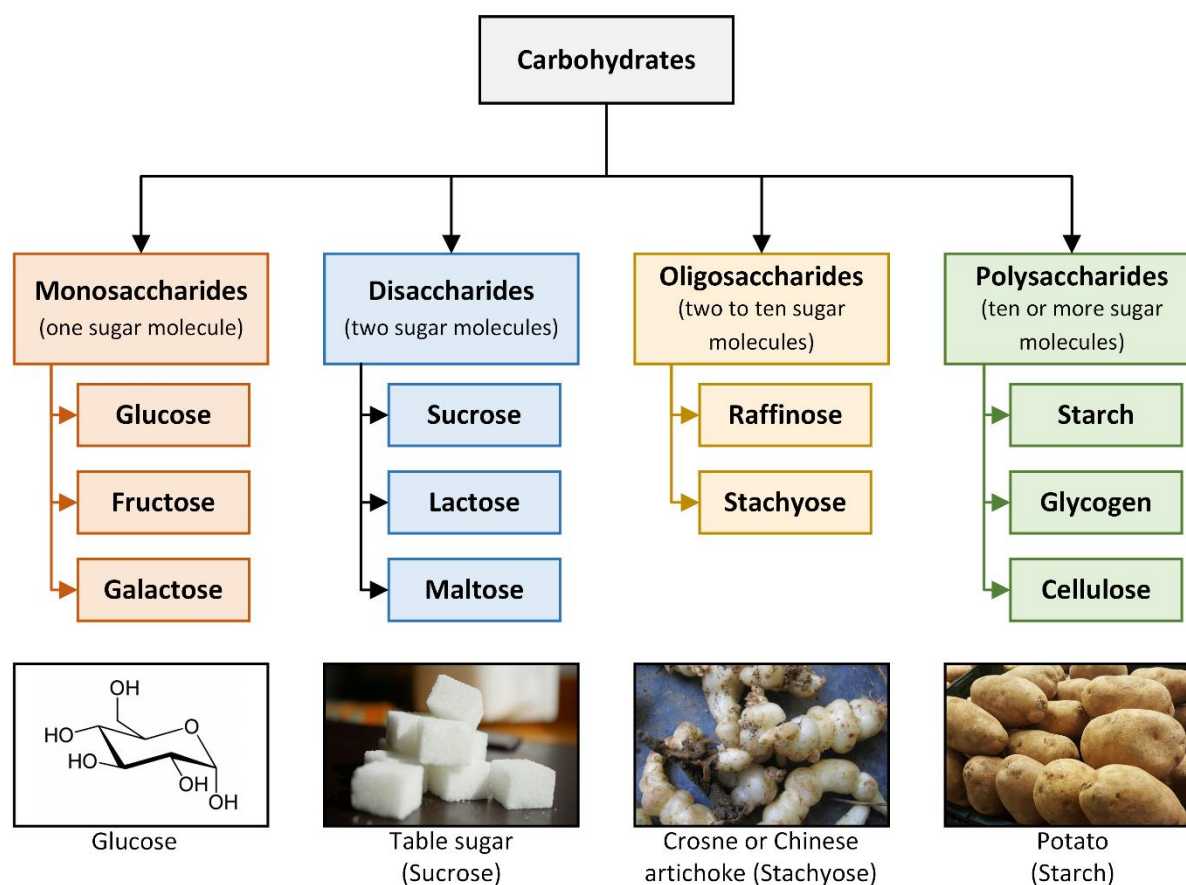


Figure 2: Carbohydrates classification

⁴ **Hydrolysis:** a chemical reaction in which a compound reacts with water to produce other compounds. (Collins dictionary) During the digestion process, covalent bonds of carbohydrates are notably cleaved by hydrolysis to form simple soluble sugars.

⁵ **Polymer:** any of a class of natural or synthetic substances composed of very large molecules, called macromolecules, which are multiples of simpler chemical units called monomers. (Encyclopædia Britannica)

view, all these molecules belong to the carbohydrates group and represent between 40 and 60% of the daily energy intake of healthy people in western countries.

In regard to nutrition, the overall objective of human beings is to supply their body with all the natural compounds it needs to maintain vital metabolic processes. In nature, glucose is found in the form of rather complex molecules grouped together under the term carbohydrates. To use it as a fuel, the human body therefore developed over time the ability to convert complex carbohydrates molecules into smaller glucose molecules that can be used by its cells. Due to their hydrophilicity, the hydrolysis of carbohydrates naturally occurs in water. However, in the gastro-intestinal tract, this long process is catalysed by enzymes. Each molecule hydrolysis is processed with the help of specific enzymes – e.g., lactase eases the digestion of lactose (milk sugar). The **duration of the digestion** of di- or polysaccharide molecules **increases with the complexity** of the molecule. Due to their rather low complexity, disaccharides are quickly processed and the glucose resulting from their hydrolysis rapidly “crosses” the intestinal barrier to reach the bloodstream. The fact that they contain sucrose (a disaccharide) therefore explains why high-sugar products are more likely to induce quick rises of the blood glucose level. On the other hand, the digestion process of polysaccharides – which can be composed of up to 10 000 molecules of glucose – could be rather long. Starchy foods like pasta or rice are slowly digested and therefore induce a steady glucose intake even few hours after the meal. The latter property explains why people practicing endurance sports do privilege this kind of food before a physical effort.

Carbohydrates type and food structure, greatly influence the duration of the digestion process, and thus the glucose rate of appearance in the bloodstream. To measure the influence of carbohydrates on blood glucose variations, the widespread dichotomy between slow and fast carbohydrates has been refined by two key concepts: the glycaemic index and the glycaemic load. The **Glycaemic Index (GI)** was introduced in 1981 by Jenkins et al. [1] to compare the glycaemia response to the intake of different types of food. A 50-g portion of food is given to the subject and the area under curve of the resulting glucose level response is computed and compared to the glycaemic response obtained with a reference food (either glucose or white bread – see **Figure 3A**). The areas are computed on a 2-hour window after the food ingestion. GI is then formulated as the ratio between these two areas expressed as a percentage. As a consequence, the GI of glucose is 100 when the reference food is glucose. The GI of many different food has been estimated and is regularly published online [2]. Examples for some staple food products, taken from Atkinson et al. [2], are presented in **Table 1**.

The **Glycaemic Load (GL)** is computed by multiplying the carbohydrate content of a food serving by the GI of this food divided by 100:

$$GL = GI \times \text{Carbohydrate content per serving (g)} \div 100$$

Ex: The glycaemic index of a banana cake made with sugar is about 47. The carbohydrates content of a 60-gram serving of this cake is about 29 grams. The glycaemic load of a 60-gram serving of banana cake is then 14.

Table 1: Average GI of common food products compiled in atkinson et al. (2008)

High-carbohydrates foods		Breakfast cereals	
- White wheat bread	75 ± 2	- Cornflakes	81 ± 6
- Specialty grain bread	53 ± 2	- Muesli	57 ± 2
- Corn tortilla	46 ± 4	Dairy products	
- Spaghetti, white	49 ± 2	- Milk, full fat	39 ± 3
Snacks		- Yogurt fruit	41 ± 2
- Chocolate	40 ± 3	Fruits	
- Rice crackers	87 ± 2	- Apple, raw	36 ± 2
- Popcorn	65 ± 5	- Pineapple, raw	59 ± 8
Sugars		- Watermelon, raw	76 ± 4
- Fructose	15 ± 4	Vegetables	
- Glucose	103 ± 5	- Potato, boiled	78 ± 4
- Sucrose	65 ± 4	- Potato, French fries	63 ± 5
- Honey	61 ± 3	- Carrots, boiled	39 ± 4

Data are means ± SEM

This indicator provides a tool to compare food servings of different nature and size. Calculating the GL of each food serving which compose a meal allows an estimation of the carbohydrates content of the meal and predicts the associated postprandial⁶ excursion of the blood glucose level as if this meal was only containing glucose (see **Figure 3B**).

The GI is the subject of a debate in the scientific community [2]–[4]. This index has been thought as an intrinsic characteristic of food. However, numerous factors do influence the glycaemic response to food products, i.e. the computed GI value of these products [5]. The most significant are the time of day when the test is realised, the tested subject own physiological characteristics, and the way food has been processed and cooked. As a consequence, there is no consensus for the recommendation of low-GI diets as part of diabetic

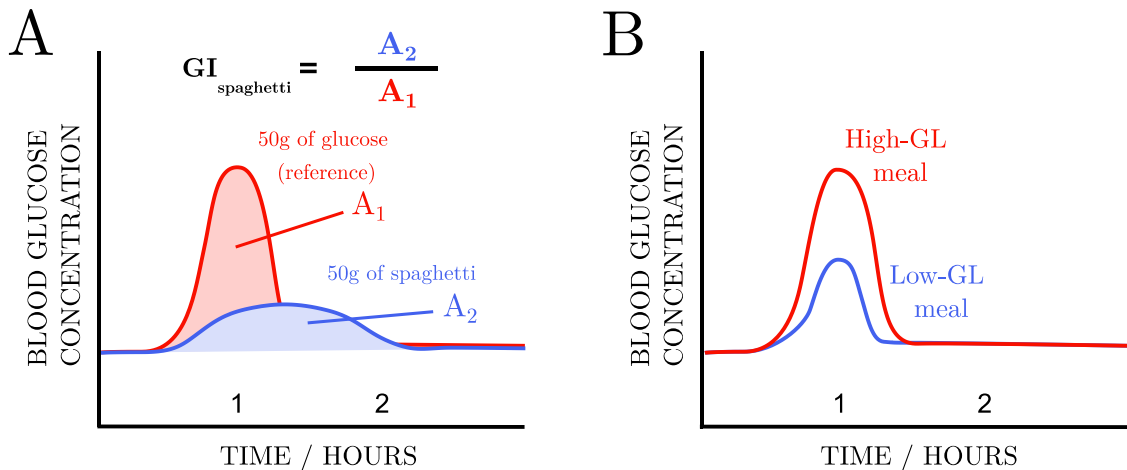


Figure 3: Two metrics to characterise carbohydrate content of meals **A**) GI calculation method (in the case of spaghetti) **B**) Illustration of the normal blood glucose response to meals containing a high Glucose Load (GL) in red and a low GL in blue.

⁶ Postprandial: happening after lunch or dinner. (Cambridge dictionary)

patients' treatment. The American Diabetes Association (ADA) rather recommends individualized diets focusing on the reduction of the total amount of carbohydrates per meal [5]. Nevertheless, GI highlights the influence of food processing and cooking on glucose level response. For example, depending on the variety and the processing and cooking method, the GI of potato can range from 23 to 144 [6]. GI is then a valuable tool to characterise food products and, when combined with GL, provides diabetic patients with a method to assess the **influence of meal composition** on their postprandial glycaemia variations.

1.1.2. Glucose homeostasis

We have seen that all body cells can process glucose to obtain energy, with some of them exclusively relying on this molecule to maintain their vital metabolic processes. To ensure a continuous energy supply to their cells, human beings therefore need to keep their blood glucose concentration above a certain level. This threshold varies from one individual to the other, but an average value has been estimated at **70 mg/dl** (3.9 mmol/l). A prolonged time below this limit elicits the symptoms of **hypoglycaemia**. These symptoms worsen as the glycaemia continues to fall or if hypoglycaemia lasts longer. Common symptoms are trembling, palpitations, sweating, anxiety, hunger, nausea, tingling, difficulty concentrating, confusion[7]. They can be self-treated most of the time; however, if hypoglycaemia is not treated in time it can eventually lead to unconsciousness, coma and death when the glycaemia persists below 55 mg/dl.

In contrast, high concentrations of glucose are toxic for many body cells and can have severe consequences on the long-term. In the case of diabetes, long-term complications elicited by repeated and prolonged high blood glucose levels concern mainly blood vessels and their cells, leading to a wide range of pathologies from retinopathy, nephropathy and neuropathy to increased risk of stroke and cardiovascular disease (further described in section 1.2.2) [8]. The **hyperglycaemia limit** is traditionally set to **180 mg/dl** (10 mmol/l) for diabetic patients and to 140 mg/dl for healthy individuals.

By nature, the nutrition process results in an intermittent glucose rate of appearance in the bloodstream. To avoid harmful concentrations of glucose in blood (e.g., due to meals with a high glycaemic load ingested in a short period) and to ensure a steady energy supply to cells, evolution equipped higher organisms with the ability to extract glucose from the bloodstream to store it. Indeed, glucose can be **stored under the form of glycogen** in the **liver** and the **muscles**. It can also be stored in **adipose tissues** disseminated throughout the body and therefore constitute energy reserves under the form of fat.

To ensure a continuous energy supply to the body and prevent hypoglycaemic events, the glucose storing mechanism requires a counterpart: the ability for the body to **release the stored glucose** into the bloodstream. The mobilisation of this energy reserve is particularly necessary considering the long digestion process induced by some types of food and when the glucose consumption suddenly increases (stress, physical effort...). The glucose release mechanism mainly takes place in the liver.

As previously mentioned, body cells can be supplied with energy through three main pathways using amino acids, fatty acids and glucose. To keep supplying the glucose-dependent

cells with energy when the glucose reserves are lessening, the body is also able to synthesize glucose with non-carbohydrate precursors such as amino acids in a metabolic process called **gluconeogenesis**. This set of metabolic processes help the body to survive to periods of starvation lasting few days to few weeks.

The combination of the glucose storage/release mechanisms enables **glucose homeostasis** and allows human beings to maintain their glycaemia in a safe range named normoglycaemia or euglycaemia. In this work, we used the most common definition of **euglycaemia limits: 70 to 180 mg/dl**. The extraction and release of glucose from and into the bloodstream is finely **regulated** through complex physiological processes but the main regulatory circuit uses endocrine pathways and is orchestrated by the **islets of Langerhans in the pancreas**.

1.1.3. Endocrine regulation via insulin and glucagon secretion

Glucose homeostasis is maintained in healthy individuals through the coordinated action of two hormones secreted by the endocrine pancreas: **insulin and glucagon**. The first one triggers several physiological responses that help diminishing the blood glucose level and the second one stimulates physiological processes leading to the opposite effect. In this section, we will describe the characteristics of each one of these hormones, the cells they target, and their mode of operation, starting by insulin.

Insulin is an endocrine peptide hormone – as opposed to steroid hormones – which signifies that it is composed of a chain of **amino acids**. This 51-amino acid hormone is synthesized from a single-chain proinsulin precursor in the **β cells** of the islets of Langerhans. Proinsulin undergoes enzymatic cleavage resulting in the production of an insulin molecule (an A chain connected to a B chain by two disulphide bonds – see **Figure 4**) and a C-peptide [9]. Parenthetically, as insulin and C-peptide are secreted in equimolar amounts by β cells, C-peptide dosing is a common technique to assess the remaining pancreatic insulin secretion in diabetic patients treated with exogenous insulin infusion.

Insulin is closely **regulated by glucose** concentration in blood, i.e., high and low blood glucose levels respectively stimulate and inhibit insulin secretion. Insulin membrane-bound receptors are expressed in many cell types but, concerning the glucose homeostasis, the main target cells of insulin, the classical triad, are located in the liver, skeletal muscles and adipose tissues. During the recent years it has become apparent that insulin also regulates other tissues such as brain, heart and even the islets

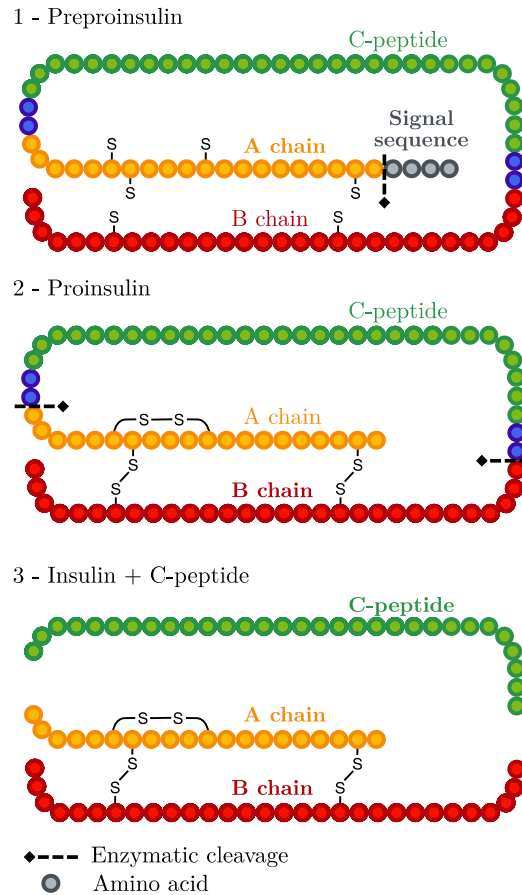


Figure 4: Insulin synthesis process in the β cells

such as brain, heart and even the islets

themselves. To decrease blood glucose level, insulin stimulates or inhibits several metabolic processes [10]. It activates the synthesis of energy storage molecules (glycogen in liver and muscles, fat in adipocytes), it increases glucose transport across insulin target cells' membrane, and modulates the expression of numerous genes involved in glucose homeostasis. Finally, as the main anabolic⁷ hormone, insulin does not only play a role in the metabolism of glucose but also in the metabolism of other nutrients (e.g., proteins and lipids) [11], which further explains the severity of diabetes.

Glucagon is a peptide hormone, like insulin, secreted by **α cells** in the endocrine pancreas. As glucagon is a main counter-regulatory hormone of insulin, its secretion is also predominately regulated by glucose concentration in blood. Glucagon transmembrane receptors are mainly expressed in liver, kidney, and **β cells** [12]. Concerning glucose homeostasis, the most important physiological responses induced by glucagon are the promotion of glycogenolysis (hydrolysis of glycogen), inhibition of glycogen synthesis and potentiation of gluconeogenesis in the liver, and the inhibition of glycolysis (hydrolysis of glucose occurring in ATP synthesis – see **Figure 1**) [11], [13]. Glucagon also plays a key role in other major metabolic processes: protein metabolism, lipid metabolism, bile acid metabolism, energy expenditure regulation and food intake regulation. Their understanding being less important here, they will not be further described.

1.1.4. Anatomy and physiology of the human pancreas

The human **pancreas** can be divided into three parts (head, body and tail – see **Figure 5A**) with varying cell populations in term of both cell type and cell spatial distribution. In addition to its physical partition, the pancreas can be divided in two functional parts: the exocrine pancreas and the endocrine pancreas.

The **exocrine pancreas** participates to the digestion process by secreting digestive fluids in the duodenum. It is mainly composed of acinar and ductal cells. Acinar cells are in charge of the secretion of various digestive enzymes such as proteases which convert proteins and peptides into amino acids, amylase which process starch and maltose or pancreatic lipase which converts lipids into glycerol and free fatty acids. For their part, ductal cells secrete a fluid rich in bicarbonate which, thanks to its amphoteric properties, increases the pH of the gastric chyme⁸ in order to provide a suitable operating environment to the pancreatic digestive enzymes.

Yet, in the context of diabetes, the relevant part of the pancreas is its endocrine part. The **endocrine pancreas** regulates several metabolic processes through the secretion of various hormones in the bloodstream. It is composed of isolated cells or clustered cells gathered in small **structures** named **islets of Langerhans** (see **Figure 5B**). The endocrine pancreas rarely exceeds 5% of the whole pancreas in mass [14]. It is composed of five main cell types:

- **α cells** secrete the above-mentioned hormone glucagon.
- **β cells** secrete the above-mentioned hormone insulin.

⁷ Anabolism: a metabolic process in which complex molecules are synthesized from simpler ones with the storage of energy. (Collins dictionary)

⁸ Gastric chyme: the thick fluid mass of partially digested food that leaves the stomach. (Collins dictionary)

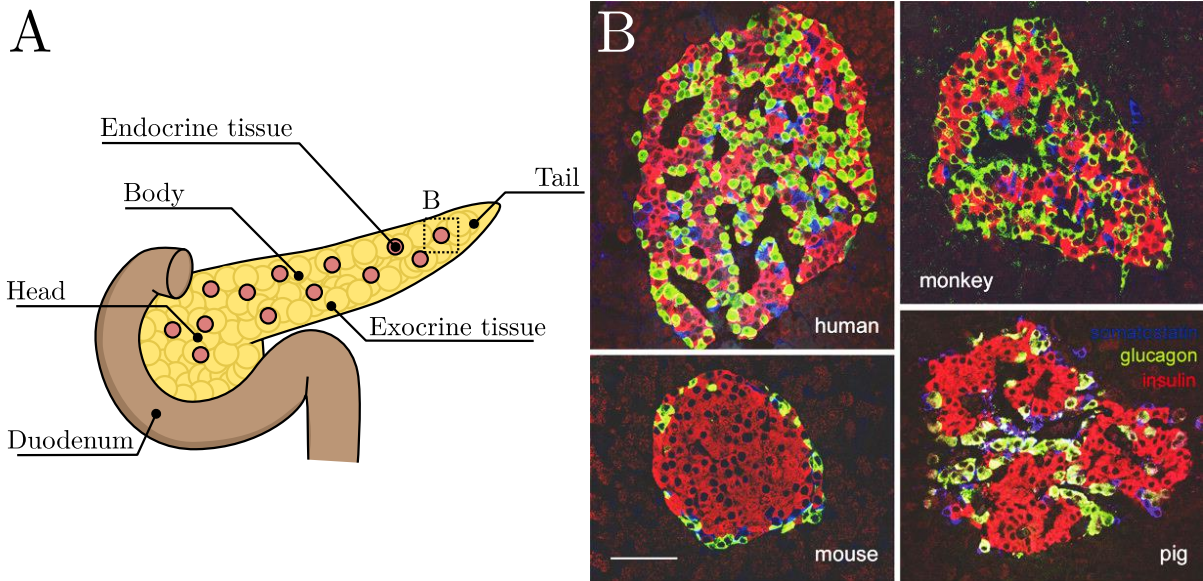


Figure 5: Anatomy of the pancreas **A)** Schematic of the human pancreas structure **B)** Cytoarchitecture of the human islet and comparison with other species. The pictures show representative immunostained pancreatic sections containing islets of Langerhans from human, monkey, mouse and pig. Interestingly, insulin-immunoreactive (red), glucagon-immunoreactive (green), somatostatin-immunoreactive (blue) cells were all found randomly distributed in human and monkey islet. (adapted from Cabrera et al.)

- δ cells secrete the hormone somatostatin which presents a paracrine⁹ action by inhibiting secretion of both insulin and glucagon, and by inhibiting exocrine pancreas secretion.
- PP cells secrete pancreatic polypeptide which is also involved in the regulation of pancreatic secretion (both exocrine and endocrine).
- ϵ cells secrete ghrelin and compose up to 10% of the endocrine cells in the embryonic pancreas but their proportion falls to less than 1% in the adult pancreas.

The proportion of endocrine cells largely varies from one individual to the other. This composition variation is partly age-dependent [15] but pancreas also presents regional variations as described in Wang et al. [14]. In general, in human adults, the islets of Langerhans are assumed to be composed of 60-70% of β cells, 5-30% α cells and the remainder being divided between the other above-mentioned cell types, for a total exceeding the thousands of endocrine cells [11], [16].

The total number of islets in the human endocrine pancreas has been estimated to range from 3.2 to 14.8 million islets [16], [17]. Using advanced imaging techniques and two estimation methods, Ionescu-Tirgoviste et al. estimated the average islet diameter to be of 108.92 μm (± 6.27) [16], and that islets occupy only 4.487% of the total pancreas volume of their donor. It is also worth noting that mouse islets present a characteristic structure where a β cell core is surrounded by a mantle of α and δ cells, when human islets do not show anatomical subdivisions. Indeed, Cabrera et al. [18] found insulin-immunoreactive beta cells, glucagon-immunoreactive alpha cells, and somatostatin-containing delta cells scattered throughout the human islet, and compared it to other mammalian species (see **Figure 5B**). Larger human islets seem to be

⁹ **Paracrine:** of, relating to, promoted by, or being a substance secreted by a cell and acting on adjacent cells. (Merriam-Webster dictionary)

more vascularised than smaller ones. Either way, the endocrine pancreas is a highly vascularised and innervated organ which receive an abundant flow of blood from splenic and pancreaticoduodenal arteries [11].

1.1.5. Other regulatory circuits of insulin secretion

Insulin secretion is mainly regulated by the prevailing **glucose level**. However, insulin playing a role in other nutrients metabolism, and to cope with a variety of physiological states and perturbations, insulin secretion is also finely regulated by **lipids and amino acids** plasma levels, other hormones and neurotransmitters.

Fatty acids and few amino acids present a stimulatory action on β cells which further increases the insulin secretion consecutive to a meal. Note that fatty acids taken by a meal increase only after 60 to 90 min in the circulation. The ingestion of food and the associated absorption of nutrients also result in the stimulation of intestinal endocrine cells and the secretion of several insulin secretagogues¹⁰. Among them, the **glucagon-like peptide-1 (GLP-1)**, the gastric inhibitory polypeptide (GIP) and cholecystokinin (CCK) act as potent glucose-dependent **stimulator** of insulin secretion [11]. In contrast, an increase in **adrenaline** concentration results in an **inhibition** of insulin release to satisfy the associated increase in glucose consumption by muscles.

To anticipate oncoming situations of need or excessive absorption of glucose, pancreatic secretions are also regulated by the **nervous system**. Feeding activates the parasympathetic innervation which stimulates all endocrine islet cells and especially insulin secretion by releasing acetylcholine from nerve terminals close to β cells. In situation of need, such as starvation, fright or physical activity, the sympathetic innervation is activated to lower insulin secretion.

Finally, the pancreas endocrine secretions are also finely auto-regulated by a paracrine action of each hormone on the others with a hierarchy established by the position of the secreting cells in the intra-islet portal system. For example, glucagon stimulates insulin and somatostatin secretion while insulin is a general inhibitor of pancreatic hormones secretion. Pancreatic polypeptide is an inhibitor of pancreatic endocrine and exocrine secretions.

This first section outlined the **central role of glucose metabolism** in the human body. The glucose metabolism supplies the body with the energy it needs to function and also provides precursors for many physiological relevant molecules. Although numerous safeguards do exist to withstand extreme situations, glucose remains the preferred energy source of some essential cell types (e.g., red blood cells, brain cells). The nutrient metabolism is an intricate machinery involving various anatomical structures disseminated throughout the body and precisely directed by its conductor - the endocrine pancreas. Among the numerous molecules involved in the different regulatory circuits, insulin occupies a prominent position as the main anabolic hormone. This explains why type 1 diabetes is such a serious disease which, untreated, can lead to death within months, and whose long-term consequences remain severe in the absence of perfectly satisfactory treatment.

¹⁰ Secretagogue: a substance that stimulates secretion. (Collins dictionary)

1.2. Diabetes mellitus

Diabetes mellitus is referring to a group of **chronic metabolic disorders** characterized by prolonged hyperglycaemia and altered lipid profiles. The term gathers various diseases with specific clinical pictures but a common origin: an impairment in insulin secretion, insulin action or both. Three main types were described: Type 1 Diabetes (T1D), Type 2 Diabetes (T2D) and gestational diabetes. Other forms of diabetes do exist, with specific clinical pictures, but their incidence is too low for them to constitute a separate subgroup. Each type of diabetes pairs with adequate and preferred therapeutic approaches depending on the main symptoms and on the pathogenesis of the disease (see **Table 2**). **T1D** being characterized by a **loss in β cell mass** resulting in impaired insulin secretion, the main treatment still consists in the injection of **exogenous insulin** to cope with postprandial hyperglycaemia. Note that T1D can be further divided in two subtypes: type 1A (autoimmune) and type 1B (idiopathic¹¹). Though the pathogenesis of these two types is different, they share the same diagnostic methods, long-term complications and treatment approaches. In this work, we use the term T1D to refer to the **most prevalent autoimmune** type but most of the following subsections remains valid for both types. **T2D**, in contrast, is characterized by an **insulin resistance** resulting in an impaired insulin action. Though genetic factors do play a role in disease development, T2D is a lifestyle disease associated with obesity and sedentariness. As a consequence, the prime treatment is the introduction of lifestyle modifications (e.g., low-carb diet, increased physical activity).

Table 2: Comparison of clinical features of type 1 and type 2 diabetes (adapted from Atlas of diabetes, Springer US, 2012, P.66)

Characteristics	Type 1 Diabetes	Type 2 Diabetes
<i>Onset</i>	Abrupt	Progressive
<i>Endogenous insulin</i>	Low to absent	Normal, elevated, or depressed
<i>Age at onset</i>	Any age	Vast majority of adults
<i>Body mass</i>	Usually nonobese	Obese or nonobese
<i>Treatment</i>	Insulin	Diet, oral hypoglycemics, insulin
<i>Family history</i>	10-15%	30%

The survival of T1D patients relies on an adapted insulin therapy, while such a therapy is only part of the treatment of a limited number of T2D patients. The fine tuning of the exogenous insulin infusion importantly conditions the long-term outcome of T1D. Our work, by providing a better picture of the patient physiological state resulting in a finer management of insulin infusion, firstly applies to the **treatment of T1D**. The next subsections therefore focus on the description of this disease.

1.2.1. Pathogenesis of type 1 diabetes

The causes of T1D are not fully understood yet although they received increased attention during the last two decades. The disease appears to result from an interplay between genetic

¹¹ Idiopathic: refers to a disease or medical condition which origin is unknown.

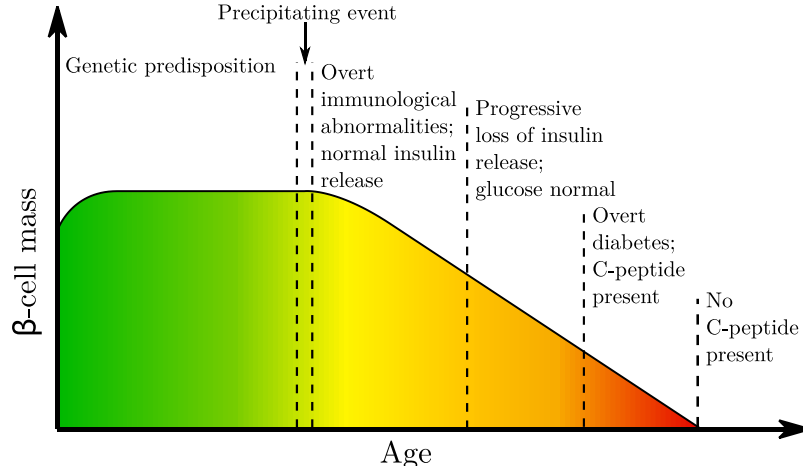


Figure 6: Eisenbarth model of type 1 diabetes pathogenesis (derived from Eisenbarth et al.)

predisposition, environmental factors and microbiome, and individual characteristics [19]. T1D patients present genetic risk factors which means that the disease results from a complex polygenic inheritance but is not hereditary and needs environmental triggers to develop. As a consequence, children who have a parent with diabetes present a risk to develop the disease which does not exceed 9%. In 1984, George S. Eisenbarth proposed a conceptual model of the pathogenesis of T1D in the form of a chart (see **Figure 6**) presenting the **evolution of βcell mass** during the **development of the disease** [20]. From genetic predisposition and before overt diabetes, patients firstly present immunological abnormalities with the presence of pancreatic islet autoantibodies in blood inducing an immune response specifically targeting pancreatic βcells. The true trigger of this abnormal immune response is not known yet, but it has been hypothesized that environmental causes such as changes in microbiome composition or viral infections could play a precursory role. As a consequence of the autoimmune response, β cell mass starts diminishing and insulin secretion is progressively impaired. First, blood glucose level is not affected, but after a period lasting few months to years insulin secretion becomes insufficient and diabetes appears. As knowledge of the disease increased, the model was completed to highlight the interventions that may be considered to curtail the diminution of βcell mass at different stages of the disease.

Contrary to T2D which mostly appears in adults, and due to its specific pathogenesis, type 1 diabetes can appear at any age. The incidence variation of genetically defined T1D across age categories is limited (28 to 89 cases for 100000 population) when compared to T2D (0 to 3500 cases for 100000 population)[21]. As the only diabetes type frequently diagnosed in children, T1D was formerly known as juvenile-onset diabetes. However, up to 50% of T1D cases are diagnosed in adults but a significant part of these cases is mistakenly diagnosed with T2D in the first place. Although, diagnostic techniques, such as C-peptide dosing, do exist to characterize severe impairment of insulin secretion, no clinical feature can undoubtedly distinguish type 1 from non-type 1 diabetes at diagnosis [19].

1.2.2. Diagnosis and pathophysiology

As a metabolic disorder causing a severe impairment in insulin secretion, T1D induces a wide range of symptoms depending on the advancement of the disease at diagnosis and the

age of the patient. Although the pathophysiology¹² of T1D is well described, the diagnosis of T1D remains challenging since the clinical picture greatly vary with patient age. In children, the clinical picture suggesting diabetes often includes polyuria (frequent urination), polydipsia (excessive thirst), and weight loss. These symptoms are less frequent in adults, who present a more diversified clinical picture at disease onset. Despite these differences, the diagnostic is always confirmed by blood glucose level measurements. Diabetes is typically diagnosed when a fasting blood glucose level above 126 mg/dl is measured, when casual blood glucose levels above 200 mg/dl and other diabetes symptoms are detected, or when a non-physiological response to a glucose tolerance test is observed [22]. Additionally, a measurement of the glycated haemoglobin concentration (HbA1c)¹³ can confirm the diagnosis or help in detecting the disease when the measured concentration exceeds 6.5%.

As stated above, the **main symptom** caused by T1D is impaired blood glucose homeostasis in the form of prolonged high blood glucose levels. **Hyperglycaemia** being harmful for the patient on the long-term (see section 1.1), the infusion of exogenous insulin transforms the disease from a possibly lethal one into a treatable one. However, it does not annihilate the risk of complications due to difficulties to perfectly restore the endogenous insulin action. An increased risk of hyperglycaemia persists and, despite the treatment, complications can gradually develop throughout the years. The risk of **diabetes complications** substantially depends on the duration of the disease, the adopted treatment, the insulin dosing adequacy and the patient acceptance of his treatment.

The long-term complications of T1D are linked to pathological alterations of blood vessels that can lead to renal insufficiency, the necessity of limb amputations, blindness and heart attacks. They are coarsely classified in two categories: microvascular and macrovascular complications.

Microvascular diabetes complications are due to a higher vulnerability of specific body cells to elevated extracellular glucose concentration [23]. This damaging mechanism mainly affects the capillary endothelium¹⁴ of the retina, the mesangial cell in the kidney and the Schwann cell of peripheral nerves, and explains the specific retinopathy, nephropathy and neuropathy associated with diabetes. Other organs, such as the brain and the heart, can be affected by both microvascular and macrovascular complications (atherosclerosis, thrombosis) leading to an increased risk of heart attack or stroke. These macrovascular complications also affect extremities resulting in a vulnerability to skin infections which can lead to amputation in severe and untreated cases.

Risk factors for complications include juvenile-onset of the disease, chronic hyperglycaemia, and repeated hypoglycaemic events. Puberty seems to play a role in complications development

¹² Pathophysiology: refers to the study of abnormal changes in body functions that are the causes, consequences, or concomitants of disease processes. (*Encyclopedia of Behavioral Medicine*, 2013 Edition)

¹³ Glycated haemoglobin is the product of a slow and spontaneous reaction occurring in blood and consisting in the bonding of a glucose molecule to the haemoglobin protein of a red blood cell. This reaction is therefore catalysed by prolonged hyperglycaemia. Red blood cells life span is about three months, it is therefore possible to estimate the mean blood glucose level over the last three months via HbA1c dosing in blood.

¹⁴ Endothelium: the thin layer of cells that cover the inside walls of the blood vessels, heart and some other body parts. (Cambridge Dictionary)

[24] as well as patient sex, with girls presenting increased rates of all-cause premature mortality and vascular events than men. Concerning non-glycaemic risk factors, education and income levels were associated with inversely proportional risk of both micro- and macrovascular complications. As a good predictor of poor glycaemic control, poor quality of life also influences long-term outcome of the disease.

Other complications associated with T1D do not directly result from the disease, but from its treatment. In 1993, the Diabetes Control and Complications trial (DCCT) assessed the benefits of **intensive insulin therapy** – implemented with external insulin pumps – compared with multiple daily injections of insulin (3 to 4 a day) on a large cohort of 1441 T1D patients [25]. The study was unprecedented due to the long follow-up duration achieved (6.5 years in average) and the size of the patient cohort. This major clinical trial demonstrated that intensive blood glucose control significantly **reduces the incidence of most common complications** of T1D and impedes their progression. However, the study also highlighted **an increased incidence of hypoglycaemic** events (up to two- to three-fold). This latter statement emphasized the need to pair the reduction of mean blood glucose level, induced by intensive insulin therapy, with a mitigation of the hypoglycaemic risk. Indeed, the repetition of acute hypoglycaemic events is associated with increased hypoglycaemia unawareness and the occurrence of more severe subsequent hypoglycaemic events. However, it is worth noting that, despite the difficulties to optimize insulin delivery in real-life conditions, the risk of microvascular and macrovascular complications have substantially decreased over the last 25 years [26].

1.2.3. Epidemiology

Epidemiology is defined in the Encyclopædia Britannica as follows:

“The branch of medical science that studies the distribution of disease in human populations and the factors determining that distribution, chiefly by the use of statistics. Unlike other medical disciplines, epidemiology concerns itself with groups of people rather than individual patients and is frequently retrospective, or historical, in nature. It developed out of the search for causes of human disease in the 19th century, and one of its chief functions remains the identification of populations at high risk for a given disease so that the cause may be identified and preventive measures implemented”.

In the case of T1D, epidemiological studies aim at identifying **environmental and genetical causal factors** of the disease in order to improve its understanding and imagine innovative approaches for both treatment and prevention. Risk factors for development of T1D are manifold [27]. We have already discussed the increased risk for complications associated with age, sex and the influence of genotype in disease development. In this section, we focus on risks associated with geographic location and race, and we finally discuss the worldwide temporal trends of diabetes incidence.

Few epidemiological data about the worldwide incidence of T1D in adults is available, as a vast majority of studies focused on children. Among them, the large-scale worldwide DIAMOND study is worth mentioning: it was initiated by the World Health Organization

(WHO) to evaluate the incidence¹⁵ rate variation of T1D in 50 countries. The incidence of T1D in children ≤ 4 years of age, from a population of 75.1 million children and between 1990 and 1994 was reported in 2000 [28]. A 350-fold difference in age-adjusted T1D incidence rates was reported with a minimum of 0.1/100000 per year (China, Venezuela) and a maximum of 36.5-36.8/100000 per year (respectively Finland and Sardinia).

Worldwide differences in T1D incidence by race/ethnicity is rarely discussed in epidemiological studies due to the relative homogeneity of studied populations or to lacking data for political or study design reasons. These differences can be confounded with geographical differences in countries presenting a large race/ethnicity homogeneity. However, the mobility of populations around the world, accelerated by globalisation, revealed a link between T1D and race/ethnicity. For example, people of European descent present an increased risk of developing T1D. It is particularly noticeable in countries such as New-Zealand where significant differences can be observed between people of European descent and people of Maori descent [29]. In the United States, the SEARCH for Diabetes in Youth study gave some valuable insight on the relationship between race/ethnicity, age and sex, and T1D incidence [30]. Conducted on more than 10 million American children/years, SEARCH highlighted significant particularities: T1D incidence and prevalence rates were higher in non-Hispanic white youth as compared to four other race/ethnicities (African American, Hispanic, Asian and Pacific Islander and Navajo) [27].

In 2006, The DIAMOND Group Project published an updated report describing the worldwide evolution of **childhood T1D** incidence rate between 1990 and 1999. The report concluded that the average annual **increase in incidence** was about 2.8% (95% CI¹⁶ 2.4–3.2%). The annual increase was slightly higher in the period 1995-1999 (3.4% - 95% CI 2.7–4.3%), than in the period 1990-1994 (2.4% - 95% CI 1.3–3.4%) [31]. This trend was observed almost all over the world and has been confirmed by several recent studies [29]. In France, a similar trend was observed over the 2010-2015 period with an increase by 4% of childhood T1D incidence rate [32].

The International Diabetes Federation publishes, on a regular basis, estimations and forecasts on global and regional **diabetes-related health expenditure** (see Appendices 1 and 2). These data, which gather estimations of all expenditure relative to both T1D and T2D, are particularly useful to assess the worldwide evolution of the disease and the associated economic burden for patient families, health systems and national economies. It is worth noting that both diagnosed and undiagnosed prevalence¹⁷ estimates are considered. The last report underlined a **steady upward trend** in the estimated global health expenditure among adults with diabetes since 2006. The total diabetes-related health expenditure was estimated to be USD 230 billion in 2006 and USD 760 billion in 2019. The health expenditure is projected to grow to USD 825 billion per year by 2030 and USD 845 billion by 2045 : the world is facing

¹⁵ **Incidence:** in epidemiology, the occurrence of new cases of disease, injury or other medical conditions over a specified time period, typically calculated as a rate or proportion. (Encyclopaedia Britannica)

¹⁶ **CI:** Confidence Interval

¹⁷ **Prevalence:** in epidemiology, the proportion of a population with a disease or a particular condition at a specific point in time (point prevalence) or over a specified period of time (period prevalence). Prevalence is often confused with incidence, which is concerned only with the measure of new cases in a population over a given interval of time. (Encyclopaedia Britannica)

a **worldwide epidemic of diabetes** [33] (see Appendix 1). This epidemic results in diabetes market forecasts highlighting the necessity and viability of research projects aiming at developing cutting-edge technologies to **improve diabetes management** and reduce the psychological, economic and social burdens associated with the disease.

1.3. Current and future therapies for type 1 diabetes

This section details the **therapeutic interventions** currently available to prevent, treat or cure diabetes, and the most promising research in the domain: interventions aiming at **preventing diabetes** for people at risk, and interventions aiming at **treating or curing** for people with overt diabetes. After a brief history of the mainstay treatment, the insulin therapy, we will focus on the tremendous progress achieved throughout the last century, transforming a disease leading to a certain death within months into a treatable or even curable one. Finally, we will show how the development of mobile technologies aims at revolutionising diabetes treatment to improve quality of patient's life.

1.3.1. Preventive treatments

Early interventions to prevent diabetes aim at **hampering autoimmunity development** and consecutive β cell mass decline (see Pathogenesis of type 1 diabetes). In first-degree relatives of T1D patients which present high risk of developing the disease (tested positive for at least two pancreatic autoantibodies), such intervention often raises an ethical and clinical conflict - also referred to as treatment dilemma. A wide body of evidences supports early interventions to modulate the autoimmune response as the most effective means to prevent diabetes. However, the reliability of disease prediction methods increases as T1D onset approaches. The most effective interventions should therefore imply the treatment of individuals that might never develop symptoms. That dilemma raised the need for benign form of pre-onset therapy that has not been met yet [34]. As a result, immunomodulatory therapies are often implemented at disease onset to preserve the remaining insulin secretion and therefore struggle to cure diabetes in the strict sense. The Epidemiology of Diabetes Interventions and Complications (EDIC) Study enrolled the DCCT patient cohort (see section 1.2.2) to assess the influence of an average of 6.5 years of intensive diabetes therapy (achieved during the DCCT trial) on long-term disease-related complications. The patients were followed for an average of 17 years after DCCT ending. EDIC study demonstrated the importance of early diabetes treatment by highlighting a 57% decrease in the risk of major cardiovascular events in the population treated with intensive insulin therapy more than a decade before the beginning of the EDIC trial. Consistent results were still observable after adjustment for EDIC HbA1c level differences between compared populations. The DCCT/EDIC Research Group therefore concluded that the reduction in cardiovascular disease risk in treatment population could be attributed to the 6.5 years of intensive insulin therapy, and associated low HbA1c levels, achieved during the DCCT trial [26]. The underlying physiological mechanism leading to this decreased cardiovascular risk was named “metabolic memory”. This mechanism is not completely understood yet. Still, a growing body of experimental evidences supports the early adoption of an aggressive treatment to reduce hyperglycaemia in T1D as soon as possible [35].

1.3.2. Cures for type 1 diabetes

No efficient and widely accessible cure is available yet. Due to the above mentioned “treatment dilemma”, immunomodulatory therapies cannot be considered as a universal intervention. The use of **allogeneic**¹⁸ **transplantation** techniques successfully led few patients to a sustained insulin independence [36], [37]. Simultaneous transplantation of pancreas and kidney from cadaveric donors has greatly evolved and is now considered as a standard-of-care treatment for T1D patients presenting an end-stage renal failure [19]. Performed in experienced centres, such intervention can offer to the patient up to 80% chance of insulin independence over 5 years. This therapeutic option however suffers from major limitations: a substantial surgical risk remains, donors are lacking and an immunosuppressive treatment is required to avoid both graft rejection and recurrent autoimmune islet destruction [34].

For the last two decades, **islet transplantation** has developed as an alternative to pancreas-kidney transplantations. The landmark TRIMECO study [38], demonstrated, in a multicentre randomised controlled clinical trial, the superiority of islet transplantation over intensive insulin therapy in reducing the hypoglycaemic risk of patients presenting severe hypoglycaemia, hypoglycaemia unawareness, or kidney grafts with poor glycaemic control. However, notwithstanding the reduced surgical risk, the need for continuous immunosuppressive treatment and the lack of organ donors still constitute major limitations to the wide spreading of such therapy. Recently, a promising approach, residing in the **differentiation of stem cells** (either embryonic or pluripotent induced stem cells) into insulin-producing β cells, has been investigated to address the donor shortage. Mass-produced, these cells could make transplantation therapies accessible to a larger population of T1D patients but mass production and potential clinical application is still in its infancy.

1.3.3. Insulin therapy as the mainstay of treatment

Immunomodulatory and cell transplantation therapies appear as the most promising research approaches to prevent and cure diabetes. However, at this time, they still suffer from the major limitations depicted in last subsections. On the other hand, the DCCT and the subsequent EDIC study demonstrated that intensive delivery of exogenous insulin enables satisfactory improvements in T1D patients’ HbA1c level leading to a beneficial effect on long-term health outcome. Benefiting from an easier implementation, **insulin therapy** therefore remains the mainstay of T1D treatment.

A brief history of insulin therapy

The successful and repeatable extraction of insulin is attributed to Frederick Banting and his assistant Charles Best in 1921. They developed a new method to isolate insulin from a dog’s pancreas. Insulin discovery and its use as a treatment for diabetes was developed under the supervision of John Macleod and in collaboration with James Collip who developed a process to purify insulin extracts, making them suitable for clinical use. The first patient treated with insulin is Leonard Thompson a 14-year-old boy dying from diabetes. In January 1922, in the Toronto hospital, Thompson received an injection of insulin which resulted in a rapid reduction

¹⁸ **Allogeneic**: relating to or denoting tissues or cells which are genetically dissimilar and hence immunologically incompatible, although from individuals of the same species. (Oxford Languages)

of its blood glucose level. The treatment was confirmed on six more patients and published over the next months. For this major advancement in diabetes treatment and the associated discovery of insulin, Banting and Macleod received the Nobel Prize in Physiology or Medicine in 1923 and decided to share it with Best and Collip.



Figure 7: Frederick Banting (right) and Charles Best (left) in 1924

During the next decades, large-scale production developed using bovine and porcine extracts [39]. These animal-sourced preparations, containing insulin molecularly very similar to human insulin, conserved their full biological properties once administered to diabetic patients. Side effects, such as allergic reactions, were still associated with these insulin preparations but a solution emerged in 1978 with the production of the first human insulin in modified *E. Coli* bacteria. With the refinement of insulin production processes and the use of modern technologies such as genetic recombination, the purity of insulin solutions dramatically increased and material supply is not a problem anymore. Manufacturers also developed slow-acting insulins which, combined with regular insulin, enable a more accurate insulin therapy. Lately, research has focused on the development of a variety of insulin analogues presenting characteristics which allow healthcare providers to finely adapt insulin treatment to patient individual needs.

Insulin analogues development

Progress in biotechnological processes for generating insulin, and a better understanding of insulin chemical and physical properties, enabled the development of molecules similar to insulin but presenting genetic alterations resulting in different pharmacokinetics and pharmacodynamics [9]. The latter differences are used to classify these **analogues of insulin**. In particular, the following properties are used to differentiate the soluble formulations available on the market:

- **Onset:** time before injected insulin starts to act,
- **Peak action time:** time to maximum effect,
- **Duration of action,**
- **Concentration:** the concentration of insulin in soluble formulations can vary from one country to another,
- **Route of delivery:** mostly subcutaneous and intravenous routes but aerosolized formulations such as insulin Afrezza do exist.

The insulin analogues available on the market provide a variety of tools that diabetic patients can use to finely tune their insulin therapy. **Rapid acting insulin** analogues are particularly useful to reduce **postprandial hyperglycaemia** while the injection of **long acting insulin** analogues is a precious therapeutic tool to limit the number of daily injections and to **control glycaemia overnight**.

Rapid-acting insulin is the only insulin analogue used in modern insulin pump, it is therefore the only insulin modelled in the **insulin pump models** used in this work. As a consequence, the possibilities offered by all the insulin analogues available on the market are not fully exploited in the T1DM Simulator. However, **insulin onset, peak and duration of action** are discussed in this manuscript as they are pivotal concepts to understand glycaemia variations in response to meal perturbations in insulin-treated patients. They depend on numerous factors such as dose, injection site, injection route, presence of insulin autoantibodies, and physical activity [9]. These concepts and other patient characteristics (e.g. insulin sensitivity, insulin clearance by liver, insulin clearance by kidney) are also fundamental elements that explain the **inter- and intra-subject differences** in insulin therapy outcomes described in Chapters 3 (intravenous injection route) and 4 (subcutaneous injection route).

Restoring a healthy endogenous insulin secretion profile

In the healthy individual, normal **insulin secretion** profile is constituted by the alternation of **stimulated secretion phases** consecutive to meals and **secretion plateaux** at a basal secretion rate. Stimulated secretion typically results in plasmatic insulin peaks reaching 50-80 $\mu\text{U/mL}$, whereas basal plasmatic insulin is comprised between 5 and 15 $\mu\text{U/mL}$ [40]. In the T1D patient treated with insulin therapy, the objective is to restore this healthy insulin secretion profile via multiple injections of exogenous insulin. This technique – referred to as **Multiple Daily Injection (MDI)** – requires the patients to assess the carbohydrates content of their meals and inject an insulin dose in consequence. Measurement of the prevailing blood glucose level are also used to fine-tune insulin dosing with an individualised correction factor. Relying on repeated capillary glucose testing, optimal blood glucose control with MDI is complicated to achieve and can be very challenging or impossible for patients. The development of rapid-acting insulin reduced insulin onset and enabled bolus injection at the start or right after a meal. To achieve optimal blood glucose control, healthcare providers work with each patient to individualise the basal insulin level and an insulin-to-carbohydrates ratio (also referred to as Carbohydrates Ratio or CR) used to compute **meal boluses** from carbohydrates counting¹⁹.

Traditionally, **Self-Monitoring of Blood Glucose (SMBG)** was achieved by depositing a finger-prick drop of blood on glucose oxidase test strips and insulin was injected with syringes. Over time, many medical devices were developed to alleviate the psychosocial burden associated with regular blood glucose testing and insulin injection. Test strips are now used in conjunction with **electronic blood glucose meters** to improve both accuracy and readability of SMBG. These devices have data storing and data sharing functions to help both patients and clinicians in analysing trends in time to improve blood glucose control. Insulin syringes were replaced by insulin pens which reduce pain and waste (for the models equipped with replaceable cartridges). Insulin pens are often favoured to syringes as they are less time consuming, easy to use and discrete which is particularly important for visually impaired patients and children respectively.

In the 1970s, the discovery that **interstitial glucose** could be used as a proxy for estimating blood glucose variations with a sufficiently short time lag to comply with diabetes clinical

¹⁹ Insulin bolus (in insulin units) = insulin-to-carbohydrates ratio \times amount of carbohydrates (in grams)

constraints raised the hope to achieve a more physiologic insulin delivery [41]. During the next two decades, the growth of **mobile health**²⁰ has continuously provided new tools to achieve this goal. By revolutionising diabetes management, mobile health aims at improving both clinical outcome of the disease and quality of patient's life [42]. The first device that could be associated with mobile health, the insulin pump, was invented in the late 1970s. Since then, the pumps were refined to take the form of compact wearable devices which are remotely programmable with a smartphone. With insulin pumps, the development of a **bio-mechanical pancreas** appeared as a potential cure for T1D. This approach truly became realistic in the mid-2000s with the advent of **real-time Continuous Glucose Monitoring (CGM)** systems to provide inputs to a feedback control loop for insulin pumps [43]. The joint use of a CGM sensor and an insulin pump to improve glycaemic control of T1D patients is now referred to as **Sensor-Augmented Pump (SAP)** therapy.

Other aspects of diabetes treatment

At times, other diabetes medications are prescribed to patients as a complement to the main treatment with insulin. Pramlintide, an amylin²¹ analogue, is the only one to be approved for improved blood glucose control with T1D. Several T2D medications such as metformin are reportedly used off-label but, contrary to T2D, the use of other medications than insulin remains marginal and only concerns 5.4% of patients affected by T1D [44]. T1D being a chronic metabolic disease, several lifestyle modifications, such as personalized diet plan, can also be implemented to improve both blood glucose control and long-term outcomes of the disease. Regular practice of physical exercise is also recommended with the major benefits being a reduction of the long-term cardiovascular disease risk and an increase in insulin sensitivity (in addition to the usual benefits of physical exercise).

The successful management of all T1D treatment compartments (diet, exercise, medications, and insulin doses) can be very challenging and requires the patient to have high levels of health literacy²² and numeracy²³. As a consequence, another essential aspect of diabetes treatment for healthcare providers is **educating patients** to help them self-manage their diabetes. Education can range from better understanding the numerous factors influencing blood glucose response to meal stimulations, to an introduction to the numerous personalisation possibilities offered by modern medical devices and applications.

The development of mobile health also permitted the advent of some valuable **decision support tools**. Indeed, many applications (either third-party applications running on a smartphone or applications provided by medical device manufacturers) were developed to

²⁰ Mobile health: delivery of health services and improvement of health outcomes via mobile and wireless devices. Mobile health interventions often employ modalities such as short message service (SMS) text messaging, smartphone applications and wearable technology.

²¹ Amylin: a peptide hormone co-secreted with insulin by pancreatic β cells which inhibits glucagon secretion, delays gastric emptying and promotes satiety.

²² Health literacy: the degree to which an individual has the capacity to obtain, communicate, process, and understand basic health information and services to make appropriate health decisions. (US Patient Protection and Affordable Care Act definition).

²³ Health numeracy: the degree to which individuals have the capacity to access, process, interpret, communicate, and act on numerical, quantitative, graphical, biostatistical, and probabilistic health information needed to make effective health decisions. [137]

reduce the burden associated with the multiple aspects of disease management. Individualisation of insulin boluses to reduce postprandial hyperglycaemia amplitude is now facilitated by **bolus calculators** and frequent remote exchanges with physician. Improved CGM **dataset visualisation** helps the patient in better understanding his or her own glycaemic response to meals and prevent harmful glycaemic events. Keeping a digital daily diary allows patients to keep track of physical exercise sessions or meal contents, and facilitate diet follow-up and personalisation. Daily diaries and CGM datasets are also powerful tools for the subsequent analysis of **adverse glycaemic events genesis**.

Finally, the **benefits of SAP therapy over MDI therapy** on various health outcomes were outlined in several large studies. In particular, Bergenstal et al. published, in 2010, the results of a multicentre, randomized clinical trial comparing SAP therapy to MDI therapy in 485 patients (329 adults and 156 children) with suboptimal glucose control. After 1 year, patients in the pump-therapy group presented a significantly higher decrease of HbA1c level (-0.2% vs -0.8%) with a greater proportion of patients reaching the target (<7%) [45]. Since then, SAP therapy became the **standard of care** in developed countries and is often used as the control therapy in studies aiming at assessing the clinical benefits of the Artificial Pancreas. The latter, by introducing decision-making algorithms between the sensor and the pump to reduce the number of necessary patient interventions, aims at improving both health outcomes and quality of life of patients under SAP therapy.

1.4. The Artificial Pancreas

This section provides an overview on the different ways of implementing an Artificial Pancreas (AP) so that the reader can better perceive the building blocks necessary to validate **AP systems *in silico***. Questions that can be addressed using simulation will be highlighted, and the benefits and limitations of the AP use to treat T1D will be discussed. The section will also provide an overview of the AP systems available on the market or at a research stage, in order to compare our device and identify its added-value.

In 2006, the Juvenile Diabetes Research Foundation (JDRF) launched a project to develop a commercially-viable bio-mechanical pancreas via the sponsoring of several research centres in the USA and Europe. This project is named the **Artificial Pancreas Project**. A strategic funding plan was defined with priorities for research associated with each product development stage. This 6-step plan (see **Figure 10**) describes incremental advances to develop increasingly automated devices. Numerous approaches have been investigated to develop an AP with notably different degree of automation, different degree of integration and various additional features to facilitate T1D patients' life. Yet, an AP can always be formally described by three blocks: a **sensor** to estimate the patient metabolic status, an **insulin pump** to infuse exogenous insulin, and a **control algorithm** (i.e., a controller) for the necessary decision-making in between.

1.4.1. Sensor

To this day, the vast majority of sensors used in AP systems are **glucose-only sensors**. Different measurement principles have been investigated but only few of them were developed in commercially-viable products [46]. Among them, the **catalysis of glucose reduction** to

produce a glucose concentration-dependent electrical signal is the most commonly used glucose measurement principle. Taking advantage of the fact that capillary glucose equilibrates in the interstitial fluid [47], the sensors' core element is a flexible electrode plated with glucose oxydase and inserted just beneath the skin. The subcutaneous glucose concentration is converted into an electrical signal measured by a small external electronic device connected to the electrode and attached to the skin. In latest sensors, subcutaneous glucose is measured with a sampling time ranging from 3 to 5 minutes.

In 2014, Abbott launched the Freestyle Libre sensor which embeds a memory to store up to 8 hours of glucose readings. To access the data, the patient simply has to “flash” the sensor with a proprietary reader or with an NFC-enabled device (smartphone or tablet). As a lightweight, factory-calibrated and fairly accurate glucose sensing device guaranteeing a 2-week life span, it was found to be very useful to MDI users by replacing the regular finger-stick testing. However, due to the lack of continuous data stream, **Flash Glucose Monitoring (FGM)** – also referred to as intermittent CGM – is not suitable for SAP therapy and AP systems. It was also demonstrated that FGM is inferior to CGM when it comes to improve diabetic patients blood glucose control [48]. As a consequence, we will now focus on “true” CGM sensors.

Contrary to the Freestyle Libre, the other CGM sensors rely on **external devices to store** glucose data. Using a wireless connection, CGM readings are transmitted to a reader provided by the sensor manufacturer or a smartphone (see **Figure 8**). A special purpose application then allows enhanced data visualisation and the triggering of alarms when glycaemia reaches user-configured limits. CGM readings can also be transferred to a compatible insulin pump to implement **SAP (Sensor-Augmented Pump)** therapy. CGM sensors have provided a major advance in assessing glucose variability at resolutions unattainable through traditional Self Monitoring of Blood Glucose (SMBG) or HbA1c measurement, thus enabling intensive glycaemic control [49]. **CGM is now recommended** to improve glucose control for patients using both MDI and Continuous Insulin Infusion (CSII) as its use demonstrated a positive impact on HbA1c and mean glucose [50]. While latest sensors do not require regular calibration anymore, improvements still have to be achieved to improve sensors' life expectancy and accuracy while reducing sensor lag and susceptibility to pharmacologic interferences.



Figure 8: The Guardian Connect CGM system (Medtronic): a wireless transmitter paired with a dedicated mobile application.

1.4.2. Insulin Pump

Over the last forty years, **insulin pumps** greatly evolved, becoming more accurate and reliable. The use of lighter material, together with increasingly integrated electronics and miniaturized mechanical pumping systems, allowed for the development of very compact devices. Easy to wear and dissimulate, these small insulin pumps have encountered a better acceptance by patients. The availability of recombinant insulin analogues with improved

pharmacokinetics (reduced onset and peak action time) also contributed to a greater use of insulin pumps. As a matter of fact, a study analysing the large T1D Exchange clinic registry denoted a **foreseeable increase** in insulin pumps use from 2010-2012 to 2016-2018 (increase from 57% to 63%, respectively) [51].

Nowadays, insulin pumps are small programmable electronic devices (see **Figure 9**) that provide the patient with a **Continuous Subcutaneous Insulin Infusion (CSII)**. The insulin pump is powered by a rechargeable battery and insulin is stored in a refillable cartridge. Traditionally, insulin was infused via a catheter connected to a cannula but now tubeless pumps using soft cannula placed just beneath the pump case are available, making the device even more compact and discreet. In practice, continuous infusion is achieved by the delivery of tiny boluses of rapid-acting insulin with a steady time interval ranging from 1 to 5 minutes between insulin pump



Figure 9: Tandem t:slim X2 insulin pump

boluses (this time interval varies from one manufacturer to the other). In so doing, insulin pumps provide the patients with a user-friendly and very convenient means to adapt their basal insulin infusion level throughout the day and in every situation (e.g., physical exercise, inactivity, and sick days). They also allow the patient to administer premeal or correction boluses to cover meal-related carbohydrates intake or correct above-target glycaemia levels. Pumps sometimes propose advanced features such as a built-in bolus calculator or automated bolus correction based on previously injected insulin. Patient have to adequately set a CR (Carbohydrates Ratio)²⁴, a Correction Factor (CF)²⁵, and provide an estimation of the amount of carbohydrates ingested during the meal. The bolus calculator then computes a recommended bolus which is sometimes corrected by taking into account previously administered boluses and prevailing glucose level in order to minimize the risk of iatrogenic²⁶ hypoglycaemia. Rules of thumb do exist to initialize CR and CF parameters in pump settings; however, optimal blood glucose control often requires the patient to **fine-tune these parameters** and configure a daily variation profile for each of them (e.g., to account for the circadian variation of patient sensitivity to insulin).

Currently available commercial devices only automate insulin delivery. However, many multi-hormone infusion pumps have been investigated. Infusion of exogenous glucagon appears as the best candidate to help the patients to avoid and recover from severe hypoglycaemic events. Pramlintide, an analogue of amylin (the hormone co-secreted with insulin in the healthy pancreas), is for example also studied as a potential candidate for dual-hormone systems since early results demonstrated a positive impact on postprandial glucose excursion. To this day, these alternative approaches still face practical and physiologic challenges such as solubilisation and stabilisation of glucagon at ambient temperature, and their benefit. still needs to be confirmed by extensive studies [43].

²⁴ **CR**: the insulin to carbohydrate ratio is defined as the amount of carbohydrate (in grams) covered by each unit of (100 IU strength) insulin.

²⁵ **CF**: the insulin sensitivity factor is defined as the drop-in blood glucose level caused by each unit of insulin taken.

²⁶ **Iatrogenic**: relating to illness caused by medical examination or treatment.

Many studies and meta-analyses demonstrated the benefits of CSII over MDI [52], [53]. However, CSII still suffers some limitations. In particular, the delay resulting from the insulin diffusion in the subcutaneous space greatly alters CSII performance, and many research projects aim at addressing this issue by developing **implantable systems** that deliver insulin directly in the intraperitoneal space. Although more invasive, such systems could also improve patient acceptance by removing external signs of T1D treatment. Nonetheless, major challenges still need to be overcome to power these devices and supply them with insulin. In any case, insulin pumps remain expensive and require from the patient a high level of health numeracy and literacy. Education is part of the solution but represents an additional cost for healthcare systems which, associated with insulin pump cost, explain why CSII spreading is confined to the more developed countries. Although the pain associated with MDI is removed by using insulin pumps, many patient interventions are still necessary (fine-tuning of pump settings, carbohydrates counting). Still, the AP represents a promising approach to close the loop between glucose sensors and insulin pumps while strongly limiting the need for patient interventions thanks to increasingly automated systems.

1.4.3. Closing the loop

Traditional diabetes treatment approaches such as MDI or their modern counterparts based on CGM or CSII are referred to as **open-loop therapies**. That term signifies that a **patient intervention** is required to close the loop between blood glucose measurement (or estimation with a CGM sensor) and the subsequent delivery of exogenous insulin. Fear of hypoglycaemia is a known phenomenon which leads the patient to underestimate the amount of insulin that should be administered for optimal blood glucose control. Misestimation of meal carbohydrates content is another source of errors that greatly affect insulin therapy performance. To reduce the risk of iatrogenic hypoglycaemia resulting from patient's errors and improve their quality of life, several partly automated systems were developed in line with the Artificial Pancreas Project (APP) development pathway (**Figure 10**). These systems are referred to as **hybrid closed-loop systems**.

According to the APP 6-step development plan (see **Figure 10**), the first hybrid closed-loop systems that have been developed were able to suspend basal insulin delivery based on CGM information (Step 1). This functionality is referred to as **Low Glucose Suspend (LGS)**. In some systems, this feature is enhanced by mathematical models of glucose dynamics, which allow for insulin infusion adaptation based on prediction, and named **Predictive LGS (PLGS)**. Features that take into account previously injected insulin and prevailing glucose level to automatically correct insulin boluses were then implemented to reduce hypoglycaemic risk (Step 2). When the blood glucose level measured between two meals is above target, some systems trigger an **alarm** to recommend the injection of a correction bolus in order to reduce **hyperglycaemic risk** (Step 3). Finally, **hybrid closed-loop** systems that **continuously adapt basal rate**, without any patient intervention, have recently been approved by the US Food and Drug Administration (FDA): the Medtronic MiniMed 670G and the Tandem t:slim X2 with Control IQ (Step 4). The ultimate goal is to develop **fully automated systems** which do not rely on patient input to handle meal-related carbohydrates intake. Although there is currently no such system on the market, many AP are under development. The main challenge is the development of a sophisticated control algorithm which closes the loop by

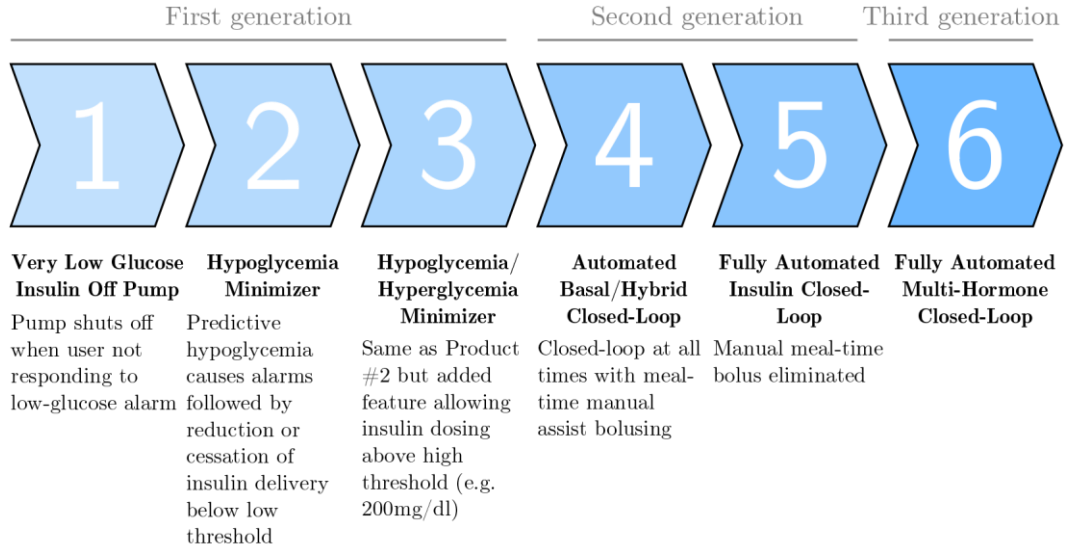


Figure 10: 6-step development plan of the Artificial Pancreas Project

computing a command signal, for an insulin pump (Step 5) or for a multi-hormone pump (Step 6), based on blood glucose estimation provided by a CGM sensor.

1.4.4. Control algorithms

With the intensification of research on this topic over the last decade, many **control algorithms** were proposed for the AP. Among them, the most popular are the Proportional-Integral-Derivative (PID) algorithm and the Model-Predictive-Control (MPC) algorithm. Other strategies involving robust H_∞ methods or fuzzy logic are also investigated but remain less frequent. PID appears as a straightforward strategy and was used in the first generation of AP systems. MPC are more complex algorithms that require the definition of a dynamic model of glucose-insulin interactions. MPC has long been seen as more powerful than PID [54]. However, it is worth noting that both PID and MPC are generic labels that cover a variety of practical implementations. In [55], B. Wayne Bequette details how MPC controllers can achieve the same level of robustness as PID controllers, while PID can achieve top of the art performance when appropriately tuned and in association with advanced features (anti-reset windup, derivative filter, and insulin feedback to name a few). Indeed, Medtronic is using a PID controller with model-based insulin-feedback (PID-IFB) in its hybrid closed-loop system MiniMed 670G. The latter system aims at improving controller performance by considering the already administered insulin. In so doing, the delayed action of exogenous insulin is taken into account, which mitigates the risk of reactive hypoglycaemia (postprandial hypoglycaemia due to overly aggressive insulin infusion). For their part, MPC algorithms are often favoured for their great versatility and their ability to conveniently manage multivariable systems [55]. Recently, various adaptive MPC strategy have also been proposed [56]. These strategies interestingly take into account intra- and inter-day variability of patient characteristics (e.g., insulin sensitivity) as in Toffanin et al. [57].

1.4.5. Benefits and limitations

During the last decade, numerous inpatient and controlled outpatient studies have been published demonstrating the **safety and efficacy of AP systems** [58]. In 2018 a meta-

analysis highlighted that the benefits are particularly visible in term of time spent in the different glycaemic ranges [59]. This analysis of 40 studies (1027 participants) aimed at comparing insulin-only AP systems (35) and dual-hormone AP systems (9) to the current standard of care (SAP therapy). It reported an average hyperglycaemia reduction of almost 10% with AP systems, hypoglycaemia being meanwhile reduced by 1.5%. HbA1c level was not significantly reduced (-0.26%) due to consistent reduction of hypoglycaemia. Of course, reduction of the hypoglycaemic risk is beneficial to T1D patients but current technology does not allow for a concomitant normalisation of HbA1c level [60]. It is also worth noting that this meta-analysis highlights the greater benefits of overnight AP use compared with daytime.

Apart from biomedical outcomes, the growing use of technology in diabetes management also raises questions concerning the **psychosocial impact** of AP systems on T1D patients. Assess and understand these aspects of disease management is of prime importance to promote a sustained and effective technology use. In 2018, a review focusing on this topic outlined that “reported benefits extended beyond improved glycaemic control and reduced fear of hypoglycaemia to include reassurance for users and family members (e.g. partners and parents), reduced anxiety, improved sleep, confidence, ‘time off’ from diabetes demands, greater freedom to engage in activity, excitement and empowerment” [61]. It also noted that using AP systems for longer periods is associated with increased satisfaction.

Frequently reported psychosocial burdens are also described in Farrington et al. [61], with the most cited burdens being “**technical difficulties**, alarm intrusiveness and interrupted sleep, increased time spent thinking about diabetes, size and appearance of the equipment, limitations on exercise, and perceptions of deskilling and data obsession”. Together with high cost, these burdens constitute major barriers to the wide adoption of AP systems by patients and to the reimbursement by healthcare systems. They are notably responsible for the large **drop-out rate** reported after 12 month of Medtronic Minimed 670G use [62]. In addition, although the AP removes some limitations associated with the use of CGM and CSII technologies such as the need for numerous patient interventions (CGM trend analysis, configuration of insulin infusion), it still suffers from the remaining limitations of each of its constituents. Indeed, control algorithms are particularly convenient to adapt insulin treatment to individual specificities but are still constrained by the imperfections of closed-loop system components (e.g., glucose sensing inaccuracies, pump delivery errors) [63].

Full automation cannot yet be achieved in unsupervised home settings yet due to remaining barriers such as the slow pharmacokinetics of subcutaneous insulin and sensor lag. Daily variations of blood glucose mostly result from an increased glucose intake (meals), a decrease in glucose consumption (sleep) and an increase in glucose consumption (stress, physical activity). Sleep and stress are well managed by current hybrid closed-loop systems by continuously adapting basal insulin infusion. However, the management of **meals and physical activity remains highly challenging** for these systems and requires the patient to provide information to the control algorithm. The incorporation of **inputs beyond glucose concentration** to provide information about nutrition, physical activity, and stress level of the patient, and the concomitant development of **multi-hormone** pumps could therefore provide the missing piece of the puzzle and enable the restoration of physiological glucose homeostasis with a fully automated biomechanical AP.

1.5. An islet-based biosensor for the Artificial Pancreas

In section 1.4, we outlined the prime importance **of the sensor and the control algorithms** to achieve optimal glucose control with an AP. Particularly, we argued that, in the absence of information other than patient’s subcutaneous glucose level, dealing with large disturbances remains an unattainable objective. To lighten the burden of the numerous patient interventions still necessary to achieve optimal glucose control with current AP systems, **new sensors** should be developed that provide the control algorithm with additional information about the patient’s physiological state. Sensors monitoring the heart rate and integrating accelerometers are notably being considered to control glucose level during physical exercise. However, their cointegration with traditional enzymatic glucose sensors in a compact wearable device remains a challenge.

This thesis work is part of a broader project whose objective is to develop an **innovative sensor** - a cell-based biosensor – able to provide the AP algorithm with all the information necessary to **regulate** exogenous insulin infusion in a **physiological manner**. In the healthy individual, the sensor, control algorithm and actuator involved in the closed-loop regulation of insulin secretion are gathered in the same anatomical structure: the **pancreatic islet of Langerhans**. The secretion is **qualitatively adapted** to the prevailing metabolic status of the patient by the coordinated action of β cells in the islets, while the **quantitative adaptation** to patient needs is achieved through the replication of this islet structure in the pancreas. The core idea of our biosensor is to use the **sensing ability of the β cell**, via extracellular monitoring of islets’ electrical activity, and use it to compute the **control signal** of an insulin pump. The β cell being sensitive to **all the modulators of insulin secretion**, this sensing paradigm could provide the information missing to AP control algorithms to deal with large disturbances (e.g., meals, physical activity). This consideration has already led other research teams to develop healthy islets transplantation techniques or, more creatively, to develop highly engineered membranes to encapsulate healthy cells, thus, providing them with all the necessary nutrients while protecting them from the destructive immune response [60], [64]. However, these approaches are limited by their biological actuator (the component which secretes insulin) and its constrained sourcing (human donors, see section 1.3). Our strategy is to take the best of the two traditional approaches: automated insulin delivery devices and cell therapy [60]. Indeed, we designed a biosensor which takes advantage of the sensing ability of the islets of Langerhans and could, in an AP system, benefits from the virtually unlimited insulin infusion capabilities of artificial insulin pumps and the advanced features of modern control algorithms. By providing a means to access the pancreatic islets’ endogenous algorithm and exploit them in a closed-loop system, we propose here a new biosensing paradigm in the context of AP.

In this section, we will first describe the electrophysiology of the β cell and the islets of Langerhans and relate it to our islet-based biosensor principle and design. Thereafter, we will explain how such a sensor can pursue the medical devices validation process in the context of the AP and we will show how the simulation of AP systems supports that process. In the end, this section will lead us to formulate the **scientific question** that this thesis work addresses.

1.5.1. Electrophysiology of the endocrine pancreas

Electrophysiology is the branch of physiology concerned with the electrical activity of bodily processes. Its extended scope spans from the electrical monitoring of unicellular activity to the characterization of larger anatomical structures like the heart or neural networks. It involves the measurement of voltages and currents but, contrary to electronics where electrical charges are carried by freely moving electrons, electrophysiology is dealing with **ionic**. In body cells, a lipid bilayer - the cell membrane - isolates the intra- and extracellular medium which thus present different ionic composition and distribution. The cell membrane is scattered with many transmembrane proteins which allow specific molecules and ions to cross the membrane or act as receptors which, when bound to the adequate extracellular molecule, induce changes in cell activity. Both actions aim at stimulating or inhibiting cell processes (e.g., secretion, energy supply). The ion channels are transmembrane proteins which enable the passive diffusion of ions through the membrane, thus creating ionic currents. The two main functions of these currents are to change the **membrane potential**²⁷ (e.g., neural communication) and to transiently increase the intracellular concentration of a particular ion to trigger **ion concentration-dependent cell events** (e.g., secretion, contraction) [65]. While some ion channels are opened or closed in response to cell events, others are permanently open and therefore act as ion pump. The unbalanced exchange of electrical charges through these ion pumps explains the baseline difference in electric potential across the plasma membrane. Ranging between -60 and -80 mV, this difference is named the resting membrane potential.

Similarly to neurons, **pancreatic β cells are excitable cells**. In particular, they have a measurable electrical activity in response to variations of glucose concentration in their vicinity. Glucose is transported through the membrane by the GLUcose Transporters (GLUT 1-4 – a group of transmembrane proteins) and metabolized by mitochondria which results in a neat increase of high-energy Adenosine TriPhosphate (ATP). The resulting rise of the ATP/ADP ratio causes the closing of ATP-dependent potassium (K^+) channels and the subsequent increase in intracellular K^+ ion concentration. It results in a depolarization of the membrane leading to the opening of voltage-dependent calcium (Ca^{2+}) channels which generates a positive ion influx thus hyperpolarizing the membrane. Meanwhile, Ca^{2+} ion concentration increases and triggers a Ca^{2+} ion concentration-dependent cell event named exocytosis. Exocytosis consists in the fusion of Insulin Secretory Granules (ISGs are vesicles containing insulin) with the cell membrane enabling the release of insulin outside the cell, i.e., the **secretion of insulin** (**Figure 11**) [66]. As with neurons, the depolarization/hyperpolarization of the pancreatic β cell membrane occurring during insulin secretion is called an **action potential**. Exocytosis and action potential generation are extremely fast processes that happen in few tens of milliseconds (about 90 ms for β -cell action potentials) and up to 12 times per second in secretory conditions [67]. The noteworthy element here is the central role played by these ionic and electrical events in **the stimulus-secretion coupling** of the β cells.

As described in section 1.1, insulin secretion is also modulated by **other regulatory mechanisms** to ensure nutrient homeostasis in a variety of physiological states. A number of

²⁷ The word potential refers here to the electric potential difference (as usually defined in electronics) between the intra- and extracellular medium (the extracellular potential being taken as the reference).

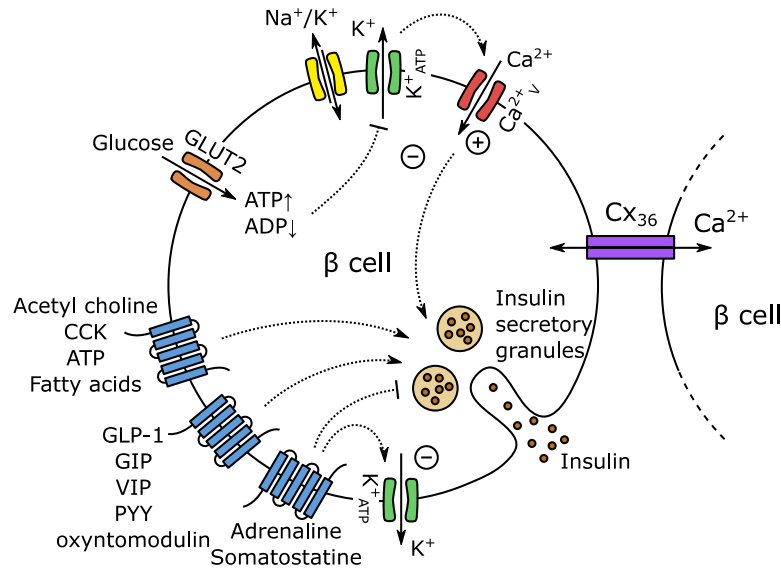


Figure 11: Electrophysiology of the β cell

molecules whose associated receptors are expressed on β cell membranes affects ion fluxes via different signaling pathways. As a consequence, their action on insulin secretion is also electrically measurable. In particular, GLP-1, GIP, CCK, peptide YY (PYY), and oxyntomodulin are potentiators of insulin secretion released from the gut in response to food intake, when adrenaline and somatostatin present an inhibitory action. Other potentiators of secretion include vasoactive intestinal peptide (VIP), fatty acids, and acetyl choline.

In addition to the above-mentioned unicellular mechanism, intercellular communication between juxtaposed β cells is responsible for a synchronized secretory activity [68]. This coordinated secretion is the result of Ca^{2+} ion exchanges between β cells via specific gap-junction proteins - named Connexin 36 (Cx_{36}) - and is lost in dissociated cells. It was demonstrated that this synchronicity also improves islet response towards a glucose stimulation (e.g., a meal) by suppressing insulin release at low glucose levels and by increasing it at high glucose levels.

To characterize membrane potential variations of a unique cell, invasive techniques, such as patch-clamp, are available and present an excellent signal-on-noise ratio. They however do not allow for long-term recording of islet activity as cells cannot survive long in these conditions. Recording the electrical activity of multiple cells over weeks therefore requires other techniques: by placing a conductive electrode beneath an islet (constituted of multiple interconnected β cells), it is possible to record the extracellular potential variations resulting from the complex summation of ionic fluxes generated by islet's cells in contact with the electrode at the cost of a reduced signal-on-noise ratio (compared to patch clamp). The coordinated **insulin secretion** is correlated with a coordinated electrical activity which takes the form of a **slow oscillation (<1 Hz) of the extracellular potential**. This phenomenon was first described in [69] and characterized by our partners from the CBMN laboratory [70]. It presents a shape and properties which are reportedly unique to pancreatic islets and will be, in the following, referred to as **Slow Potentials (SP)**.

1.5.2. The islet-based biosensor

A **biosensor** is commonly defined as an analytical device that converts a change in the immediate environment of the sensor into an electrical signal [71]. This conversion is usually obtained through the association of two elements: **a sensitive biological element** (biological material responsive to the analyte) and **a transducer** whose function is to transform the resulting signal into an electrical signal conducive for subsequent processing. At times, **processing electronics** is integrated to the device in order to condition the electrical signal and improve the sensor overall performance. Ideally, the estimation of the physical variable of interest, provided by the sensor, should also be independent from other environmental physical parameters (e.g. pH, temperature). At this point, it is worth noting that CGM sensors also satisfy this broad definition of a biosensor. Our sensor belongs to the subgroup of **cell-based biosensors** as its biological sensing element is a whole pancreatic islet. Even though cell-based biosensors have existed for years [72], and have found many applications in biomedicine [73], this one is the first of its kind as pancreatic islets have never been utilized to sense insulin demand in the past.

The **hybrid bio-electronic sensor** (see **Figure 12**) studied in this thesis work is the result of a decade of research by our research group and its partners. This patented technology [74] benefits from the natural sensing features of islets: it uses a Micro-Electrode Array (MEA) as a transducer to measure, on multiple recording sites, the extracellular electrical activity of a few murine or human islets. This transducer is linked to an electronic acquisition board achieving the real-time processing of the measured signals [75], [76]. The electrical signals are conditioned by a first analogue stage for their subsequent analysis by a dedicated digital architecture. The biosensor is able to measure, with a high signal-on-noise ratio, the unicellular activity (i.e., action potentials or spikes) and the synchronised multicellular activity (SPs) of islet cells (**Figure 12B**). It also computes on line AP or SP characteristics of interest such as frequency or amplitude (**Figure 12C**). Thanks to the on

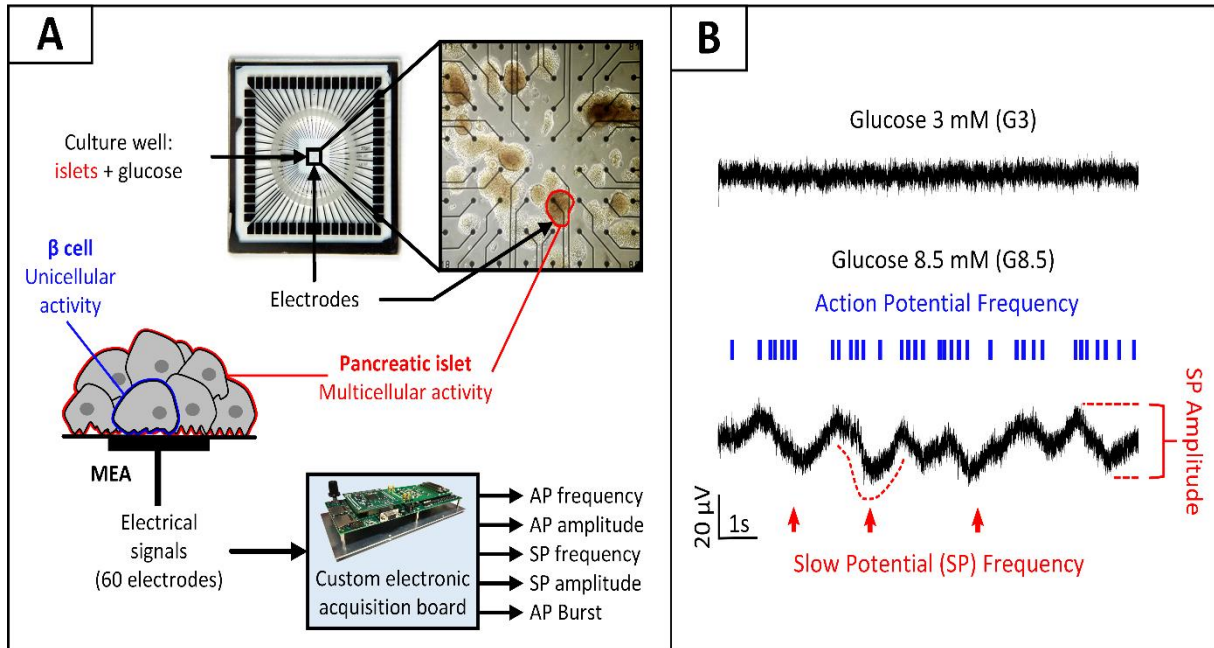


Figure 12: Biosensor description and working principle

-chip islets, the biosensor integrates the action of all the mediators of insulin secretion. As β cells, glucagon-secreting α cells generate APs. Drawing a distinction between APs originating from β cells and APs originating from α cells can therefore be very complicated when glucose concentration is moderate (i.e., both types of cell are stimulated). For this reason, and because they showed a good correlation with glucose concentration [70], **SPs are the preferred biosensor output signals** in the context of its inclusion in an Artificial Pancreas. This decision is reinforced by the fact that, as already mentioned, SPs appear as an image of the true physiological insulin secretion.

1.5.3. Towards a wearable medical device

A laboratory prototype of our biosensor is already in use and provides our partners a unique means to study the electrophysiology of pancreatic islets submitted to different stimulations (e.g., glucose, hormones) [70], [77]. Note that this prototype still relies on commercial solutions for some elements of the acquisition chain. Besides, this sensor module is currently used in a clinical study for *in vitro* quality control of human donor islets prior to transplantation [78]. Embedded in a **wearable device**, this technology would also constitute a valuable alternative to CGM sensors which currently limit the efficacy of commercially-available AP systems. This ongoing work necessitates the integration and packaging of the electronic acquisition chain together with a microfluidic setup containing the islets and an insulin pump in a compact housing. The device needs to be reliable enough to efficiently control the blood glucose of diabetic patients while ensuring their safety.

In the prospect of becoming a **medical device**, it needs to pass several validation stages to be endorsed by national regulatory authorities. The development and validation process, can be roughly described with four stages [79]. The first stage concerns the discovery and basic research work leading to the first proof of concept. During the second stage, the preclinical development, design specifications for fabrication, packaging and labelling are established. If applicable, efficacy is assessed with a preclinical trial using animals. The design of protocols for future research and clinical trials also takes place during this stage. The third stage aims at assessing the safety and efficacy of the proposed solution in a controlled environment, i.e. a clinical trial. This latter stage, when validated, leads to the market approval process (fourth stage). The current status of our research positions us in the second stage in that development path, i.e., the **preclinical validation**.

1.5.4. *In silico* preclinical validation

The ability of our biosensor to access the endogenous algorithms of pancreatic islets was demonstrated and published [70]. Preclinical validation of the technology is now necessary and requires the design of a new version of the acquisition board to incrementally converge to a compact wearable sensor. While the specifications of the final device are under study, the protocol for *in vivo* experiments has been submitted and accepted. This trial aims at assessing the ability of our sensor to regulate the blood glucose level of 10 T1D patients in a controlled clinical environment. A hybrid closed-loop will be studied with the healthcare staff controlling the command signal transmitted to the insulin pump by the controller algorithm. Due the

complexity of such trials for a very limited number of patients, we simultaneously investigate the *in silico* validation of our sensor.

Simulation of metabolic processes has a recognised clinical relevance in developing solutions for the treatment of diabetes [80]. Simulations offer the possibility to perform **extensive tests** with significant time- and cost- savings. Preclinical trials on animals are frequently replaced by or assisted with *in silico* trials to reduce the time and cost of the traditional medical device validation process (see **Figure 13**). In the context of diabetes, **models** have been developed, both for **T1D** and **T2D**, to study patient's response to treatment (e.g., drugs, insulin delivery systems) or long-term therapeutic outcomes and costs [80]. A variety of models have also been developed to be used in **AP controllers** [54]. A milestone in the development of this research area is the **approval by the US FDA** of the first *in silico* model, the **UVA/Padova T1DM Simulator (T1DMS)**, that can substitute for animal studies in the preclinical testing of diabetes treatment by means of artificial pancreas (AP) systems [81]. To this day, the T1DMS is the most complete solution to model the glucose-insulin dynamics in insulin-treated diabetic patients. It provides a high-fidelity metabolic model together with an AP testing environment with built-in CGM sensor and insulin pump models. Its **cohort of virtual T1D patients** comprises 11 adults, 11 adolescents and 11 children which can be submitted to a variety of glucose intake scenarios and metabolic tests. It was therefore chosen to develop a model of our islet-based biosensor and validate its closed-loop performance in an AP.

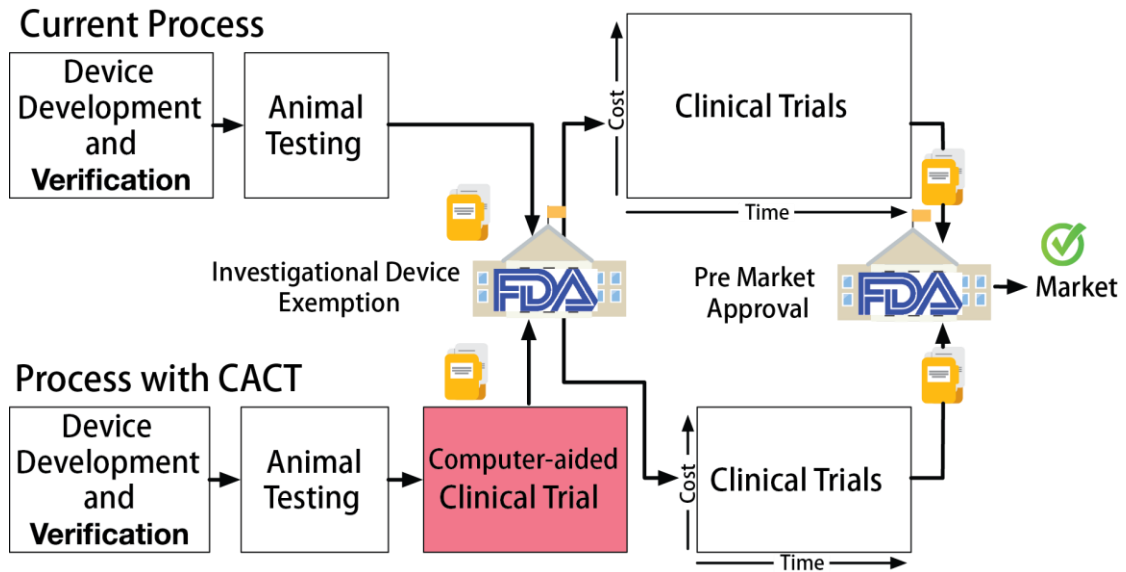


Figure 13 : Alternative medical device validation process using computer-aided simulation: the example of the validation of a new drug or implantable drug infusion pump in the US

1.5.5. Contribution of this thesis work

This thesis work is part of a broader set of research projects named DIABLO (grant agreement DIABLO DIABLO N°ANR-18-CE17-0005-01) and DIAGLYC (grant agreement DIAGLYC N°3538519), supported respectively by the ANR and by the FEDER/Région Nouvelle-Aquitaine. The research consortium is highly interdisciplinary:

- **The group of Prof. Sylvie RENAUD** (ELIBIO team - IMS Laboratory, UMR CNRS 5218) has an expertise in electronics engineering and is in charge of the biosensor device design, including the algorithms implementation on hardware.
- **The group of Prof. Jochen LANG** (CBMN Laboratory, UMR CNRS 5248) has expertise and set-ups for islets preparation, molecular cell biology, electrophysiology & microfluidics.
- **The group of Prof. David HENRY** (ARIA team – IMS Laboratory, UMR CNRS 5218) is specialized in control theory, fault diagnosis and fault tolerant theories to guarantee an operational autonomy of complex safety-critical systems. It is in charge of the control law design based on matured techniques in a complex environment.
- **Prof. B. CATARGI** is head of a Diabetes Unit in CHU-Bordeaux, and an internationally renowned specialist in diabetes treatment by insulin pumps and CGM. He is involved in fundamental research in the closed-loop field in diabetes.

With the DIABLO project, this consortium aims at developing an *in silico* AP model integrating our biosensor model and a novel *ad hoc* regulation controller robust to patients' variability: while current controllers only consider glucose for their input, our consortium designs a controller which benefits from the biosensor properties to also consider hormonal levels to regulate glycaemia. To validate the approach on humans, the controller predictions will be compared to standard CGM's first in the T1DMS testing environment. Second, as mentioned in 1.5.4, our entire setup will be tested directly in T1D patients equipped with an extracorporeal version of our biosensor (and a current commercial CGM and pump). Our objectives are:

- **Objective 1:** Assess the human *in silico* biosensor model in physiological conditions (glucose and hormones), using advanced multiparametric identification techniques,
- **Objective 2:** Enhance the reference whole human body single-input T1DMS by integrating the biosensor model from Obj. 1, and an innovative multi-parametric controller,
- **Objective 3:** Design and perform experiments to validate the biosensor and the controller via (i) an *in silico* clinical trial on the T1DMS and (ii) the previously mentioned *in vivo* and *extra corpore* clinical trial with diverse daily scenarios; compare to classical CGM and demonstrate the benefits of a novel 1) hybrid bio-electronic sensor paired with 2) an *ad hoc* robust controller.

The scientific question of this thesis work is to determine if simulation constitutes a valid support to validate the concept of using pancreatic islets algorithms via electrophysiological measurements in a biosensor. In a second time, the objective is to design an *in silico* clinical trial to assess the performance of a biosensor-based AP that regulates the blood glucose of virtual T1D patients, and compare it to standard treatment approaches.

Conclusion

In this first chapter, we have seen that the **glucose metabolism**, as part of the nutrient metabolism, is a vital **physiological process** which provides human beings with the necessary energy and natural compounds to enable growth and reproduction. The complex interplay of numerous physiological processes is required to cope with the molecular diversity and the intermittence of food intake, while withstanding demanding situations (e.g., intense physical exercise, starvation).

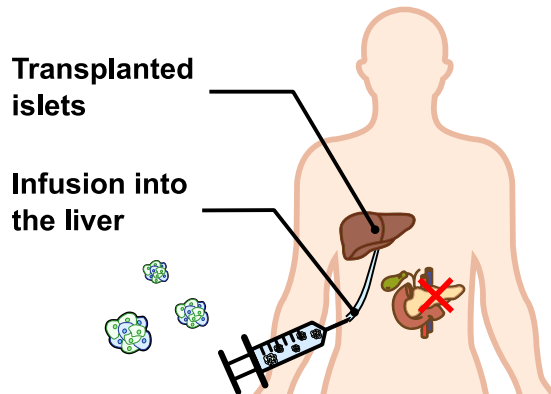
Type 1 diabetes is a severe autoimmune disease leading to death within months in the absence of treatment. The immune system targets the **pancreatic β cells**, causing a severe impairment of insulin regulation which culminates in the complete suppression of its secretion. The disease severity resides in the unique and predominant role insulin plays in the metabolism of nutrients. The main anabolic hormone being suppressed, the primary symptom of diabetes takes the form of chronic hyperglycaemia and needs to be treated to avoid the development of serious complications.

In 1921, the discovery and isolation of insulin by Banting and colleagues opened the door to the development of a treatment for type 1 diabetes. During the last century, insulin production processes were refined and the development of insulin analogues provided the patient with a means to restore physiological insulin profiles. Pivotal studies such as the DCCT/EDIC demonstrated the benefits of intensive **insulin delivery** to achieve a tight **glycaemic control** and improve long-term health outcome of type 1 diabetic patients. Towards the day-to-day burden associated with the challenging implementation of tight glycaemic control, mobile health aims at developing solutions to improve patients' quality of life. The development of continuous **glucose sensors** and **insulin pumps** have achieved a first step in that direction. One step further is the **Artificial Pancreas**, which combines these wearable devices with sophisticated algorithms in a closed-loop configuration and removes the need for patient interventions. Although promising, automated closed-loop systems still suffer from major limitations and struggle to manage meals and physical activity due to limited information on patient physiological status.

As outlined by Frederick Banting in its Nobel lecture: "insulin is not a cure for diabetes; it is a treatment", i.e., patients are not cured with insulin and need to bear a life-long dependency to exogenous insulin infusion. An alternative approach, based on cell therapy, therefore aims at curing diabetes with transplantation techniques. This approach greatly suffers from the lack of donors and the lifelong immunosuppressive treatment required to avoid graft rejection. In this context, closed-loop technologies still appear as viable alternatives to replace the endocrine pancreas and have a continuing innovation potential.

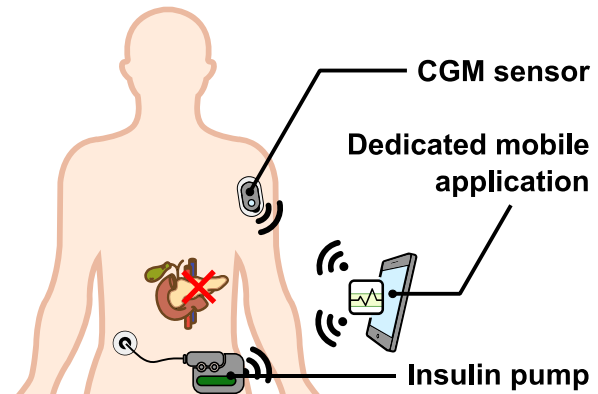
In the last decade, **computer-aided simulation** has emerged as a time- and cost-effective support to develop medical devices for the treatment of diabetes. As highlighted by concepts such as the glucose index and the glucose load, the molecular diversity of food intake and the complexity of the digestion process can be simplified and modelled as the rate of appearance of smaller molecules (e.g., glucose, fructose, fatty acids, and amino acids) in blood. In the context of diabetes, where glucose metabolism is primarily affected, carbohydrates intake can thus be reduced to the resulting **glucose rate** of appearance in blood, i.e. meals can be

Cell Therapy



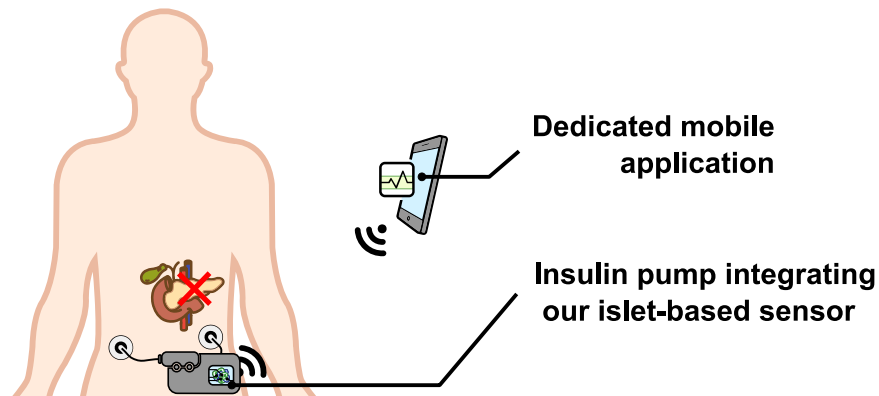
- 👍 restore glucose homeostasis
- 👎 chronic immunosuppression
- 👎 limited cell supply

Artificial Pancreas



- 👍 faster pace of development
- 👍 no need for other medication
- 👎 alarm fatigue
- 👎 psychosocial impact of wearing several devices

Islet-based Artificial Pancreas



- 👍 exquisite sensing capabilities of biological cells
- 👍 inner regulation capabilities of pancreatic islets
- 👍 unlimited insulin supply and power of modern algorithms
- 👎 psychosocial burden of wearing an electronic device
- 👎 high technological complexity

Figure 14: The Biomimetic Artificial Pancreas. This islet-based AP takes advantage of the exquisite sensing and blood glucose regulation capabilities of healthy pancreatic islets to ensure the closed-loop control an insulin pump in a physiological manner.

modelled as glucose intake. Nonetheless, **modelling the complex endocrine regulation** of glucose homeostasis and the interplay between all the involved organs, is mandatory to accurately represent the glucose-insulin dynamics in T1D patients.

By associating the natural sensing abilities of the islets of Langerhans, the advanced features of modern closed-loop algorithms and the virtually unlimited supply of insulin pumps, our project proposes a **new paradigm for the Artificial Pancreas** (see **Figure 14**). Using the high-fidelity UVA/Padova T1DMS testing environment and its virtual cohort, we aim at establish an *in silico* proof of concept for the use of our innovative biosensor in an AP system.

Chapter 2

Material and methods

To a certain extent, this manuscript is organised as a scientific paper. After an introductory chapter depicting the scientific context of this PhD work, the second chapter then presents the necessary material and the methods developed to achieve the results described and discussed in Chapters 3 and 4. Although the main material and methods are provided in the chapter, supplementary content is also available in the appendices and additional information is provided as the results are described. This structure was favoured to improve the readability of the manuscript.

The subject of this thesis covers numerous research areas. A first section further details the actual implementation of the biosensor. It describes the components of the current electrophysiological measurement setup as well as the next version (currently under development) designed to perform experiments using microfluidics. A second section describes the modelling approach that has been adopted to design the biosensor models. The *in vitro* experiments which provided the datasets necessary to identify these data-based models are then presented together with the identification methodology. A fourth section describes the UVA/Padova T1DM Simulator whose testing environment was used to assess the closed-loop performance of a biosensor-based AP system. Finally, a last section details the methodology we implemented to assess the performance of our BG regulation closed-loop systems.

The vocabulary and representations used in this chapter comes from the engineering community. Although the description of the islets as a “device”, i.e., the description of islet inputs processed by endogenous algorithms to provide outputs, might unsettle the reader with a background in biology, it has been voluntarily chosen to encourage the reader to consider the pancreatic islet as a sensor component. The objective is to underline that, unlike traditional CGM sensors, the biosensor is a multi-input sensor (sensitive to numerous molecules) even if its models are single-input (glucose-only models).

As stated in section 1.5.2, the association of a sensitive biological element and a transducer

[illegible]

(when compared to other techniques such as patch-clamp). It notably enables the recording of both unicellular and multicellular signals.

In vitro MEAs are usually composed of a substrate covered with multiple electrodes connected to contact pads via conducting metal lines. Electrodes and conducting lines are insulated in non-conductive material to limit crosstalk. As cells are directly cultured in a well on the MEA, all materials are carefully chosen to ensure biocompatibility. The materials typically used are transparent glass for the substrate (to allow microscope observation), silicon nitride (SiN) for the insulator and titanium (Ti) or indium tin oxide (ITO) for the conductor. Electrodes use diverse conductive materials depending on the application, including gold (Au), titanium nitride (TiN), platinum (Pt), stainless steel, aluminium (Al), and iridium oxide (IrOx) [83].

The biosensor models presented in this work were derived from experimental data acquired with commercial *in vitro* MEAs from Multichannel Systems (MCS, Reutlingen, Germany). Static experiments (see section 2.3) were performed with these MEAs. Commercial MEAs provide reliability, comfort of use and satisfactory signal-to-noise ratio. However, they are not specifically designed for the recording of islets (making it difficult to position the islets on the electrodes for example) and their size would not suit a wearable implementation of the biosensor (gold standard MEAs are a squared glass wafer with sides 45mm in length and topped with a 6-mm high glass cylinder).

Furthermore, additional **microfluidic** appeared to be necessary in order to study the dynamics of the endocrine pancreas response with more accuracy using time-varying stimulation patterns. Microfluidic MEAs²⁸ ease the characterisation of the pancreatic islets for the purpose of designing a dynamical model of these islets. Commercial microfluidic MEAs (Qwane Biosciences, Lausanne, Switzerland) were used in the past but did not fulfil our needs. The decision to develop application-specific microfluidic MEAs was finally taken and resulted in the development of a first prototype (see **Figure 16**). The advantages of this solution are that the islets can be trapped in a specifically-designed PDMS chip, electrodes can be engineered to improve signal-to-noise ratio, and an increased integration level can be reached for the sensing part of the biosensor. This solution however requires an important and time-consuming work to achieve the sensitivity and reliability of their commercial counterparts, and the models described in this chapter were thus calibrated with the most reliable experimental data we obtained using traditional MEAs.

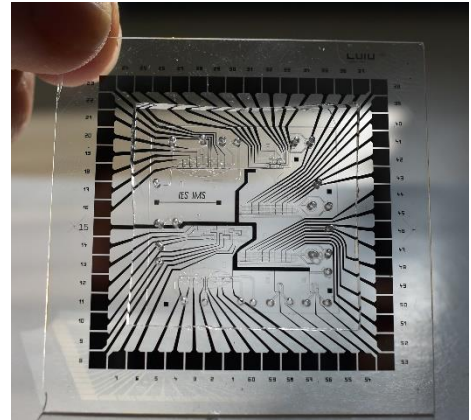


Figure 16: Application-specific microfluidic MEA developed in collaboration with IES Laboratory (UMR 5214, Montpellier).

²⁸ By « microfluidic MEA » we mean the assembly of a MEA with dedicated microfluidic channels fabricated in a biocompatible material and used to control fluid circulation over the MEA electrodes.

2.1.2 Signal conditioning front-end

The recorded electrical biosignals of pancreatic islets go through a **first stage of amplification** achieved by a commercial discrete **preamplifier** (MCS MEA1060-Inv). This 60-channel preamplifier is compatible with MCS *in vitro* MEAs. It provides a first stage of amplification close to the recording site in order to limit the degradation of the signal-to-noise ratio of recorded signals. A first stage of filtering is also applied with a customized bandwidth ranging from 0.1 to 3000Hz. In addition to electrical signal conditioning, the preamplifier maintains the MEA culture medium at a temperature close to 37 degrees Celcius, thus guaranteeing true-to-life response of islets. Temperature is regulated thanks to a programmable heating plate driven by a proprietary MCS temperature controller (MCS TC01).

2.1.3 Biosignal processing with the Multimed system

The ELIBIO team designed a **versatile processing system**, called Multimed [84], to cover a wide range of applications with a single electronic acquisition board. To design such a versatile system, a modular strategy was adopted to ensure flexibility (see **Figure 17**). The Multimed acquisition system is composed of three interconnected electronic boards:

- an acquisition board, named “*Tethys*”, that provides a second stage of amplification of the recorded biosignals and multichannel analogue-to-digital conversion,
- a digital processing board, named “*Titan*”, embedding a FPGA²⁹ that runs a dedicated digital signal processing architecture,
- an interface board, named “*Dock*”, containing numerous features to connect Multimed to other devices, enable configuration by the user, save datafiles, and distribute power to other boards. It notably embeds switches, buttons, USB (Universal Serial Bus) port, Video Graphics Array (VGA) port, digital I/Os, SD (Secure Digital) card slots, and a JTAG (Joint Test Action Group) connector.

Multimed is thus a generic **hardware platform with acquisition and processing capabilities** centred on an FPGA. Taking advantage of the reconfigurable logic of FPGAs, it can be reprogrammed, upgraded, and shared between research projects with different cellular material (e.g., *in vitro* pancreatic cells, *in vitro* neurons, or ex-vivo spinal cord), all the while proposing dedicated hardware processing architectures with very low (sub-millisecond) latency. While the global VHDL (VHSIC Hardware Description Language) architecture (handling both processing and interfacing) is identical between projects, the processing functions and their arrangement are application-specific.

On its FPGA, Multimed embeds a digital architecture dedicated to the real-time processing of electrical biosignals. The real-time processing modules are designed to have a short, well-

²⁹ **FPGA (Field Programmable Gate Array)**: are semiconductor devices that are based around a matrix of configurable logic blocks (CLBs) connected via programmable interconnects. FPGAs can be reprogrammed to desired application or functionality requirements after manufacturing. This feature distinguishes FPGAs from Application Specific Integrated Circuits (ASICs), which are custom manufactured for specific design tasks (definition by Xilinx, top FPGA design company).

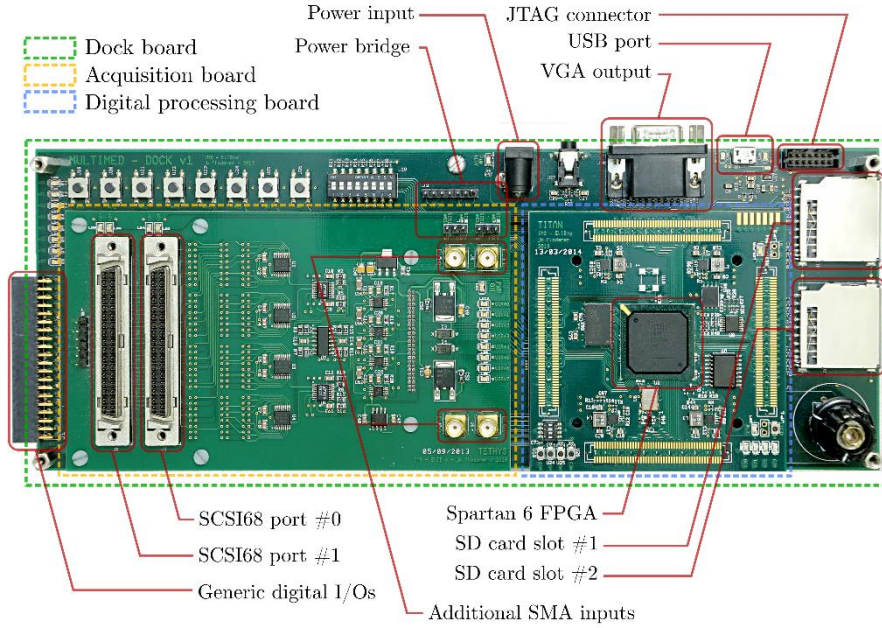


Figure 17: Multimed biosignal acquisition and processing system

characterized latency. To do so, they are fully described in VHDL, which permits a total control over computation procedures. The team design strategy was to build a library of processing modules that can interoperate while keeping the processing flow fluent, predictable, and latency-efficient. Hosting the processing architecture in an FPGA also makes it adaptable, while keeping the exact same hardware from one application to the other. Once digitalised, the recorded electrical biosignals are processed using various techniques (e.g., wavelet filters, min-max detection, and threshold-based detection to name a few) to extract the electrical signatures of interest (e.g., action potentials, Slow Potentials, and plateau fraction). The numerous signal processing capabilities of the Multimed system, an in-depth description of its hardware, and computation cost and latency estimations for all the modules of its digital architecture were published in [84]. In the context of the DIABLO project, this dedicated processing electronics with multichannel capabilities serves to **extract electrical signatures** such as action potentials and SPs (Slow Potentials) from the electrical signals recorded on the islets embedded in the biosensor.

2.1.4 System for Acquisition with Microfluidics (SYAM)

To eliminate the dependence on proprietary technologies, a custom electronic system was developed under the name **System for Acquisition with Microfluidics**. It integrates the functions of the MCS equipment (i.e., MEA support, low-noise amplification, bandpass filtering, and temperature control). This system also provides grounds for further integration and represents, as does the use of microfluidic MEAs, one more step towards the incorporation of the biosensor in a closed loop regulating the BG of diabetic patients. Indeed, at this stage of the project, we anticipate that a wearable implementation of the biosensor would require a fully integrated system containing a microfluidic system to supply islets with patient's fluids, a microfluidic chip to trap the islets and ensure a satisfactory recording when the patient is moving, and all the electronics necessary to power the system, control the environment

(temperature), process the islets biosignals and establish a wireless communication with a programming device.

SYAM was designed to fit acquisition and thermal control in a single device, in contrast with MCS equipment that achieves the same function with three separate pieces of equipment (see **Figure 18**). It is composed of two main sub-systems: the main body, which includes electronics for thermal control, backlighting, user controls, and electromagnetic shielding, and an acquisition stage. SYAM is thus a complete electrophysiology acquisition system allowing for the stimulation of the islets with a microfluidic setup and the recording of their activity via electrical or optical measurements. To conclude, SYAM was designed according to the following specifications and constraints:

- 60-channel, 16-bit, 10 kHz data acquisition³⁰
- Temperature control at 37°C
- Easy access to the MEA for insertion and manipulation of microfluidic tubing
- Must include a Faraday cage

The system is powered by a 12 V, 5.42 A power supply. This system was developed during my PhD thesis, I participated to the setting of its specifications but I have never been directly involved in its development. Besides, no data acquired with this system were used to develop the models presented in this work as they were only available recently.

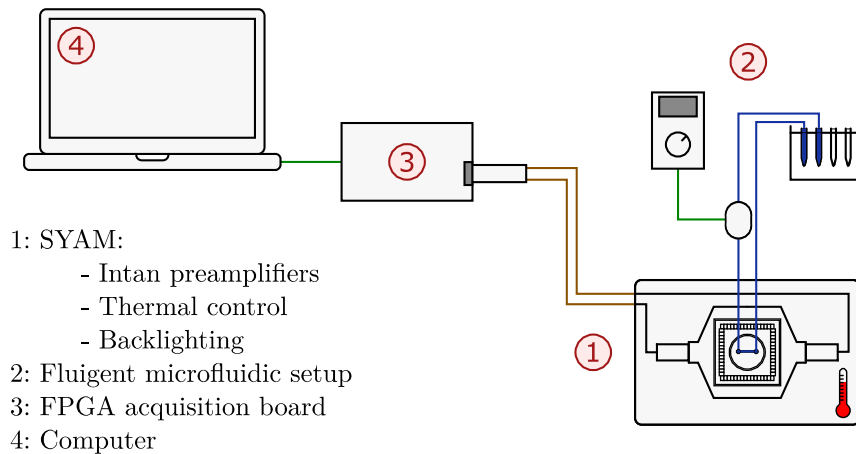


Figure 18: Scheme of the microfluidic measurement setup integrating SYAM.

³⁰ Legacy from the MCS equipment, which has identical specifications

2.2 Biosensor modelling approach

« Models describe our beliefs about how the world functions. »

Glenn Marion in [85]

With mathematical models, beliefs about how the world functions are translated in the language of mathematics, i.e., a combination of equations with numeric parameters. Mathematics enable the formulation of ideas with precision and concision, and the clear identification of underlying assumptions. In addition, mathematical modelling offers the possibility to benefit from all the results that mathematicians have proved over hundreds of years. Nowadays, it also opens the access to the tremendous power of **computer-aided simulation**. In its “Introduction to Mathematical Modelling” [85], Glenn Marion highlights that: “There is a large element of compromise in mathematical modelling. The majority of interacting systems in the real world are far too complicated to model in their entirety. Hence the first level of compromise is to identify the most important parts of the system. These will be included in the model, the rest will be excluded.” This statement is particularly true for the **modelling of biological systems** which can present a marvellous complexity as we have seen in Chapter 1. Indeed, modelling the physiological processes occurring in the islets of Langerhans requires major simplifications and behavioural assumptions.

In this section, we will describe the design of a mathematical model of our biosensor for the purpose of assessing, *in silico*, the ability of this sensor to provide valuable information to an AP. It is important to note that the biosensor models used in this work were developed by a former PhD student of the team and are presented here to ease the understanding of the reader. They were updated in the course of my PhD thesis but the modelling work, strictly speaking, was already done. This section provides a description of the revised modelling approach and the underlying simplifications and assumptions.

As previously described, our biosensor monitors the electrical activity of healthy pancreatic islets and processes it to continuously assess their insulin secretion. When it comes to **modelling the biosensor**, its most important part, i.e., the part which mostly contributes to the dynamics of the biosensor output, is then the pancreatic islet. In the context of diabetes, the most interesting “output” of islets is insulin (represented by an insulin secretion rate). The dynamics of the insulin secretion result from the complex interplay between a large number of molecules and the pancreatic β cells. As a consequence, a mathematical model aiming at modelling the islets in their entirety would take all the mediators of insulin as inputs. These mediators can be classified in three categories: nutrients, hormones, and neurotransmitters³¹. Nutrients act as initiators of insulin secretion when the two other categories only regulate (either upward or downward) an insulin secretion initiated by a previous intake of nutrients. In the context of this work, a simplified model of the pancreatic islet could therefore be represented as shown in **Figure 19**.

³¹ Note that, a fourth category of mediators could be taken into account, namely the pharmacological drugs, but their effect will not be discussed in this work as they are not the research focus of our partners at CBMN laboratory and the focus here will be set on the natural mediators of insulin secretion.



Figure 19: Simplified model of the pancreatic islet:

A second level of complexity appears with the synchronised activity of the β cells. We described in section 1.5.2, how the biosensor is able to account for this coordinated response to nutrients intake. Indeed, the overall objective of our project is to use the islets' electrical activity, and particularly the frequency of the Slow Potentials, as a proxy to assess the secretory activity of these same islets, i.e., the dynamics of the insulin secretion. The islet model could therefore be completed by considering the measurable electrical activity as the main readout of the pancreatic islet model (see **Figure 20**).



Figure 20: Simplified model of the pancreatic islet adapted for the biosensor context

As previously described, the islet is the sensitive element of our biosensor, but we have seen that the biosensor also integrates data acquisition to process the information (see sections 1.5.2 and 2.1). Building a complete model of the biosensor therefore requires the modelling of the electronic acquisition/computation system (Multimed - see 2.1.3). As does the real acquisition board, its model takes the islet electrical activity as an input. Nonetheless, the model output differs from the outputs of the real biosensor (see Pirog et al. [84] for an extensive list of the measured signals) as we limited it to the sole measured SP frequency signal. **Figure 21** shows the resulting schematic of the complete biosensor model.

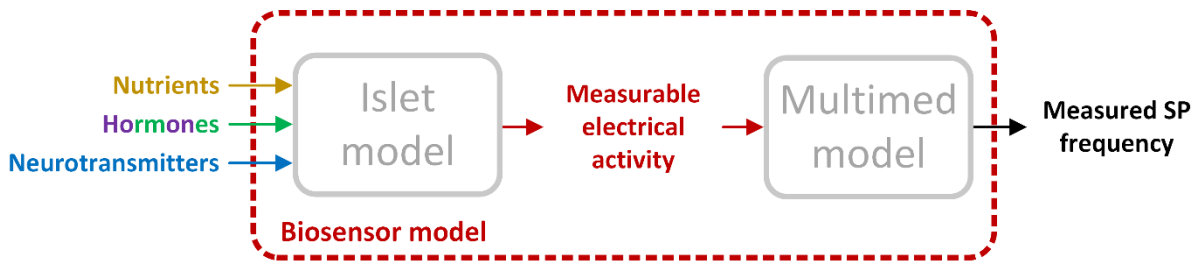


Figure 21: Simplified model of the whole biosensor

Prior to this work, several biosensor models were developed using this formalism by a former PhD student, Dr Antoine Pirog, who is now working in the ELIBIO team as a postdoctoral researcher. These models were developed using the Python programming language and first closed-loop simulation results were obtained using a Python implementation of the glucose-insulin system model published by Dalla Man et al. [86].

Simulation is part of electronic products development in order to detect design errors or unexpected behaviours due to the parasitic elements of real electronic components, and to account for complex physical phenomena. It enables the correction of errors at an early stage

of product development, i.e., at a stage where corrective actions remain less expensive. In the context of this project, the variability of the biosensor output is (and must be) largely attributable to the physiology of the islets embedded in this sensor. Simulations highlighting an excessive contribution of the acquisition electronics should therefore lead us to rethink the design of the acquisition system. At this stage of the project, a proof of concept validating the biosensor as a valuable input to an AP control algorithm is still required. As a consequence, the accurate modelling of the real implementation of the SP measurement algorithms embedded in the acquisition board is not yet a priority. The models developed by A. Pirog in Python were thus simplified to the islet model and implemented in the MATLAB Simulink environment to be used with a commercial meal simulator developed in the same environment. These **biosensor models**, whose associated simulation results are presented in this work, can be represented as shown in **Figure 22**.

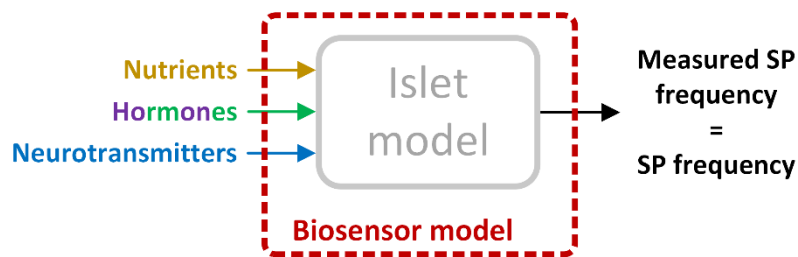


Figure 22: Reduced model of the biosensor used in this work

It is important to underline the assumptions hidden behind this formalism. The first assumption is taken from our experience with the biosensor over time. It is assumed that the main electrical signature in the electrical activity of islets, i.e., the most interesting signal, are the SPs. In particular, their frequency is the most interesting feature as it is directly correlated to glucose concentration and modulated by GLP-1 and adrenaline as does the insulin secretion response. [70] SPs amplitude variations seem to be less consistent throughout the different *in vitro* experiments. However, they are still under study as they could provide quantitative information to assess the size of an islet or the quantity of insulin it secretes compared to the other islets of the MEA. The second assumption is that it is possible to measure the SPs frequency with little biasing influence of the acquisition electronics. In other words, it is relevant, in a first approach, to neglect the influence of the acquisition system when modelling the biosensor. This hypothesis is mainly justified by the fact that SPs are a slow (period ranging between 1 and 10 seconds) signal with good repeatability.

To conclude, this work is part of a scientific approach which considers **an idealized version of the biosensor** to validate its working principle. In particular, our objective is to validate its ability to provide valuable information about a T1D patient metabolic status to the controller of an Artificial Pancreas. To do so, the extensive characterisation of islets response to the initiators and modulators of insulin secretion is required for the purpose of designing a dynamical model of the islets and of our biosensor at the same time. In a coherent manner, this approach supposes that the thorough modelling of the biosensor hardware and its processing algorithms should be postponed to a second stage of the modelling project. Indeed, it appears more profitable to model these aspects of the biosensor during the development of a commercial product with definitive design choices.

2.3 Data-based modelling

The endogenous algorithms of murine pancreatic islets have extensively been characterised via electrical measurement with our biosensor [77], [84]. Using these experimental data, it is then possible to model the islet electrical activity response to insulin secretion mediators and thus model the biosensor response to these same mediators, as we have seen in the previous section. Many approaches do exist to develop a **model based on experimental data**. “Black box” approaches are a set of techniques that do not use *a priori* knowledge about the system under consideration to identify a model of this system and the model parameters. In practice, *a priori* knowledge is often necessary, and “grey-box” approaches are preferred: some *a priori* knowledge is injected at different stages of the modelling process but the equations and the parameters of the model do not necessarily have any physical meaning. Lastly, “white-box” identification techniques rely on a parameterized model which aims at representing the system under consideration. The identification then becomes an optimization problem where an algorithm is used to find estimate of model parameters which minimizes the estimation error following a predefined criterion. The models used in this work were developed using a technique which can be classified in the “**white-box approaches**” category. Yet, the ARIA team at IMS, which officially joined the project in 2019 and is now in charge of the biosensor modelling work, is currently using “grey-box” approaches to design alternative versions of the biosensor model.

In the last section we have also seen that designing a relevant mathematical model requires to define the most important parts of the system to model. The ideal islet model for us, i.e., the model which best matches the context of this project, is outlined in the first subsection to come. Then, general principles of extracellular electrophysiology and the methodology utilized during the *in vitro* experiments are briefly described. An overview of the retrieved experimental data is provided in the third subsection, followed by the description of the actual **parameterized** models that have been used in our study. Finally, the identification techniques which provided the best fit to experimental data are detailed.

2.3.1 Contextualised model of the pancreatic islet

In Chapter 1, we emphasized the tremendous complexity of the human body. In particular, the glucose homeostasis results from the complex interplay of multiple organs, precisely orchestrated by the endocrine pancreas. To cope with a variety of physiological states and perturbations, the pancreatic islets integrate numerous signalling pathways and molecules. Modelling their complexity in its entirety is utopian. Yet, it is possible to design a simplified - but not simplistic - **islet model**, describing its response to numerous molecules, based on *in vitro* characterisation. In view of the difficulty to monitor the islet output in real time (the insulin secretion rate), the biosensor, and its ability to monitor extracellularly the electrical activity of the islets, appears as a valid information source to develop a mathematical model of the islets. The ideal functional islet model takes all the **initiators and modulators of insulin secretion** as inputs and outputs the **insulin secretion rate** (see **Figure 23**). In our context, we consider an islet model with a second output, the **measurable electrical activity**. Our ideal model can therefore be represented as shown in **Figure 23**.

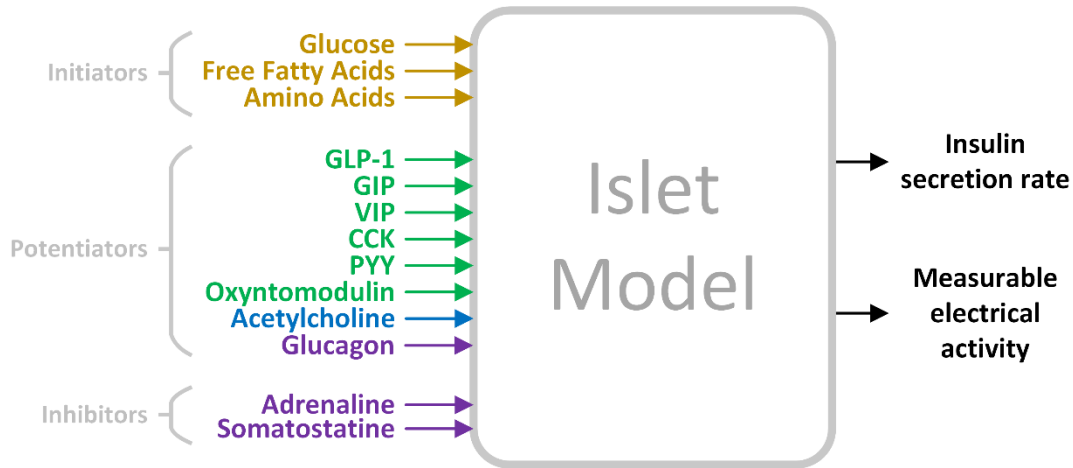


Figure 23: Contextualised model of the islet of Langerhans. The main initiators, potentiators, and inhibitors of insulin secretion are considered as inputs of the model: nutrients (dark yellow), neurotransmitters (blue), gut hormones (green), and other hormones (purple).

2.3.2 *In vitro* characterisation of islet endogenous algorithms

The *in vitro* characterization of the islets endogenous algorithms with the biosensor took place at CBMN laboratory in Prof. J. Lang's team³². Murine pancreatic islets were obtained by enzymatic digestion and handpicking, and were cultured directly on MEAs by CBMN. Human islets, provided by the GRAGIL³³, were also used but their transportation makes their culture complicated and thus deteriorates the reproducibility of the experiments. Due to a limited availability of human data, the **biosensor models were fitted on data** obtained with murine islets. As a consequence, we will focus on the results obtained with these **murine islets**.

Islets are usually cultured on MEAs for 2 to 7 days prior to the electrophysiology experiments. Experiments then consist in perfusing the culture chamber with various solutions depending on the desired objective. Islets electrical activity is recorded as detailed in 2.1 and the **static behaviour** of islets is usually characterised by averaging the **frequency and amplitude of SPs** (Slow Potentials) on a short time window (few minutes) and on several electrodes once the steady state for a given condition is reached. The **dynamical characterization** of islets behaviour requires to continuously record these signals while applying a step of glucose. In so doing, the **transient response** to the condition under study is captured and characteristic time-dependent behaviour of the islets can be brought to light.

The solutions utilized to stimulate the islets contain the necessary ions to ensure a physiological response or to induce a specific response (e.g., inhibition of SPs with a supraphysiological concentration of calcium). To **assess islets response to nutrients**, the solutions are also carefully dosed to attain the desired **glucose concentration**. More conveniently, a given glucose concentration is referred to as **GX**, where G stands for glucose

³² Prof. J. Lang, Dr M. Raoux, Dr F. Lebreton, Dr M. Jaffredo, E. Puginier.

³³ The GRAGIL (Geneva-Rhine-Rhone-Alps Group for the transplantation of Islets of Langerhans) consortium is a network of several transplantation centres from France (Grenoble, Lyon) and Switzerland (Geneva University Hospital) that act as a central islet production structure.

and X for the concentration in glucose in mmol/l (e.g., G5.5 refers to a solution with a glucose concentration of 5.5 mmol/l). Moreover, both physiological and supraphysiological concentrations in nutrients and insulin modulators are used during the experiments to better understand pancreatic islets physiology.

2.3.3 Experimental protocols

We have seen that, ideally, modelling the endogenous algorithms of the islet of Langerhans would require the characterisation of their response to many molecules (**Figure 23**). Indeed, a mathematical model accounting for all the initiators and modulators of insulin secretion is a Holy Grail. Yet, multiplying the experiments to extensively study the islets is time and resource-consuming. Together with our partners at CBMN, we therefore decided to focus resources on the most interesting and accessible molecules. At the time of writing, the pancreatic islets' response to glucose has been well studied but data with other initiators of insulin secretion, such as lipids or amino acids, is still lacking. Concerning the modulators of insulin secretion, the response to GLP-1 has been studied together with the response to adrenaline. **Figure 24** summarizes the experiments that have been performed (the molecules, the stimulation patterns, and the islet response to these stimulations are detailed) and the main “features” (i.e., the characteristic response to these different stimulants) of the endogenous algorithms that have been reported.

These very characteristic responses of the islets have been identified applying the methodology depicted in section 2.3.2.

In a series of static experiments consisting in applying increasing followed by decreasing ramps of glucose to cultured murine islets, we observed a characteristic **hysteretic response**. Mouse islets were cultured for 3 to 13 days on MEAs. During the experiments, the electrical activity of these islets was recorded while the glucose concentration was raised, step by step (variable amplitude but 0.5 mmol/l most of the time), from 3 mmol/l to 15 mmol/l (G3 to G15) and decreased back to 3mmol/l. A deeper analysis of this glucose-induced electrical activity revealed that the frequency of the SPs was correlated with glucose concentration, showing a sensitivity to both the concentration and its direction of change. During the rising phase, SP frequency increased with a median effective concentration (EC50) of 7.5 mmol/l (maximal effect at 10 mmol/l glucose), while the EC50 shifted to 8.7 mmol/l during the decreasing phase. From a functional perspective, this characteristic response of the islet endogenous algorithms ensures a quick reaction to hyperglycaemia while preventing reactive hypoglycaemia (by lowering rapidly the secretion of insulin when the glucose level is decreasing).

Concerning the modulators of insulin secretion, the **effect of GLP-1** concentration on glucose-induced electrical activity was studied. A potentiation of the electrical activity induced by steady concentrations of glucose was observed. Using steady concentrations of glucose (G8.2 and G15) associated with picomolar concentrations of GLP-1, we notably observed an increase of SP frequency correlated with the increase of GLP-1 concentration (from 0.5 pmol/l to 50 pmol/l) [70]. The stress hormone adrenaline was also tested as it is a known inhibitor of beta cell electrical activity. Glucose-induced SPs were reversibly inhibited by relatively high

concentrations of adrenaline. The design and results of these experiments are further detailed and discussed in Lebreton et al. [70].

The transient response of the murine pancreatic islets was also studied using steps of glucose concentration. Cultured islets were maintained at a glucose concentration of 3 mmol/l. Glucose steps at 5.5 mmol/l (G5.5, at the activation threshold), 6 mmol/l (G6, immediately above the activation threshold), and 8.2 mmol/l (G8.2, close to post-prandial BG levels) were then applied. The instantaneous SP frequency presented a characteristic biphasic response over time in all three cases with the amplitude of this biphasic response correlated with the glucose step concentration. The first phase lasted on average 8.40 ± 1.18 min, was followed by a drop of global activity, and by a second phase presenting a plateau of lower activity than the first phase. During the second phase, SPs become pulsatile (both in amplitude and frequency)

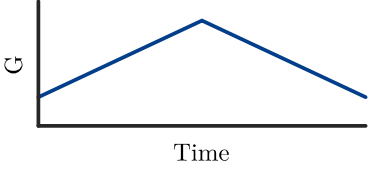
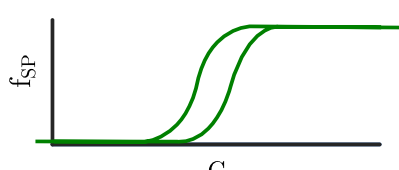
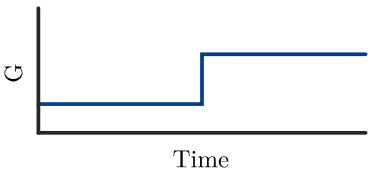
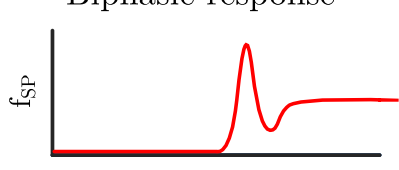
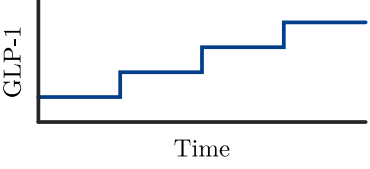
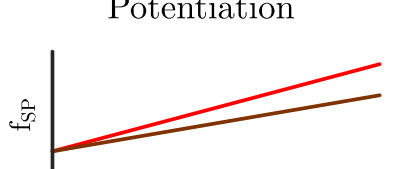
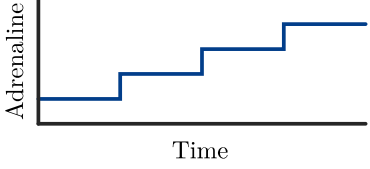
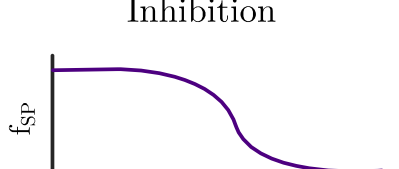
Stimulant	Stimulation pattern	Islet response
Glucose		
Glucose		
GLP-1 (+ steady glucose)	 at G8.2 or G15	
Adrenaline (+ steady glucose)	 at G15	

Figure 24: Summary of the main islet endogenous algorithms that have been characterised *in vitro* with the biosensor.

presenting a general pattern which reminds the biphasic insulin secretion patterns [87]. These results related to the islet biphasic response to glucose steps are published in [77].

2.3.4 A mathematical model of islet electrical activity

The **endogenous algorithms** of murine pancreatic islets have been **statically and dynamically characterised *in vitro*** (see sections 2.3.3 and 2.3.2). Sensitivity to glucose concentration and direction of change, the potentiating effect of GLP-1, the inhibiting effect of adrenaline, as well as biphasic response profiles were described with sufficient resolution and repeatability to be exploited in a modelling approach. During his PhD, Dr A. Pirog developed **models of SP frequency** variation in response to glucose ramps and steps in Python. He then modelled the effect of GLP-1 and adrenaline as SP frequency modulation parameters.

This work deals with the use of simulation to validate the biosensor as a valuable input to the control algorithm of an AP. My first task was then to develop a MATLAB implementation of A. Pirog's biosensor models, to make them compatible with the UVA/Padova T1DMS. The implementation of the models in the MATLAB Simulink environment did not pose major technical difficulties, but we had to limit the models' inputs to glucose only since the simulator only reproduces the dynamics of glucose, insulin, and glucagon. Indeed, the dynamics of the other mediators of insulin secretion (such as GLP-1 and adrenaline) are not modelled in the simulator, we therefore implemented in MATLAB mathematical models which express the **SP frequency as a function of glucose concentration only**.

The previously described **hysteretic response** to ascending and descending ramps of glucose, was first modelled using a **Hill equation** [88] widely utilized to model biological processes. This model does not account for the asymmetry observed depending on the direction of change of glucose concentration but, in a first approach, it provides a simple mathematical model which correctly fits the experimental data. Following the method described by Stamper and Wang [89] an activation function was defined (see **Equation 1**).

$$A(G) = \begin{cases} \frac{[G - G_0]^n}{[G_{50} - G_0]^n + [G - G_0]^n} & \text{if } G \geq G_0 \\ 0 & \text{otherwise} \end{cases} \quad (1)$$

With G_{50} a half-activity constant, G_0 an activation threshold and n the Hill coefficient. A scaling factor f_M representing the maximum SP frequency was then added to de-normalize the model and fit the experimental data. The SP frequency is then computed with **Equation 2**.

$$f_{SP} = f_M \times A(G) \quad (2)$$

To account for the sensitivity of islets to glucose direction of change, a second mathematical model was developed using a custom implementation of the **Preisach model of hysteresis** [90]. This model is widely accepted to model hysteretic phenomena. It decomposes a hysteresis envelope into a summation of N discrete hysteretic elements, the relay hysteron (see **Figure 25A**). An hysteron of amplitude 1 can be described as a two-valued operator denoted $R_{\alpha,\beta}$ with

α and β the “switch-off” and “switch-on” thresholds respectively (see **Figure 25B**). Mathematically, the output of $R_{\alpha,\beta}$ is expressed by **Equation 3**.

$$y(x) = \begin{cases} 1 & \text{if } x \geq \beta \\ 0 & \text{if } x \leq \alpha \\ k & \text{if } \alpha < x < \beta \end{cases} \quad (3)$$

Where $k = 0$ if the last time x was outside of the boundaries $\alpha < x < \beta$, it was in the region of $x \leq \alpha$; and $k = 1$ if the last time x was outside of the boundaries $\alpha < x < \beta$, it was in the region of $x \geq \beta$. Although more complex, this model has been extensively used in this work as it better accounts for the hysteretic response of the islets.

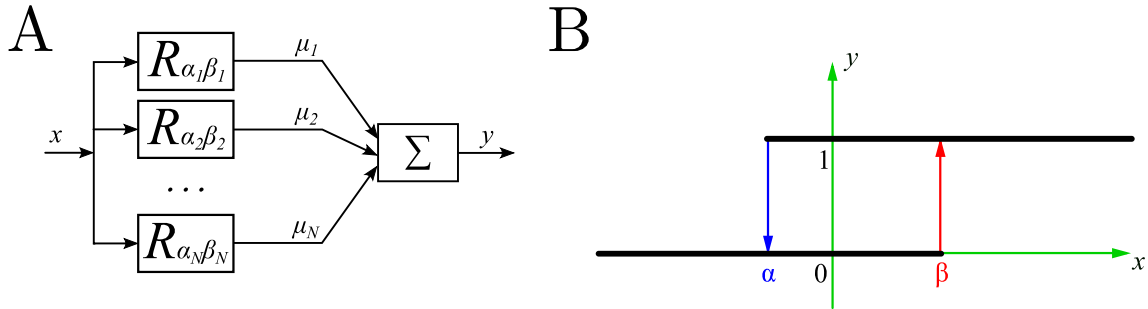


Figure 25: Working principle of the Preisach model. A) Summation of N discrete hysteretic elements of amplitude μ_i B) Transfer function of a unitary hysteron $R_{\alpha,\beta}$.

A dynamical model aiming at reproducing the **biphasic response** to a glucose step was also developed in Python. Preliminary data obtained in Python did not show any significant improvement of the closed-loop results when using this much more complex model (data not shown in this manuscript). Therefore the implementation of this model in the MATLAB Simulink environment was not a priority and was not completed during this thesis. Furthermore, the ARIA team joined the project consortium in 2019 to develop a dynamical model of our biosensor and a control algorithm specifically designed to integrate the biosensor in an AP, using a grey-box approach which is quite different than the approach we used (white-box approach).

2.3.5 Model parameters identification

The experimental data recorded as described in Lebreton et al. [70] were used for the **parameters extraction of the two models** presented in the previous section. Recorded signals were filtered using a Butterworth 0.2-2.0 Hz filter, and SP events were detected using the algorithm presented in Pirog et al. [91] with a 6 μV threshold. The average frequency of those events was calculated, and normalized, at steady state during the last 3–7 min of each glucose condition (see Chapter 3 – **Figure 38**).

The static model (based on the Hill equation) was identified using the method of least squares solved by the Trusted Region Reflective algorithm. Concerning the hysteretic model, experimental data were split between increasing and decreasing glucose conditions, and fitted to two separate static models using the same method in order to avoid propagation of

measurement errors within the model. The region between the two resulting curves was then utilized to generate a hysteresis envelope and converted in the Preisach matrix to establish the final model.

Identification of the static model was initially done in Python 2.7 using `scipy.optimize`'s `curve_fit` function during Antoine Pirog's thesis. I then translated the resulting model in Matlab to satisfy compatibility with the T1DMS. Likewise, and for the same reasons, the Preisach model was initially identified in Python 2.7 with an algorithm adapted from Janičić et al. which takes the hysteresis envelope as an input [92]. The hysteretic model was then translated in Matlab. During this thesis, the **models were refined**, as the experimental data were analysed with detection parameters that had been improved in between. Both the static and the hysteretic models were identified on the newly-processed data to obtain updated versions of these models. During this new identification phase, homogeneity between models was promoted by constraining the maximal frequency parameter (f_M). As a consequence, and contrary to the previous versions, the new versions of the models now have the same bounds (see section 3.2).

2.4 Simulation environment

With the growing interest of simulation to assess therapeutic approaches in the diabetes field, many **models** aiming at describing the **glucose-insulin system** were developed. The most popular ones are the Bergman Minimal Model [93], the Hovorka's Model [94], the Sorensen's Model [95], and the Dalla Man's Model [86] to name a few. As previously mentioned, they have notably been used to develop MPC (Model Predictive Control) algorithms or other features relying on prediction such as PLGS (Predictive Low Glucose Suspend). Among them, the Dalla Man's Model has proven to be the most successful. This model is included in the UVA/Padova Type 1 Diabetes Mellitus Simulator (**T1DMS**), which has a recognized physiological accuracy, and obtained the approval of the US FDA as a substitute for preclinical animal trials. The UVA/Padova T1DMS is now a renowned and commercially-available testing environment for glucose sensors, control algorithms, and pumps involved in modern T1D therapy. Indeed, it was specifically designed to facilitate the **development of AP systems**.

2.4.1 UVA/Padova T1DM Simulator testing environment

The core element of the UVA/Padova T1DMS is a comprehensive mathematical model of the glucose-insulin dynamics. In 2007, the team of Pr. Cobelli (University of Padova, IT) published this metabolic model which accurately describes the physiological events that occur consecutively to the ingestion of a mixed meal. A compartmental model was built benefiting from several separate models of the literature. Model parameters were set to fit the mean of a large **clinical dataset** generated using an innovative triple-tracer meal protocol [96]. The cohort submitted to this protocol was constituted of 203 individuals with different age and sex, and a normal tolerance to glucose. As a consequence, the UVA/Padova metabolic model originally described an **healthy individual**. The same strategy was then applied to a smaller dataset to extend the model to T2D. The modelling strategy, the model equations, and parameters for a normal individual and a T2D patient were published in Dalla Man et al. [86].

In 2008, the metabolic model was extended to T1D. The insulin secretion module was replaced by a subcutaneous insulin infusion module to **model a T1D patient** treated with insulin therapy. Adjustments were made on few model parameters to match the differences between healthy individuals and T1D patients reported in the literature (e.g., basal glucose level, endogenous glucose production, insulin clearance rate). A MATLAB/Simulink implementation of the model was then published to provide diabetes researchers with a simulation platform enabling the testing of insulin infusion algorithms, decision support systems and the assessment of CGM sensors [97]. In 2008, the S2008 version of the simulator was approved by the **US FDA as a substitute for pre-clinical animal trials** [81]. The simulator included a T1D patient cohort consisting in 100 adults, 100 adolescents, and 100 children. As it did not model the circadian variation of insulin sensitivity, the simulator was only approved for single meal scenarios.

A second version of the simulator was published in 2014 and obtain the FDA-approval the same year. This latter version (S2013) incorporated new modules to take into account the counterregulatory action of glucagon, an exogenous glucagon infusion route, alternative insulin administration routes, and a glucose-insulin system which models insulin secretion dynamics with more accuracy, especially during hypoglycaemia. Furthermore, the virtual T1D patients of the S2013 version were generated with an enhanced statistical method to better match the variability of metabolic parameters observed in real T1D patients [98]. Both version were regularly compared to real clinical data showing satisfactory results. The T1D cohort of the S2013 version notably demonstrated to be representative of the T1D population of a clinical trial [99].

The UVA/Padova T1DMS is commercialized by The Epsilon Group. A licence of the version 3.2 (S2013) of the simulator was bought in 2017 to meet the needs of our project. The T1DMS testing environment provides a complete solution including all the components necessary to assess AP systems (see section 1.4), i.e., a cohort of 33 T1D patients (11 adults, 11 adolescents and 11 children – see Appendix 4), built-in models of numerous commercial CGM sensors and insulin infusion pumps, as well as a metabolic model of T1D patients. The latter simulates the glucose-insulin interactions in virtual T1D patients subjected to glucose intake scenarios with physiological accuracy. It takes the **meal (glucose intake)** scenario and the **insulin infusion rate** as inputs, and outputs the patient's **glucose concentrations** (e.g.,) following the equations described in Dalla Man et al. [98] (model equations are provided in Appendix 3). For the AP controller, the variables of interest are glucose (either intravenous or subcutaneous concentration) and insulin (also intravenous or subcutaneous - see **Figure 26**). Meal scenarios are user-defined (see section 2.4.3) and set the timing and levels of glucose intakes. The simulator also provides a built-in meal announcement feature to simulate the interactions between the patient and the control algorithm. In addition the simulator includes a customizable controller module which allows for the implementation of a variety of control algorithms. To adapt this testing environment to our investigations, we inserted in the T1DMS the model of our biosensor - developed as described in the last section - in place of built-in CGM sensor models.

2.4.2 Closing the loop *in silico*

Traditional insulin therapy is tedious as it involves self-monitoring of blood glucose and consequent multiple injections of insulin throughout the day. Nowadays, technological advances help therapy evolve towards more automated and unburdening solutions: CGM sensors measure subcutaneous glucose, insulin pumps inject the necessary insulin, and a controller closes the loop helping with the necessary decision-making in between.

Control algorithms are a key component in an artificial pancreas. However, the diversity of control algorithms will not be investigated in this work, not focused on control theory. To close the artificial pancreas loop, we used simple **Proportional-Integral-Derivative (PID) controllers** for the sake of demonstration. We assessed variants of this architecture to match the specificities of each simulation configuration, i.e., the input-output configuration of the T1DMS. Two distinct configurations have been used. In the first one, the biosensor is fed with intravenous (IV) glucose and the insulin is infused intravenously. This configuration will be referred to as the **IV/IV configuration** and the associated results are presented in Chapter 3. The second configuration uses subcutaneous (SQ) glucose measurement and subcutaneous insulin infusion. It will be referred to as **SQ/SQ configuration** and the associated results are presented in Chapter 4.

It is important to emphasize the unconventional nature of the biosensor in this work. The image of the patient's physiological state (see **Figure 26**) is the output of the biosensor which is therefore an **insulin demand** signal, resulting from the processing of glucose levels by the islet endogenous algorithms, rather than a glucose level signal. As a consequence, the output of the sensor is not compared to any desired setpoint, like traditional PID control, and is directly used as an **error signal**. The setpoint is in fact **encoded in the endogenous algorithms** of the pancreatic islets.

With the **IV/IV configuration**, our objective is to validate the SP frequency signal as a relevant indicator of insulin need. The insulin infusion signal is generated using a model of SP frequency variations in series with a gain K which ensures the adaptation necessary to match the daily insulin need of each patient. When the model is connected to the simulator using IV measurement and IV insulin infusion routes (no insulin pump in the loop – see **Figure 26**), the insulin regulation is performed without diffusion delays (as would be the case with the healthy endocrine pancreas). This configuration is used to **evaluate the electrically-characterised endogenous islet algorithms alone**, i.e., without any error compensation from a controller. It emphasizes the inborn regulation capabilities of pancreatic islets.

The **SQ/SQ configuration** uses the subcutaneous (SQ) insulin delivery route as it is systematically used to ensure patient safety in actual T1D therapy. Islets are now considered as embedded in **an extracorporeal implementation of the biosensor** and fed with patient's subcutaneous fluid. T1DMS configured in SQ/SQ simulates an AP with a sensor and a pump (both extracorporeal) which is the reference therapy for T1D patients (see Chapter 1). The main difference with IV/IV configuration is the presence of delays resulting from glucose diffusion in the SQ space and from SQ insulin absorption which delays insulin onset of action. We use the T1DMS in SQ/SQ configuration to simulate, as best as the software currently allows, the everyday life of patients by pairing it to realistic glucose intake scenarios when

assessing an **AP system integrating the biosensor**. It is also used to compare this system to more conventional AP systems (i.e., AP systems integrating a CGM sensor) or to open-loop therapies such as MDI.

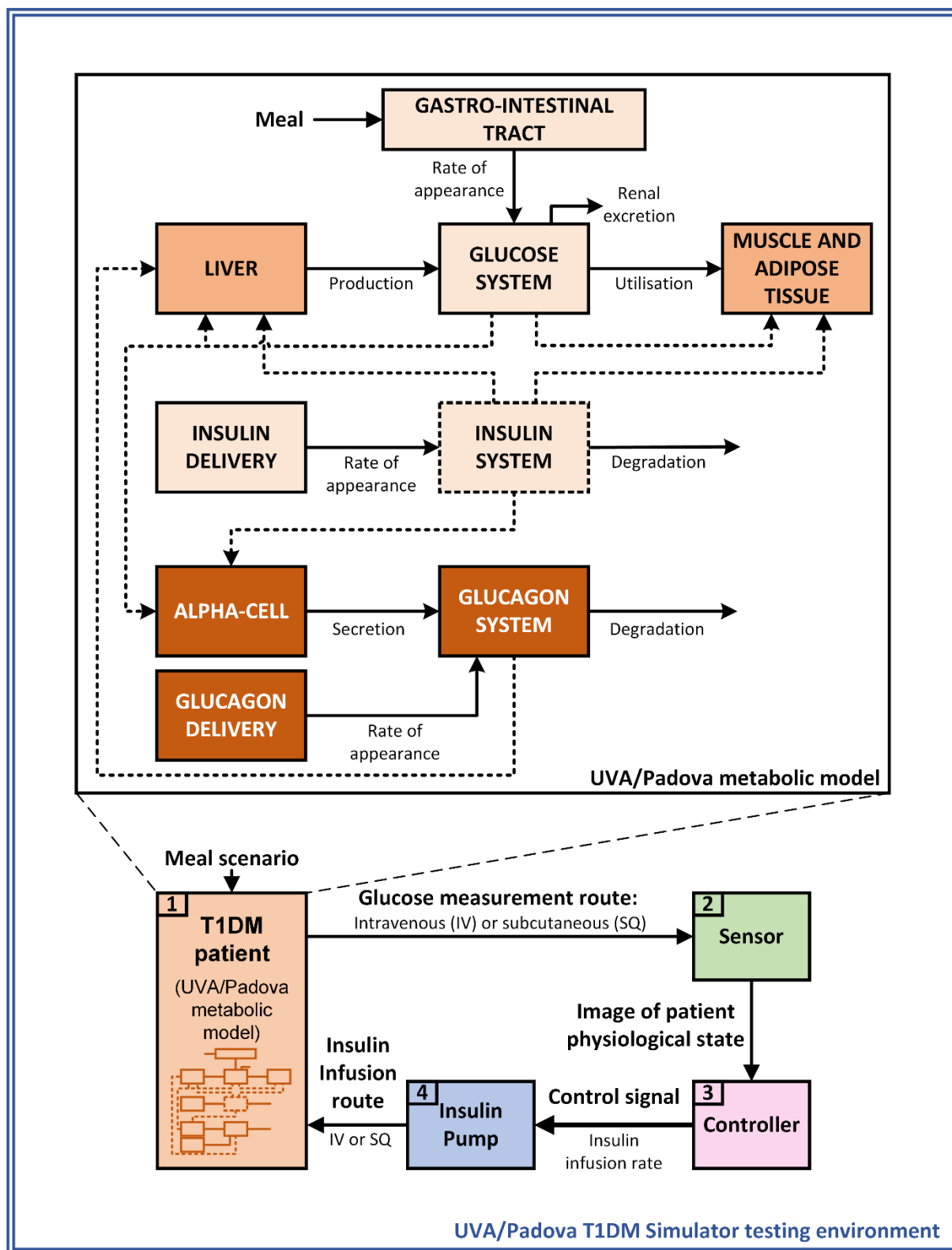


Figure 26: UVA/Padova T1DM Simulator testing environment

Controller tuning methodologies.

In an AP, the function of the controller is to determine the appropriate quantity of insulin to be delivered in response to significant disturbances, such as a meal or physical effort. To do so, the controller takes into account present and past sensor readings, but also anticipates the future states determined by glucose insulin interactions and insulin onset of action. To achieve optimal performance, the controller needs to be appropriately tuned. In particular, in the context of diabetes treatment, the controller needs to be tuned to match **patient's insulin needs**. Indeed, the large inter-patient variability in terms of sensitivity to insulin, body weight, and T1D duration (see Appendix 4) is a serious issue in designing easily adjustable devices. The amount of insulin required to bring BG level back to the normal range after a meal greatly varies from one patient to the other. To handle this variability, and to ensure reliability and stability of the closed-loop system, a **fine tuning of the AP controller's parameters** is necessary.

To achieve that tuning, several methods were implemented. When only one parameter had to be set, optimal tuning was achieved with the joint use of **parametric analyses and a performance criterion** (see subsections 2.5.1 and 3.3.2). To tune several controller parameters at once, we developed an *in silico* tuning method based on a **Genetic Algorithm** (GA, see **Figure 27**). In [100], K. F. Man describes GA as a technique “inspired by the mechanism of natural selection, a biological process in which stronger individuals are likely be the winners in a competing environment”. The numerical GA technique implements the same method to find the most suitable solution to a complex problem [101], [102]. A first population of solutions is generated (vectors of controller parameters in our case). Its members are evaluated with the cost function and the most fitted are bred by a crossover function to form the next generation. The algorithm then iterates over generations to converge to a solution. To avoid local minima, GAs also introduces random mutations in the solutions, i.e., random variations of the controller parameters, whenever a new generation is computed. It is theoretically proven that this process guarantees

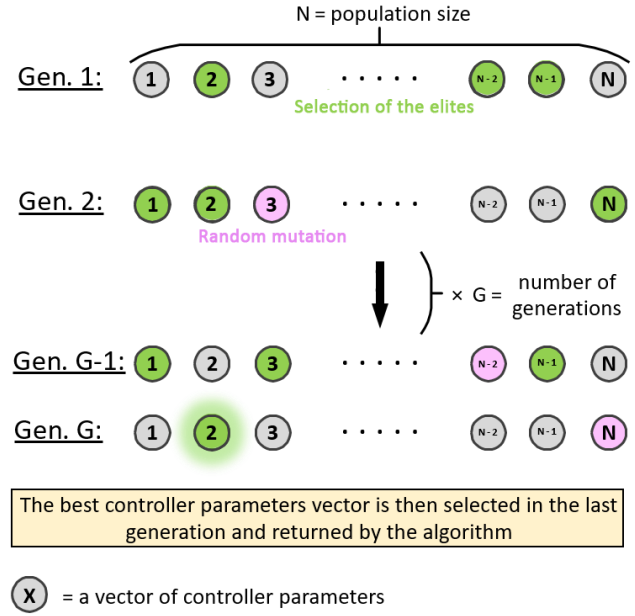


Figure 27: Genetic algorithm working principle

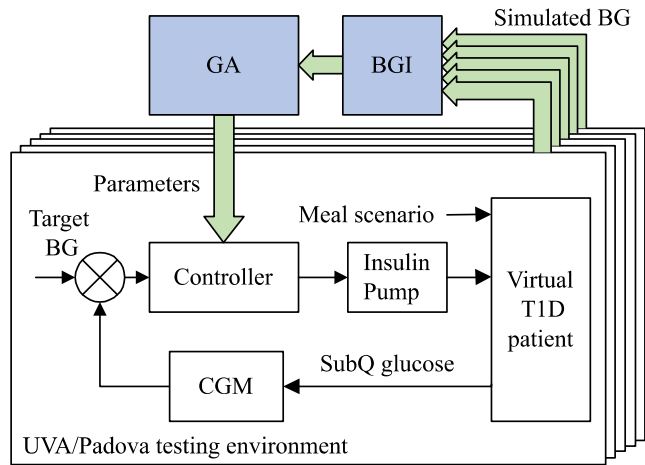


Figure 28: Principle of operation of the GA-based controller tuning method involving a cost function assessing glucose control with BGI.

convergence to the global optimal solution, in a statistical sense [101], [102]. The *fmincon* function is then used in a hybrid optimization scheme to continue the optimization after *ga* terminates and ensure that a minimum has been reached.

GA requires careful joint design of the initial population and of the cost function to converge to an optimal solution. In this work, GA is paired with a **cost function** that computes the **mean Blood Glucose Index** (BGI - further described in 2.5.2) of BG profiles resulting from the simulation of 5 single meals (see **Figure 28**). Thanks to the clinical risk assessment capabilities of BGI, this algorithm optimizes controllers that minimize the clinical risk associated to patient's glycaemia. This tuning method is further detailed in Olçomendy et al. [103]. Thereafter, another method with a minor difference have been developed to improve the tuning results with CGM: the *fmincon* function is no longer used to select the optimal parameters of the controller. Instead, average parameters are derived from the 10 best controllers provided by the GA, i.e., the ten best controllers of the last generation. This eliminates an unfair disadvantage induced by *fmincon* when it comes to tuning controllers paired with noisy CGM sensors.

2.4.3 Glucose intake scenarios

To produce the results presented in Chapters 3 and 4, countless simulations have been performed with a variety of glucose intake scenarios. Rather than listing all these scenarios, we will describe in this section the methodology we used to define these scenarios.

For **development purpose** (either biosensor model development or controller parameters tuning), **single meal scenarios** were mostly used. Both unrealistic and realistic T1D patient's meals were simulated and the meal duration was always set to 15 minutes. Realistic glucose intakes were defined in accordance with the total daily carbohydrates intake observed in American T1D adults [104]. Meal times were set in function of the objective of each simulation.

For **validation purpose** (either biosensor models comparison or AP system performance assessment), **multi-meal scenarios** were used. These scenarios mostly involved realistic daily glucose intakes and the predefined meal pattern of the T1DMS (3 meals, 2 snacks a day) was used. Meal duration was also set to 15 minutes. The meal scenarios being investigated for validation purpose were realistic 48-hour scenarios but the performance assessment was always performed on the second day in order to remove any initial transient dynamics from the analysis. Performance analysis was performed on 24 hours so that the metrics expressed as a percentage were computed on a whole day and could be compared from one scenario to the other. The scenarios used for development purpose were shorter scenarios (typically 10-hour long scenarios).

Finally, the number of times a **scenario was repeated** to compute performance metrics was set to 25 as soon as random phenomena were modelled in the simulation (e.g., CGM noise, carbohydrates counting errors).

2.4.4 A framework to improve research work robustness

A **versatile framework** was developed to simulate various architectures of AP systems with a unique Simulink file. The framework relies on a modified version of the T1DMS testing platform. This testing platform implements a **highly configurable AP architecture**. It

relies on custom configuration functions, structures, and databases (see **Figure 29**). Two separate databases were built: a database containing all the versions of the biosensor models and another one containing the controllers that have been designed.

This framework has been designed to be easily upgraded. Indeed, two selection modules are implemented in the Simulink testing platform file to build any AP system from a set of sensors and controllers. In addition, the sensor and controller models were standardized and are highly configurable via a set of parameters (stored in the dedicated database). For example, an enable parameter is implemented to activate or to deactivate the integral action of the PID controller so that the same PID Simulink module could serve for the simulation of a PD or a PID controller. This design notably anticipates the need to compare our controllers with the controllers developed by the ARIA team. The framework accelerates the simulation work as it allows the user to write MATLAB scripts automating the comparison of several AP architectures. Indeed, the user can now launch several repetitions of several scenarios (built-in features of the T1DMS) with various AP systems at the same time (added feature). An appropriate data logging system was also designed. It completes the native T1DMS results structure with information describing the AP system (i.e., which sensor-controller pair is being simulated). Finally, a systematic performance analysis of the results is performed and added to the results structure. All the information and simulation results are automatically stored in a dedicated directory to ease the subsequent interpretation work. In so doing, this framework **substantially increases the robustness of the *in silico* investigations**.

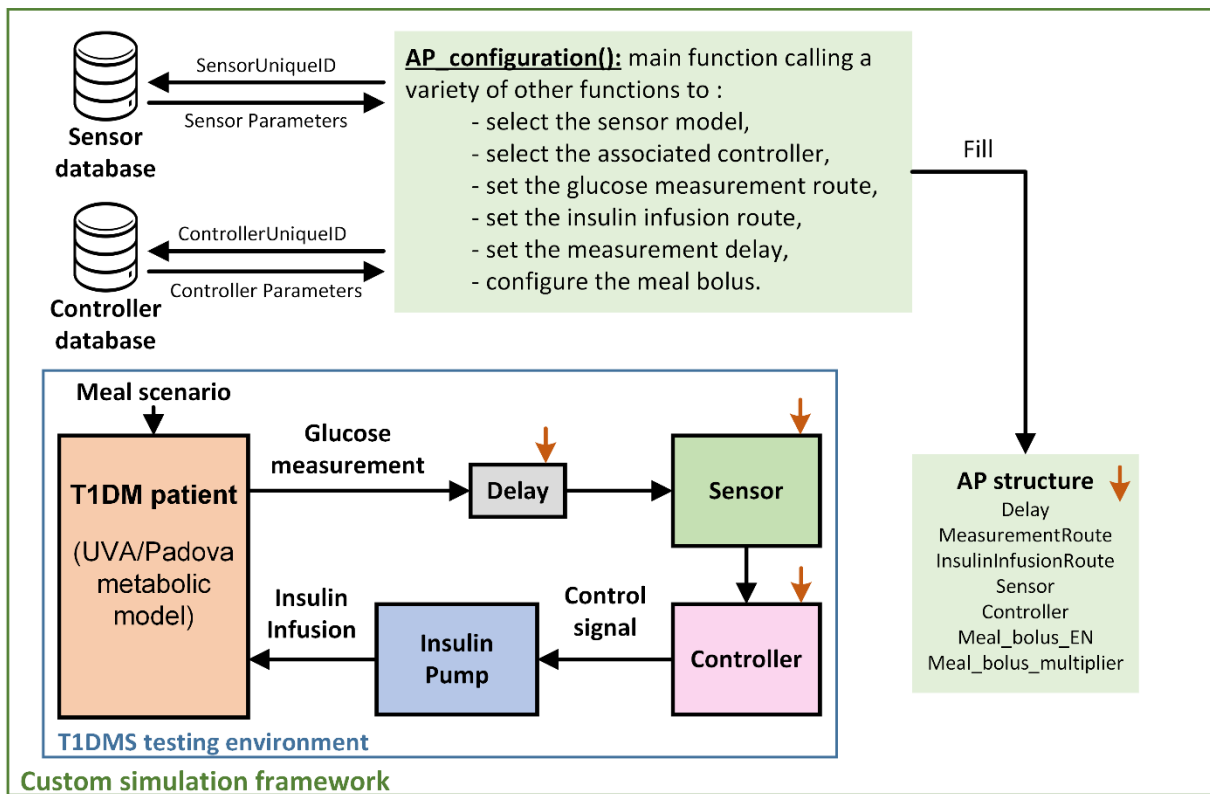


Figure 29: Illustrative scheme of the custom simulation framework mode of operation

2.5 Glucose control assessment

One of the most important questions I had to answer with this doctoral thesis could be formulated as:

What is a normal (healthy) response to glucose intake?

This question may appear simple, but it actually requires a thorough answer. Indeed, it exists as much healthy glycaemic response to a meal as individuals presenting a normal glucose tolerance. This reportedly high inter-subject variability [105] is completed by both daily and day-to-day intrasubject variabilities which further complicate the definition of a reference healthy glucose profile.

In this section, I will present the methods and metrics used both as criteria during the development phase (e.g., biosensor model development, controller calibration) and as performance indicators during the validation phase (e.g., models comparison, closed-loop performance assessment). I will not only focus on the techniques I finally selected but also on the techniques that I have used earlier on, as the pathway I followed appropriately outlines: 1) the subtle discrepancies between countries when it comes to define a healthy glucose response to meals, 2) the difficulties that answering this question could cause (e.g., lack of international consensus, differences between recommendations by health authorities), and 3) the prime importance of considering these choices when interpreting the obtained results.

To address my initial question, and to define the characteristics of a healthy glycaemic response to carbohydrates intake, three sources of information were used on a regular basis. Prof. Bogdan Catargi, diabetologist, provided us with insights on the common practices at Bordeaux University Hospitals while sharing with us his expertise on diabetes treatment. Recommendations published by health authorities in the US and Europe were studied. Finally, a careful bibliographic research has been sustained to update our set of **performance assessment metrics**. To further emphasize this latter aspect, I will present these criteria in their chronological order of use.

2.5.1 A criteria to assess glycaemic profiles

Mean glucose - For decades, the only means to assess glycaemic control on extended periods of time was **HbA1c level** measurement. HbA1c is commonly expressed as a percentage representing the fraction of glycated haemoglobin relative to total haemoglobin. It was first proposed in 1976 by Koenig et al. to assess diabetes management [106]. As mentioned in Chapter 1, the DCCT/EDIC studies established that lowering HbA1c level of T1D patients has a positive impact on the risk for severe complications observed in these patients on the long-term. HbA1c therefore became both **the ‘gold-standard’ metric** to optimize insulin therapy and the prime outcome of many clinical trials. The World Health Organization (WHO) notably recommends an HbA1c of 6.5% as a cut-point for diagnosing diabetes. According to an online conversion calculator provided by the American Diabetes Association, this HbA1c level is equivalent to a mean blood glucose of 140 mg/dl. Nowadays, **CGM** enables the computation of the **mean blood glucose level** of patients with an increased flexibility (e.g., daily, weekly, and monthly averages), compared to HbA1c which can only be used as a proxy

to estimate a three-month average of blood glucose level. CGM thus tends to replace HbA1c level measurement to assess glycaemic control of T1D patients [49]. In this work, the mean blood glucose of virtual patients was routinely computed to assess blood glucose profiles.

Time spent in euglycaemia - Although well correlated with long-term outcomes, HbA1c is intrinsically poorly reflecting acute hyper- and hypoglycaemic events. Thus, tight glycaemic control long required the patients to multiply finger-prick blood testing throughout the day. Nowadays, CGM sensors enable the estimation of blood glucose concentration with an exquisite resolution. The growing adoption of CGM technology notably permitted the development of a variety of new glucose control metrics. Among them, the CGM-derived times in the glucose ranges have been acclaimed. In particular, the time in the **euglycaemic range (70-180 mg/dl)** is becoming a gold-standard. It appropriately completes the computation of the average blood glucose level by taking into account the occurrence of extreme glycaemic events. Furthermore, it is generally preferred to other metrics thanks to its straightforward meaning for real-life diabetology. It will be further referred to as the **Time In Range (TIR)**.

Time spent in a predefined target area - While demonstrating the importance of lowering the mean blood glucose level of patients suffering from diabetes, the DCCT also emphasized the increased risk for hypoglycaemia induced by intensive insulin treatment. Mitigating both the risk for long-term complications, i.e., reducing HbA1c level, and the occurrence of hypoglycaemic events therefore requires **diminishing glucose variability**. As a consequence, this latter parameter is increasingly considered as a primary marker of glycaemic control and several related metrics were developed [49]. HbA1c and TIR fail to thoroughly represent glucose variability and mean glucose level: as illustrated in **Figure 30**, identical HbA1c or TIR values (here respectively 6.5% and 100%) represent many glycaemia profiles.

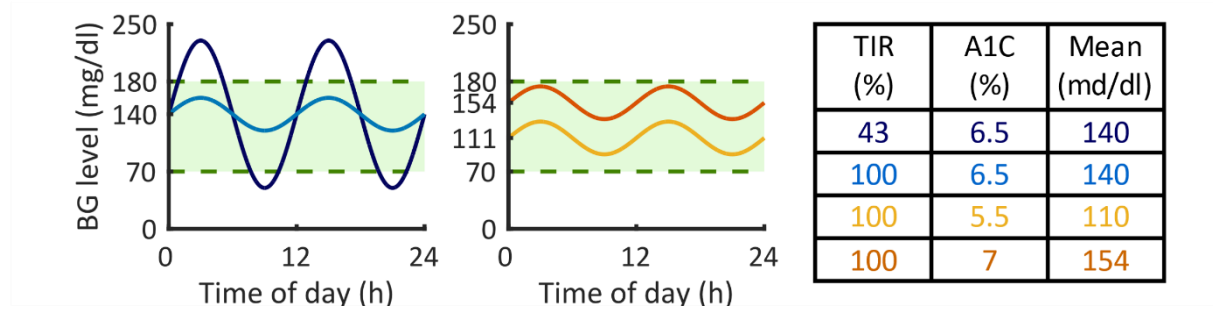


Figure 30: Many faces of 6.5% A1C and 100% TIR.

To account for the between-meal variability of glycaemia, we then developed a method consisting in the **definition of a target area** (see **Figure 31**).

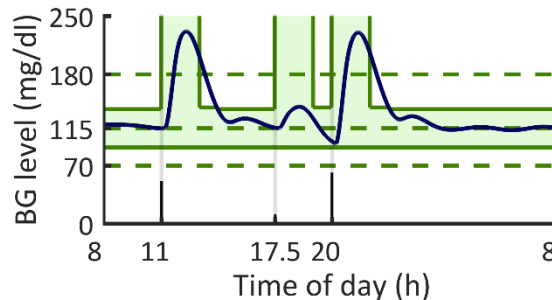


Figure 31: Definition of a target area (in green) based on meal scenario

Between meals, the target area is narrowed to an 80-120% range centred on the target blood glucose level (115 mg/dl in this example). For each meal, the upper limit is removed for a 2-hour period beginning with the start of the meal, and set to 140 mg/dl during the third hour after the meal. This target definition matches the ADA definition of a normal glucose tolerance [107]. The definition of this target area enables the computation of a metric, further referred to as the **time in target area**, which determines how “physiological” the considered glucose profile is.

The Blood Glucose Index - Although providing satisfactory results, the performance assessment using the time in a predefined target area as no recognized clinical relevance and requires choices (e.g., target width, duration of mealtime window) which were difficult to relate to official recommendations for patients. In contrast, Kovatchev et al. introduced, in 2005, the **Blood Glucose Index (BGI)**, a metric designed to analyse the BG dynamics from a **risk perspective** [108][109]. The BGI associated with a glucose concentration G is defined by **Equation 4**.

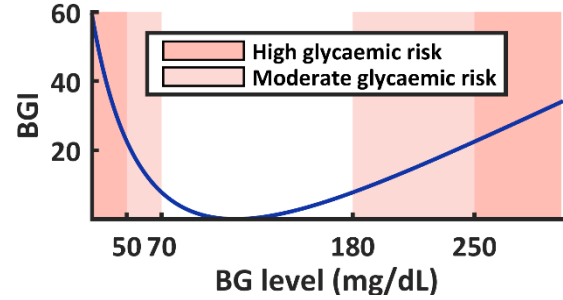


Figure 32: Blood Glucose Index risk function

$$\text{BGI}(G) = 10 \times (1.509 \times (\ln(G)^{1.084} - 5.381))^2 \quad (4)$$

The BGI provides a symmetrical index to handle the asymmetric risk distribution around the patient target BG level: elevated glucose levels can be tolerated by a patient for some time, while hypoglycaemia quickly becomes life-threatening (see **Figure 32**). This index relevantly penalises the major adverse glycaemic events, i.e., acute hypo- and hyperglycaemia, excessive variability, high mean BG level. As a very complete metric to assess glycaemic profiles, it was then regularly used in this work to algorithmically assess large sets of glucose profiles or in the cost function of optimization algorithms.

2.5.2 Systematic performance assessment with reference metrics

The considerable progress and increased popularity of CGM [110] resulted in a need for standardization of performance metrics in both closed- and open-loop insulin therapies. To this end, **recommendations regarding CGM metrics** were formulated in 2017 [111]–[113]. At the 2019 Advanced Technologies & Treatments for Diabetes (ATTD) annual congress, a panel of international CGM technologies experts agreed on these metrics and defined their clinical targets for different diabetes populations. The consensus was published and endorsed by several diabetes professional associations such as the American Diabetes Association (ADA) and the European Association for the Study of Diabetes (EASD) [114]. We selected and integrated in a function for systematic performance eight of these recommended metrics and their associated targets, all detailed below. These metrics have been preferentially used on validation results but also during the development stages.

- **Mean Glucose:** mean glucose is a common performance indicator of insulin delivery therapies. In an *in silico* environment, estimating the blood glucose concentration does

not require the use of HbA1c as a proxy or of CGM datasets. The mean glucose is directly computed with the blood glucose concentration values provided by the simulator.

- **Time In Range (TIR):** time spent in a given range by the glycaemia of a patient is a widely used indicator to assess performance of AP systems. TIR refers to the time spent in normoglycaemia (70-180 mg/dl).
- **Time Below Range (TBR 1 and TBR 2):** the time spent below a given BG level. The first considered level is 70 mg/dl (TBR 1) and the second one is 54 mg/dl (TBR 2).
- **Time Above Range (TAR 1 and TAR 2):** the time spent above a given BG level. The first considered level is 180 mg/dl (TAR 1) and the second one is 250 mg/dl (TAR 2).

As T1DMS does not label “high risk patients” (according to the nomenclature used in Battelino et al. [114]) in its cohort, we therefore considered that the whole cohort was constituted of “normal” T1D patients. The simulation results were therefore compared to the targets below, recommended for this diabetes population [114]: **TBR 2 < 1%, TBR 1 < 4%, TIR > 70%, TAR 1 < 25%, and TAR 2 < 5%.**

In 2005, together with the previously-mentioned BGI, Kovatchev et al. [108] introduced two additional metrics derived from BGI:

- **Low BGI (LBGI):** This metric is a measure of the frequency and extent of low BG readings and has been validated as an excellent predictor of severe hypoglycaemic events.²⁹ The T1DMS User Guide indicates that LBGI can be considered minimal ($LBGI < 1.1$), low ($1.1 \leq LBGI < 2.5$), moderate ($2.5 \leq LBGI < 5$), and high ($LBGI > 5.0$).
- **High BGI (HBGI):** This metric is a measure of the frequency and extent of high BG readings and showed reliable performances in predicting risk for hyperglycaemia.²⁹ HBGI can be considered minimal ($HBGI < 5.0$), low ($5.0 \leq HBGI < 10.0$), moderate ($10.0 \leq HBGI < 15$), and high ($HBGI > 15.0$).

In addition, the **Total Daily Insulin (TDI)** is systematically computed for performance analysis during both development and validation phases. There are neither official recommendations nor targets concerning the TDI infusion for T1D patients because insulin needs vary greatly across the patient population according to their diet, physical activity or their own physiological characteristics. However, TDI still is an interesting indicator to objectively compare different regulation strategies for a given patient. It is also useful to detect deficient or excessive aggressiveness in the tuning of the controllers.

Normality of the performance metrics data was also tested, when necessary, using the Shapiro-Wilk test to subsequently assess statistical significance using either the two-sided paired sample t-test or the two-sided Wilcoxon signed rank test. P-values lower than 0.01 were considered significant.

Chapter 3

In silico validation of the biosensor's working principle

The first chapter provided key knowledge about the physiological mechanisms ensuring nutrient homeostasis, about its impairment induced by diabetes, and the currently available therapeutic options. It also provided a description of our biosensor, its working principle, and the research project which permitted its development. The second chapter detailed the material and methods which yielded the results presented and discussed in Chapters 3 and 4, from the *in vitro* experimental data obtained with murine islets to the mathematical modelling of the biosensor in order to implement an *in silico* biosensor-based AP and test it in the UVA/Padova T1DM Simulator.

In this third chapter, a first series of simulation results are presented. The chapter is structured in chronological order to emphasize the progression of my scientific reasoning throughout these three years. The answers I gave to the questions that arose are presented together with the issues I encountered, the solutions I envisaged and the ones I explored.

This chapter focuses on the use of **simulation for fundamental research purposes**. The actual biosensor models implemented in the UVA/Padova T1DMS testing environment are described. They are then compared by using a well-suited configuration of the T1DMS. It uses intravenous glucose measurement and insulin infusion routes to limit the number of external elements which skew the comparison between models and to reproduce the natural environment of the healthy endocrine pancreas. The pancreas model is “removed” from the virtual diabetic patient model and replaced by a **behavioural model of the pancreatic islets electrical activity**, calibrated using *in vitro* experimental data acquired with our biosensor.

The blood glucose regulation capabilities of the electrically-characterised islet algorithms are investigated *in silico* using their mathematical models. As the islets are the main constituent of the biosensor, this work aims at **assessing the performance of the islet algorithm models** in a blood glucose control loop. In so doing, it would provide an *in silico* **proof-of-concept** validating electrical measurement as a means to characterise and study the secretory activity of islets of Langerhans (either murine or human islets) with our sensor.

The first subsection reviews the results obtained with biosensor models and a T1DM simulator implemented using the Python programming language by Dr Antoine Pirog³⁴, who formerly worked in the ELIBIO team as a PhD student [115]. This section also presents preliminary results obtained with a very similar closed loop implemented in the MATLAB/Simulink environment. Although the structure of the islet algorithm models

³⁴ In the following chapters, any result not obtained directly by the author is explicitly attributed to its owner.

remained unchanged, a new calibration was performed using new experimental data to promote homogeneity across models. These updated models are presented in a second subsection. The following subsection describes the development of a methodology enabling the computation of insulin need in virtual patients thanks to the output of the islet algorithm models whose input is the patient's blood glucose level. For the sake of concision, this third subsection is illustrated with the results of a single patient and using only one islet algorithm model. Contrariwise, the fourth subsection presents extended results obtained with the whole virtual T1DM cohort of the UVA/Padova T1DMS and a comparison between two different islet algorithm models. Finally, the closing subsection discusses the different results presented in this chapter.

3.1. Preliminary results

This subsection presents the very first simulation results obtained during my PhD thesis. First, I tried to reproduce the results obtained by Dr Pirog with a Python-based BG regulation closed loop [115]. Even though my final objective was to implement this closed-loop in the MATLAB-based UVA/Padova testing environment, it allowed me to better understand how the different constituents of the closed-loop had been developed (e.g., the biosensor models, the UVA/Padova T1DM metabolic model) and were interacting together to yield the results obtained by Dr Pirog during his PhD thesis. This work has proved to be essential to outline some **limitations of the S2008 version** of the simulator and to conceive my own research approach using the S2013 version. It also allowed me to **identify some errors and weaknesses** in the design of our biosensor-based closed loop. The second part of this subsection presents preliminary results obtained with a MATLAB/Simulink implementation of the biosensor models. These results permitted to **highlight the differences between the S2008 and S2013 versions** of the UVA/Padova T1DM Simulator and to **learn how to use the simulator (S2013)**. This preliminary stage also allowed me to **refine my research approach** by defining both the objectives that could realistically be achieved using simulation and a working plan for the three years of this PhD thesis.

3.1.1. A custom implementation of the S2008 T1DM Simulator

3.1.1.1. Dalla Man's meal simulator of glucose-insulin system

The preliminary results presented in subsection 3.1.1 were obtained using a custom implementation (Python language) by Dr Pirog of the **meal simulator of glucose-insulin system** published by Dalla Man et al. in 2007 [86]. As described in Chapter 2, this simulator models the glucose-insulin interactions consecutive to a glucose intake at both organ/tissue and whole-body levels. The first version of this metabolic model accurately simulates the response of a healthy individual to a meal. As our research is focused on T1D, the model's parameters were modified to account for the physiological differences induced by T1D following the method published by Dalla Man et al. [97]. The insulin secretion module was substituted with a subcutaneous insulin infusion module to enable the simulation of insulin therapy. To account for the higher basal glucose level observed in T1D patients, the basal endogenous glucose production is higher (as a result, plasma glucose clearance is lower than normal). The simulated subject is assumed to achieve good glycaemic control, all the other parameters are then kept at values of the normal subject.

3.1.1.2. Closing the loop with a model of the biosensor

To regulate the blood glucose level of the virtual T1D patient described in the last section, an *in silico* closed loop involving our biosensor and an “insulin pump” was then implemented. The biosensor model was rather complex. It was constituted of a Cell SP model generating a SP signal connected to a Python implementation of the processing algorithms embedded in the Multimed acquisition system (see 2.1.3) which outputs the measured SP frequency (see **Figure 33**). The Cell SP model was built from two separate blocks: a SP frequency generation block (see 2.3.4) and a SP waveform generation block able to synthesize

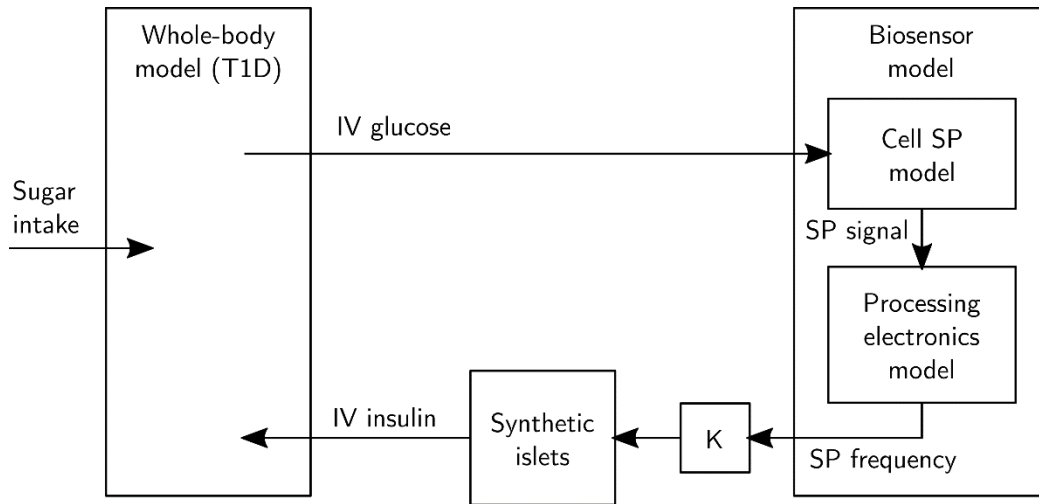


Figure 33: *In silico* blood glucose regulation closed loop implemented using a Python implementation of Dalla Man's meal simulation model

frequency-modulable SP waveforms using an average SP shape converted into a periodic function using Fourier series. The SP frequency signal generated by the biosensor model was then scaled by a factor K (which could be seen as a proportionate controller). No insulin pump model was available at this time, Dr Pirog then decided to use a synthetic islet model instead [89]. The unitary output of this islet model was then scaled up to simulate a population of 80 000 secreting islets. The simulations using this closed-loop aimed at verifying that SP frequency could indeed control insulin infusion and mimic physiological insulin secretion using the most direct measurement and injection routes (IV glucose, IV insulin). While unrealistic from a clinical point of view, these methods of measurement and infusion seemed fair in the absence of a dedicated regulation controller.

3.1.1.3. Closed-loop results

Using the Python implementation of Dalla Man's meal simulator of glucose-insulin system, we simulated a **realistic 3-meal 2-snack glucose intake** scenario to assess the performance of the closed-loop regulation scheme presented in the previous section. In these simulations (see an illustration in **Figure 34**) we compared a virtual healthy subject (its model parameters are available in [86]) to a virtual T1D subject (its model parameters are derived from the healthy subject as in [97]) treated with a biosensor-based closed-loop insulin therapy. Two versions of the latter regulation scheme are presented. The first one involves the Static model of islet response to glucose concentration variation when the second one involves the Hysteretic model (see 2.3.4). The simulations yielded plasma insulin profiles which clearly depict the differences between the two models with the hysteretic model responsible for shorter but higher insulin peaks in response to meals. On a broader level, the biosensor-based regulation schemes ensured very **satisfactory performance** with near normal glucose profiles: the TIR were 97.2% and 100%,³⁵ and the mean glucose level were 119 mg/dl and 117 mg/dl (for Static and Hysteretic models respectively).

³⁵ TIR: Time In Range (see section 2.5.1)

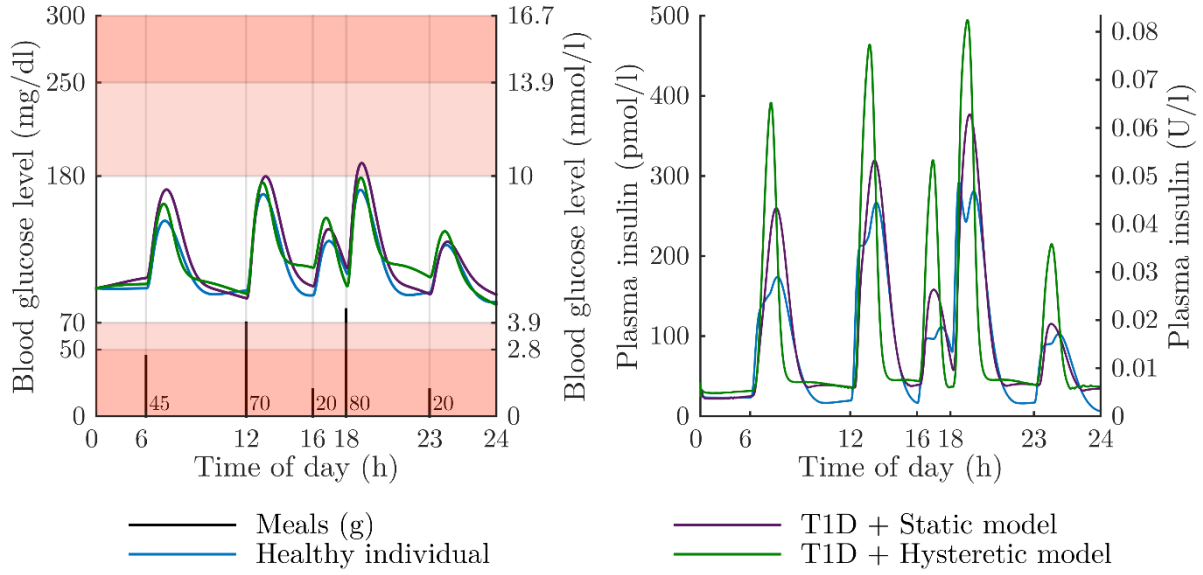


Figure 34: Blood glucose profiles of a healthy individual and a virtual T1D patient submitted to a realistic 24-h glucose intake scenario composed of 3 meals and 2 snacks. Insulin infusion of the T1D patient is regulated using the output of the biosensor model (two different models are simulated).

3.1.1.4. Limits of these preliminary results

Using the Python programming language, Dr Pirog demonstrated the **feasibility of modelling a BG regulation closed-loop** including a model of our hybrid bio-electronic sensor. He notably achieved satisfactory results with a virtual T1D patient as highlighted by the time spent in the normoglycaemic range and the quasi-normal shape of the glycaemic response (see **Figure 34**).

Although the analysis of the insulin profiles clearly emphasizes the contribution of the Cell SP model, this *in silico* closed loop suffers from **major limitations** which prevent us to draw any stronger conclusions. Indeed, the use of a synthetic islet model as an insulin pump model interferes in the result interpretation and makes it difficult to understand whether the good results should be attributed to the Cell SP model or to the synthetic islet. As in some sense, the biosensor's output acts as an image of the patient BG concentration, the synthetic islet model fed with the output of the biosensor could be seen as a gross model of the pancreas, thus explaining the satisfactory results obtained with this closed loop.

Another limitation concerns the definition of the virtual T1D patient. As previously mentioned, the virtual T1D patient used here is a healthy individual which was rendered diabetic by modifying few parameters. Although this method is satisfactory in a first approach, it does not allow to fully capture the modifications induced by the disease in the patient's body. Another issue comes with the use of a single patient which prevents to model the inter-patient variability observed in a real T1D cohort.

In my opinion, this last point also emphasizes a limit of this preliminary work: the adaptation gain K used to calibrate the closed loop was set manually and without any objective criterion. Although this method is satisfactory and efficient when working with a single virtual patient and proved to yield good results, the study of more than one patient requires the

definition of a standardized method to set this parameter both for efficiency and reliability purpose. It would also strengthen the comparison between patients by removing the random level of optimisation induced by the manual tuning of K value.

The preliminary results presented in section 3.1.1.3 are a comparison between the response to meals of an insulin-treated virtual T1D patient and a healthy individual. They thus raise another question: **how to define a healthy individual or a physiological glycaemic response to a meal?** This question is one of the key scientific questions I have attempted to answer throughout this PhD thesis. It is a complex question since the response to a meal is highly variable in the population with normal glucose tolerance. The direct comparison of glucose profiles therefore seems limited and a better method is required.

Some of the limitations described above (e.g., T1D patient definition, insulin pump model) result from constraints imposed by our custom implementation of Dalla Man’s simulator [86]. The purchase, at the beginning of my thesis, of a licensed version of the UVA/Padova T1DM Simulator (S2013) provided a solution to these problems. Indeed, the S2013 simulator includes built-in insulin pump models and a cohort of “true” virtual T1D patients. Indeed, virtual patients generation have been refined and model parameters were obtained using the data of real T1D patients who underwent a triple tracer protocol to study the glucose-insulin dynamics with a great precision [96], [98]. The virtual T1D cohort contains 11 adults, 11 adolescents and 11 children, and matches the real-life variability of T1D patients (see Appendix 4).

Although the S2013 simulator did solve some issues raised by these preliminary Python results, essential questions remained unaddressed. Thereupon, my objective was to develop a research approach that addresses these questions which can be succinctly formulated as follows:

- Q1: How to define a normal response to glucose intake?**
- Q2: How to assess a glycaemic profile using an objective criterion?**
- Q3: Which is the best criterion to assess glycaemic profiles?**
- Q4: Is there a unique gain K value that ensures optimal performance?**
- Q5: How to meaningfully compare the different biosensor models?**
- Q6: How to quantify the contribution of our biosensor in the overall closed-loop performance of the control system?**

3.1.2. Implementation of the biosensor models in the MATLAB/Simulink environment

This subsection presents early results obtained with the **S2013 commercial version of the UVA/Padova T1DMS**. These preliminary simulations (which were conducted during several months) allowed me to better master the simulator while refining my research approach. They also helped consolidate a research plan for my PhD thesis.

The T1DMS is a set of MATLAB scripts which provides a highly configurable testing environment for AP systems. A GUI³⁶ allows the user to define the simulation scenario, i.e., the simulation duration, the initial conditions, the meals and the open loop treatment parameters. It also provides a convenient interface to select the patients and the hardware (e.g., CGM sensor, noise-free insulin pump) to simulate, and the outcome measures to compute (see 2.4.1 for further details about the T1DMS). Thanks to its easy-to-use GUI the simulator does not require any programming skills. The T1DMS however lacks features enabling automated simulations. It is possible to repeat a given scenario several times but the user manual does not mention any command-line mode of operation or any feature enabling the launch of simulations from a custom MATLAB script. Thereupon, I decided to develop my own **set of scripts to automate simulation**, results saving in a well-organised repository, logging, and systematic performance analysis (using the metrics described in section 2.5.2). This task seemed achievable thanks to the design of the T1DMS which relies on text files and MAT-files to store data (e.g., model parameters, scenarios, simulation results) and could thus be read from any custom script.

The T1DMS also embeds a testing platform, in the form of a configurable Simulink file, where the user can implement a custom system (either a controller or an algorithm) to drive the insulin pump which ensures continuous insulin infusion to the virtual T1D patients. My first task with the T1DMS, was thus to implement the closed loop described in section 3.1.1.2 with a difference residing in the absence of the synthetic islet model, which was replaced by the built-in insulin pump model. Only few technical difficulties had to be overcome since Python and MATLAB programming languages are similar.

Another difference with 3.1.1 lies in the virtual patient definition: the unique T1D adult patient was replaced by a cohort of 33 patients. As a consequence, the K value had to be adapted to this new configuration and a strategy had to be chosen to handle the inter-patient variability. In a first approach, K value was tuned individually with a single meal scenario (70g) and using a methodology aiming at minimizing the TIR.

Early results, obtained with this coarsely calibrated closed loop, highlighted two sensitive points:

- **Initial conditions setting**

The T1DMS offers the possibility to either set the initial glucose level to a value configured by the user (the same for all patient) or set it to the fasting glucose level of the patient (an individualized parameter provided by the simulator). This setting has a limited influence on the whole simulation (see **Figure 35**) and, after discussion with our clinical partner (Prof. B. Catargi), I decided to set the **initial glucose level to the Subject Specific Fasting BG**. This choice appeared to be the more realistic from a clinical point of view and eases inter-day comparisons (in the case of scenarios lasting more than 24 hours).

³⁶ GUI = Graphical User Interface

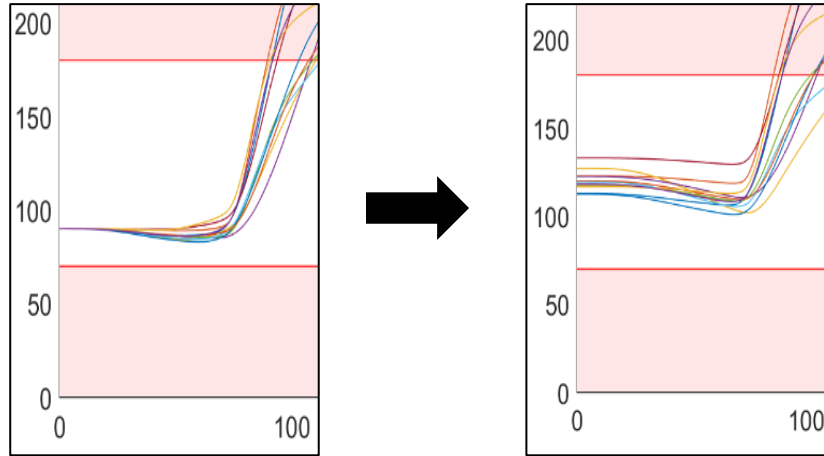


Figure 35: Initial 100 minutes of a T1DMS simulation: modification of the initial blood glucose level setting. Left: unique initial glucose level. Right: initial value is set to the patient fasting glucose level.

- Influence of the Multimed processing algorithms model

The first simulations also revealed the critical impact of some parameters of the processing algorithm models on the closed-loop performance (results obtained with the Static model are displayed in **Figure 36**). In the Multimed system (see 2.1.3), the average frequency of the SPs (Slow Potentials) is computed over a configurable time window using a low-pass filter whose cut-off frequency F_c is set via a parameter named n (see **Equation 5** - the higher the parameter n is set, the lower the cut-off frequency is).

$$\frac{1}{F_c} = 2^n \left(1 - \frac{1}{2^n}\right) 2\pi T_s, n \in [0; 17] \quad (5)$$

This filter computes the average frequency and thus smooths the signal to limit oscillations of the biosensor's output. A trade-off therefore appears between the responsiveness of the system and the smoothness of the output. The parameter n influences the overall responsiveness of the system and impacts the closed-loop performance: the higher is the time-window used to compute the SP frequency, the lower are the responsiveness of the system and the performance. **Figure 36** displays the best results obtained with a basic tuning algorithm of the K value. It consists in a parametric analysis from which the K value which ensures the highest time spent in normoglycaemia is selected. The comparison between panel A ($n=7$, $F_c \simeq 21,66$ Hz) and panel B ($n=9$, $F_c \simeq 5,40$ Hz) emphasizes the impact of the cut-off frequency of the Multimed averaging filter. The tuning algorithm selected K values which were much higher (leading to a more aggressive regulation) when F_c was higher thanks to the resulting better responsiveness of the closed-loop system. The loss in performance between three configurations ($n = 7$, $n = 9$, and a reference condition without any filter) was then quantified using three performance indicators: the Time In Range, the mean BG level, and the mean Blood Glucose Index (BGI) (see **Figure 36C**).

This responsiveness/smoothness trade-off is the consequence of technical choices in the design of Multimed, motivated by FPGA resources savings, but other solutions do exist to

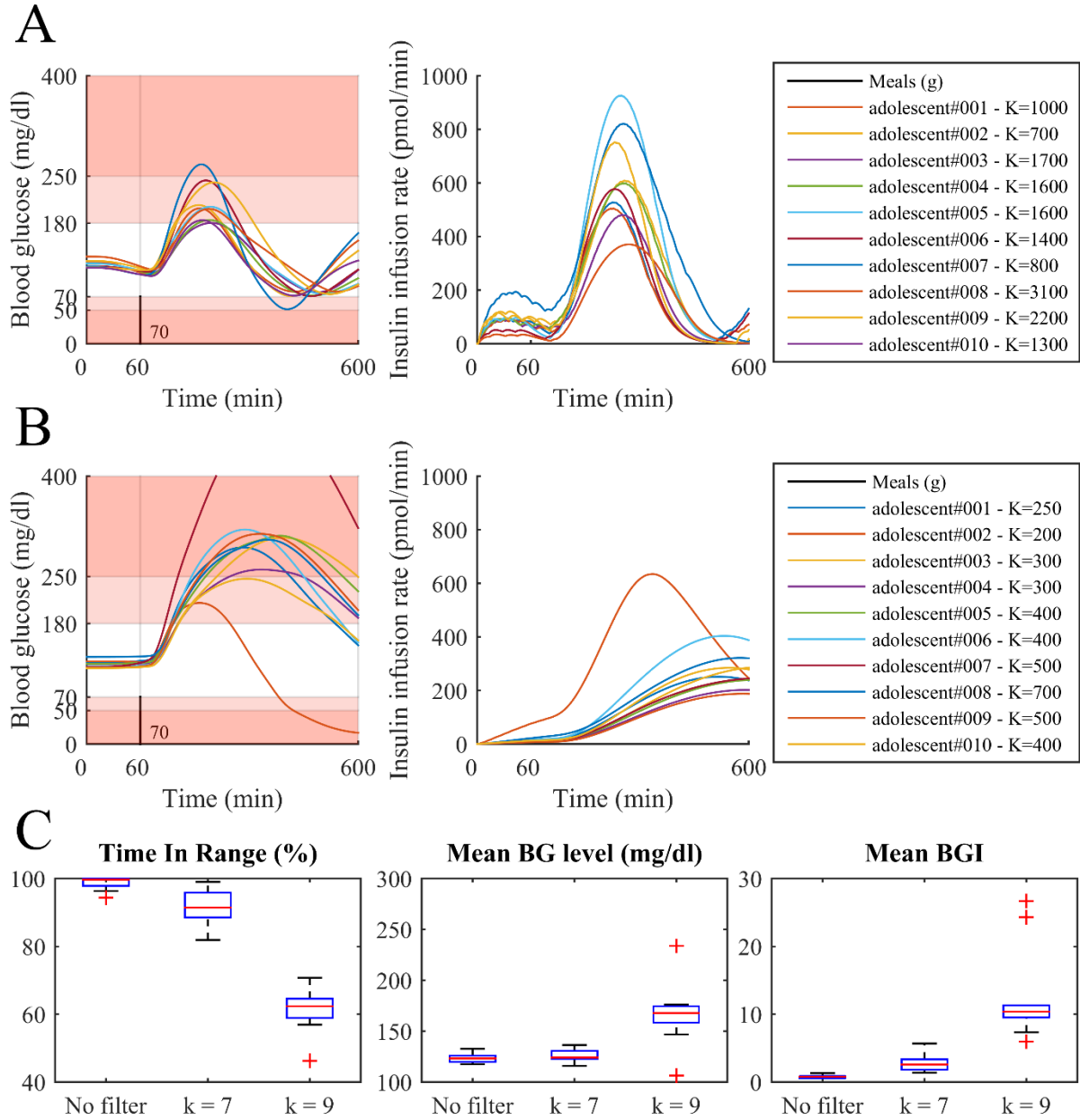


Figure 36: Impact of the low-pass filter cut-off frequency. A) Blood glucose level and subcutaneous insulin infusion profiles for 10 adults subjected to a 70-g meal ($n = 7$, $F_c \approx 21,66$ Hz) B) Blood glucose level and subcutaneous insulin infusion profiles for 10 adults subjected to a 70-g meal ($n = 9$, $F_c \approx 5,40$ Hz) C) Impact of Multimed averaging filter on the closed-loop performance assessed with Time in Range, Mean Blood Glucose (BG) level, and Mean Blood Glucose Index (BGI).

compute a frequency value in real-time. Making the assumption that measuring the SP frequency in real-time with minimal delay does not constitute a technological barrier, I removed the model of Multimed from the biosensor model implemented in the T1DMS. In so doing, we assess the potential of our technology as if the acquisition system performs an **ideal recording of the embedded islets' activity**, i.e., without any significant bias. This choice is also justified by the fact that the acquisition system is likely to be modified in the future and that the purpose of this *in silico* work is to evaluate its working principle rather than the performance of its actual physical implementation. As a consequence, the biosensor model has been reduced to the **islet algorithm model**.

3.1.3. A consistent research strategy

The first year of my PhD thesis yielded preliminary results which highlighted some limitations of our approach and raised scientific questions as stated in 3.1.1.4. They thus permitted to settle a working plan for the following two years which addresses my thesis objectives. These results highlighted the need to develop **algorithms to automate tasks included in the simulation work** (e.g., glucose profile evaluation, parameter tuning, data saving, systematic performance assessment). I thus spent a significant amount of time developing automation scripts and set it as a priority during the second year. My objective was then to intensively use the automation scripts to ease and hasten the research work during the third year. The results yielded by this strategy are presented later in this chapter and in Chapter 4.

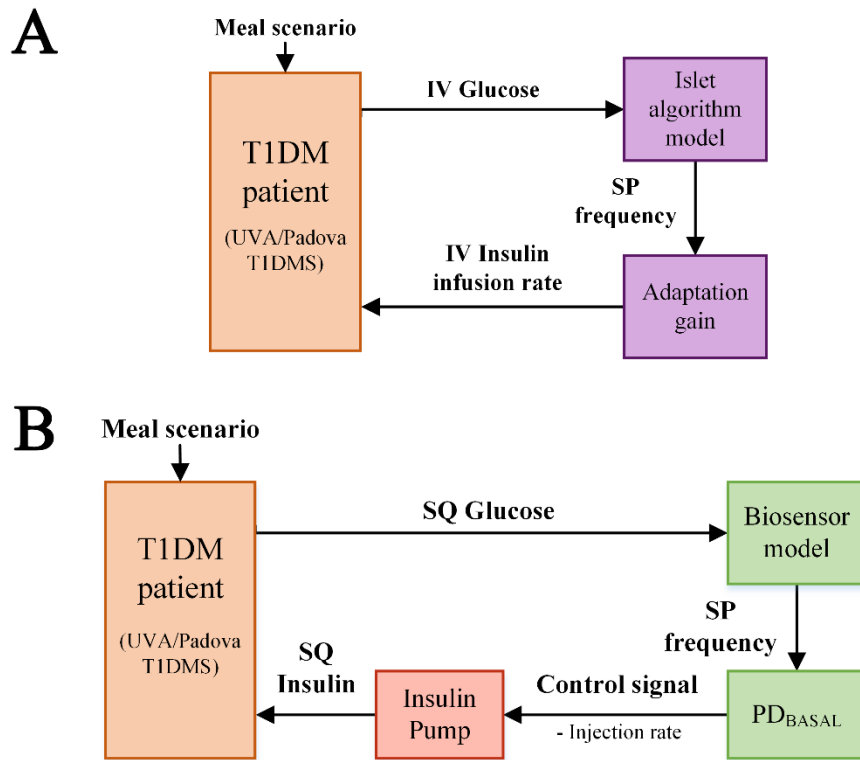


Figure 37: Two separate *in silico* research axes A) IV/IV configuration of the T1DMS used in Chapter 3 B) SQ/SQ configuration of the T1DMS used in Chapter 4

The adopted strategy consisted in splitting the simulation work into two separate research axes. These approaches rely on **two configurations of the T1DMS**: the first one uses intravenous (IV) glucose measurement and insulin infusion routes (it will be referred to as **IV/IV configuration** – **Figure 37A**), whereas the second one uses subcutaneous (SQ) routes (**SQ/SQ configuration** – **Figure 37B**). These two configurations serve distinct objectives: the IV/IV configuration aims at validating the **SP frequency** - measured by the biosensor - as a relevant **indicator of insulin need**, while the SQ/SQ configuration aims at simulating the traditional operating environment of an AP (**Artificial Pancreas**) system to assess the **ability of our biosensor** to provide relevant information to such a system. As the

biosensor model was reduced to its primary component, the islet algorithm model, both approaches use the same models (described in subsection 2.3.4).

In the **IV/IV** configuration, a minimal regulation scheme is implemented. The defective pancreas is “replaced” by a **model of the endogenous islet algorithms** (see 2.2 and 2.3) in series with **an adaptation gain K** enabling the islet model to match the insulin need of the patient. The K value is then individually tuned to handle inter-patient variability. By using the IV routes, this configuration was designed to virtually **place the islet algorithms in their usual environment of operation** (the pancreas is a highly vascularized organ – see 1.1.4) without any delay induced by subcutaneous routes. Our objective here is to assess the potential of the SP signal to provide information on the secretory activity of the islets. By limiting the number of elements affecting the closed-loop performance, this configuration is also convenient to **compare islet algorithm models** presenting a varying level of accuracy to experimental data, in order to assess which characteristic of the islet response to glucose (see 2.3.3) has a physiological relevance for glucose homeostasis.

The **SQ/SQ** configuration aims at simulating an AP with a sensor and a pump (both extracorporeal) which is the **state-of-the-art therapy for T1D patients**. The main difference with IV/IV configuration is the presence of **delays** resulting from **glucose diffusion** in the SQ space and from **SQ insulin absorption** which delays insulin onset of action (see subsection 1.3.3). To notably handle these delays, a controller needs to be designed to close the loop between the sensor and the pump. The SQ/SQ configuration is used to **compare different T1D therapies**: Multiple Daily Injection, a CGM-based AP, and a biosensor-based AP. This approach falls within one objective of our research consortium, which is to design an *in silico* clinical trial to assess the performance of the association of our hybrid bio-electronic sensor paired with the *ad hoc* robust controller developed by the ARIA team at IMS (see section 1.5).

3.2. Islet algorithm models

As explained in subsection 2.3.5, the experimental data recorded during stimulation of the islets with ascending followed by descending glucose ramps (see **Figure 38** and subsection 2.3.3) were **re-analysed with refined detection parameters**. As models did not fit anymore the analysed data (see left panel of **Figure 38**), they needed to be updated. This update was also the occasion to **promote homogeneity between models**. In particular, the maximal frequency is now set close to the same value for all models (see **Figure 38** and **Table 3**). To that end, the parameters of a Hill equation were fit to the experimental data obtained during the ascending glucose ramp and the resulting maximal frequency was subsequently used to constrain the maximal frequency of all the models during their respective identification processes. Two Hill equations were also used to generate the envelope used to generate the Preisach matrix (see subsection 2.3.5) when the former models were using sigmoid functions for that purpose. **Figure 38** presents the differences between former and updated versions of the models.

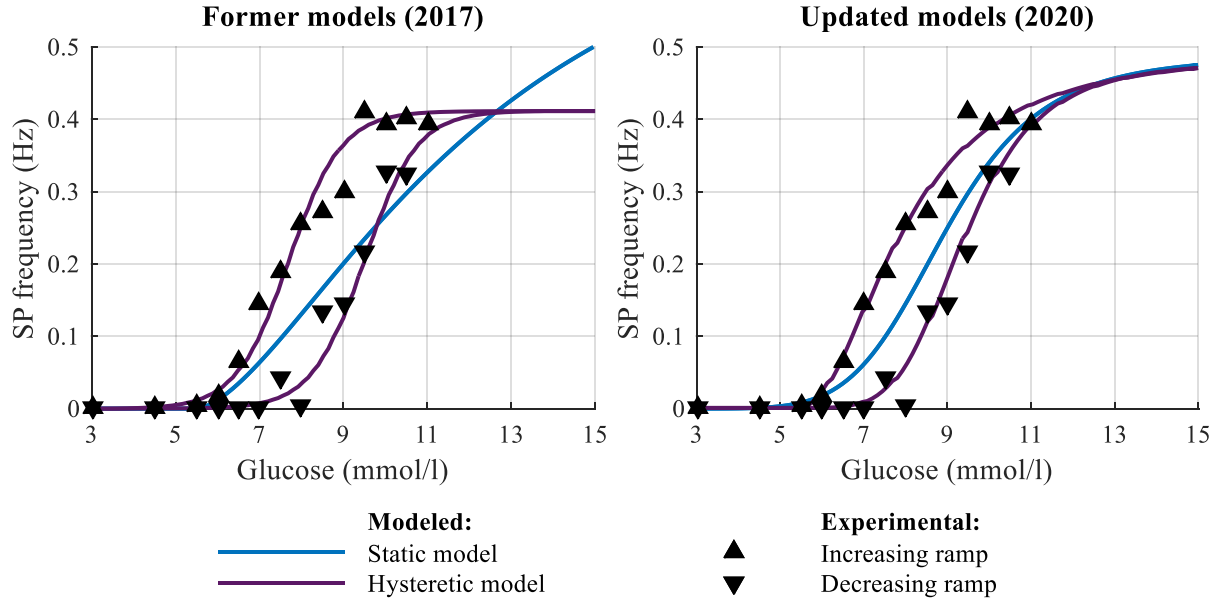


Figure 38: Comparison of former and updated versions of the Static and Hysteretic models. The Static models (blue) and Hysteretic models (purple) are superimposed on the experimental data recorded during the ascending glucose ramp (black upward-pointing triangles) and descending glucose ramp (black downward-pointing triangles).

Table 3 presents the parameters of the Static model and of the Hill equations used to generate the envelope of the Hysteretic model. It has to be noted that the Static model is fitted to the whole experimental dataset whereas this dataset is split in two halves to generate the hysteretic envelope. **Table 3** also presents the goodness of fit achieved with each model (assessed with the coefficient of determination R-squared). It notably highlights the **better modelling** of the experimental data yielded by the **hysteretic model** as compared to the static model (0.82 vs 0.98).

Table 3: Model parameters for Static and Hysteretic models, and corresponding coefficient of determination R^2 . Results are value (standard error)

Parameter	Static model	Hysteretic model		Unit
		Upper envelope	Lower envelope	
G_0	2.0164 (21.5693)	5.3595 (0.5640)	5.6991 (2.2138)	mM
G_{50}	8.9334 (1.7512)	7.9733 (0.1036)	9.6062 (0.0964)	mM
n	5.8934 (23.5199)	2.1880 (0.5418)	4.2883 (2.6972)	.
f_M	0.4867 (0.3388)	0.4921 (0.1001)		Hz
R^2	0.8317	0.9859	0.9790	

3.3. Adaptation to patient needs

Our hybrid bio-electronic sensor records the electrical activity of the islets it embeds. We demonstrated that SP frequency is sensitive to various regulators of insulin secretion (see subsection 2.3.3). The biosensor thus appears to be a potential **proxy to estimate islet secretion**. In contact with the fluids of a patient, we hypothesize that the biosensor output can help determine their insulin need. The real biosensor embeds several islets, but its mathematical model simulates the electrical activity of a single islet (in the form of a SP frequency signal). As a consequence, the model virtually accounts for the secretion of a unique islet and its output signal has to be “scaled” to represent the secretion of the whole pancreas, i.e., the prevailing insulin need of the patient. This section presents different methods to perform this scaling operation. For the sake of concision, results are limited to one patient (adolescent#001) and one endogenous islet model (the hysteretic one) in this subsection. Results for the whole cohort are presented in the following one.

3.3.1. Description of the problematic

To scale the output of the biosensor so that it represents the patient insulin need, the K value needs to be tuned. This tuning process requires some form of assessment of the closed-loop regulation to ensure optimal performance and a quasi-normal response to glucose intake. In other words, a preliminary work is to answer the **Question 1** (mentioned in section 3.1):

Q1: How to define a normal response to glucose intake?

Discussions with our partners Dr M. Raoux (from CBMN laboratory) and Prof. B. Catargi (from CHU-Bordeaux) yielded a first answer to this question. In their daily practice, clinicians assess patient glucose control with indicators such as the TIR or the mean BG level (assessed either on CGM datasets or via HbA1c dosing). However, assessing the response to glucose intake also requires to take into account numerous variables (such as the patient’s age, other pathologies, or T1D duration to name a few) and thus requires the eye of an experienced clinician.

In the context of this simulation work, the information concerning the virtual patients is limited and the physiological variables which are simulated only relate to the action of glucose, insulin, and glucagon. In a will to develop a standardized and automated approach to assess glucose profiles I therefore selected the TIR and the mean BG level as two potential metrics.

Q2: How to assess a glycaemic profile using an objective criterion?

The objective here is to answer the **Question 2**:

A literature search permitted to identify other potential metrics (see section 2.5). A **systematic performance assessment algorithm** including all these metrics was developed and is run for every single simulation. Finally, a last metric was designed based on the

American Diabetes Association (ADA) definition of a normal response to an OGTT³⁷. ADA considers that individuals whose glycaemia is below 140mg/dl two hours after the ingestion of a special sweet drink, present a normal glucose tolerance [107]. We therefore developed a metric consisting in **the time spent in a target area** whose bounds are set using the meal scenario and the ADA definition (see subsection 2.5.1 for details).

In order to develop a tuning algorithm for the parameters of BG regulation systems, we needed to choose a unique objective criterion or a limited set of criteria with clinical relevance. For that purpose, we developed a methodology to compare the different metrics. This approach aims at answering **Questions 3, 4 and 4bis**:

Q3: Which criterion is best to assess glycaemic profiles?

Q4: For each patient, is there a unique K value that ensures optimal performance?

Q4bis: How to choose this K value with a standardized and automated method?

3.3.2. Parametric analyses

To choose the best objective criterion to include in a tuning algorithm, we conducted **parametric analyses**. This type of analysis is not realistic from a clinical point of view. Yet, it constitutes one of the main advantages of simulation and allowed me to gain experience with the simulator, improve my understanding of glycaemia dynamics, and better assess inter-patient variability. Three metrics were investigated: the mean Blood Glucose (BG) level, the Time In Range (TIR), and the Time In the Target Area (TITA). At first, these analyses permitted to determine if these metrics present a unique global maximum when K varies (with the same glucose intake scenario). Then, a second series of analyses permitted to investigate the influence of the amount of glucose being ingested on the conclusions yielded by the first series of parametric analyses.

3.3.2.1. A mathematical criterion to assess glucose control from blood glucose profiles

The analyses presented in this subsection were performed with a **10-hour single meal** scenario consisting in the ingestion of 70 grams of glucose 4 hours after the beginning of the simulation. The scenario was simulated for all the T1D patients (11 adults, 11 adolescents, and 11 children) with K values varying from 100 to 10 000 (by increments of 100).

An algorithm was written to select **the K value that optimizes the regulation performance** according to each one of the three metrics of interest. The algorithm output thus consists in three ranks of the simulated K values (one rank per criterion). A first version of this ranking algorithm highlighted some issues: a rule had to be added, for mean BG and TIR, in order to avoid hypoglycaemia (which is much more life-threatening than hyperglycaemia). In case of a tie between two K values, another rule had to be implemented

³⁷ OGTT: Oral Glucose Tolerance Test.

to rank the results. The first issue was simply handled by downgrading the K values yielding hypoglycaemic events. In the case of a tie, the results were ranked based on the total insulin injected throughout the simulation (the fewer insulin is injected, the better). Later on, discussions with Prof. B Catargi led us to change this rule to favour the K value whose associated mean BG level is the closest to the “target” BG level, i.e. 105 mg/dl, used here as the target for the TITA criterion. The reason is that, in real-life, the prime objective is to lower the HbA1c level of the patient rather than minimize the amount of insulin delivered by the pump. One can note here that this BG level is not the target of the regulation process (as there is no setpoint in our regulation scheme) but this BG level is frequently set as a target in the literature. **Table 4** shows the best K values selected by our ranking algorithm together with the level of performance achieved for each criterion: Mean BG, TIR and TITA. Mean BG levels and total injected insulin are also provided to ease the comparison.

Figure 39 shows the BG profile associated with the best K value selected for each criterion. For **criteria 1 and 2**, the algorithm logically selected profiles that brush with the hypoglycaemia threshold without exceeding it as they both **maximize the time spent in the normoglycaemic range** and **minimize the mean BG level**. **Criterion 3** induced the selection of a profile which appears **more physiological** and safer (in the sense that the regulation is less aggressive, i.e., less insulin is injected) than those selected with the other criteria.

The ranking algorithm provided a first method to set the optimal value for K based on the performance assessment provided by the three studied metrics. However, with the data representation we used until now (**Table 4** and **Figure 39**), the selectivity of each criterion is difficult to assess. To address this issue, we observed the **evolution of the studied performance assessment metrics as a function of K**. In addition, we also computed the range of K values that ensures 98% of the best performance for each criterion in order to characterise the selectivity of each criterion (see **Figure 40**). The first observation is that the

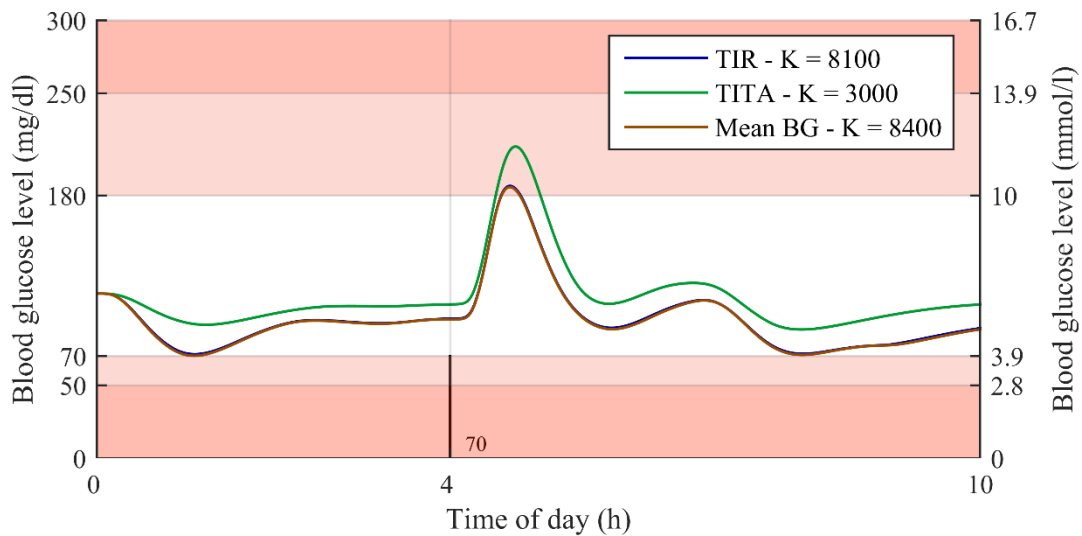


Figure 39: BG profiles selected by the ranking algorithm. The response of adolescent#001 to a single meal consisting in 70 grams of glucose ingested 4h after the beginning of the simulation is displayed for the three values of K selected by the algorithm.

Table 4: Comparison of three criteria to select the optimal value of K: mean Blood Glucose (BG) level, Time In Range (TIR), and Time In Target Area (TITA)

Criterion 1: Mean BG level (the lower the better)					
Rank	K	TIR (%)	TITA (%)	Mean BG level (mg/dl)	Injected insulin (U)
1	8400	97.8	61.2	95.0	21.2
2	8300	97.8	61.4	95.2	21.0
3	8200	97.8	61.9	95.4	20.9
4	8100	97.8	62.4	95.6	20.7
Criterion 2: Time In Range (the higher the better)					
Rank	K	TIR (%)	TITA (%)	Mean BG level (mg/dl)	Injected insulin (U)
1	8100	97.8	62.4	95.6	20.7
2	8200	97.8	61.9	95.4	20.9
3	8300	97.8	61.4	95.2	21.0
4	8400	97.8	61.2	95.0	21.2
Criterion 3: Time In Target Area (the higher the better)					
Rank	K	TIR (%)	TITA (%)	Mean BG level (mg/dl)	Injected insulin (U)
1	3000	94.8	100	110.5	12.4
2	2900	94.8	100	111.1	12.2
3	2800	94.7	100	111.7	12.1
4	2700	94.5	100	112.3	11.9

best TIR (97.8%) was obtained for K values ranging from 8100 to 8400 while the best TITA (100%) was obtained for a broader range spanning from 1600 to 3000. The second observation was that 98% of the best performance was obtained for K values ranging from 4400 to 8400 for the TIR while a narrower range spanning from 1300 to 3000 was obtained for the TITA. As the mean BG level is conversely proportional to the amount of insulin delivered to the patient, it is also conversely proportional to the value of K and a unique maximum is only ensured, for the criterion 1, by the condition we added to prevent hypoglycaemia. A first conclusion is that regardless of the selected criterion, **a continuous range of K values can be considered optimal**. Of note, the results presented here concern patient adolescent#001 but a similar behaviour was observed for all the virtual patients of the T1DMS cohort.

As criteria 1 and 2 tended to select higher K values resulting in an excessively aggressive regulation of the BG level, we decided to **favour the criterion 3**. Indeed, the TITA offered the advantage to select K values leading to a BG response presenting both a safety margin to

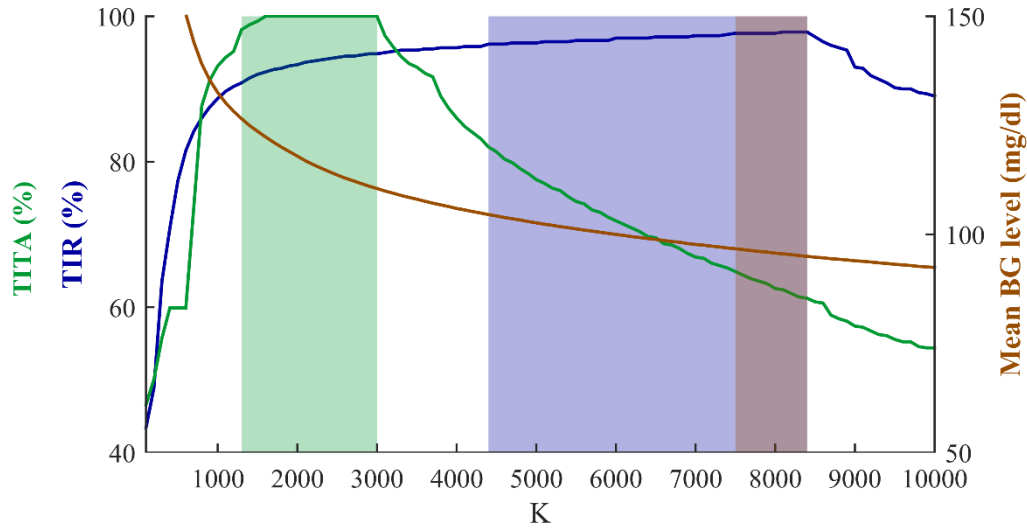


Figure 40: Evolution of the closed-loop regulation performance assessed with Time In Range (TIR), Time In Target Area (TITA) and mean Blood glucose (BG) level, as a function of K . Coloured areas highlight the range of K values that ensure 98% of the best performance for each criterion.

guard against the risk of hypoglycaemia and a satisfactory time spent in the normoglycemic range (94.8%).

3.3.2.2. Virtual patient's response to glucose intake

We outlined the existence of a continuous range of K values which maximizes the closed-loop regulation performance. The fact that, depending on the selected criterion, this range can importantly shift highlights the importance of the choice of the criterion used to tune the parameters of the regulation closed loop. Prior to making a definitive choice, we decided to study how a variation of the amount of glucose ingested during the simulated meal affects the trends we observed in the last subsection.

This section presents a second batch of parametric analyses. The analyses presented in 3.3.2.1 were reproduced with **16 single meal scenarios**. The scenario characteristics are the same as those of the 70-g single meal scenario previously used except that the **glucose intake is varied** from 10 to 160 g (10 g steps). These analyses generated large amounts of data which allowed me to better understand how glucose intake influences the variations of T1D patient's glycaemia. To facilitate the analysis of these large datasets, we generated surface plots presenting the evolution of the TIR as a function of K and of the glucose intake. These maps capture the high inter-patient variability of the response to single meals and the differences induced by the different biosensor models (see **Figure 41**).

For each scenario, the criterion 3 (TITA) was used to select the optimal value of K which was then represented on the surface plot (red dots). **Figure 41C** displays the evolution of this optimal K value through the 16 scenarios for adolescent#001. Interestingly, we noted that the values selected for the Static model were highly variable while those selected for the **Hysteretic model were steadier** throughout the 16 scenarios. **Figure 41D** also displays the TIR associated with the optimal K values selected by the ranking algorithm, but no significant differences between models were observed. A consistent behaviour was observed for almost all the patients of the cohort.

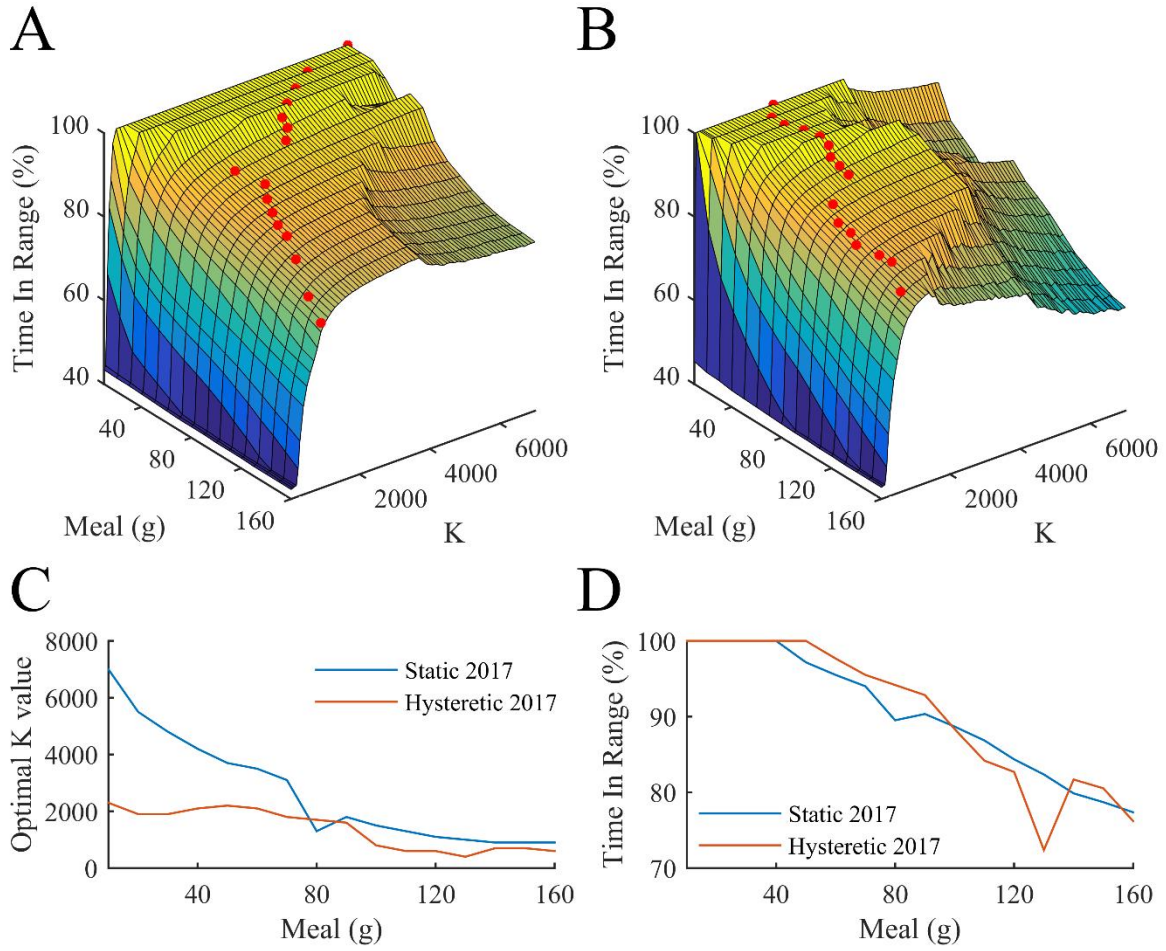


Figure 41: Parametric analysis characterising the response of adolescent#001 to different glucose intakes (10g to 160g single meal scenarios). A-B) Evolution of the Time In Range (TIR - expressed as a percentage) as a function of K and of the glucose intake for two different models of the islet endogenous algorithms: the Static model (version 2017 – panel A) and the Hysteretic model (version 2017 – panel B). C) Evolution of the optimal K value selected by the ranking algorithm using the Time In Target Area criterion (see previous subsection). D) TIR corresponding to the optimal K values.

This second batch of parametric analyses was performed using the former versions of the biosensor models (see section 3.2). As these analyses are time- and resource-consuming they were not reproduced with the updated models. They however confirmed the existence of a continuous range of K values ensuring the maximal performance as assessed with the criterion 3 (Time In Target Area) and for the 16 simulated scenarios. We also observed that this range was narrowed by increasing glucose intakes. Another important conclusion (data not shown here) was that it was possible **to select a K value ensuring 100% of TITA** for glucose intakes varying between 10 and 120g for the hysteretic model and for almost all patients. This optimal K value was always close to the K value selected for the 70g scenario and we therefore selected this method as the **standardized method to tune K**.

3.4. *In silico* results under realistic scenario

As we have seen above, in the IV/IV configuration, the defective pancreas of the virtual T1D patient is replaced by the islet algorithm model in series with a scaling factor K to restore the glucose homeostasis. In the last section we described our standardised methodology to tune K in order to handle the **large inter-patient variability** which characterises the response to glucose stimulation of the T1DMS virtual T1D cohort. The methodology chosen consisted in setting K to the value which maximizes the TITA for a 70g single meal scenario. Once this tuning process was achieved for the whole T1D cohort of the T1DMS, we used a realistic multi-meal scenario to assess the performance of this islet algorithm-based regulation closed loop. This scenario consisted of a **3-meal/2-snack daily pattern** in which a total of 235 g of glucose is ingested each day. The meals are distributed as follows: a breakfast of 45 g of glucose ingested at 6 a.m., a lunch of 70 g at noon and a dinner of 80 g at 6 p.m. Two 20 g snacks are added at 4 p.m. and 11 p.m. The scenarios were simulated for all the T1DMS virtual patients (i.e., 11 adolescents, 11 adults, and 11 children) and using the two updated versions of our biosensor model presented in section 3.2 (Static 2020 and Hysteretic 2020). **Figure 42** displays the mean BG profiles for each regulation scheme; profiles are averaged over the 11 patients of each population.

The closed-loop performance was assessed by calculating internationally recommended metrics (see subsection 2.5.2) for each patient category (Adults, Adolescents, Children) and each regulation scheme (Static and Hysteretic). Results are presented in **Table 5** as mean (standard deviation). Detailed results for each patient are provided in Appendices 5 to 7.

The **regulation schemes based on islet endogenous algorithms** (Static and Hysteretic models) ensured excellent performance of the BG regulation closed-loop. The mean TIR was above 90% for all patient categories and very close to 100% for adults. The biosensor algorithms maintained the **BG level in the normoglycaemic range** during the major part of the simulation with a **very low risk of extreme glycaemic events** (mean BGI < 2 in all

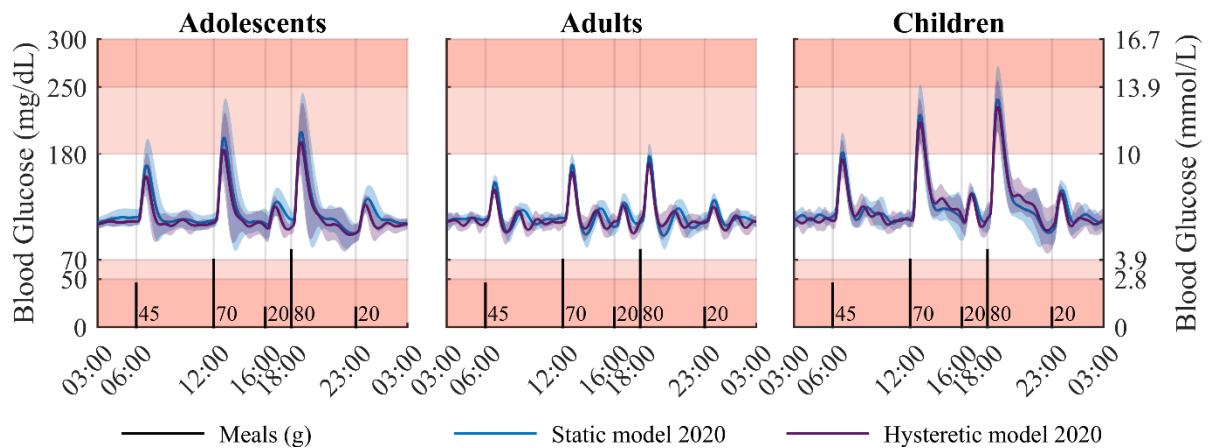


Figure 42: Simulation results for a 48-hour, 5-meal scenario (last 24 hours are displayed) in adults, adolescents, and children, for two regulation schemes (Static model 2020, Hysteretic model 2020) using IV glucose measurement and insulin infusion routes. Mean glucose profile (curve) and standard deviation (coloured patch) are displayed. Regions with no glycaemic risk, moderate glycaemic risk and high glycaemic risk are color-coded, respectively in white, pink and red.

Table 5: Performance metrics for two regulation schemes in all three patient categories.

Adults									
Category	TBR 2 (%)	TBR 1 (%)	TIR (%)	TAR 1 (%)	TAR 2 (%)	LBGI (.)	HBGI (.)	Mean BG (mg/dl)	TDI (U)
Static	0.0 (0.0)	0.0 (0.0)	99.3 (1.1)	0.7 (1.1)	0.0 (0.0)	0.2 (0.1)	0.5 (0.2)	115.9 (3.8)	53.1 (13.1)
Hysteretic	0.0 (0.0)	0.0 (0.0)	99.8 (0.4)	0.2 (0.4)	0.0 (0.0)	0.2 (0.1)	0.3 (0.1)	113.4 (3.5)	54.3 (14.5)
Adolescents									
Category	TBR 2 (%)	TBR 1 (%)	TIR (%)	TAR 1 (%)	TAR 2 (%)	LBGI (.)	HBGI (.)	Mean BG (mg/dl)	TDI (U)
Static	0.0 (0.0)	0.0 (0.0)	94.5 (6.6)	5.5 (6.6)	1.0 (2.2)	0.2 (0.1)	1.3 (1.4)	120.9 (11.9)	42.1 (11.7)
Hysteretic	0.0 (0.0)	0.4 (1.5)	95.8 (5.4)†	3.8 (4.7)	0.5 (1.5)	0.3 (0.3)	0.9 (0.9)	115.5 (7.8)	44.0 (13.3)
Children									
Category	TBR 2 (%)	TBR 1 (%)	TIR (%)	TAR 1 (%)	TAR 2 (%)	LBGI (.)	HBGI (.)	Mean BG (mg/dl)	TDI (U)
Static	0.0 (0.0)	0.0 (0.0)	92.7 (3.5)	7.3 (3.5)	1.4 (1.8)	0.2 (0.2)	1.8 (0.9)	127.2 (7.6)	26.1 (7.4)
Hysteretic	0.0 (0.0)	0.6 (1.5)	92.6 (2.7)	6.8 (2.4)	0.6 (0.9)	0.2 (0.3)	1.6 (0.5)	126.4 (7.7)	25.4 (7.6)

Nine metrics are computed: the Time Below Range (TBR level 1: 70 mg/dl, level 2: 54 mg/dl), the Time In Range (TIR), the Time Above Range (TAR level 1: 180 mg/dl, level 2: 250 mg/dl), the Low Blood Glucose Index (LBGI) and its counterpart the High Blood Glucose Index (HBGI), the Mean Blood Glucose level (Mean BG), and the Total Daily Insulin (TDI) administered to the patient. All metrics are mean (SD). Symbol † indicates statistical significance ($p < 0.01$) with respect to the Static model.

patient categories), thus successfully restoring the glucose homeostasis of the patient. Concerning the mean TIR, IV/IV results showed a consistent trend **in favour of the Hysteretic model**. This trend is statistically significant for adolescents ($p = 0.010$) but not for adults and children (respectively $p = 0.098$ and $p = 0.492$). Overall, this led us to choose the Hysteretic model for the test of the *in silico* AP in an SQ/SQ configuration presented in Chapter 4).

3.5. Discussion

The overall objectives of the IV/IV simulation campaign were: 1) to answer the scientific questions which emerged during the preliminary phase; 2) to validate electrical measurement as a means to both characterize the islet endogenous algorithms and use them to regulate the BG level of virtual T1D patients. To that aim, a simulation environment and a methodology facilitating the comparison of different versions of the biosensor model were developed. By limiting the number of elements constituting the regulation closed-loop, we were able to highlight the contribution of the biosensor to the closed-loop performance.

We have seen that the answer to **Question 1** cannot be obvious. Indeed, a “normal response” to glucose stimulation is often determined by the clinicians based on various metrics and the characteristics of the patients, completed by years of experience. Still, a consensus has emerged around the definition of the normoglycaemic range (70-180 mg/dl) and the normal fasting BG level (<100mg/dl). To answer **Question 2**, the TIR and the mean BG level can thus be considered as objective criteria to assess BG profiles. We have seen that another objective criterion can be built based on ADA’s definition of a normal glucose tolerance (we named this criterion TITA). Objectivity is key in our work; indeed, by developing a **standardized methodology** based on an objective criterion to tune our closed-loop parameters, we can hypothesize that **the same level of optimization** is achieved for all patients and biosensor models which enables a valid comparison of these models.

The parametric analyses presented in subsection 3.3.2 demonstrated the **superiority of the TITA** as a criterion that accounts for all the **clinical risks** associated with glycaemia: hypoglycaemia, hyperglycaemia, and glucose variability³⁸. Indeed, an additional condition to avoid hypoglycaemia was necessary to tune K with our ranking algorithm when the TIR and mean BG level were used as objective criteria. Despite the addition of this condition, these criteria still induced an excessively aggressive tuning of K highlighted by important values of total injected insulin and BG profiles brushing with the hypoglycaemia threshold. In contrast, the use of TITA resulted in BG profiles which seem physiological and present both satisfactory TIR and mean BG level, while ensuring a sufficient safety margin towards hypoglycaemia. The parametric analyses also highlighted the existence of a **single K value** (or a continuous range of K values) which ensures optimal performance of the islet algorithm-based regulation scheme (as assessed with TITA). This latter point is particularly interesting to develop an **optimization algorithm**³⁹ to get rid of the resource and time-consuming parametric analyses. Such an algorithm was designed and used to tune the parameters of the controllers necessary to handle the delays induced by subcutaneous routes (see Chapter 4 for associated results). While developing this optimization algorithm, we replaced the TITA-based cost function by a **BGI-based**⁴⁰ **cost function** as BGI is a well-established metric. That decision was justified by a comparison of the ranking of K values when based on TITA and BGI (see **Figure 43** and **Table 6**).

The first observation is that BGI is more selective than TITA and permits a better discrimination of K values contrary to TITA (16 values of K present a TITA of 100% - see **Figure 43**). In view of this, and considering that mean BGI is strictly decreasing up to its minimum and is strictly increasing afterwards, this **metric is perfectly suited to be used in the cost function of an optimization algorithm**. Concerning the tuning of K, i.e., the

³⁸ Glucose variability: refers to blood glucose oscillations that occur throughout the day, including hypoglycaemic periods and postprandial increases, as well as blood glucose fluctuations that occur at the same time on different days (Suh et al. [138]).

³⁹ Optimization algorithm: a procedure which is executed iteratively by comparing various solutions till an optimum or a satisfactory solution is found. With the advent of computers, optimization has become a part of computer-aided design activities.

⁴⁰ BGI = Blood Glucose Index

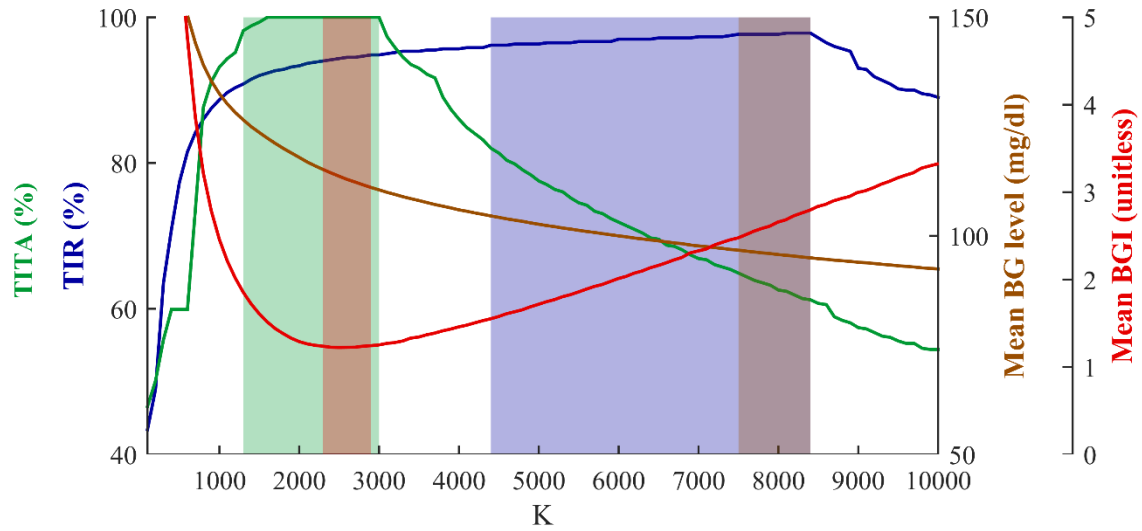


Figure 43: Evolution of the closed-loop regulation performance assessed with Time In Range (TIR), Time In Target Area (TITA), mean Blood glucose (BG) level, and mean Blood Glucose Index (BGI) as a function K. Coloured areas highlight the range of K values that ensure 98% of the best performance. For TIR and TITA, the best performance is the highest value reached during the parametric analysis. In contrast, it is the lowest value for Mean BG and Mean BGI.

selection of a unique optimal K value for each virtual T1D patient, both criteria yield very similar results (see **Figure 44**).

To answer **Question 3, 4 and 4bis**, TITA was chosen as the best objective criterion to assess blood glucose profiles in a first time and was replaced by the mean BGI afterwards. In addition to the advantages mentioned above, this metric was favoured for its **well-established**

Table 6: Comparison of TITA and BGI as two objective criteria to assess blood glucose profiles.

Criterion 1: Time In Target Area (the higher the better)						
Rank	K	TIR (%)	TITA (%)	Mean BGI (mg/dl)	Mean BG level (mg/dl)	Injected insulin (U)
1	3000	94.8	100	1.25	110.5	12.4
2	2900	94.8	100	1.24	111.1	12.2
3	2800	94.7	100	1.24	111.7	12.1
4	2700	94.5	100	1.23	112.3	11.9
Criterion 2: Mean BGI (the lower the better)						
Rank	K	TIR (%)	TITA (%)	Mean BGI (mg/dl)	Mean BG level (mg/dl)	Injected insulin (U)
1	2500	94.3	100	1.22	113,6	11,5
2	2600	94.5	100	1.23	112,9	11,7
3	2400	94.2	100	1.23	114,4	11,3
4	2700	94.5	100	1.23	112,3	11,9

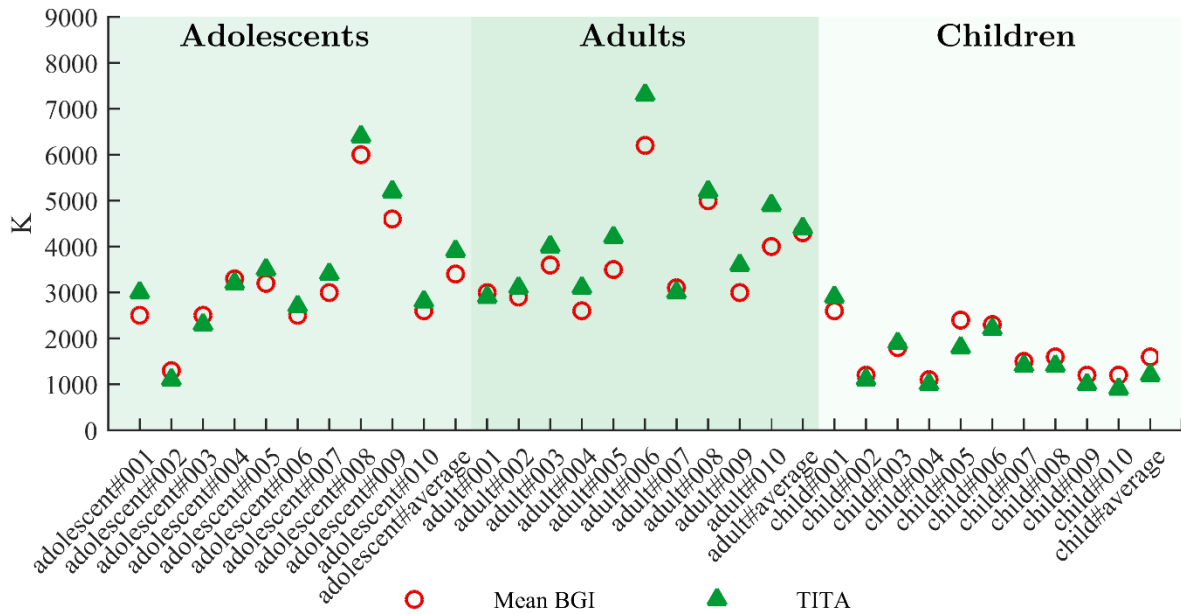


Figure 44: Results of the K tuning process for all the patients of the T1DMS's virtual T1D cohort for two criteria: TITA (green triangles) and Mean BGI (red circles).

clinical relevance and because its definition does not involve arbitrary choices (such as the lower and upper limits in TITA).

As previously mentioned, the IV/IV configuration together with the use of an objective criterion in an automated process (using either parametric analyses or an optimization algorithm) enables a **fair comparison between the different biosensor models**. Indeed, with K values optimally tuned for each patient, this methodology is an answer to **Questions 5 and 6**: any difference in performance highlights the differences between the biosensor models presenting different degrees of accuracy. The Hysteretic model, providing a better fit to experimental data presented slightly better IV/IV results than the Static model at the cost of an increased computation time (2% to 4% increase). At the current stage of our research, computational cost is not an issue (as opposed to computation cost in medical devices), the biosensor-based AP was thus developed using the **more accurate hysteretic model** (see Chapter 4).

As healthy pancreatic islets constitute the core element of our biosensor, the presented IV/IV results provide a successful **proof of concept** of its working principle. The excellent results in IV/IV simulations validate the use of **electrical measurements of islet activity** as a means to characterize and exploit the **inborn algorithms of pancreatic islets** in a BG regulation closed-loop. Indeed, the simulator's T1D cohort was maintained in the normoglycaemic range (70 to 180 mg/dl) for a minimum of 97%, 82%, and 86% of the simulation length (for adults, adolescents, and children respectively) with reduced glycaemia-related risk (assessed with BGI).

Chapter 4

Integration of the biosensor in an *in silico* Artificial Pancreas

After the description of the scientific context and the material and methods, we presented a first series of simulation results which permitted to answer some of our scientific questions concerning glucose control assessment (see Chapter 3). In particular, we investigated various methods to assess the performance of a BG regulation closed-loop. In so doing, we highlighted **the existence of an optimum of performance of the regulation closed loop** in all patients. It thus allowed us to envision the development of an automated algorithm to optimally calibrate the regulation closed loop by minimising the glycaemia-related clinical risk. In addition, we highlighted the slight increase of closed-loop performance permitted by the **Hysteretic model** (as compared to the Static one). We therefore chose this model to assess the biosensor ability to perform in an AP system.

To a certain extent, the simulations in Chapter 3 rely on a diverted use of the UVA/Padova T1DM Simulator which was originally designed to simulate AP systems. In Chapter 4, the T1DMS is now used in a more conventional manner to simulate our **biosensor-based AP system (Bios-AP)** and compare it to other reference therapies for T1D: a **CGM-based AP (CGM-AP)** and **MDI therapy**. In actual T1D therapies, **subcutaneous routes** are both used for continuous glucose monitoring and insulin infusion in order to ensure patient safety. The subcutaneous routes mitigate the occurrence of complications frequently associated with the use of intravenous routes (infections being the main complication). However, subcutaneous measurement of glucose is associated with a delay due to the slow kinetics of glucose diffusion from the vascular to the interstitial space. Similarly, subcutaneous infusion of insulin delays its onset of action as explained in Chapter 1. These sensor and pump delays, induced by the subcutaneous diffusion kinetics, are further referred to as **subcutaneous delays**. To simulate a realistic AP system, the simulations presented in this chapter therefore use the SQ/SQ configuration of the T1DMS (see subsection 2.4.2). To illustrate the impact of subcutaneous delays, we present in **Figure 45** a comparison of the BG regulation with the Hysteretic islet algorithm model using IV and SQ insulin delivery routes. Postprandial excursion highlights the delayed onset of insulin action which results in a hyperglycaemic event followed by a life-threatening hypoglycaemic event for almost all patients. This postprandial hypoglycaemia, due to an excessive delivery of insulin while the BG level continues to rise, **requires a controller** to be anticipated and mitigated.

The first section of this chapter describes the methodology we developed to individually tune the parameters of a controller for each patient of the T1DMS cohort. The obtained controllers were paired with the default built-in CGM sensor at first and with the biosensor model afterwards. The second subsection provides a comparison of the closed-loop performance of the resulting Bios-AP, to reference therapies with the most realistic scenarios that can be simulated with our version of the simulator. The third subsection discusses the contribution of

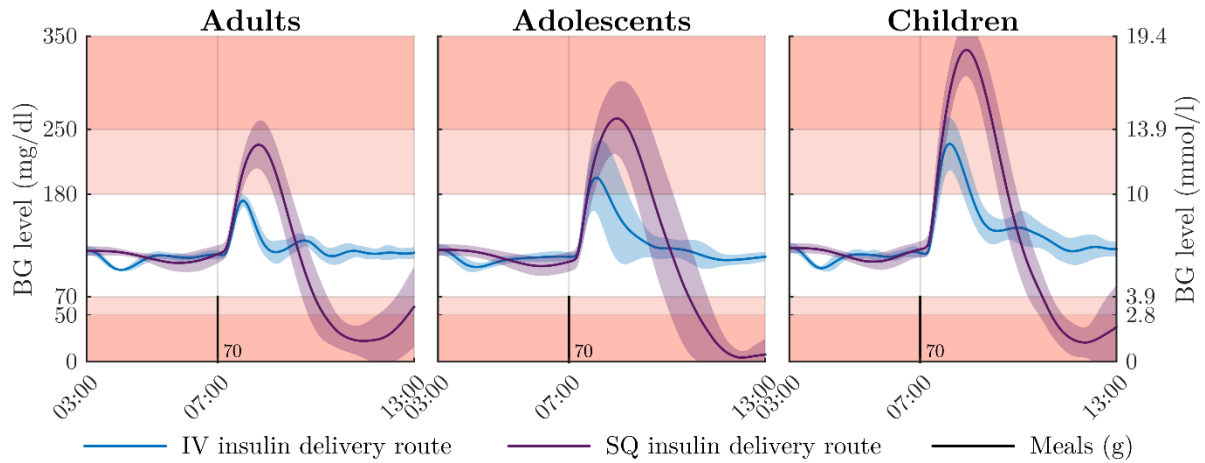


Figure 45: Comparison of BG level figures with intravenous (IV) and subcutaneous (SQ) insulin delivery routes when regulation is achieved by the Hysteretic islet algorithm model. All patients are submitted to a 70-g single meal scenario. Mean BG profiles (curves) and standard deviation (coloured patches) are displayed.

mathematical modelling and simulation to the development of a biosensor-based AP. The concluding subsection finally attempts to lay the groundwork for future development of a real-world implementation of such an AP system.

4.1. Design of an individualised controller to handle the subcutaneous delays

In the overnight fasted state, the delay induced by the subcutaneous measurement of BG level has been estimated by Basu et al. [47] to fall within a 4.8 to 9.8 minutes range for T1D patients. Similarly, the delayed onset of action of subcutaneously-infused insulin ranges from 20 to 60 minutes depending on the type of insulin administered. By diminishing their overall reactivity, subcutaneous delays negatively affect closed-loop performance of BG regulation systems. As a consequence, **AP systems require a controller to ensure optimal and reliable performance**. The controller takes into account present and past glucose readings, but also anticipates the future states determined by glucose-insulin interactions and the infusion delays of subcutaneous interfaces. This dynamic control can be achieved through a variety of algorithms, among which the most common are the Model Predictive Control (MPC) and the Proportionate Integral Derivate (PID) control [116]. As this work is not focused on control theory and **for the sake of demonstration**, we used simple **Proportional-Integral-Derivative (PID) controllers** to handle the subcutaneous delays induced by the SQ/SQ configuration. This control algorithm was favoured for its simple handling, the many variants that can be easily implemented, and because PID control has already demonstrated its effectiveness to regulate the BG level of T1D patients [55].

It is important to remind the unconventional nature of our biosensor. Its output is an image of electrical islet activity and thus integrates the action of all the regulators of insulin secretion as well as physiologically important intra-islet regulations [117]. It provides an image of the patient's physiological state and represents an insulin demand signal rather than a glucose level signal. In the healthy individual, islets act as the natural sensor, control algorithm and actuator that enable glucose homeostasis. Monitoring their electrical activity therefore amounts to monitoring the natural control algorithm output. To account for this uniqueness, the setpoint of the controllers paired with the biosensor in this work is set to 0 (no insulin need) while the setpoint of the controllers paired with a CGM sensor is set to the desired BG level target (110 mg/dl). In this way, the **biosensor signal acts as an error signal**, rather than a sensor signal, as soon as the BG level exceeds a target intrinsically defined by the islet endogenous algorithms.

4.1.1. Controller tuning

In this subsection, we describe a **methodology to individually tune the controller** of an AP system to match the insulin need of a virtual patient. Individualisation of the controller parameters seems necessary to reach the optimum of closed-loop performance highlighted in Chapter 3. It also permits to cope with the reportedly high interpatient variability observed in real T1D patients and modelled in the T1DMS. In addition, the *in silico* approach facilitates individualisation thanks to the possibility of repeated and fast simulations with identical scenarios and patients.

Control performance of closed-loop systems is greatly dependent on the adequate tuning of controller parameters. For the most part, classical tuning techniques for control algorithms rely on the modelling of the controlled device dynamics. Model-based techniques turn out to be

very effective and convenient but are limited when the model-system mismatch is too great. This is particularly true for biological systems. In an effort to overcome this issue, “model-free” techniques have been developed. Among them, **iterative optimisation algorithms** have shown promising results. They attempt to compute a vector of parameters best suited to solve a given problem through repeated attempts and corrections. In [118], Soylu et al. compare three of these algorithms to tune the parameters of a PID controller involved in the closed-loop BG control of virtual T1D patients. Whether the optimisation method be iterative or heuristic, these algorithms rely on the definition of an objective cost function to assess performance. Traditional optimisation criteria, such as integral of absolute error (IAE) minimisation, are not well suited for performance assessment in the case of glycaemia regulation. As explained in subsection 1.1.2, deviations from the target BG cannot be treated symmetrically: while elevated glucose levels can be tolerated for a limited period of time, an equivalent deviation in the hypoglycaemic direction may already constitute a life-threatening event.

For their tuning algorithms, Soylu et al. opted for a cost function which compares the T1D patient’s simulated BG profile to a healthy BG profile in an attempt to minimise the absolute error between the two. As explained in Chapter 2 and illustrated in Chapter 3, the **assessment of clinical risk** based on glucose profiles is a complex question. In particular, it is not possible to define a unique healthy response to glucose intake. We therefore improved the method published by Soylu et al., by using the same meta-heuristic approach, which involves a genetic algorithm (GA)-based optimisation technique, with a cost function directly assessing the quality of closed-loop control from the simulated glucose profiles. As explained in subsection 2.4.2, the numerical GA technique reproduces the mechanisms of natural selection to find the most suitable controller parameters, i.e., the controller parameters which minimises the cost function.

The controller tuning method was first developed with a classical **PID controller**. Three parameters were therefore needed tuning to match the patient’s insulin need: the proportional gain K_p , the integration time T_i and the derivative time T_d . The MATLAB ga function was used with a custom cost function. As mentioned in section 3.5, the ga function was at first associated with a cost function computing the **TITA** (Time In Target Area – see subsection 2.5.1) of the glucose profile resulting from the simulation of a 70-g single meal scenario. This cost function was straightforwardly defined by **Equation 6**.

$$Cost = 100 - TITA(\%) \quad (6)$$

Where *Cost* is the output of the cost function which has to be minimised by ga and *TITA* the percentage of time spent by the glycaemia in the predefined target area throughout the simulated scenario.

Lacking experience with numerical optimisation, we adopted a “trial and error” methodology to optimally set the MATLAB ga function parameters. A satisfactory convergence speed was obtained with a population size of 200 and a number of generations varying between 5 and 10 (see **Figure 46**). Indeed, the mean performance of the 10 best controllers is almost constant on the last 4 generations with a narrow standard deviation.

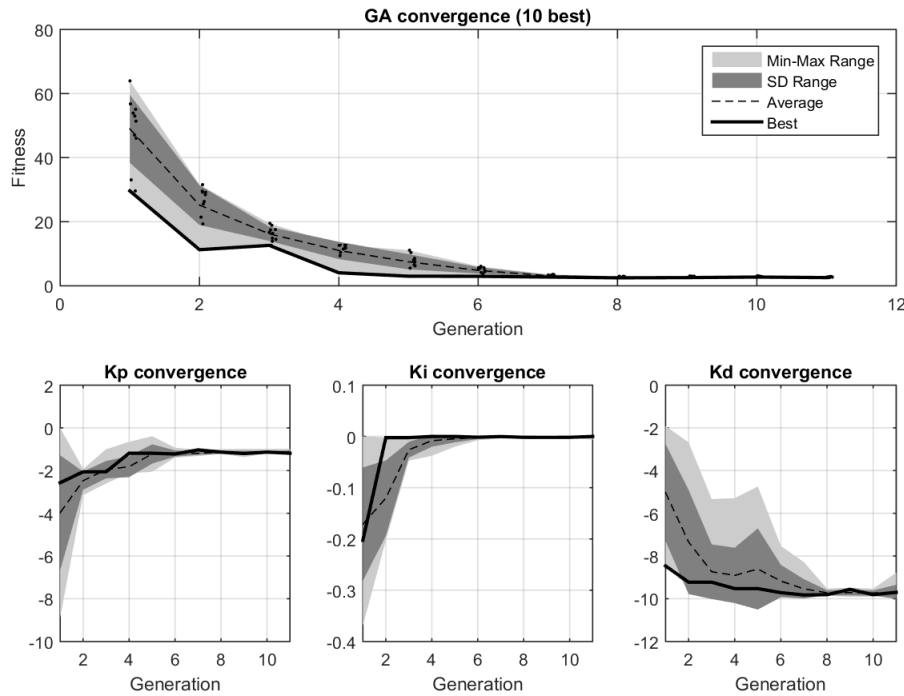


Figure 46: GA-based tuning of a PID controller parameters. The top panel displays the evolution of the performance of the ten elites (ten best controllers as assessed with the TITA-based cost function) over the eleven generations. The ten elite controllers' parameters are plotted on the three bottom panels.

Afterwards, the TITA metric was replaced in the cost function by the **BGI**, a well-recognised indicator of the asymmetric glycaemia-related clinical risk of T1D patients. Instead of maximising the percentage of time spent in a given glycaemic range or target area, the objective therefore became to minimise the glycaemia-related clinical risk. Satisfactory convergence speed was also obtained with this clinically-relevant cost function. The subsequent validation of the resulting controllers with realistic multi-meal scenarios highlighted some weaknesses of our tuning process: the tuning with 70-g scenarios resulted in an excessively aggressive regulation leading to hypoglycaemia with scenarios involving snacks (20-g glucose intake). To address this issue, we modified the cost function to base the performance assessment with BGI on the mean performance over 5 scenarios with **various glucose intakes**. A loss in performance was observed on the 70-g single meal scenario used during the tuning process but better glucose control was obtained with realistic validation scenarios.

The GA-based controller tuning method was first developed with a single patient. Thereafter, the ga function settings (e.g., number of generations, parameter bounds) were refined with two patients of each category to save time and the definitive method was validated with the whole T1DMS cohort. The final method consists in the ga-based tuning of an AP controller using a cost function computing the mean BGI over five 10-hour single meal scenarios (with glucose intakes varying between 20 and 100 grams). To achieve this result, the ga function is set as follows:

PopulationSize : 50
CrossoverFraction : 0.8000
Generations : 5
SelectionFcn : @selectionroulette
CrossoverFcn : @crossoverheuristic
MutationFcn : {[@mutationuniform] [0.2000]}
HybridFcn : @fmincon

All other parameters are set at their default value.

Satisfactory glucose control was obtained for the 11 virtual T1D adults equipped with an AP system involving a CGM sensor and PD_{BASAL} controllers. The tuning method and the associated closed-loop results were thus presented at the 2020 IEEE EMBC virtual conference and published in the conference proceedings [103].

4.1.2. PID controller architectures

As previously mentioned, numerous variants of the PID controller architecture co-exist. To gain experience, we tested different configurations of controllers whose parameters were tuned with the method described in the last section. At first, we tested variants which do not implement a continuous basal infusion of insulin, unlike MDI and modern hybrid closed-loop systems (see Chapter 1). However, our experience and the literature suggest that basal insulin delivery is necessary to limit the BG level variability, induced by the closed-loop control with important sensor delay and insulin onset of action. The PID control architectures presented in this work all include a steady basal insulin delivery.

Many configurations have been tested with features such as anti-windup, saturation block on the PID output, and deactivation of the integral action to implement a PD_{BASAL} controller. The four most performing configurations are described in this section:

Controller 1: a PD_{BASAL} controller whose basal insulin infusion rate was set to the Subject Specific Basal (SSB) parameter provided by the T1DMS for each virtual patient.

Controller 2: a PD_{BASAL} controller whose basal infusion rate was tuned by GA.

Controller 3: a PID_{BASAL} controller whose basal infusion rate was tuned by GA.

Controller 4: a PID_{BASAL} controller including a saturation block on the PID output.

A comparison of these four architectures is presented in **Figure 47** and **Table 7**. The variations of the BG level, the Insulin Infusion Rate (IIR) and the plasmatic insulin level resulting from the simulation of a 70-g single meal scenario are shown. The comparison between controllers 3 and 4 highlights the influence of a **saturation block** placed on the PID output (see **Figure 47A** and 2F-I). This saturation block limits the PID output to 0 so that the minimal IIR is the basal infusion rate. It induces a less aggressive tuning of the controller by the GA: the postprandial maximal IIR is significantly lower as compared to other controllers (600 pmol/min with saturation block versus 950, 1020 and 1150 pmol/min without saturation). It also results in a **better stability** of the BG level at the cost of decreased rapidity of the

regulation (see **Figure 47A**) and **lower performance** (as assessed with TIR and mean BGI – see **Table 7**).

Interestingly, the comparison between PID_{BASIL} and PD_{BASIL} controllers whose parameters are all tuned by GA (controller 2 versus controller 3) showed only little difference. Both the BG level profiles and the associated performance metrics are quite similar, with a slight advantage for the PD_{BASIL} controller. The TIR were 90.7% and 89.7% and the mean BGI were 1.91 and 2.37 for the controller 2 and 3 respectively. The more pronounced difference observed with BGI should be attributed to the **lower stability of the PID_{BASIL}** controller which induces more variability of the BG level.

To discuss the design of an AP controller, another key parameter is the sampling period. As a starting point, all our controllers were using a 15-min sampling period. Afterwards, we implemented versions our controllers with a sampling period of 1 and 5 minutes. Unsurprisingly, the **regulation performance increased with lower sampling** period due to a better reactivity of the closed-loop system and a more aggressive tuning of the controllers by the GA. However, we decided thereafter to set the **sampling period to 5 minutes** as currently available commercial devices rarely use lower values.

4.1.3. Is there a “best architecture”?

A first conclusion after comparing controllers was that a **steady basal insulin infusion was necessary** to achieve good performance. However, the controller including a saturation block on the PID output (see **Figure 47**) yielded lower performance than the controllers able to reduce the IIR to zero. This result is not surprising and can be explained by the **derivative action of the PID** controller which acts as a very simple prediction model. When the insulin delivered by the controller in response to a meal starts to act, the BG level starts decreasing. As the BG level rate of variation decreases, the contribution of the derivative action increases (this contribution is negative as the error is decreasing) and the derivative action suspends the basal insulin delivery. It therefore limits postprandial reactive hypoglycaemia exactly **like the PLGS (Predictive Low Glucose Suspend)** feature implemented in modern hybrid closed-loop systems does (see Chapter 1). This mechanism explains why our GA-based method tends to be overly aggressive in the tuning of the derivative time T_d , which results in **excellent performance of the closed-loop regulation** at the cost of an **increased BG level variability** between meals. This issue could be addressed with a **meal detection feature** activating or deactivating a saturation block on the output of the PID based on the BG level

Table 7: Comparison of closed-loop regulation performance of four PID architectures. The same patient (adolescent#001) was submitted to a 70-g single meal scenario each time.

Category	TBR 2 (%)	TBR 1 (%)	TIR (%)	TAR 1 (%)	TAR 2 (%)	LBGI (.)	HBGI (.)	Mean BG (mg/dl)	TDI (U)
Controller 1	0.0	0.0	89.9	10.1	0.0	0.14	1.78	124.0	26.0
Controller 2	0.0	0.0	90.7	9.3	0.0	0.31	1.60	118.8	26.9
Controller 3	0.0	0.0	89.7	10.3	0.0	0.45	1.92	119.3	27.0
Controller 4	0.0	0.0	86.6	13.4	0.0	0.44	2.25	121.4	24.9

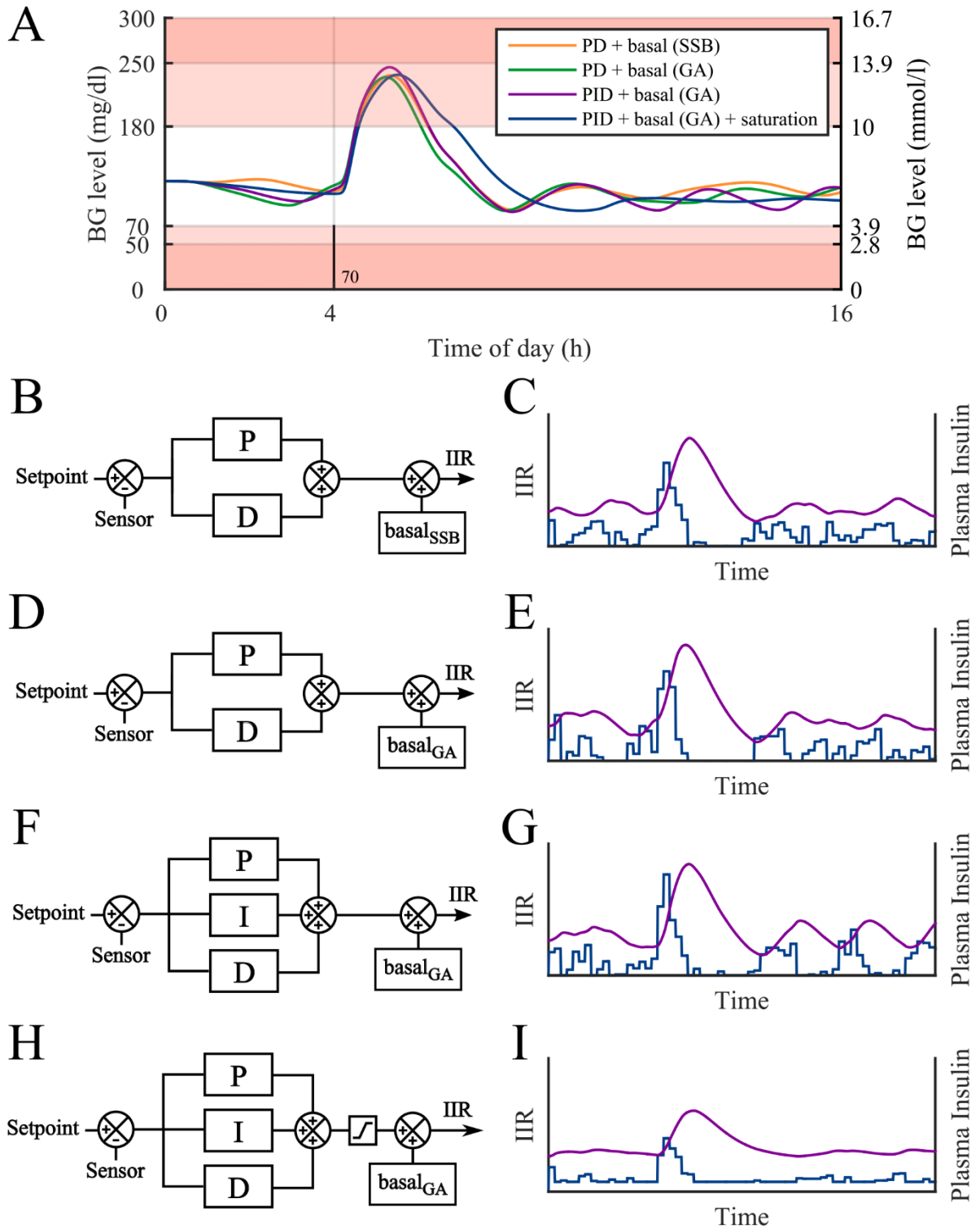


Figure 47: Four variants of the PID control architecture. Panel A: Blood Glucose (BG) variations resulting from the simulation of a 70-g single meal scenario with these four controller architectures; panels B to H: architecture schematic of four controllers (left), related Insulin Infusion Rate (IIR) and plasma insulin variations (right); Panels B-C: PD_{BASAL} controller whose basal infusion rate was set to the Subject Specific Basal (SSB) parameter provided by the T1DMS for each patient (Controller 1); panels D-E: PD_{BASAL} controller whose basal infusion rate was tuned by GA (Controller 2); panels F-G: PID_{BASAL} controller whose basal infusion rate was tuned by GA (Controller 3); panels H-I: PID_{BASAL} controller including a saturation block on PID output (Controller 4).

rate of variation. This solution was not investigated further as the control algorithm is not the main focus of this work.

Our work was presented at the 2020 IEEE EMBC conference as a **ready-to-use method to tune the parameters of a controller** involved in closed-loop BG regulation. This method could be adapted to every type of controller or for the tuning of specific parameters in a closed-loop BG regulation system. It is however more suited for controllers with few parameters such as the PD_{BASAL} controller. The latter demonstrated satisfactory performance, even compared to other PID architectures. However, one should keep in mind that this version of the metabolic model does not implement the patient-specific circadian variations of insulin sensitivity. Moreover, the CGM sensors models used in this study do not account for any static error which would impose a correction from the controller. On a real patient, these elements would certainly **require an integral correction**, which suggests a proper PID would present better results than PD_{BASAL} controller (as suggested in [119]).

For this *in silico* work, we decided to use **PD_{BASAL} controllers** to limit the number of parameters which needed to be tuned by the ga function to 3 and thus increase the convergence speed. We also used the Subject Specific Basal (SSB) parameter, provided by the T1DMS for each patient to implement the MDI therapy, to **set the basal insulin delivery** of our PD_{BASAL} controllers. This modification permitted to reduce the number of parameters to optimise to 2 with a negligible impact on the closed-loop performance of the system (see **Figure 47** and **Table 7**).

4.1.4. Correcting an unfair disadvantage for the CGM-AP

The controller tuning method was validated with multi-meal scenarios (as opposed to the single meal scenarios used during the development phase). We observed a surprisingly high

Method 1: The optimal parameters are the average parameters of the ten best controllers of the last generation computed by the GA (10 elites). This method is referred to as ‘*mean*’.

Method 2: The optimal parameters are the parameters of the best controller of the last generation computed by the GA. This method is referred to as ‘*best*’.

Method 3: The optimal parameters are computed with the hybrid optimisation scheme presented in subsection 4.1.1 (GA + *fmincon*). This method is referred to as ‘*fmincon*’.

frequency of postprandial reactive hypoglycaemic events **with the CGM-AP controllers**, which did not match the level of regulation performance that could be expected looking at the tuning process results. We therefore investigated further the selection method used to compute the optimal PID parameters from the last generation of controllers yielded by the ga function. We investigated three methods to select the optimal PID parameters:

We then compared the values of the K_p and T_d parameters selected with these methods together with the regulation performance of the associated controllers (assessed with the BGI-based cost function). **Figure 48** presents the result of this comparison for the 33 virtual patients of the

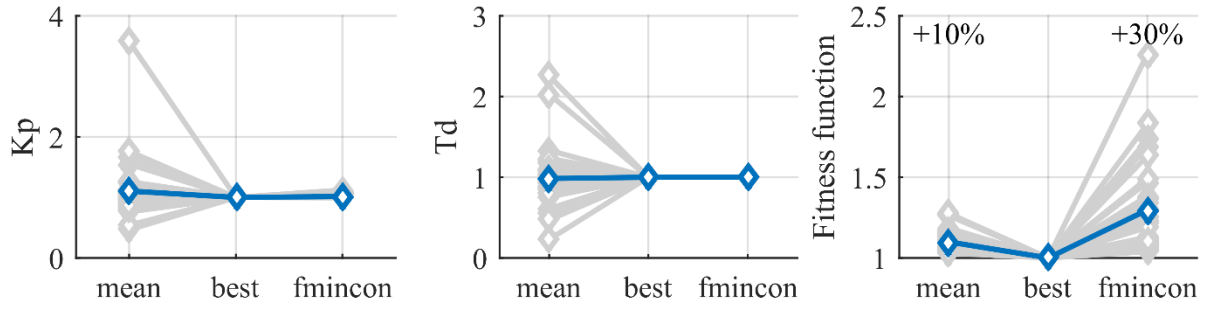


Figure 48: Comparison of 3 methods to select the optimal PID parameters for the CGM-AP controllers. From the last generation of controllers, the first method consists in computing the average parameters of the 10 best controllers (mean), the second selects the parameters of the best controller (best), and the third selects the parameters computed with *fmincon* by taking the best controller as a starting point (*fmincon*). Normalized parameters (K_p and T_d) and performance (fitness function) are presented for the three selection methods taking ‘best’ as a reference.

T1DMS. Results are normalized with ‘best’ method taken as the reference. Surprisingly, this comparison revealed a large difference of performance (**Figure 48**, right panel) between the controllers selected by *best* and *fmincon* methods while the associated controller parameters were very similar (**Figure 48**, left and center panels). In average, a 30% drop of the normalized performance was observed with the *fmincon* selection method. In comparison, the *mean* selection method yielded a 10% drop in performance. With a closed-loop system including a CGM sensor, two consecutive T1DMS simulations of the same glucose intake scenario do not yield the same results due to the modelling of **random sensor noise**. It therefore appears that the *best* controller is the result of advantageous sensor noise conditions (e.g., an overestimation the BG level right before a meal results in an increase of the IIR and acts as a small meal bolus). We thus attributed this difference in performance between *best* and *fmincon* methods to the sensor noise model included in the CGM sensor model. To improve the tuning process for the CGM-AP controllers we decided to use the **mean selection method** which ensures a good level of performance and a more reproducible behaviour than the other investigated methods. By providing a statistical mean for each controller parameter, this method is less sensitive to the CGM sensor noise.

We then tested the three selection methods mentioned above for the **Bios-AP controllers** to assess the potential impact of a modification of our GA-based tuning method (see **Figure 49**). No difference was observed between the performances of the controllers selected with the

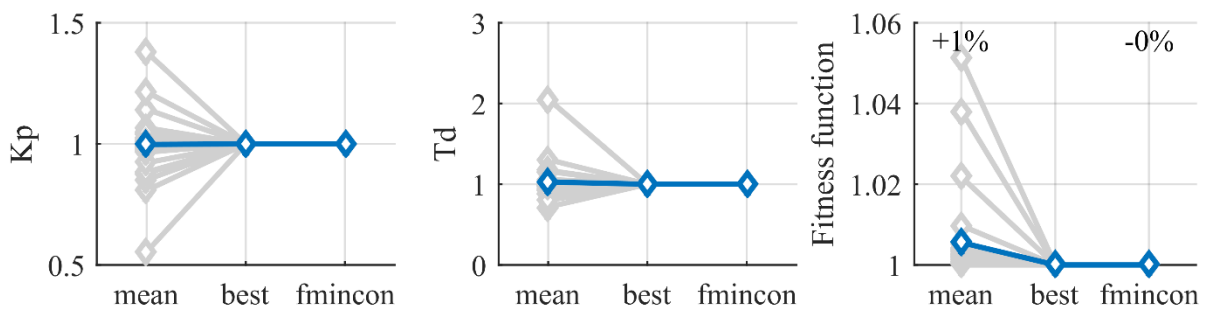


Figure 49: Assessment of the 3 selection methods in the case of the Bios-AP controllers. “mean”, “best” and “fmincon” are defined as in Figure 48. Normalized parameters (K_p and T_d) and performance (fitness function) are presented for the three selection methods taking ‘best’ as a reference.

best and *fmincon* methods. The *mean* method yielded a slight decrease of performance (average fitness function result increases by 1% - see **Figure 49** right panel). This result confirmed our conclusion: the initial hybrid optimisation scheme using *fmincon* **cannot handle the CGM sensor noise** which generate an unfair disadvantage for the CGM-AP. Our overall objective was to develop a standardised tuning method to perform a reliable comparison between the CGM-AP and the Bios-AP. We thus modified the tuning method to consider the **average parameters of the ten elites** of the last generation as the optimal PID parameters. In so doing, we greatly improved the performance of the CGM-AP with a very limited impact on those of the Bios-AP and allows a more **unbiased comparison** between these two AP systems.

4.2. Comparison of the Bios-AP with two reference treatments

After the proof of concept of our biosensor's working principle (Chapter 3), we assess in this section the SQ/SQ performance of the Bios-AP and compare it to standard treatments: a CGM-based AP and MDI therapy. To better handle the subcutaneous delays, the two compared AP systems use controllers whose parameters were tuned using the method described in the previous section. Note that the controllers of the CGM-AP and the Bios-AP do not benefit from any meal announcement from the patient (contrary to MDI therapy). **Three realistic case studies** were designed to validate the controller tuning method and to compare the three regulation schemes. The glucose intake scenarios were then **individualised in a body weight-dependent** manner to account for the natural variability of energy requirements. This second series of simulation provides an assessment of the Bios-AP performance where the stimulation of the BG regulation system (i.e., the glucose load of the meal) is more homogenous from one patient to the other.

4.2.1. Controllers' validation with multi-meal scenarios

With SQ glucose measurement and insulin infusion routes (see **Figure 50**), the T1DMS is exploited in a more realistic configuration from a clinical standpoint. The Bios-AP system is compared to two standard insulin therapy paradigms: MDI and a CGM-AP. A comparison based on three case studies is performed to assess the performance and robustness of these therapies. SQ/SQ configuration is paired with realistic multi-meal scenarios to simulate, as

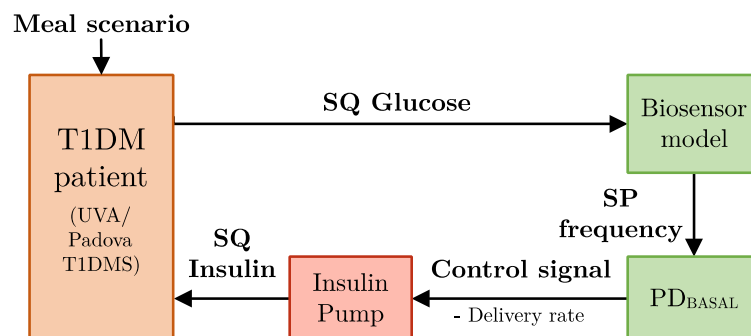


Figure 50: Closed-loop regulation scheme of the Bios-AP connected to the virtual patient through subcutaneous (SQ) glucose measurement and insulin infusion routes (as defined in Chapter 2, Figure 12).

best as the software currently allows, the everyday life of T1D patients. For each case study, the mean BG profile of the 11 adults is presented in **Figure 51**.

The first case study uses a 48-h multi-meal scenario consisting in a 3-meal/2-snack daily pattern in which a total of 235 g of glucose is ingested each day (the same scenario was used for the IV/IV validation presented in Chapter 3). The meals are distributed as follows: a breakfast of 45 g of glucose ingested at 6 a.m., a lunch of 70 g at noon and a dinner of 80 g at 6 p.m. Two 20 g snacks are added at 4 p.m. and 11 p.m. (see subsection 2.4.3 for further details on the methodology). In case study 1, both the CGM-AP and the Bios-AP allowed 9 adults to reach the recommended targets (see subsection 2.5.2 for details on the international consensus on performance metrics and their targets). With the Bios-AP, the mean TIR presents a significant increase of 4.4% in the adult population (compared to CGM-AP) with a mean BGI⁴¹ reduction of 0.9 (2.7 vs 3.6). Mean LBGI and HBGI of the 11 adults are minimal for both CGM- and Bios-APs and the mean glucose level is respectively equivalent to a mean HbA1C level of 6.6% and 6.4%⁴². MDI therapy showed excellent results with all the adults (11) reaching the targets with a mean BGI of 1.7. Performance metrics are presented in **Table 8** as mean (standard deviation). Detailed results for each patient are provided in Appendices 8 to 10.

The second case study uses the same meal scenario, but implements the method published by Herrero et al. [18] in simulations involving MDI to account for the **reported errors in carbohydrates counting by patients** (ranging from -30% to +40%). That scenario is used to quantify the impact of meal announcement accuracy, a leading cause in the top-of-the-art performance of the MDI therapy observed with scenario 1. A drop in the performance achieved by the MDI therapy was observed with only 5 adults reaching the targets (11 in case study 1) and a mean LBGi increasing from 0.2 to 0.8. That result highlights the crucial **dependency of MDI on accurate meal announcement**. As there are no meal announcements in the

⁴¹ BGI = LBGI + HBGI (defined in Kovatchev *et al.*[108])

⁴² The conversion was computed using the online eAG/A1C Conversion Calculator provided by the American Diabetes Association.

Table 8: Performance metrics for three blood glucose level regulation schemes in the three case studies, for all adults.

Case study 1										
Categor	TBR 2	TBR 1	TIR	TAR 1	TAR 2	LBGI	HBGI	Mean BG	TDI	
y	(%)	(%)	(%)	(%)	(%)	(.)	(.)	(mg/dl)	(U)	
Adu.	MDI	0.0 (0.0)	0.0 (0.0)	95.3 (4.1)	4.7 (4.1)	0.0 (0.0)	0.2 (0.2)	1.5 (0.7)	127.7 (9.2)	91.1 (20.7)
	CGM	0.1 (0.7)	0.4 (1.5)*	83.7 (7.3)*	15.9 (7.2)*	1.4 (3.1)	0.2 (0.4)	3.4 (1.6)*	140.5 (11.6)*	86.8 (19.1)
	Bios.	0.0 (0.0)	1.6 (3.2)	88.1 (5.4)*†	10.3 (3.4)*†	0.2 (0.7)	0.7 (0.6)	2.0 (0.7)†	124.4 (4.3)†	92.8 (21.7)†
Case study 2										
Categor	TBR 2	TBR 1	TIR	TAR 1	TAR 2	LBGI	HBGI	Mean BG	TDI	
y	(%)	(%)	(%)	(%)	(%)	(.)	(.)	(mg/dl)	(U)	
Adu.	MDI	0.7 (2.4)	2.9 (5.6)	93.0 (7.1)	4.2 (4.9)	0.0 (0.0)	0.8 (1.1)	1.5 (0.9)	123.5 (11.5)	92.6 (20.3)
	CGM	0.0 (0.3)	0.1 (0.8)*	83.7 (7.3)*	16.1 (7.3)*	1.5 (3.3)	0.1 (0.2)*	3.4 (1.7)*	141.1 (12.0)*	86.7 (19.0)*
	Bios.	0.0 (0.0)	1.6 (3.2)	88.1 (5.4)*†	10.3 (3.4)*†	0.2 (0.7)	0.7 (0.6)†	2.0 (0.7)*†	124.4 (4.3)†	92.8 (21.7)†
Case study 3										
Categor	TBR 2	TBR 1	TIR	TAR 1	TAR 2	LBGI	HBGI	Mean BG	TDI	
y	(%)	(%)	(%)	(%)	(%)	(.)	(.)	(mg/dl)	(U)	
Adu.	MDI	2.8 (5.4)	6.8 (8.9)	81.8 (8.4)	11.5 (5.1)	0.3 (1.2)	1.8 (2.3)	2.1 (0.9)	122.0 (13.1)	93.7 (20.6)
	CGM	0.8 (2.1)	2.9 (4.3)	81.4 (5.1)	15.7 (2.7)*	6.0 (3.9)*	1.1 (1.1)	3.7 (1.2)*	129.6 (6.9)	91.2 (20.5)
	Bios.	0.0 (0.0)*	0.0 (0.0)*†	83.4 (3.6)†	16.6 (3.6)*	5.9 (4.9)*	0.1 (0.1)*†	3.8 (1.6)*	137.3 (9.5)*†	87.4 (19.2)*†

Simulation results were analysed for adults (Adu.) after closed-loop simulations of three regulation schemes: Multiple Daily Injections (MDI), a CGM-based AP (CGM), and a biosensor-based AP (Bios.). Case studies 1 and 2 consider a realistic daily glucose intake pattern consisting in three meals (45, 70 and, 80g) and two snacks (20g). Case study 3 considers a challenging daily glucose intake pattern consisting in two meals (100 and 120g) and one snack (20g). No meal announcement is implemented for CGM and Bios. closed-loop schemes. Random errors in carbohydrates counting provided to MDI algorithm are implemented in case studies 2 and 3. The metrics extracted for this comparison are the Time Below Range (TBR) percentage (level 1 and 2), Time In Range (TIR) percentage, Time Above Range (TAR) percentage (level 1 and 2), Low- and High- Blood Glucose Index (LBGI and HBGI) (unitless), mean Blood Glucose (Mean BG) concentration in mg/dl, and Total Daily Insulin (TDI) in units of insulin. All metrics are mean (SD). Symbol * indicates statistical significance ($p < 0.01$) with respect to MDI and symbol † indicates statistical significance ($p < 0.01$) with respect to CGM.

CGM- and Bios-APs, their performance indicators are identical to the ones from case study 1. The third case study uses a **more challenging 2 meal/1 snack** pattern in which a total of 240 g of glucose is ingested each day. The meals are distributed as follows: a large brunch of 100 g of glucose ingested at 10 a.m. and a large dinner of 120 g at 8 p.m. A 20 g snack is added at 5 p.m. The MDI therapy (with random errors) and CGM-AP failed to maintain the patients in the targets; however, the **Bios-AP allowed 4 adults to reach the targets**, and kept both LBGI and HBGI minimal for all adults except adult#007 (see Table 8).

4.2.2. Discussion on this first comparison

In the first case study, the MDI therapy outperformed closed-loop therapies. This result may come as a surprise considering the well-known superiority of sensor-augmented insulin-pump therapy over MDI, as demonstrated in clinical trials [120]. The absence of meal announcement places the closed-loop regulation schemes at a disadvantage, therefore benefitting the non-causal MDI therapy. MDI also benefits from the absence of errors in the patient-provided carbohydrates counting which is unrealistic according to the literature [121]. This point was addressed in case study 2 with a more realistic implementation of the meal announcement (see Herrero *et al.* [122]) which led to a decrease in MDI performance. For its part, the Bios-AP was less efficient than the MDI therapy but still outperformed the CGM-AP with a 4.4% difference in the mean TIR and a lower cumulated glycaemia-related risk (lower LBGI and HBGI, see **Table 8**). The third case study (challenging glucose intake scenario with two large meals and one snack) further emphasized the **impact of carbohydrates counting errors on MDI performance**. The hypoglycemic risk increased even more and the mean TIR for MDI therapy decreased below that of the closed-loop schemes.

The Total Daily Insulin (**TDI**) indicator particularly highlights the **ability of the biosensor to modulate insulin delivery**. Using the same controller settings for all case studies, we observed that the Bios-AP injected more insulin than the CGM-AP in the first two

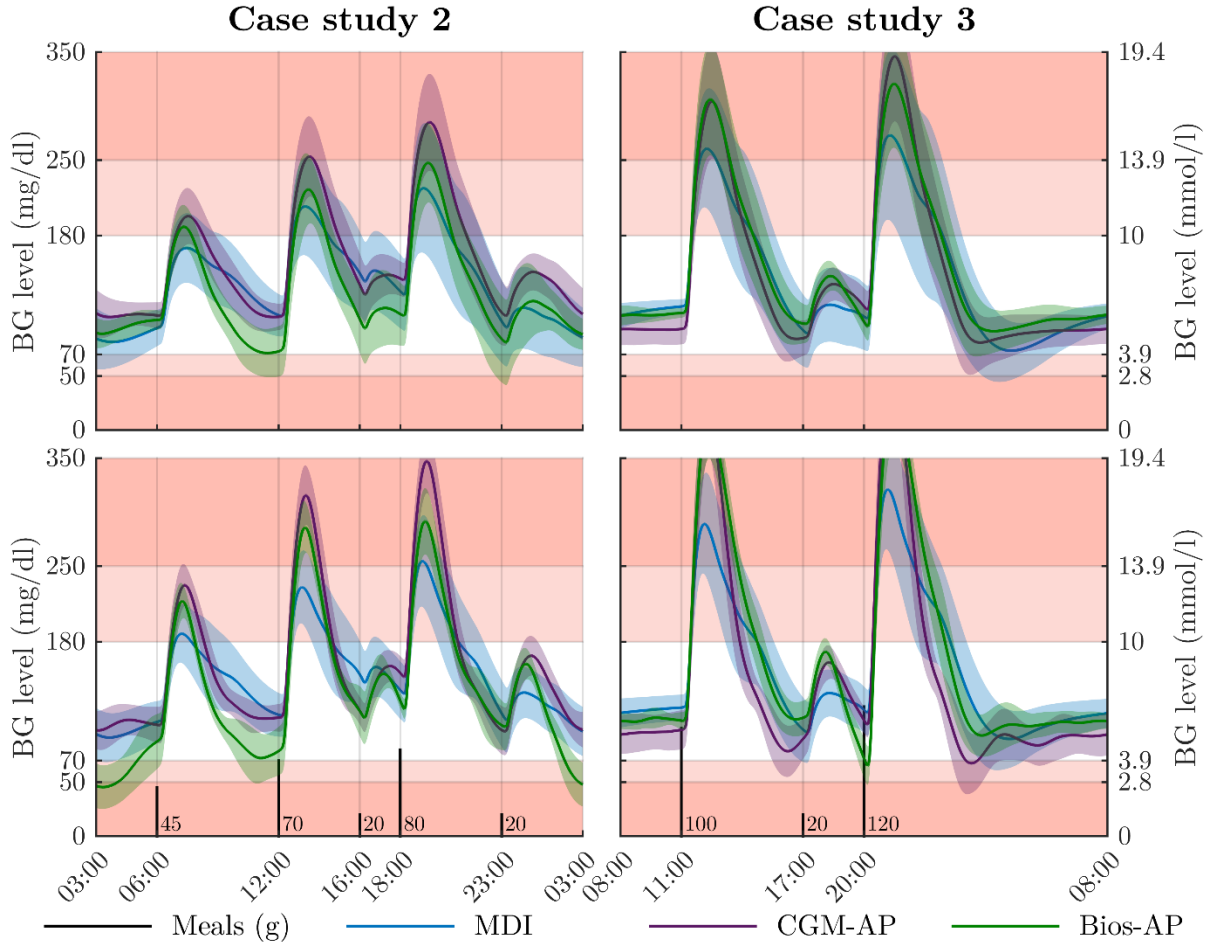


Figure 52: Comparison of the Bios-AP with two reference therapies for the 11 adolescents and 11 children of the T1DMS virtual cohort. The same color-coding as in the previous figure is used for standard deviation and glycaemic risk areas.

case studies, whereas in the third one, it injected significantly less insulin than the CGM-AP. Although the same controller tuning methodology was used in both cases, this modulation, induced by the biosensor, enabled the **Bios-AP to lower the mean BGI** of the adult T1D cohort in all case studies.

This first series of SQ/SQ results was submitted for publication in IEEE Transactions on BioMedical Engineering (TBME, revised manuscript submitted after a first round of peer-reviewing). The SQ/SQ results of adolescents and children were not presented in the TBME article, as we considered them to be inconsistent and required further investigations. They are presented and discussed in this manuscript (see **Figure 52**). Our Bios-AP could not mitigate the hypoglycemic risk of these patients, which therefore presented elevated mean LBGI values (2.5 and 3.3 for adolescents and children respectively - see **Table 9**) when compared with the CGM-AP (0.2 and 0.3). The mean TIR of adolescents the Bios-AP outperformed the CGM-AP (75.1% vs 67.3%) while the opposite happened in children (67.3% vs 71.9%) for no obvious reason. Analysing the insulin infusion rate patterns and the TDI, we also found that our methodology tends to be **overly aggressive** in the tuning of the derivative action of the PD_{BASAL} controllers, in particular with the Bios-AP controllers. We explain that difference by the noise of the CGM sensor which induces a more conservative tuning by GA. Although this downside seems well tolerated by adults, it certainly participates in the poor results observed in children. More importantly, the **meal scenarios represent excessive (and unrealistic) daily glucose intake** for young adolescents and children, which makes the controller's task even harder. We therefore decided to investigate **weight-dependant meal scenarios**, a feature not available in the current version 3.2 of the T1DMS (see next subsection).

Table 9: Performance metrics for three blood glucose level regulation schemes in case study 2, for all adolescents and children.

Category		TBR 2 (%)	TBR 1 (%)	TIR (%)	TAR 1 (%)	TAR 2 (%)	LBGI (.)	HBGI (.)	Mean BG (mg/dl)	TDI (U)
Ado.	MDI	4.1 (8.1)	6.6 (10.0)	72.9 (14.9)	20.6 (17.6)	4.4 (7.7)	2.2 (3.9)	4.6 (3.8)	143.0 (28.9)	71.7 (17.6)
	CGM	0.2 (0.6)	0.6 (1.8)	72.4 (9.4)	26.9 (9.1)	7.6 (7.0)	0.2 (0.4)	6.3 (2.8)	158.0 (16.4)	67.2 (15.6)
	Bios.	3.1 (6.4)	5.8 (10.2)	75.1 (11.4)	19.0 (7.8)†	3.4 (5.0)†	2.5 (4.9)	3.9 (2.0)†	135.1 (17.1)†	74.2 (17.8)†
Chi.	MDI	1.2 (3.5)	2.6 (5.6)	71.0 (11.9)	26.4 (12.7)	5.1 (5.9)	0.7 (1.4)	5.6 (2.6)	153.1 (17.8)	38.6 (7.4)
	CGM	0.2 (0.8)	0.8 (1.6)	71.9 (4.3)	27.4 (3.9)	13.0 (2.8)*	0.3 (0.5)	7.6 (1.3)*	162.7 (6.4)	37.2 (8.1)
	Bios.	6.3 (5.6)†	10.0 (6.4)*†	67.3 (6.8)†	22.7 (1.1)†	7.9 (3.5)†	3.3 (2.9)*†	5.5 (0.8)†	143.4 (7.2)†	40.6 (9.3)†

Simulation results were analysed for the 11 adolescents (Ado.) and 11 children (Chi.) after closed-loop simulations of three regulation schemes: Multiple Daily Injections (MDI), a CGM-based AP (CGM), and a biosensor-based AP (Bios.). Nine metrics were computed on case study 2 simulation results. Symbol * indicates statistical significance ($p < 0.01$) with respect to MDI and symbol † indicates statistical significance ($p < 0.01$) with respect to CGM.

Finally, one can also note that a proper validation of the biosensor with multi-meal scenarios would also require to model **the circadian insulin sensitivity variability** observed in real patients. Although it has been studied and published [123]–[125], this feature is not yet implemented in the commercial version of the T1DMS and was not investigated in this work.

4.2.3. Controller tuning with individualised meal scenarios

The definition of meal scenarios is a limitation in our *in silico* approach. For the sake of demonstration, the same scenarios were used with all the patients of the simulator in the previous studies. The T1DMS’s design encourages the user to do so, as personalising each glucose intake scenario in a time-efficient manner is fastidious: it requires creating one scenario for each patient and running a 33-scenario simulation. This is cumbersome and prevents the use of parallelisation to reduce computation time. As a consequence, most of the published studies using the UVA/Padova T1DMS are based on unique scenarios for all patients. These meal scenarios are unrealistic from a clinical standpoint: adults and children do not have the same energy requirements, and energy requirements of patients belonging to a same category also differ. Common practice in clinical trials is therefore to define scenarios in a body weight-dependent manner.

We developed our own method to define **individualised scenarios** that stimulate all the patients in a consistent manner. This method, described in **Figure 53**, uses a body weight-dependent definition of the glucose intake scenarios to match at best what would be the energy needs of the virtual patients in real life. An additional step was added to the T1DMS execution flow: before the scenario is loaded by the software, a custom function is called. It reads the meal scenario and generates 33 individualised scenarios ensuring that the average daily glucose

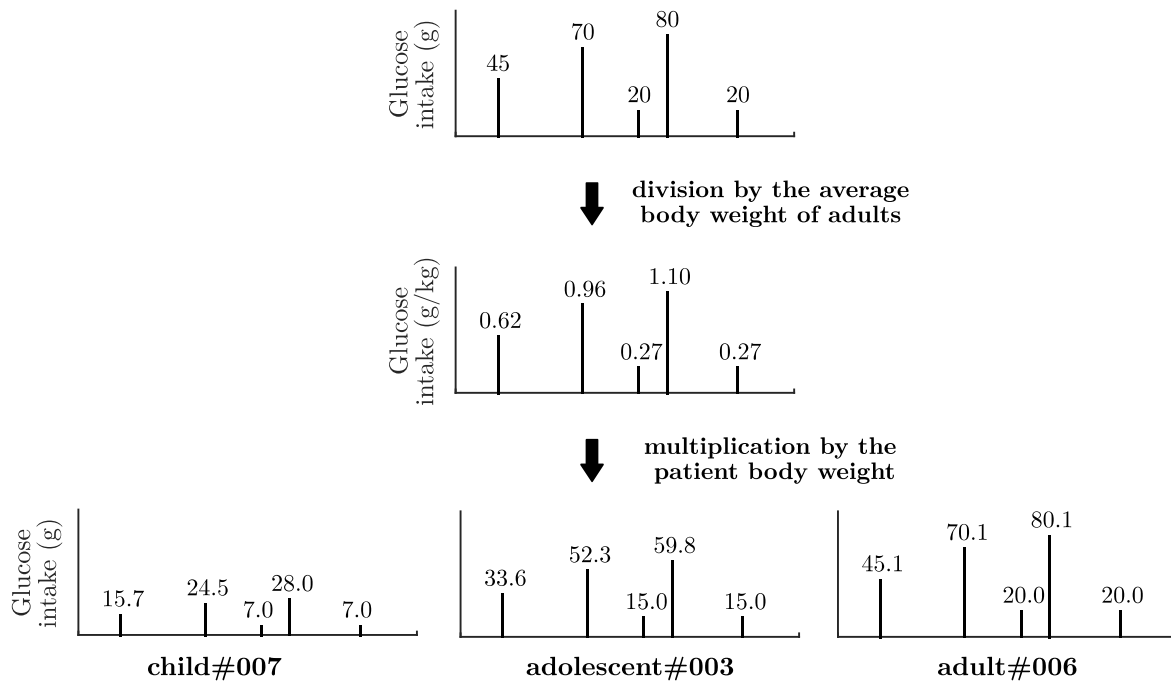


Figure 53: Body weight-dependent definition of the glucose intake scenarios. Example for child#007, adolescent#003, and adult#006.

intake of the 11 adult scenarios is the daily glucose intake of the initial scenario. Validation scenarios in previous sections were designed to match the daily glucose intake reported in the literature for American T1D adults (235 grams of glucose in average). Our method maintains this realism while generating individualised scenarios that best fit the daily intake of energy for adolescents and children. In order to achieve this result, each meal intake is divided by the average body weight of the 11 adults to obtain a meal scenario whose glucose intakes are defined in **grams of glucose per kilogram** (of body weight). The individualised scenarios are then generated by a simple multiplication with patient's body weight (see Appendix 4 for the body weight list). This upgrade of the T1DMS is **transparent for the user** as individualisation is activated by the addition of a “BWdep” key word at the end of the scenario name. Finally, all the scenarios are saved in the output structure for logging purposes.

To validate the proper functioning of this new feature, we tuned a second set of controllers with the GA-based method presented in section 4.1 using individualised scenarios. With these two sets of controllers, we first compared the mean BG profiles obtained for each virtual patient category with (1) the unique and (2) the individualised versions of the realistic 3-meal/2-snack scenario used in subsection 4.2.1. (see **Figure 54**). What is of primary importance here is that, for the first time in this work, it is relevant to **compare each patient category**. Indeed, the comparison of glucose control performance is less relevant as the perturbation induced by glucose intake is comparable between the two scenarios in adults but is far reduced in adolescents and children with individualised scenarios. We observe very **similar mean BG profiles for all categories** with the body weight-dependent scenarios, which confirms the efficiency of our individualisation method. Minimal and maximal glucose excursion are also comparable. **Figure 55** compares the closed-loop performance with the four most instructive metrics: the TIR, the Mean BGI, the Mean BG level, and the TDI. Unsurprisingly, the metrics confirm what was observed with BG profiles: **performance was greatly improved for adolescents and children** with an increase of the TIR, a decrease of both the mean BG level and the mean BGI. One can also note that mean closed-loop performance is very similar from

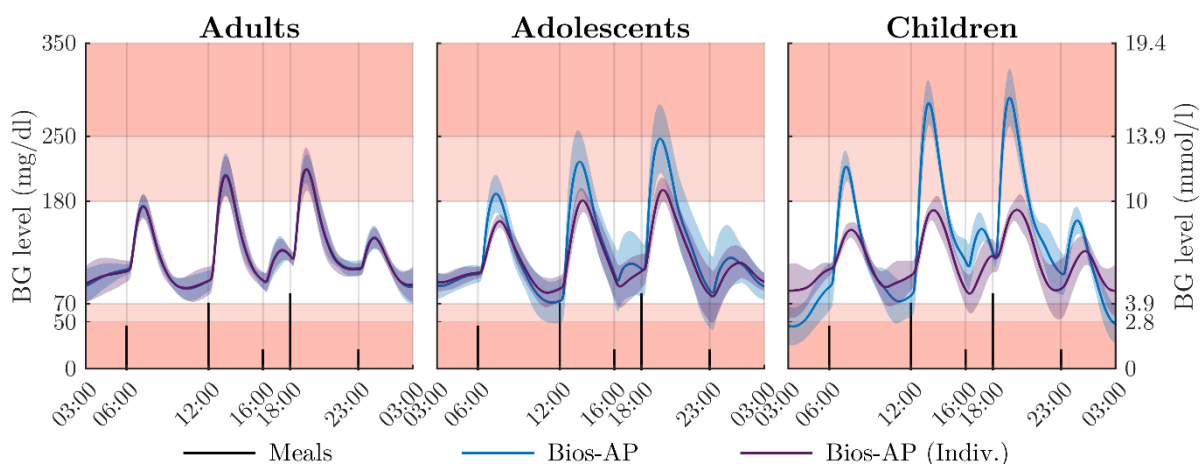


Figure 54: Comparison of mean BG profiles for the three virtual patient categories equipped with the Bios-AP and following different scenario definition strategies: a unique meal scenario is defined for all patients (blue. plot) or an individualised (Indiv.) scenario is defined for each patient (purple plot). These scenario definition strategies were used during both the controller tuning and validation phases. The same color-coding as in the previous figures is used for standard deviation and glycaemic risk areas.

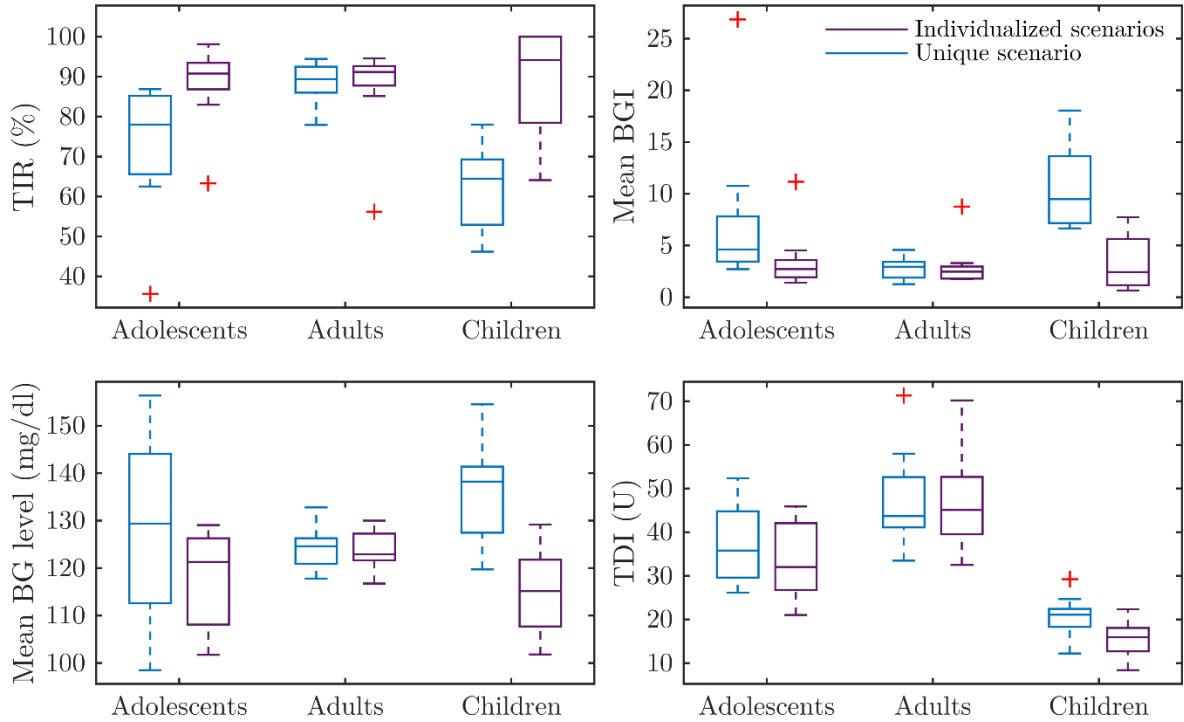


Figure 55: Influence of meal scenario individualisation on closed-loop performance assessed with boxplots of four metrics: the Time In Range (TIR), the mean Blood Glucose Index (Mean BGI), the mean Blood Glucose level (Mean BG level), and the Total Daily Insulin (TDI) are plotted for the unique scenario (blue) and for the individualised scenarios (purple).

one patient category to the other. The standard deviation is also reduced by individualisation which suggests that the inter-patient variability was partly due to an inconsistent level of stimulation by glucose: a meal consisting in 70 grams of glucose is not as challenging for a 30-year-old adult as it is for a 12-year-old adolescent. Still, the fact that the standard deviation is inversely proportional to patient category age suggests that our individualisation method could still be improved. Indeed, there is no obvious reason that explain this increased interpatient variability in children.

We performed a deeper analysis by focusing on the TDI. One conclusion that could be drawn from **Figure 55** is that the TDI logically decreases with individualisation due to a lower daily glucose intake (for a majority of patients), when compared to the unique scenario used before. We therefore analysed the evolution of the total daily glucose intake and insulin infusion for each patient in order to highlight the impact of individualisation of meal scenarios (see **Figure 56**). The upper panel, representing the daily glucose intake evolution, illustrates the principle of our individualisation method: for adults, the daily glucose intakes are equally spread on both sides of the average glucose intake represented by the 235 grams intake of the unique scenario (blue triangles), while younger (and lighter) patients receive smaller glucose intakes. In the lower panel, TDI values are normalised to TDI reference values provided by the T1DMS and corresponding to the TDI achieved by a MDI therapy as described in Dalla Man et al. [98]. Results highlight the **limited influence of individualisation on TDI except for children**. Indeed, children TDI values in the case of individualised scenarios are closer to

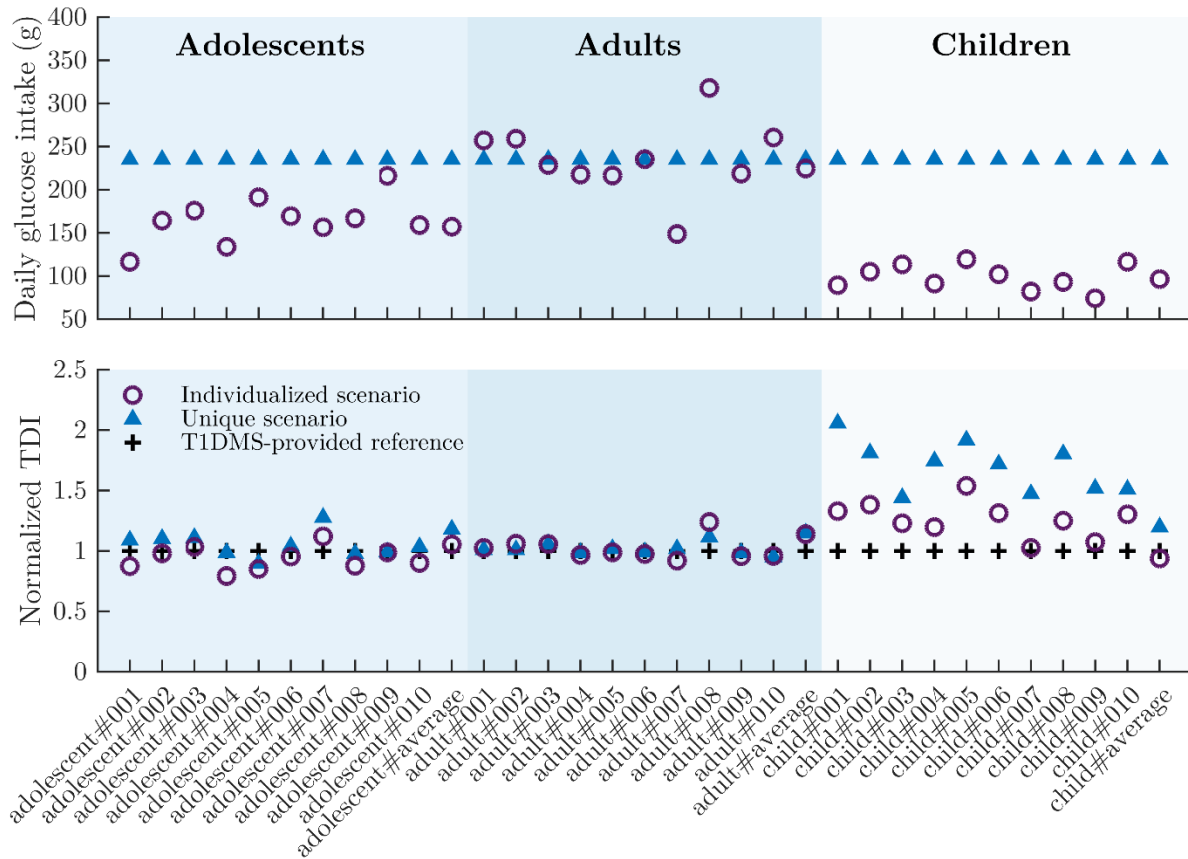


Figure 56: Comparison of the daily glucose intake and Total Daily Insulin (TDI) of each patient for the two scenario definition methods: unique scenario (in blue) and individualised scenarios (in purple). TDI values were normalized to a reference TDI value provided by the T1DMS for each patient and corresponding to the TDI achieved by a MDI therapy.

the reference and therefore appear to be more physiological. They are however still larger than those references which suggests an excessive aggressiveness of our controllers.

To conclude the analysis of this second series of SQ/SQ simulation results, we computed the **daily energy intakes** associated with the daily glucose intakes resulting from individualisation. We considered three hypotheses regarding the proportion of daily energy intake provided by carbohydrates: 45%, 55% and 65%. These hypotheses are in line with the American Diabetes Association recommendation for T1D adults: 45-60% of energy requirements covered by carbohydrates [126]. The corresponding daily energy intakes are plotted in **Figure 57** for each patient category. Unsurprisingly, the total energy intake increases when the proportion of carbohydrates decreases. The total energy intake of adults falls between 1300 to 2800 kcal/day depending on the carb proportion hypothesis. This result is consistent with the range of daily energy intakes reported in the literature for T1D adults [104], [127]. In contrast, the daily energy intakes corresponding to the individualised scenarios of adolescents are lower than those reported in the literature. The energy needs of adolescents and adults are reportedly equivalent [128], [129]. In particular, active adolescents and adolescent sportsmen can present higher energy intakes than adults. According to the average daily energy intake of Australian T1D children reported in [130] (1340 and 2340 kcal/day for 2-3 year-old and 4-8 year-old children respectively), our individualised glucose intake scenarios

also underestimate the energy intake of children. From these observations, we can conclude that the individualisation method is functional for adult patients but possibly yields underestimated daily glucose intakes for adolescents and children. A solution to address this issue could consist in introducing **nonlinearities or patient category-based rules in the body weight-dependent** definition of the scenarios.

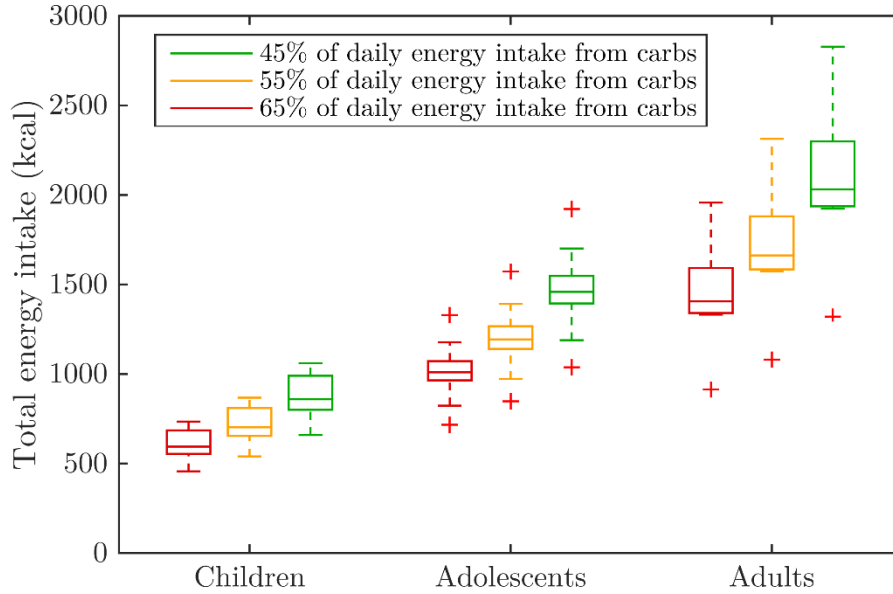


Figure 57: Boxplots of daily energy intakes corresponding to the individualised scenarios of each patient category. Three hypotheses are considered for the following proportion of energy intake covered by carbohydrates: 45%, 55%, and 65%.

4.3. The role of simulation in the Bios-AP design flow

In the last subsections, we outlined three elements restricting the extent of simulation results obtained with the version 3.2 of the UVA/Padova T1DM Simulator: circadian insulin sensitivity variation and non-glucose regulators of insulin secretion are not modelled, and the glucose intake scenarios definition is limited. Although the modelling of these sensitive points could be improved in a custom version of the simulator, one should keep in mind that *in silico* clinical trials will never perfectly reflect reality. As explained in Chapter 2, these simplifications form an integral part of the mathematical modelling process and are necessary to handle the tremendous complexity of the biological interacting systems involved in blood glucose regulation. In this section, we discuss the **contribution of simulation to the design of AP systems** taking the development of our biosensor-based AP as a case-study.

4.3.1. How to enhance the UVA/Padova T1DM Simulator?

Insulin elicits a reduction of blood glucose levels by increasing the glucose uptake of insulin-sensitive cells in muscles and adipose tissue (about two-thirds of body cells). These cells' sensitivity to insulin presents diurnal variations in both healthy and T1D people [131], [132]. This physiological process is not modelled in the **S2013 version of the T1DMS (v3.2)** which led the FDA to limit the extent of its approval to the **simulation of single-meal**

scenarios although the software allows for multi-meal scenarios. To get rid of this limitation and increase the realism of multi-meal simulations, numerous methods have been proposed to model the **intraday variation of insulin sensitivity**. A basic method, which does not require the modification of the metabolic model equations, consists in applying a variable gain on the controller output to simulate insulin sensitivity variations. This approach is convenient but provides a limited control on the diurnal variation pattern due to subcutaneous diffusion kinetics. A better solution is thus to **modify the metabolic model parameters** to implement time-dependent variations of their values. This could be achieved with a unique profile for each patient as proposed by Toffanin et al. [133], or by modelling the interpatient variability of this diurnal pattern observed in real patients, as proposed by Visentin et al. [123]. Circadian variations of insulin sensitivity was also added to the UVA/Padova metabolic model [125] but the model parameters are not published yet. As previously mentioned, a better definition of the glucose intake scenarios paired with the inclusion of intraday variations of the insulin sensitivity in a custom version of the T1DMS would **significantly improve the clinical relevance** of our multi-meal simulations.

As described in Chapter 1, pancreatic beta cell activity is regulated through different pathways involving nutrients (e.g., glucose, free fatty acids, amino acids) and hormones (e.g., GLP-1, GIP, and adrenaline), and can be modulated with various drugs [134]. We explained in Chapter 2 that these **molecules are the inputs of integrative endogenous algorithms** which provide **electrical activity and insulin secretion rate as outputs**. The added value of our biosensor partly lies in the real-time access it offers to these endogenous algorithms. As opposed to glucose-only CGM technologies, this multi-input islet-based biosensor gives new insights on the appropriate way to deliver insulin to T1D patients. As information about nutrients and hormones is integrated into a **single electrical signal**, we hypothesize that the biosensor would provide more reliable information than glucose-only sensors for controlling insulin delivery. To properly assess the ability of a biosensor-based AP to control the insulin delivery of T1D patients in a more physiological manner, the **modelling of these other regulators** of insulin secretion seems therefore necessary.

We demonstrated *in vitro* that our biosensor properly captures the modulation of islet responses induced by GLP-1 and adrenaline (Lebreton *et al.* [70]). Based on our experimental data, a modelling of the plasmatic **GLP-1 concentration varying between two states** (a basal level and a stimulating one) can be envisaged as GLP-1 influence on SPs response was found to follow an “all-or-none” mechanism rather than a dose-dependence mechanism. An alternative solution is to use the work on GLP-1-induced insulin secretion potentiation in healthy subjects and T2D patients published by Dalla Man et al. [135].

Regarding the **plasmatic adrenaline** concentration, no model of the influence of physical activity or stressful episodes in T1D patients is yet available. The work published by Schiavon et al. [136] is an interesting basis to start simulating scenarios with physical activity: it models the impact of physical activity as a **variation of insulin sensitivity** leading to variations of glucose utilization in muscles and adipose tissue.

Although sound and pragmatic, these solutions to upgrade the simulator are not completely satisfactory as they do not achieve the level of accuracy achieved by the T1DMS in modelling the glucose-insulin dynamics of T1D patients. Such a high-level of fidelity requires time and

resource-consuming clinical trials implementing complex triple-tracer methods to monitor the dynamical variations of insulin and glucose during meals, and generate reliable data for the mathematical modelling process. The development of a **multi-hormonal counterpart of the T1DMS** accounting for the intake of nutrients other than glucose thus appears as an **unachievable goal on a short to medium term basis**. Obviously, contribution of *in vitro* experiments on cultured islets, *in vivo* experiments on animal models and clinical trials on T1D patients is still necessary to fully assess the sensing capabilities of our biosensor.

4.3.2. Contribution of simulation to the design of AP systems

Due to the aforementioned limitations, *in silico* campaigns performed in a glucose-only testing environment should be dedicated to the inclusion of the biosensor in an AP system and the design of the associated control algorithm. They provide an **estimation of minimal closed-loop performance** during case studies focusing on:

- **The control algorithm:** We already mentioned the various controller architectures that have been proposed and can be tested using the UVA/Padova T1DMS. Thanks to the 33-built-in virtual T1D patients it provides⁴³, the simulator can also be used to investigate different strategies to handle interpatient variability. We investigated in this work a methodology based on the individualisation of the controller benefitting from the possibility to repeat simulations with the same patient and scenario. Strategies presenting a better compatibility regarding clinical constraints could also be tested. For example, our partners⁴⁴ investigate the application of the H-infinity theory to calibrate controllers which are robust to the interpatient variability modelled within the whole T1DMS cohort, or within a given patient category.
- **Clinically-relevant additional features:** Modern hybrid closed-loop systems all implement similar features (further detailed in 4.4) to mitigate the hypoglycaemic risk. Simulation could be used to incorporate some of them in the Bios-AP and assess their impact on closed-loop performance.
- **The impact of true-to-life challenges:** Increasing levels of realism about the evaluated therapies can also be implemented through simulations to assess the relative impact of the elements which negatively affect the closed-loop performance. The MDI therapy and the CGM-AP are rendered more realistic in this work by the introduction of errors in the carbohydrates counting and by the presence of measurement noise in the CGM sensor model (see subsection 4.2.1). In our models, the biosensor is considered as ideal since no parasitic component is implemented. This assumption is relevant considering that measurement noise does not significantly affect performance due to low SP frequency (0-2 Hz).

⁴³ A larger cohort comprising 300 patients (100 adults, 100 adolescents, and 100 children) is available upon request and payment to the Epsilon Group, the company which commercialises the UVA/Padova T1DM Simulator.

⁴⁴ The ARIA team (IMS laboratory, UMR 5218).

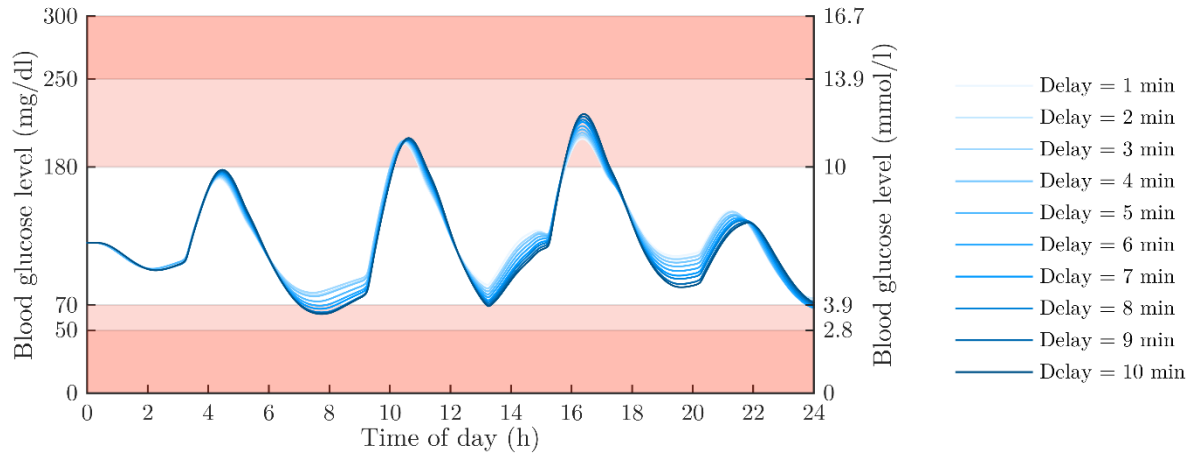


Figure 58: Evolution of the simulated blood glucose profile of adult#005 submitted to a 3-meals/2-snacks scenario for 10 values of the additional delay induced by the microfluidic setup.

- The development of a wearable device:** A wearable implementation of our biosensor would however require an osmotic pump coupled with a microfluidic chip to feed the biosensor islets with patient's interstitial fluids. Due to **tubing and perfusion** safety constraints, the microfluidic setup will certainly induce additional delay in the measurement chain thus probably degrading closed-loop performance of the AP system. Simulation certainly helps assess the **impact of this delay** on glucose control and define the specification of a wearable implementation of our sensor. **Figure 58** presents an example of parametric analysis that could be simulated for that purpose. The patient adult#005 is submitted to the realistic 3-meals/2-snacks scenario used in section 4.2. An additional delay is inserted between the patient and the biosensor to simulate the delay induced by a microfluidic chip in the biosensor. Unsurprisingly, the **magnitude of extreme glycaemic events increases** with the additional delay, thus degrading the closed-loop performance of the Bios-AP. We quantified this degradation observing the evolution of the TIR and the mean BGI as a function of the delay value (see **Table 10**). Below 5 minutes of additional delay, a performance drop of 0.4% of TIR and 0.1 of mean BGI per minute was observed while the mean drop in performance per minute regularly increases above 5 minutes. Based on these observations, one can anticipate that an additional **microfluidic delay lower than 5 minutes is acceptable** while an additional delay higher than 5 minutes significantly reduces the closed-loop performance of the Bios-AP system. These results are preliminary but they illustrate a contribution

Table 10: Evolution of the TIR and mean BGI as a function of the microfluidic delay

Units		Values									
Delay	min	1	2	3	4	5	6	7	8	9	10
TIR	%	88.5 (7.1)	88.1 (7.3)	87.7 (7.3)	87.2 (7.5)	86.2 (7.6)	85.4 (7.3)	84.6 (7.6)	83.8 (7.9)	82.7 (8.0)	82.3 (7.9)
Mean		2.62	2.73	2.82	2.93	3.10	3.21	3.33	3.48	3.64	3.75
BGI	-	(1.13)	(1.19)	(1.20)	(1.25)	(1.30)	(1.34)	(1.37)	(1.41)	(1.45)	(1.51)

Simulation results were analysed for the 11 T1D adults equipped with the Bios-AP and submitted to a 24-hour 3-meals/2-snacks scenario. All metrics are mean (SD).

of the T1DMS simulations to the development of a real-world implementation of the Bios-AP.

- **A practical biosensor device model:** For reliability purpose, a wearable biosensor device would embed several islets to provide a statistical mean and cope with biological variability. We currently foresee an **extracorporeal device embedding up to ten islets fed with patient interstitial fluids**. The continuous monitoring of islets' electrical activity would therefore yield multiple signals subsequently combined to compute the sensor output, i.e., an estimation of the patient insulin need. Our consortium (ARIA team) is currently developing a **family of biosensor models** to account for biological variability during the controller synthesis process. Using the UVA/Padova testing environment, a similar approach could be used to develop a realistic model of the biosensor incorporating several islet models, signal processing blocks and an insulin need estimation block (see an illustration with five islets in **Figure 59**). Such a model would permit to investigate various methods to compute the patient insulin need from **multiple SP frequency signals**.

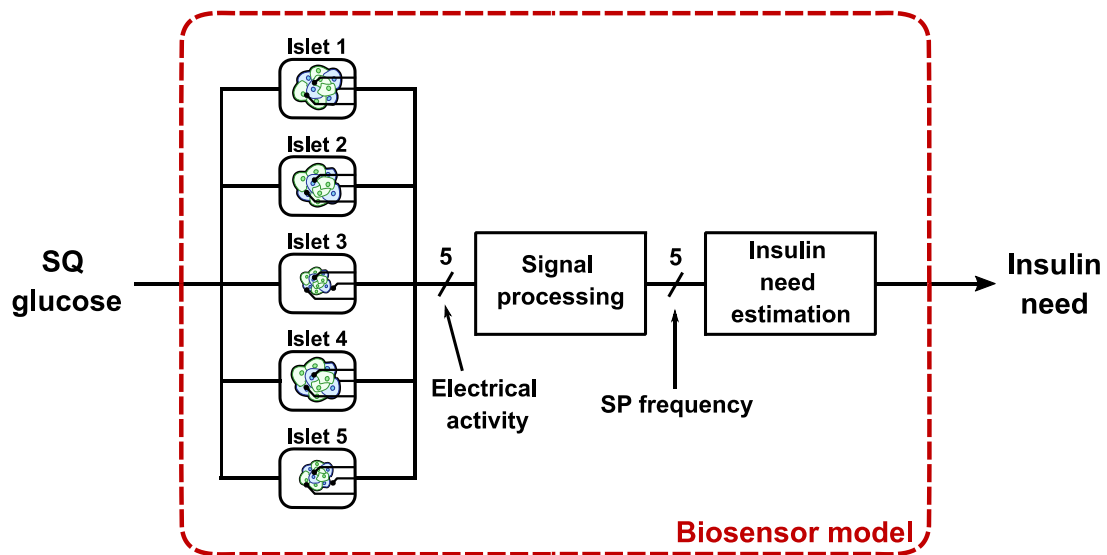


Figure 59: Model of a practical biosensor incorporating five islets whose electrical activity is monitored and processed to compute an estimation of the insulin need of a T1D patient.

4.4. Real world implementation of the Bios-AP

We found it relevant to conclude this thesis manuscript by discussing a **real-world implementation of a biosensor-based Artificial Pancreas**. We intend to depict how the aforementioned diabetes treatment problematics are managed in **state-of-the-art closed-loop systems** and underline **the blind spots of simulation in modelling everyday clinical practice**. In doing so, we will pay particular attention to the management of variability in diabetes, which is the main impediment to the development of fully automated BG regulation devices. Finally, this section proposes a **set of guidelines** for the future development of the Bios-AP.

4.4.1. Management of variability in Type 1 Diabetes

Variability in diabetes takes many forms. One may speak of interpatient, inpatient, interday, and intraday variabilities, each of which necessitating appropriate measures to limit their impact on treatment efficacy. The biosensor introduces an additional source of variability, lying in the **biological variability of the embedded islets**, which also need to be managed to allow the Bios-AP to meet the regulatory requirements of medical devices.

Interpatient variability, as the variation of body characteristics from one patient to the other, primarily originate from genetic differences but also from environmental factors as past and present lifestyles shape the body and its response to glucose intake. In the case of diabetes, interpatient variability can result in widely variable responses to a given treatment and needs to be taken into account during the development of AP systems. Disease duration also play a role in interpatient variability since patient's general condition worsens as disease develop, especially for patients with poor glucose control. Nowadays, **interpatient variability** is managed **through individualisation of the insulin therapy**, either independently by the patient or during regular meetings with the healthcare staff. Modern hybrid closed-loop systems propose a set of configurable parameters to the clinician in order to finely adapt the insulin therapy to patient needs. The same strategy should be adopted for the Bios-AP to maximise closed-loop performance and favour acceptance by both clinicians and patients. As interpatient variability is modelled in the UVA/Padova T1DMS, this testing environment is perfectly suited for the development of control algorithms robust to errors in patient-provided therapy parameters. Optimal controller parameters could for example be computed with *in silico* optimisation methods, such as our GA-based method, and subsequently related to virtual patient characteristics, thus providing a **clinically-compatible method to set the Bios-AP parameters**.

T1D patients, like healthy individuals, also present circadian variations of some of their characteristics. We have already mentioned the circadian variation of insulin sensitivity as it is the most impacting characteristic which varies throughout the day, but other characteristics such as endogenous glucose production or glucose utilization may vary depending on the patient's psychological state, nutritional status, and physical activity level. In modern closed-loop systems, **intraday variability** is handled with **daily patterns for the main therapy parameters** (e.g., basal insulin delivery, insulin-to-carbohydrates ratio, correction factor) and with **meal and physical activity announcement** features. Although the **Bios-AP** should

benefit from the exquisite sensing capabilities of the embedded healthy islets, and thus have a better picture of the patient's physiological state, the addition of **facultative meal and physical activity announcement** features would certainly be valuable to further improve regulation performance. The contribution of these different features could be investigated with simulation but some upgrades, mentioned in section 4.3.1, need to be made to the T1DMS first.

In addition to intraday variability, T1D patients also present an interday variability of their characteristics which need to be handled by any automated BG regulation device. This **interday variability** can be described at **different time scales**. A variability can be observed over several days for the reasons mentioned above (for intraday variability) and due to patient's weekly routine. Until recently, interday variability required the patient to adapt their therapy parameters themselves but with the development of CGM technologies, which monitor subcutaneous glucose concentration with an excellent resolution, and the advent of machine learning, **adaptive control algorithms** are being developed to reduce patient burden. At a longer time scale, interday variability mainly consists in body weight variation or in disease-induced modification of its body characteristics. This variability is already well managed through regular meetings with the health staff and the definition of a diet plan to improve body weight control.

To conclude this subsection, it is important to note that the **Bios-AP** introduces an additional source of variability: **the biological variability of pancreatic islets**. This variability may appear as an issue which need to be addressed via **factory calibration of biosensors** and perfect characterisation of the embedded islets. However, islets whose sizes are well characterised could also be used to virtually reconstitute the biological diversity observed in a healthy pancreas and refine patient's insulin need estimation. Although such use of the biological variability is certainly hard to achieve, we found it important to note that biological variability may not be something to reject when our overall objective is to regulate T1D patients' BG in a more **physiological manner**.

4.4.2. Integration of a CGM sensor in the Bios-AP

The DCCT/EDIC study demonstrated that **intensive glycaemic control** greatly improves long-term outcomes of T1D treatment but also induces an **increased risk of adverse hypoglycaemic events**. AP systems therefore have to both ensure a satisfactory glucose control and mitigate the hypoglycaemic risk. We have seen in Chapter 1 that modern hybrid closed-loop systems achieve this thanks to **hypoglycaemic alarm** and automated suspension of basal insulin delivery based on CGM readings analysis. Due to its working principle, the biosensor output is null when no insulin is needed. As a consequence, the information provided by the biosensor could not be used to detect hypoglycaemia and the **co-integration of a CGM sensor and the biosensor in the Bios-AP** would certainly be necessary. This choice would not only be a technical choice to improve the device performance but it would also be necessary to match the regulatory framework of medical devices. Indeed, reactive hypoglycaemia is a life-threatening complication of diabetes treatment and a CGM able to trigger an alarm is required to ensure patient safety.

4.4.3. Realistic real-world implementation of our biosensor

Although many differences do exist between the AP systems currently available on the market (e.g., form factor, user interface, configurability), some core elements are common to all of them. All hybrid closed-loop systems implement some form of **active insulin modelling** to try to estimate the amount of previously injected insulin which is still active in patient body. With hypoglycaemic alarms, this feature plays a key role in the reduction of the hypoglycaemic risk. All control algorithms are also configurable to cope with interpatient variability and benefit from patient-provided information to better handle meals and physical exercise. These core elements seem necessary to achieve top-of-the-art performance and respect the regulatory framework imposed by Health Authorities. **Figure 60** therefore presents an **illustrative schematic of a realistic real-world implementation** of the Bios-AP including all these elements.

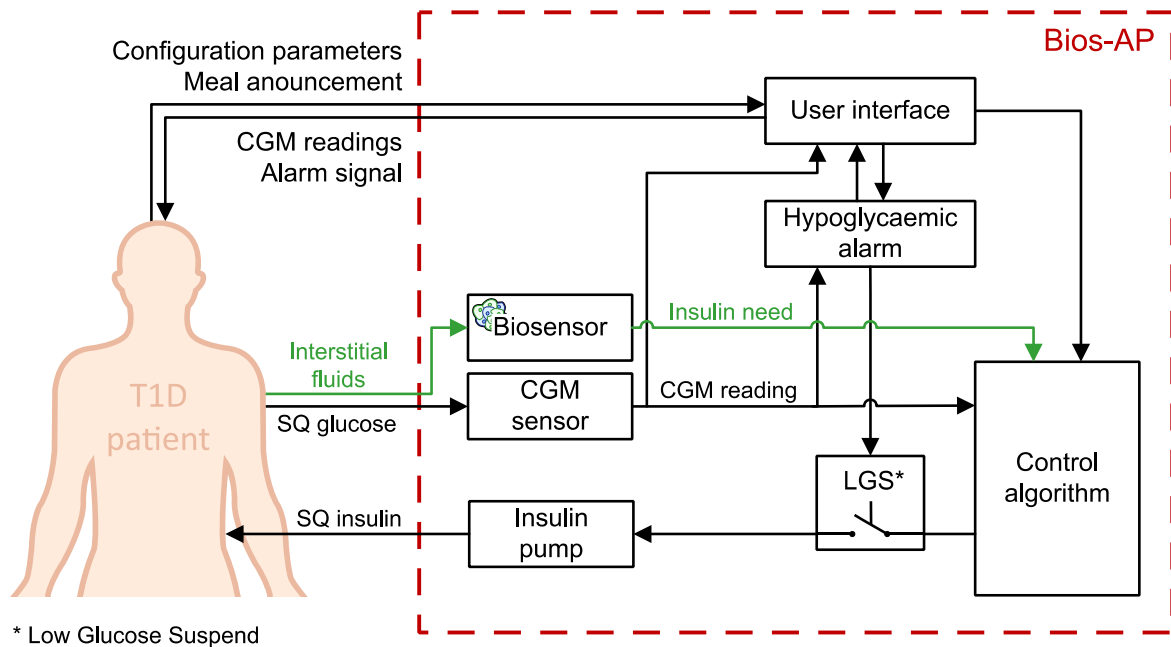


Figure 60: Practical real-world implementation of the Biomimetic Artificial Pancreas

This thesis work laid the foundations of the *in silico* design of an unconventional AP (Bios-AP) based on a new sensor paradigm. We settled simulation and analysis methodologies to explore the Bios-AP performances and prepare a future *in silico* clinical trial. A sensor benefitting from the physiological response of healthy islets is certainly valuable, but many questions remain unaddressed regarding the Bios-AP relevance for T1D patients. We truly believe that solving these issues can only be achieved through the bold combination of *in vivo*, *in vitro* and *in silico* research, requiring a symbiotic collaboration between clinicians, biologists, physicists and engineers.

Appendices

Appendix 1 - Worldwide prevalence of diabetes and forecasts (IDF Atlas 2019)

IDF DIABETES ATLAS

9th edition 2019



GLOBAL Fact sheet

Number of adults (20–79 years) with diabetes worldwide

North America & Caribbean

2045 63 million ↑ 33% increase
2030 56 million
2019 48 million

- 1 in 6 adults in this Region is at risk of type 2 diabetes
- 43% of global diabetes-related health expenditure occurs in this Region

South & Central America

2045 49 million ↑ 55% increase
2030 40 million
2019 32 million

- 2 in 5 people with diabetes were undiagnosed
- Only 9% of global diabetes-related health expenditure for diabetes is spent in this Region

Africa

2045 47 million ↑ 143% increase
2030 29 million
2019 19 million

- 3 in 5 people with diabetes are undiagnosed
- 3 in 4 deaths due to diabetes were in people under the age of 60

Middle East & North Africa

2045 108 million ↑ 96% increase
2030 76 million
2019 55 million

- 1 in 8 people have diabetes
- 1 in 2 deaths due to diabetes were in people under the age of 60

South-East Asia

2045 153 million ↑ 74% increase
2030 115 million
2019 88 million

- 1 in 5 adults with diabetes lives in this Region
- 1 in 4 live births are affected by hyperglycaemia in pregnancy

Western Pacific

2045 212 million ↑ 31% increase
2030 197 million
2019 163 million

- 1 in 3 adults with diabetes lives in this Region
- 1 in 3 deaths due to diabetes occur in this Region

WORLD

2045 700 million ↑ 51% increase
2030 578 million
2019 463 million

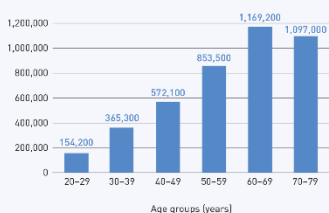
Europe

2045 68 million ↑ 15% increase
2030 66 million
2019 59 million

- 1 in 6 live births are affected by hyperglycaemia in pregnancy
- The Region has the highest number of children and adolescents (0–19 years) with type 1 diabetes – 297,000 in total

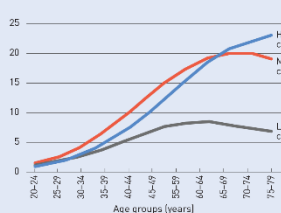
Diabetes affects people of all ages, typically showing higher prevalence with increasing age up to 60–69 years.

Deaths attributable to diabetes by age (20–79 years), 2019



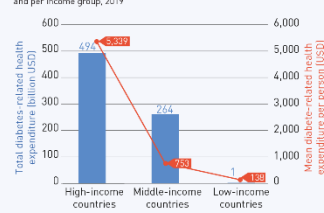
1 in 5 people older than 65 years have diabetes.

Prevalence (%) estimates of diabetes by age and income group, 2019



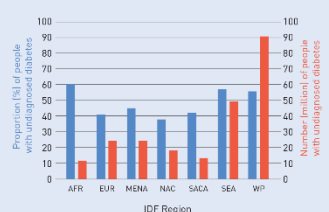
87% of diabetes-related deaths occur in low- and middle-income countries. But, only 35% of diabetes-related health expenditure is spent there.

Total diabetes-related and mean health expenditure per person and per income group, 2019



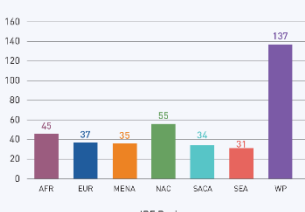
4 out of every 5 adults with undiagnosed diabetes live in low- and middle-income countries.

Number and percentage of adults (20–79 years) with undiagnosed diabetes in IDF Regions, 2019



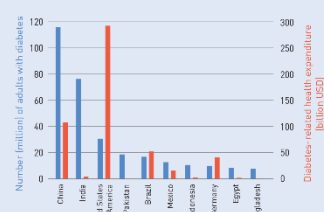
1 in 3 of adults at risk of developing type 2 diabetes, live in the Western Pacific Region.

Number (million) of adults (20–79 years) with impaired glucose tolerance per IDF Region, 2019



67% of adults with diabetes live in top 10 countries and 70% of diabetes-related health expenditure is spent in these countries.

Top 10 countries for number of adults with diabetes (20–79 years) and their health expenditure, 2019



IDF: International Diabetes Federation; AFR: Africa; EUR: Europe; MENA: Middle East and North Africa; NAC: North America and Caribbean; SACA: South and Central America; SEA: South-East Asia; WP: Western Pacific

Corporate sponsor

The 9th edition has been produced thanks to an educational grant (2018–2019) from:



With the additional support of:



Need more information?

www.diabetesatlas.org
or scan QR code
or contact atlas@idf.org



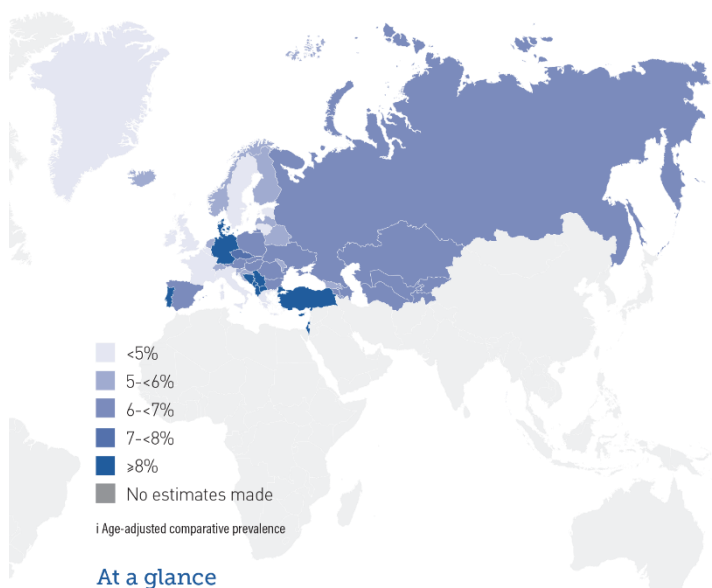
Appendix 2 - European prevalence of diabetes and forecasts (IDF Atlas 2019)

IDF DIABETES ATLAS

9th edition 2019

EUROPE

Prevalenceⁱ of diabetes (20–79 years), 2019



At a glance

	2019	2030	2045
Adult population (20–79 years)	665 million	674 million	665 million
Diabetes (20–79 years)			
Regional prevalence	8.9%	9.8%	10.3%
Age-adjusted comparative prevalence	6.3%	7.3%	7.8%
Number of people with diabetes	59 million	66 million	68 million
Number of deaths due to diabetes	465,900	-	-
Proportion of undiagnosed diabetes	40.7%	-	-
Number of people with undiagnosed diabetes	24 million	-	-
Diabetes-related health expenditure (20–79 years)			
Total health expenditure, USD	161 billion	169 billion	160 billion
Impaired glucose tolerance (20–79 years)			
Regional prevalence	5.5%	5.9%	6.1%
Age-adjusted comparative prevalence	4.4%	4.9%	5.1%
Number of people with impaired glucose tolerance	37 million	40 million	40 million
Type 1 diabetes (0–19 years)			
Number of children and adolescents with type 1 diabetes	296,500	-	-
Number of newly diagnosed children and adolescents each year	31,100	-	-

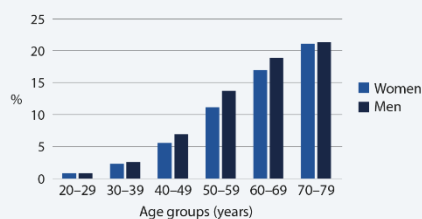
Highlights

- 1 in 11 adults have diabetes.
- 60 million people have diabetes. Immediate action is needed else the count will rise to 68 million by 2045.
- Over a third (41%) of people with diabetes have not been diagnosed and are at higher risk of developing harmful and costly complications.
- The Europe Region has the highest number of children and adolescents with type 1 diabetes 296,500 in total.
- 1 in 3 (31%) of diabetes-related deaths are in people under the age of 60 years.
- 1 in 5 live births are affected by hyperglycemia in pregnancy.
- Europe has third largest diabetes-related expenditure, total USD 161 billion which accounts for 21% of the global expenditure.

Top five countries for number of people with diabetes (20–79 years), 2019

	Millions
Germany	9.5
Russian Federation	8.3
Turkey	6.6
Italy	3.7
Spain	3.6

Prevalence of diabetes by age and sex, 2019



Corporate sponsor

The 9th edition has been produced thanks to an educational grant (2018–2019) from:



With the additional support of:



Need more information?

www.diabetesatlas.org
or scan QR code
or contact atlas@idf.org



Appendix 3 – UVA/Padova T1DMS metabolic model equations

Model Equations

Glucose subsystem:

$$\begin{cases} \dot{G}_p(t) = EGP(t) + Ra(t) - U_{il}(t) - E(t) - k_1 \cdot G_p(t) + k_2 \cdot G_i(t) \\ G_p(0) = G_{pb} \\ \dot{G}_i(t) = -U_{id}(t) + k_1 \cdot G_p(t) - k_2 \cdot G_i(t) \\ G_i(0) = G_{ib} \\ G(t) = \frac{G_p}{V_G} \\ G(0) = G_b \end{cases} \quad (A1)$$

Insulin subsystem:

$$\begin{cases} \dot{I}_p(t) = -(m_2 + m_4) \cdot I_p(t) + m_1 \cdot I_l(t) + R_{ai}(t) \\ I_p(0) = I_{pb} \\ \dot{I}_l(t) = -(m_1 + m_3) \cdot I_l(t) + m_2 \cdot I_p(t) \\ I_l(0) = I_{lb} \\ I(t) = \frac{I_p(t)}{V_l} \end{cases} \quad (A2)$$

Glucose rate of appearance:

$$\begin{cases} \dot{Q}_{sto}(t) = Q_{sto1}(t) + Q_{sto2}(t) \\ Q_{sto}(0) = 0 \\ \dot{Q}_{sto1}(t) = -k_{gri} \cdot Q_{sto1}(t) + D \cdot \delta(t) \\ Q_{sto1}(0) = 0 \\ \dot{Q}_{sto2}(t) = -k_{empt}(Q_{sto}) \cdot Q_{sto2}(t) + k_{gri} \cdot Q_{sto1}(t) \\ Q_{sto2}(0) = 0 \\ \dot{Q}_{gut} = -k_{abs} \cdot Q_{gut}(t) + k_{empt}(Q_{sto}) \cdot Q_{sto2}(t) \\ Q_{gut}(0) = 0 \\ Ra(t) = \frac{f \cdot k_{abs} \cdot Q_{gut}(t)}{BW} \\ Ra(0) = 0 \end{cases} \quad (A3)$$

with

$$k_{empt}(Q_{sto}) = k_{min} + \frac{k_{max} - k_{min}}{2} \cdot \left\{ \tanh[\alpha(Q_{sto} - b \cdot D)] - \tanh[\beta(Q_{sto} - c \cdot D)] + 2 \right\} \quad (A4)$$

Endogenous glucose production:

$$EGP(t) = k_{p1} - k_{p2} \cdot G_p(t) - k_{p3} \cdot X^L(t) + \xi \cdot X^H(t) \quad (A5)$$

$$\dot{X}^L(t) = -k_i \cdot [X^L(t) - I(t)] \quad X^L(0) = I_b \quad (A6)$$

$$\dot{I}(t) = -k_i \cdot [I(t) - I(t)] \quad I(0) = I_b \quad (A7)$$

$$\begin{aligned} \dot{X}^H(t) &= -k_H \cdot X^H(t) + k_H \cdot \max[(H(t) - H_b), 0] \\ X^H(0) &= 0 \end{aligned} \quad (A8)$$

Glucose utilization:

$$U_{il}(t) = F_{cns} \quad (A9)$$

$$U_{id}(t) = \frac{[V_{m0} + V_{mx} \cdot X(t) \cdot (1 + r_1 \cdot risk)] \cdot G_i(t)}{K_{m0} + G_i(t)} \quad (A10)$$

with

$$\dot{X}(t) = -p_{2U} \cdot X(t) + p_{2U}[I(t) - I_b] \quad X(0) = 0 \quad (A11)$$

$$risk = \begin{cases} 0 & \text{if } G \geq G_b \\ 10 \cdot [f(G)]^2 & \text{if } G_{th} \leq G < G_b \\ 10 \cdot [f(G_{th})]^2 & \text{if } G < G_{th} \end{cases} \quad (A12)$$

$$f(G) = \log\left(\frac{G}{G_b}\right)^{r_2} \quad (A13)$$

Renal excretion:

$$E(t) = \begin{cases} k_{e1} \cdot [G_p(t) - k_{e2}] & \text{if } G_p(t) > k_{e2} \\ 0 & \text{if } G_p(t) \leq k_{e2} \end{cases} \quad (A14)$$

Subcutaneous insulin kinetics:

$$R_{ai}(t) = k_{a1} \cdot I_{sc1}(t) + k_{a2} \cdot I_{sc2}(t) \quad (A15)$$

with

$$\begin{cases} \dot{I}_{sc1}(t) = -(k_d + k_{a1}) \cdot I_{sc1}(t) + IIR(t) \\ I_{sc1}(0) = I_{sc1ss} \\ \dot{I}_{sc2}(t) = k_d \cdot I_{sc1}(t) - k_{a2} \cdot I_{sc2}(t) \\ I_{sc2}(0) = I_{sc2ss} \end{cases} \quad (A16)$$

Subcutaneous glucose kinetics:

$$\dot{G}_s(t) = -\frac{1}{T_s} \cdot G_s(t) + \frac{1}{T_s} \cdot G(t); \quad G_s(0) = G_b \quad (A17)$$

Glucagon kinetics and secretion:

$$\dot{H}(t) = -n \cdot H(t) + SR_H(t) + Ra_H(t) \quad H(0) = H_b \quad (A18)$$

with

$$SR_H(t) = SR_H^s(t) + SR_H^d(t) \quad (A19)$$

$$SR_H^s(t) = \begin{cases} -p \cdot \left[SR_H^s(t) - \max\left(\sigma_2 \cdot [G(t) - G_b] + SR_H^d, 0\right) \right] & \text{if } G(t) \geq G_b \\ -p \cdot \left[SR_H^s(t) - \max\left(\frac{\sigma \cdot [G(t) - G_b]}{I(t) + 1} + SR_H^d, 0\right) \right] & \text{if } G(t) < G_b \end{cases} \quad (A20)$$

$$\text{SR}_H^d(t) = \delta \cdot \max\left(-\frac{dG(t)}{dt}, 0\right) \quad (\text{A21})$$

Subcutaneous glucagon kinetics:

$$\begin{cases} \dot{H}_{sc1}(t) = -(k_{h1} + k_{h2}) \cdot H_{sc1}(t) \\ H_{sc1}(0) = H_{sc1b} \\ \dot{H}_{sc2}(t) = k_{h1} \cdot H_{sc1}(t) - k_{h3} \cdot H_{sc2}(t) \\ H_{sc2}(0) = H_{sc2b} \end{cases} \quad (\text{A22})$$

$$Ra_H(t) = k_{h3} \cdot H_{sc2}(t) \quad (\text{A23})$$

Appendix 4 –UVA/Padova **T1DMS** virtual patients' characteristics and therapy parameters

Names	Age	Body weight	T1DM duration	CR	CF	TDI
<i>Units</i>	<i>year</i>	<i>kg</i>	<i>year</i>	<i>g/U</i>	<i>mg/dl/U</i>	<i>U</i>
adolescent#001	16	36	12	26	79	24
adolescent#002	18	51	9	20	77	26
adolescent#003	19	54	11	26	61	31
adolescent#004	17	41	16	10	48	43
adolescent#005	19	59	11	10	56	36
adolescent#006	17	53	3	24	73	26
adolescent#007	19	49	15	26	47	41
adolescent#008	16	52	2	9	37	51
adolescent#009	16	67	8	11	42	46
adolescent#010	19	49	11	15	53	36
adolescent#average	16	49	8	16	56	30
adult#001	32	80	21	19	44	42
adult#002	22	80	12	22	42	43
adult#003	42	71	38	15	35	52
adult#004	24	67	19	20	53	35
adult#005	47	67	35	13	48	40
adult#006	23	73	12	9	26	72
adult#007	47	46	3	18	43	43
adult#008	56	99	3	9	37	52
adult#009	24	68	14	20	53	34
adult#010	31	81	19	14	40	47
adult#average	32	70	11	16	43	40
child#001	3	28	2	20	108	12
child#002	12	33	1	32	120	12
child#003	5	35	2	31	96	15
child#004	5	28	5	32	176	7
child#005	3	37	3	27	120	11
child#006	2	32	1	20	80	17
child#007	2	25	1	19	102	13
child#008	8	29	6	26	137	10
child#009	4	23	2	30	151	9
child#010	7	36	4	32	96	15
child#average	6	30	4	24	110	17

Appendix 5 – Performance metrics corresponding to IV/IV results of adolescents

Adolescents										
Patient		TBR 2	TBR 1	TIR	TAR 1	TAR 2	LBGI	HBGI	Mean BG	TDI
ID		(%)	(%)	(%)	(%)	(%)	(.)	(.)	(mg/dl)	(U)
1	Stat.	0	0	93.1	6.9	0	0.3	1.3	118.6	35.1
	Hyst.	0	0	94.4	5.6	0	0.3	1.2	117.5	34.8
2	Stat.	0	0	82.9	17.1	6.3	0.1	4.2	146.3	28.4
	Hyst.	0	0	85.8	14.2	5	0.2	3.1	133.7	30.7
3	Stat.	0	0	100	0	0	0.1	0.4	116.9	34.9
	Hyst.	0	0	100	0	0	0	0.4	120.2	33.9
4	Stat.	0	0	94.2	5.8	0	0.1	1.3	124.1	53.7
	Hyst.	0	0	95.7	4.3	0	0.3	0.9	117.1	56.4
5	Stat.	0	0	99.3	0.7	0	0.2	0.5	114	38.3
	Hyst.	0	0	99.7	0.3	0	0.3	0.3	110.6	39.7
6	Stat.	0	0	100	0	0	0.1	0.2	111.5	28.7
	Stat.	0	0	100	0	0	0.1	0.2	112.8	28.3
7	Stat.	0	0	82.9	17.1	4.6	0.5	3.5	135.9	46.9
	Hyst.	0	4.9	85.8	9.4	0	1.2	1.7	116.1	51.7
8	Stat.	0	0	100	0	0	0.3	0.2	107.3	65.3
	Hyst.	0	0	100	0	0	0.5	0.1	104.4	71.1
9	Stat.	0	0	99.7	0.3	0	0.2	0.3	111.3	54.8
	Hyst.	0	0	100	0	0	0.2	0.2	109.1	56.1
10	Stat.	0	0	90.8	9.2	0	0.1	1.8	128.7	36.3
	Hyst.	0	0	94.4	5.6	0	0.2	1.1	119.5	38.4
11	Stat.	0	0	96.6	3.4	0	0.3	0.7	115.5	40.7
	Hyst.	0	0	97.6	2.4	0	0.5	0.5	109.3	43

Performance metrics computed on the last 24 hours of a 48-hour, 3-meal/2-snack scenario in adolescents for two regulation schemes: Static model 2020 (Stat.) and Hysteretic model 2020 (Hyst.). Nine metrics are computed: the Time Below Range (TBR level 1: 70 mg/dl, level 2: 54mg/dl), the Time In Range (TIR), the Time Above Range (TAR level 1: 180 mg/dl, level 2: 250 mg/dl), the Low Blood Glucose Index (LBGI) and its counterpart the High Blood Glucose Index (HBGI), the Mean Blood Glucose level (Mean BG), and the Total Daily Insulin (TDI) administered to the patient.

Appendix 6 — Performance metrics corresponding to IV/IV results of adults

Adults

Patient ID		TBR 2 (%)	TBR 1 (%)	TIR (%)	TAR 1 (%)	TAR 2 (%)	LBGI (.)	HBGI (.)	Mean BG (mg/dl)	TDI (U)
1	Stat.	0	0	99.2	0.8	0	0.1	0.5	118	48.4
	Hyst.	0	0	98.8	1.2	0	0.1	0.6	119.2	46.9
2	Stat.	0	0	97.2	2.8	0	0.2	0.9	122.5	46.7
	Hyst.	0	0	100	0	0	0.2	0.5	115.9	48.8
3	Stat.	0	0	100	0	0	0.1	0.5	118.7	60
	Hyst.	0	0	100	0	0	0.1	0.4	116.4	60.7
4	Stat.	0	0	100	0	0	0.3	0.3	112.8	40.5
	Hyst.	0	0	100	0	0	0.2	0.4	113.4	39.8
5	Stat.	0	0	100	0	0	0.3	0.3	110.5	46
	Hyst.	0	0	100	0	0	0.1	0.2	112.2	45.5
6	Stat.	0	0	97.3	2.7	0	0.2	0.7	119.5	82.9
	Stat.	0	0	99.2	0.8	0	0.3	0.4	111.7	89.8
7	Stat.	0	0	100	0	0	0.1	0.4	118.5	49.6
	Hyst.	0	0	100	0	0	0.3	0.3	114.4	50.4
8	Stat.	0	0	100	0	0	0.1	0.4	114.3	69.1
	Hyst.	0	0	100	0	0	0.1	0.4	115.8	69.6
9	Stat.	0	0	99	1	0	0.2	0.5	116.5	37.9
	Hyst.	0	0	100	0	0	0.5	0.2	107.3	41.2
10	Stat.	0	0	100	0	0	0.3	0.3	111.2	50.4
	Hyst.	0	0	100	0	0	0.4	0.2	108.3	52.3
11	Stat.	0	0	99.2	0.8	0	0.3	0.4	112.8	53.1
	Hyst.	0	0	100	0	0	0.2	0.3	112.6	52.5

Performance metrics computed on the last 24 hours of a 48-hour, 3-meal/2-snack scenario in adults for two regulation schemes: Static model 2020 (Stat.) and Hysteretic model 2020 (Hyst.). Nine metrics are computed: the Time Below Range (TBR level 1: 70 mg/dl, level 2: 54mg/dl), the Time In Range (TIR), the Time Above Range (TAR level 1: 180 mg/dl, level 2: 250 mg/dl), the Low Blood Glucose Index (LBGI) and its counterpart the High Blood Glucose Index (HBGI), the Mean Blood Glucose level (Mean BG), and the Total Daily Insulin (TDI) administered to the patient.

Appendix 7 – Performance metrics corresponding to IV/IV results of children**Children**

Patient ID		TBR 2 (%)	TBR 1 (%)	TIR (%)	TAR 1 (%)	TAR 2 (%)	LBGI (.)	HBGI (.)	Mean BG (mg/dl)	TDI (U)
1	Stat.	0	0	96.6	3.4	0	0.1	1	121.8	33.2
	Hyst.	0	0	95.7	4.3	0	0	1.3	127.9	29.5
2	Stat.	0	0	89.8	10.2	2.8	0.3	2.2	127.1	23.3
	Hyst.	0	0	89.9	10.1	1.7	0.2	2.2	127	22.9
3	Stat.	0	0	95.4	4.6	0	0.2	1.1	120.3	28.2
	Hyst.	0	0	96.3	3.8	0	0.5	0.7	113.7	29.4
4	Stat.	0	0	94.9	5.1	0	0	1.2	126.8	15.1
	Hyst.	0	0	95.7	4.3	0	0	1.2	128	14.6
5	Stat.	0	0	93.8	6.2	0	0.5	1.2	115.7	36.2
	Hyst.	0	0	93.2	6.8	0	0.1	1.3	122.1	30.9
6	Stat.	0	0	86.4	13.6	4.4	0.1	3.6	144.4	31.2
	Stat.	0	3	91.3	5.7	0	0.7	1.3	119.7	40.9
7	Stat.	0	0	90.7	9.3	0.9	0.1	2.1	131.2	35.5
	Hyst.	0	0	89.1	10.9	1.5	0.1	2.5	135.3	29.3
8	Stat.	0	0	89	11	3.8	0.3	2.6	130.4	18.9
	Hyst.	0	4.1	88.7	7.2	1.3	0.9	1.5	116.5	20.8
9	Stat.	0	0	96	4	0	0.1	1	121.9	17
	Hyst.	0	0	94	6	0	0	1.6	129.2	15.5
10	Stat.	0	0	96	4	0	0	1.1	128.3	25.2
	Hyst.	0	0	93.6	6.4	0	0	1.9	136.6	23.5
11	Stat.	0	0	91.3	8.8	2.8	0.2	2.3	131.6	23.7
	Hyst.	0	0	91.3	8.8	2.2	0	2.3	134.8	22.3

Performance metrics computed on the last 24 hours of a 48-hour, 3-meal/2-snack scenario in children for two regulation schemes: Static model 2020 (Stat.) and Hysteretic model 2020 (Hyst.). Nine metrics are computed: the Time Below Range (TBR level 1: 70 mg/dl, level 2: 54mg/dl), the Time In Range (TIR), the Time Above Range (TAR level 1: 180 mg/dl, level 2: 250 mg/dl), the Low Blood Glucose Index (LBGI) and its counterpart the High Blood Glucose Index (HBGI), the Mean Blood Glucose level (Mean BG), and the Total Daily Insulin (TDI) administered to the patient.

Appendix 8 – Performance metrics corresponding to SQ/SQ results of adolescents

Adolescents									
Patient ID	TBR 2 (%)	TBR 1 (%)	TIR (%)	TAR 1 (%)	TAR 2 (%)	LBGI (.)	HBGI (.)	Mean BG (mg/dl)	TDI (U)
1	CGM	0	0	93.1	6.9	0	0.3	118.6	35.1
	Bios.	0	0	94.4	5.6	0	0.3	117.5	34.8
2	CGM	0	0	82.9	17.1	6.3	0.1	146.3	28.4
	Bios.	0	0	85.8	14.2	5	0.2	133.7	30.7
3	CGM	0	0	100	0	0	0.1	116.9	34.9
	Bios.	0	0	100	0	0	0.4	120.2	33.9
4	CGM	0	0	94.2	5.8	0	0.1	124.1	53.7
	Bios.	0	0	95.7	4.3	0	0.3	117.1	56.4
5	CGM	0	0	99.3	0.7	0	0.2	114	38.3
	Bios.	0	0	99.7	0.3	0	0.3	110.6	39.7
6	CGM	0	0	100	0	0	0.1	111.5	28.7
	Bios.	0	0	100	0	0	0.1	112.8	28.3
7	CGM	0	0	82.9	17.1	4.6	0.5	135.9	46.9
	Bios.	0	4.9	85.8	9.4	0	1.2	116.1	51.7
8	CGM	0	0	100	0	0	0.3	107.3	65.3
	Bios.	0	0	100	0	0	0.5	104.4	71.1
9	CGM	0	0	99.7	0.3	0	0.2	111.3	54.8
	Bios.	0	0	100	0	0	0.2	109.1	56.1
10	CGM	0	0	90.8	9.2	0	0.1	128.7	36.3
	Bios.	0	0	94.4	5.6	0	0.2	119.5	38.4
11	CGM	0	0	96.6	3.4	0	0.3	115.5	40.7
	Bios.	0	0	97.6	2.4	0	0.5	109.3	43

Performance metrics computed on the last 24 hours of a 48-hour, 3-meal/2-snack scenario in adolescents for two regulation schemes: the CGM-AP (CGM) and the Bios-AP (Bios.). Nine metrics are computed: the Time Below Range (TBR level 1: 70 mg/dl, level 2: 54mg/dl), the Time In Range (TIR), the Time Above Range (TAR level 1: 180 mg/dl, level 2: 250 mg/dl), the Low Blood Glucose Index (LBGI) and its counterpart the High Blood Glucose Index (HBGI), the Mean Blood Glucose level (Mean BG), and the Total Daily Insulin (TDI) administered to the patient. CGM-AP data are averaged over 25 repetitions of the scenario.

Appendix 9 – Performance metrics corresponding to SQ/SQ results of adults

Adults										
Patient ID		TBR 2 (%)	TBR 1 (%)	TIR (%)	TAR 1 (%)	TAR 2 (%)	LBGI (.)	HBGI (.)	Mean BG (mg/dl)	TDI (U)
1	CGM	0	0	99.2	0.8	0	0.1	0.5	118	48.4
	Bios.	0	0	98.8	1.2	0	0.1	0.6	119.2	46.9
2	CGM	0	0	97.2	2.8	0	0.2	0.9	122.5	46.7
	Bios.	0	0	100	0	0	0.2	0.5	115.9	48.8
3	CGM	0	0	100	0	0	0.1	0.5	118.7	60
	Bios.	0	0	100	0	0	0.1	0.4	116.4	60.7
4	CGM	0	0	100	0	0	0.3	0.3	112.8	40.5
	Bios.	0	0	100	0	0	0.2	0.4	113.4	39.8
5	CGM	0	0	100	0	0	0.3	0.3	110.5	46
	Bios.	0	0	100	0	0	0.1	0.2	112.2	45.5
6	CGM	0	0	97.3	2.7	0	0.2	0.7	119.5	82.9
	Bios.	0	0	99.2	0.8	0	0.3	0.4	111.7	89.8
7	CGM	0	0	100	0	0	0.1	0.4	118.5	49.6
	Bios.	0	0	100	0	0	0.3	0.3	114.4	50.4
8	CGM	0	0	100	0	0	0.1	0.4	114.3	69.1
	Bios.	0	0	100	0	0	0.1	0.4	115.8	69.6
9	CGM	0	0	99	1	0	0.2	0.5	116.5	37.9
	Bios.	0	0	100	0	0	0.5	0.2	107.3	41.2
10	CGM	0	0	100	0	0	0.3	0.3	111.2	50.4
	Bios.	0	0	100	0	0	0.4	0.2	108.3	52.3
11	CGM	0	0	99.2	0.8	0	0.3	0.4	112.8	53.1
	Bios.	0	0	100	0	0	0.2	0.3	112.6	52.5

Performance metrics computed on the last 24 hours of a 48-hour, 3-meal/2-snack scenario in adults for two regulation schemes: the CGM-AP (CGM) and the Bios-AP (Bios.). Nine metrics are computed: the Time Below Range (TBR level 1: 70 mg/dl, level 2: 54mg/dl), the Time In Range (TIR), the Time Above Range (TAR level 1: 180 mg/dl, level 2: 250 mg/dl), the Low Blood Glucose Index (LBGI) and its counterpart the High Blood Glucose Index (HBGI), the Mean Blood Glucose level (Mean BG), and the Total Daily Insulin (TDI) administered to the patient. CGM-AP data are averaged over 25 repetitions of the scenario

Appendix 10 — Performance metrics corresponding to SQ/SQ results of children

Children										
Patient ID		TBR 2 (%)	TBR 1 (%)	TIR (%)	TAR 1 (%)	TAR 2 (%)	LBGI (.)	HBGI (.)	Mean BG (mg/dl)	TDI (U)
1	CGM	0	0	96.6	3.4	0	0.1	1	121.8	33.2
	Bios.	0	0	95.7	4.3	0	0	1.3	127.9	29.5
2	CGM	0	0	89.8	10.2	2.8	0.3	2.2	127.1	23.3
	Bios.	0	0	89.9	10.1	1.7	0.2	2.2	127	22.9
3	CGM	0	0	95.4	4.6	0	0.2	1.1	120.3	28.2
	Bios.	0	0	96.3	3.8	0	0.5	0.7	113.7	29.4
4	CGM	0	0	94.9	5.1	0	0	1.2	126.8	15.1
	Bios.	0	0	95.7	4.3	0	0	1.2	128	14.6
5	CGM	0	0	93.8	6.2	0	0.5	1.2	115.7	36.2
	Bios.	0	0	93.2	6.8	0	0.1	1.3	122.1	30.9
6	CGM	0	0	86.4	13.6	4.4	0.1	3.6	144.4	31.2
	Bios.	0	3	91.3	5.7	0	0.7	1.3	119.7	40.9
7	CGM	0	0	90.7	9.3	0.9	0.1	2.1	131.2	35.5
	Bios.	0	0	89.1	10.9	1.5	0.1	2.5	135.3	29.3
8	CGM	0	0	89	11	3.8	0.3	2.6	130.4	18.9
	Bios.	0	4.1	88.7	7.2	1.3	0.9	1.5	116.5	20.8
9	CGM	0	0	96	4	0	0.1	1	121.9	17
	Bios.	0	0	94	6	0	0	1.6	129.2	15.5
10	CGM	0	0	96	4	0	0	1.1	128.3	25.2
	Bios.	0	0	93.6	6.4	0	0	1.9	136.6	23.5
11	CGM	0	0	91.3	8.8	2.8	0.2	2.3	131.6	23.7
	Bios.	0	0	91.3	8.8	2.2	0	2.3	134.8	22.3

Performance metrics computed on the last 24 hours of a 48-hour, 3-meal/2-snack scenario in children for two regulation schemes: the CGM-AP (CGM) and the Bios-AP (Bios.). Nine metrics are computed: the Time Below Range (TBR level 1: 70 mg/dl, level 2: 54mg/dl), the Time In Range (TIR), the Time Above Range (TAR level 1: 180 mg/dl, level 2: 250 mg/dl), the Low Blood Glucose Index (LBGI) and its counterpart the High Blood Glucose Index (HBGI), the Mean Blood Glucose level (Mean BG), and the Total Daily Insulin (TDI) administered to the patient. CGM-AP data are averaged over 25 repetitions of the scenario.

List of publications

Loïc Olçomendy, Antoine Pirog, Fanny Lebreton, Manon Jaffredo, Louis Cassany, et al.. Integrating an Islet-Based Biosensor in the Artificial Pancreas: In Silico Proof-of-Concept. *IEEE Transactions on Biomedical Engineering*, (submitted May 2021, under revision)

Louis Cassany, David Gucik-Derigny, Jérôme Cieslak, David Henry, Roberto Franco, et al.. A Robust Control solution for Glycaemia Regulation of Type-1 Diabetes Mellitus. *IEEE European Control Conference*, Jun 2021, Rotterdam, Netherlands. [\(hal-03157045\)](#)

Roberto Franco, Alejandra Ferreira de Loza, Hector Ríos, Louis Cassany, David Gucik-Derigny, et al.. Output-Feedback Sliding-Mode Controller for Blood Glucose Regulation in Critically Ill Patients Affected by Type 1 Diabetes. *IEEE Transactions on Control Systems Technology*, Institute of Electrical and Electronics Engineers, 2021, pp.1-8. [\(10.1109/TCST.2020.3046420\)](#). [\(hal-03109830\)](#)

Roberto Franco, Alejandra Ferreira de Loza, Hector Ríos, Louis Cassany, David Gucik-Derigny, et al.. Regulación de Glucosa en la Sangre en Pacientes con Diabetes Mellitus Tipo 1 usando Control por Realimentación de Salida. *27^o Congreso Argentino Argentino de Control Automático*, Oct 2020, Buenos Aires, Argentina. [\(hal-02972043\)](#)

Loïc Olçomendy, Antoine Pirog, Yannick Bornat, Jérôme Cieslak, David Gucik-Derigny, et al.. Tuning of an artificial pancreas controller: an in silico methodology based on clinically-relevant criteria. *42nd Annual International Conference of the IEEE Engineering in Medicine and Biology Society (EMBC)*, Jul 2020, Montréal, Canada. [\(hal-02908200\)](#)

Matthieu Raoux, Manon Jaffredo, Loïc Olçomendy, Antoine Pirog, Yannick Bornat, et al.. Capteur Bio-Electronique : Analyse en Temps Réel des Algorithmes des Îlots et Exploitation en Boucle Fermée dans le Simulateur UVA/PADOVA de Patient Diabétique de Type 1. *Société Francophone du Diabète (SFD)*, Mar 2019, Marseille, France. [\(hal-02520964\)](#)

Matthieu Raoux, Manon Jaffredo, Loïc Olçomendy, Antoine Pirog, Bogdan Catargi, et al.. Real-time decoding of endogenous islet algorithms and their use in a type 1 diabetes simulator. *European Association for the Study of Diabetes (EASD)*, Oct 2018, Berlin, Germany. [\(hal-02520956\)](#)

Bibliography

- [1] D. J. A. Jenkins, T. M. S. Wolever, R. H. Taylor, *et al.*, “Glycemic index of foods: A physiological basis for carbohydrate exchange,” *Am. J. Clin. Nutr.*, vol. 34, no. 3, pp. 362–366, 1981, doi: 10.1093/ajcn/34.3.362.
- [2] F. S. Atkinson, K. Foster-Powell, and J. C. Brand-Miller, “International tables of glycemic index and glycemic load values: 2008,” *Diabetes Care*, vol. 31, no. 12, pp. 2281–2283, Dec. 2008, doi: 10.2337/dc08-1239.
- [3] M. J. Franz, “The glycemic index: Not the most effective nutrition therapy intervention,” *Diabetes Care*, vol. 26, no. 8, pp. 2466–2468, 2003, doi: 10.2337/diacare.26.8.2466.
- [4] F. Xavier Pi-Sunyer, “Glycemic index and disease,” *Am. J. Clin. Nutr.*, vol. 76, no. 1, 2002, doi: 10.1093/ajcn/76.1.290s.
- [5] M. J. Franz, J. Bantle, C. A. Beebe, *et al.*, “American Diabetes Association Position Statement: Evidence-based nutrition principles and recommendations for the treatment and prevention of diabetes and related complications,” *J. Am. Diet. Assoc.*, vol. 102, no. 1, pp. 109–118, 2002, doi: 10.1016/S0002-8223(02)90031-3.
- [6] B. Nayak, J. De J. Berrios, and J. Tang, “Impact of food processing on the glycemic index (GI) of potato products,” *Food Res. Int.*, vol. 56, pp. 35–46, 2014, doi: 10.1016/j.foodres.2013.12.020.
- [7] J. F. Yale, B. Paty, and P. A. Senior, “Hypoglycemia,” *Can. J. Diabetes*, vol. 42, pp. S104–S108, 2018, doi: 10.1016/j.jcjd.2017.10.010.
- [8] F. Giacco and M. Brownlee, “Mechanisms of Hyperglycemic Damage in Diabetes,” in *Atlas of Diabetes*, Springer US, 2012, pp. 217–231.
- [9] J. M. Beals, M. R. DeFelippis, C. D. Paavola, D. P. Allen, A. Garg, and D. B. Baldwin, “Insulin,” in *Pharmaceutical Biotechnology: Fundamentals and Applications*, Springer International Publishing, 2019, pp. 403–427.
- [10] M. C. Petersen and G. I. Shulman, “Mechanisms of insulin action and insulin resistance,” *Physiol. Rev.*, vol. 98, no. 4, pp. 2133–2223, 2018, doi: 10.1152/physrev.00063.2017.
- [11] N. H. McClenaghan and P. R. Flatt, “HORMONES | Pancreatic Hormones,” in *Encyclopedia of Food Sciences and Nutrition*, Elsevier, 2003, pp. 3150–3157.
- [12] K. M. Habegger, K. M. Heppner, N. Geary, T. J. Bartness, R. DiMarchi, and M. H. Tschöp, “The metabolic actions of glucagon revisited,” *Nature Reviews Endocrinology*, vol. 6, no. 12, NIH Public Access, pp. 689–697, Dec. 2010, doi: 10.1038/nrendo.2010.187.
- [13] G. Jiang and B. B. Zhang, “Glucagon and regulation of glucose metabolism,” *Am. J. Physiol. - Endocrinol. Metab.*, vol. 284, no. 4, pp. 47–4, 2003, doi: 10.1152/ajpendo.00492.2002.
- [14] X. Wang, M. C. Zielinski, R. Misawa, *et al.*, “Quantitative Analysis of Pancreatic Polypeptide Cell Distribution in the Human Pancreas,” *PLoS One*, vol. 8, no. 1, pp. 1–7, 2013, doi: 10.1371/journal.pone.0055501.
- [15] Y. J. Wang, M. L. Golson, J. Schug, *et al.*, “Single-Cell Mass Cytometry Analysis of the Human Endocrine Pancreas,” *Cell Metab.*, vol. 24, no. 4, pp. 616–626, Oct. 2016, doi: 10.1016/j.cmet.2016.09.007.
- [16] C. Ionescu-Tirgoviste, P. A. Gagniuc, E. Gubceac, *et al.*, “A 3D map of the islet routes

- throughout the healthy human pancreas,” *Sci. Rep.*, vol. 5, pp. 1–14, 2015, doi: 10.1038/srep14634.
- [17] K. Saito, N. Iwama, and T. Takahashi, “Morphometrical Analysis on Topographical Difference in Size Distribution, Number and Volume of Islets in the Human Pancreas,” *Tohoku J. Exp. Med.*, vol. 124, no. 2, pp. 177–186, 1978, doi: 10.1620/tjem.124.177.
 - [18] O. Cabrera, D. M. Berman, N. S. Kenyon, C. Ricordi, P. O. Berggren, and A. Caicedo, “The unique cytoarchitecture of human pancreatic islets has implications for islet cell function,” *Proc. Natl. Acad. Sci. U. S. A.*, vol. 103, no. 7, pp. 2334–2339, Feb. 2006, doi: 10.1073/pnas.0510790103.
 - [19] L. A. DiMeglio, C. Evans-Molina, and R. A. Oram, “Type 1 diabetes,” *The Lancet*, vol. 391, no. 10138. Lancet Publishing Group, pp. 2449–2462, Jun. 16, 2018, doi: 10.1016/S0140-6736(18)31320-5.
 - [20] G. S. Eisenbarth, “Type I Diabetes Mellitus,” *New England Journal of Medicine*, vol. 314, no. 21. Massachusetts Medical Society, pp. 1360–1368, May 22, 1986, doi: 10.1056/NEJM198605223142106.
 - [21] N. J. Thomas, S. E. Jones, M. N. Weedon, B. M. Shields, R. A. Oram, and A. T. Hattersley, “Frequency and phenotype of type 1 diabetes in the first six decades of life: a cross-sectional, genetically stratified survival analysis from UK Biobank,” *Lancet Diabetes Endocrinol.*, vol. 6, no. 2, pp. 122–129, Feb. 2018, doi: 10.1016/S2213-8587(17)30362-5.
 - [22] “Diagnosis and classification of diabetes mellitus,” *Diabetes Care*, vol. 28, no. SUPPL. 1. 2005, doi: 10.2337/diacare.28.suppl_1.S37.
 - [23] L. Y. Melendez-Ramirez, R. J. Richards, and W. T. Cefalu, “Complications of type 1 diabetes,” *Endocrinology and Metabolism Clinics of North America*, vol. 39, no. 3. Elsevier Ltd, pp. 625–640, 2010, doi: 10.1016/j.ecl.2010.05.009.
 - [24] C. Yh, C. Me, D. Kc, Y. Hi, E. Maria, and C. Kim, “Puberty as an accelerator for diabetes complications,” pp. 18–26, 2014, doi: 10.1111/pedi.12112.
 - [25] T. D. C. and C. T. R. Group, “The Effect of Intensive Treatment of Diabetes on the Development and Progression of Long-Term Complications in Insulin-Dependent Diabetes Mellitus,” *N. Engl. J. Med.*, vol. 329, no. 14, pp. 977–986, Sep. 1993, doi: 10.1056/NEJM199309303291401.
 - [26] J. M. Lachin, T. J. Orchard, D. M. Nathan, and D. Edic, “Update on Cardiovascular Outcomes at 30 Years of the Diabetes Control and Complications Trial / Epidemiology of Diabetes Interventions and Complications Study,” vol. 37, no. January, pp. 39–43, 2014, doi: 10.2337/dc13-2116.
 - [27] D. M. Maahs, N. A. West, J. M. Lawrence, and E. J. Mayer-Davis, “Epidemiology of type 1 diabetes,” *Endocrinol. Metab. Clin. North Am.*, vol. 39, no. 3, pp. 481–497, 2010, doi: 10.1016/j.ecl.2010.05.011.
 - [28] M. Karvonen, V.-K. Maarit, M. Elena, L. Ingrid, L. Ronald, and T. Jaakko, “Incidence of Childhood Type 1 Diabetes,” *Diabetes Care*, vol. 23, no. 10, pp. 1516–26, 2000.
 - [29] A. T. Borchers, R. Uibo, and M. E. Gershwin, “The geoepidemiology of type 1 diabetes,” *Autoimmunity Reviews*, vol. 9, no. 5. Elsevier, pp. A355–A365, Mar. 01, 2010, doi: 10.1016/j.autrev.2009.12.003.
 - [30] A. D. Liese, “The burden of diabetes mellitus among US youth: Prevalence estimates

- from the SEARCH for Diabetes in Youth Study: SEARCH for Diabetes in Youth Study Group,” *Pediatrics*, vol. 118, no. 4, pp. 1510–1518, 2006, doi: 10.1542/peds.2006-0690.
- [31] The DIAMOND Project Group, “Incidence and trends of childhood Type 1 diabetes worldwide 1990-1999,” *Diabet. Med.*, vol. 23, no. 8, pp. 857–866, Aug. 2006, doi: 10.1111/j.1464-5491.2006.01925.x.
- [32] C. Piffaretti, L. Mandereau-Bruno, S. Guilmin-Crepon, C. Choleau, R. Coutant, and S. Fosse-Edorh, “Trends in childhood type 1 diabetes incidence in France, 2010–2015,” *Diabetes Res. Clin. Pract.*, vol. 149, pp. 200–207, 2019, doi: 10.1016/j.diabres.2018.11.005.
- [33] R. Williams, S. Karuranga, B. Malanda, *et al.*, “Global and regional estimates and projections of diabetes-related health expenditure: Results from the International Diabetes Federation Diabetes Atlas, 9th edition,” *Diabetes Res. Clin. Pract.*, vol. 162, 2020, doi: 10.1016/j.diabres.2020.108072.
- [34] M. A. Atkinson and G. S. Eisenbarth, “Type 1 diabetes: New perspectives on disease pathogenesis and treatment,” *Lancet*, vol. 358, no. 9277, pp. 221–229, 2001, doi: 10.1016/S0140-6736(01)05415-0.
- [35] R. Testa, A. R. Bonfigli, F. Prattichizzo, L. La Sala, V. De Nigris, and A. Ceriello, “The ‘Metabolic Memory’ Theory and the Early Treatment of Hyperglycemia in Prevention of Diabetic Complications,” *Nutrients*, vol. 9, no. 5, 2017, doi: 10.3390/nu9050437.
- [36] R. P. Robertson, “Prevention of recurrent hypoglycemia in type 1 diabetes by pancreas transplantation,” *Acta Diabetologica*, vol. 36, no. 1–2. Springer Verlag, pp. 3–9, 1999, doi: 10.1007/s005920050138.
- [37] A. M. J. Shapiro, J. R. T. Lakey, E. A. Ryan, *et al.*, “Islet Transplantation in Seven Patients with Type 1 Diabetes Mellitus Using a Glucocorticoid-Free Immunosuppressive Regimen,” *N. Engl. J. Med.*, vol. 343, no. 4, pp. 230–238, Jul. 2000, doi: 10.1056/NEJM200007273430401.
- [38] S. Lablanche, M. C. Vantyghem, L. Kessler, *et al.*, “Islet transplantation versus insulin therapy in patients with type 1 diabetes with severe hypoglycaemia or poorly controlled glycaemia after kidney transplantation (TRIMECO): a multicentre, randomised controlled trial,” *Lancet Diabetes Endocrinol.*, vol. 6, no. 7, pp. 527–537, 2018, doi: 10.1016/S2213-8587(18)30078-0.
- [39] L. Moroder and H. J. Musiol, “Insulin—From its Discovery to the Industrial Synthesis of Modern Insulin Analogues,” *Angew. Chemie - Int. Ed.*, vol. 56, no. 36, pp. 10656–10669, 2017, doi: 10.1002/anie.201702493.
- [40] J. Galloway and R. Chance, “Improving Insulin Therapy: Achievements and Challenges,” *Horm. Metab. Res.*, vol. 26, no. 12, pp. 591–598, Dec. 1994, doi: 10.1055/s-2007-1001766.
- [41] K. Rebrin, G. M. Steil, W. P. Van Antwerp, and J. J. Mastrototaro, “Subcutaneous glucose predicts plasma glucose independent of insulin: Implications for continuous monitoring,” *Am. J. Physiol. - Endocrinol. Metab.*, vol. 277, no. 3 40-3, pp. 561–571, 1999, doi: 10.1152/ajpendo.1999.277.3.e561.
- [42] R. Shan, S. Sarkar, S. S. Martin, S. R., S. S., and S. S. . O. <http://orcid.org/000.-0002-7021-7622> Martin S.S. AO - Martin, “Digital health technology and mobile devices for the management of diabetes mellitus: state of the art,” *Diabetologia*, vol. 62, no. 6, pp.

- 877–887, 2019, doi: 10.1007/s00125-019-4864-7.
- [43] E. Latres, D. A. Finan, J. L. Greenstein, A. Kowalski, and T. J. Kieffer, “Navigating Two Roads to Glucose Normalization in Diabetes: Automated Insulin Delivery Devices and Cell Therapy,” *Cell Metab.*, vol. 29, no. 3, pp. 545–563, 2019, doi: 10.1016/j.cmet.2019.02.007.
 - [44] S. K. Lyons, J. M. Hermann, K. M. Miller, *et al.*, “Use of adjuvant pharmacotherapy in type 1 diabetes: International comparison of 49,996 individuals in the prospective diabetes follow-up and T1D exchange registries,” *Diabetes Care*, vol. 40, no. 10, pp. e139–e140, 2017, doi: 10.2337/dc17-0403.
 - [45] R. M. Bergenstal, W. V. Tamborlane, A. Ahmann, *et al.*, “Effectiveness of Sensor-Augmented insulin-Pump therapy in Type 1 Diabetes,” *N. Engl. J. Med.*, vol. 363, no. 4, pp. 311–320, Jul. 2010, doi: 10.1056/nejmoa1002853.
 - [46] H. C. Wang and A. R. Lee, “Recent developments in blood glucose sensors,” *Journal of Food and Drug Analysis*, vol. 23, no. 2. Elsevier Taiwan LLC, pp. 191–200, Jun. 01, 2015, doi: 10.1016/j.jfda.2014.12.001.
 - [47] A. Basu, S. Dube, S. Veettil, *et al.*, “Time lag of glucose from intravascular to interstitial compartment in type 1 Diabetes,” *J. Diabetes Sci. Technol.*, vol. 9, no. 1, pp. 63–68, 2015, doi: 10.1177/1932296814554797.
 - [48] C. Uduku, M. Reddy, and N. Oliver, “Clinical impact of CGM use,” in *Glucose Monitoring Devices*, Elsevier, 2020, pp. 135–158.
 - [49] B. P. Kovatchev, “Metrics for glycaemic control-from HbA1c to continuous glucose monitoring,” *Nat. Rev. Endocrinol.*, vol. 13, no. 7, pp. 425–436, 2017, doi: 10.1038/nrendo.2017.3.
 - [50] D. Rodbard, “Continuous glucose monitoring: A review of recent studies demonstrating improved glycemic outcomes,” *Diabetes Technol. Ther.*, vol. 19, pp. S25–S37, 2017, doi: 10.1089/dia.2017.0035.
 - [51] N. C. Foster, R. W. Beck, K. M. Miller, *et al.*, “State of Type 1 Diabetes Management and Outcomes from the T1D Exchange in 2016-2018,” *Diabetes Technology and Therapeutics*, vol. 21, no. 2. Mary Ann Liebert Inc., pp. 66–72, Feb. 01, 2019, doi: 10.1089/dia.2018.0384.
 - [52] J. C. Pickup and A. J. Sutton, “Severe hypoglycaemia and glycaemic control in Type 1 diabetes: Meta-analysis of multiple daily insulin injections compared with continuous subcutaneous insulin infusion,” *Diabetic Medicine*, vol. 25, no. 7. Diabet Med, pp. 765–774, Jul. 2008, doi: 10.1111/j.1464-5491.2008.02486.x.
 - [53] K. Jeitler, K. Horvath, A. Berghold, *et al.*, “Continuous subcutaneous insulin infusion versus multiple daily insulin injections in patients with diabetes mellitus: Systematic review and meta-analysis,” *Diabetologia*, vol. 51, no. 6, pp. 941–951, Jun. 2008, doi: 10.1007/s00125-008-0974-3.
 - [54] A. Nath, S. Biradar, A. Balan, R. Dey, and R. Padhi, “Physiological Models and Control for Type 1 Diabetes Mellitus: A Brief Review,” *IFAC-PapersOnLine*, vol. 51, no. 1, pp. 289–294, 2018, doi: 10.1016/j.ifacol.2018.05.077.
 - [55] B. W. Bequette, “Algorithms for a closed-loop artificial pancreas: The case for model predictive control,” *J. Diabetes Sci. Technol.*, vol. 7, no. 6, pp. 1632–1643, 2013, doi: 10.1177/193229681300700624.

- [56] A. Cinar, "Multivariable Adaptive Artificial Pancreas System in Type 1 Diabetes," *Curr. Diab. Rep.*, vol. 17, no. 10, 2017, doi: 10.1007/s11892-017-0920-1.
- [57] C. Toffanin, R. Visentin, M. Messori, F. Di Palma, L. Magni, and C. Cobelli, "Toward a Run-to-Run Adaptive Artificial Pancreas: In Silico Results," *IEEE Trans. Biomed. Eng.*, vol. 65, no. 3, pp. 479–488, 2018, doi: 10.1109/TBME.2017.2652062.
- [58] B. Kovatchev, "The year of transition from research to clinical practice," *Nat. Rev. Endocrinol.*, vol. 14, no. 2, 2017, doi: 10.1038/nrendo.2017.170.
- [59] E. Bekiari, K. Kitsios, H. Thabit, *et al.*, "Artificial pancreas treatment for outpatients with type 1 diabetes: Systematic review and meta-Analysis," *BMJ*, vol. 361, 2018, doi: 10.1136/bmj.k1310.
- [60] E. Latres, D. A. Finan, J. L. Greenstein, A. Kowalski, and T. J. Kieffer, "Navigating Two Roads to Glucose Normalization in Diabetes: Automated Insulin Delivery Devices and Cell Therapy," *Cell Metab.*, vol. 29, no. 3, pp. 545–563, 2019, doi: 10.1016/j.cmet.2019.02.007.
- [61] C. Farrington, "Psychosocial impacts of hybrid closed-loop systems in the management of diabetes: a review," *Diabet. Med.*, vol. 35, no. 4, pp. 436–449, 2018, doi: 10.1111/dme.13567.
- [62] R. A. Lal, M. Basina, D. M. Maahs, K. Hood, B. Buckingham, and D. M. Wilson, "One year clinical experience of the first commercial hybrid closed-loop system," *Diabetes Care*, vol. 42, no. 12, pp. 2190–2196, 2019, doi: 10.2337/dc19-0855.
- [63] H. Thabit and R. Hovorka, "Coming of age: the artificial pancreas for type 1 diabetes," *Diabetologia*, vol. 59, no. 9, pp. 1795–1805, 2016, doi: 10.1007/s00125-016-4022-4.
- [64] J. Magisson, A. Sassi, D. Xhema, *et al.*, "Safety and function of a new pre-vascularized bioartificial pancreas in an allogeneic rat model," *J. Tissue Eng.*, vol. 11, p. 204173142092481, Jan. 2020, doi: 10.1177/2041731420924818.
- [65] C. Hammond, *Ionic gradients, membrane potential and ionic currents*, Fourth Edi. Elsevier Ltd, 2015.
- [66] J. Lang, "Molecular mechanisms and regulation of insulin exocytosis as a paradigm of endocrine secretion," *Eur. J. Biochem.*, vol. 259, no. 1–2, pp. 3–17, Jan. 1999, doi: 10.1046/j.1432-1327.1999.00043.x.
- [67] H. P. Meissner and H. Schmelz, "Membrane potential of beta-cells in pancreatic islets," *Pflügers Arch. Eur. J. Physiol.*, vol. 351, no. 3, pp. 195–206, 1974, doi: 10.1007/BF00586918.
- [68] R. K. P. Benninger and D. W. Piston, "Cellular communication and heterogeneity in pancreatic islet insulin secretion dynamics," *Trends in Endocrinology and Metabolism*, vol. 25, no. 8. Elsevier Inc., pp. 399–406, Aug. 01, 2014, doi: 10.1016/j.tem.2014.02.005.
- [69] Y. Palti, G. Ben David, E. Lachov, Y. H. Mika, G. Omri, and R. Schatzberger, "Islets of Langerhans generate wavelike electric activity modulated by glucose concentration," *Diabetes*, vol. 45, no. 5, pp. 595–601, 1996, doi: 10.2337/diab.45.5.595.
- [70] F. Lebreton, A. Pirog, I. Belouah, *et al.*, "Slow potentials encode intercellular coupling and insulin demand in pancreatic beta cells," *Diabetologia*, vol. 58, no. 6, pp. 1291–1299, 2015, doi: 10.1007/s00125-015-3558-z.
- [71] P. Mehrotra, "Biosensors and their applications - A review," *Journal of Oral Biology and Craniofacial Research*, vol. 6, no. 2. Elsevier B.V., pp. 153–159, May 01, 2016, doi:

- 10.1016/j.jobcr.2015.12.002.
- [72] J. J. Pancrazio, J. P. Whelan, D. A. Borkholder, W. Ma, and D. A. Stenger, "Development and Application of Cell-Based Biosensors," *Ann. Biomed. Eng.*, vol. 27, no. 6, pp. 697–711, 1999, doi: 10.1114/1.225.
 - [73] Q. Liu, C. Wu, H. Cai, N. Hu, J. Zhou, and P. Wang, "Cell-Based Biosensors and Their Application in Biomedicine," 2014, doi: 10.1021/cr2003129.
 - [74] J. Lang, B. Catargi, S. Renaud, M. Raoux, G. Charpentier, and Y. Bornat, "Sensor for measuring the activity of beta-pancreatic cells or of islets of Langerhans, manufacture and use of such a sensor," no. WO/2011/086105. p. 33, 2011, [Online]. Available: <https://hal.archives-ouvertes.fr/hal-00667612>.
 - [75] Y. Bornat, M. Raoux, Y. Boutaib, *et al.*, "Detection of electrical activity of pancreatic beta-cells using micro-electrode arrays," *Proc. - 5th IEEE Int. Symp. Electron. Des. Test Appl. DELTA 2010*, pp. 233–236, 2010, doi: 10.1109/DELTA.2010.60.
 - [76] M. Raoux, Y. Bornat, A. Quotb, B. Catargi, S. Renaud, and J. Lang, "Non-invasive long-term and real-time analysis of endocrine cells on micro-electrode arrays," *J. Physiol.*, vol. 590, no. 5, pp. 1085–1091, 2012, doi: 10.1113/jphysiol.2011.220038.
 - [77] M. Jaffredo, E. Bertin, A. Pirog, *et al.*, "Dynamic uni- and multicellular patterns encode biphasic activity in pancreatic islets," *Diabetes*, p. db200214, Jan. 2021, doi: 10.2337/db20-0214.
 - [78] M. Raoux, F. Lebreton, Y. Bornat, *et al.*, "Diabetachip, a novel method for quality control and long-term monitoring of beta-cells and islets," *Diabetes*, vol. 63, pp. A220–A220, 2014.
 - [79] S. Al-Jawadi, P. Capasso, and M. Sharma, "The road to market implantable drug delivery systems: a review on US FDA's regulatory framework and quality control requirements," *Pharm. Dev. Technol.*, vol. 23, no. 10, pp. 953–963, 2018, doi: 10.1080/10837450.2018.1509348.
 - [80] K. Fritzen, L. Heinemann, and O. Schnell, "Modeling of diabetes and its clinical impact," *J. Diabetes Sci. Technol.*, vol. 12, no. 5, pp. 976–984, 2018, doi: 10.1177/1932296818785642.
 - [81] B. P. Kovatchev, M. Breton, C. Dalla Man, and C. Cobelli, "In silico preclinical trials: A proof of concept in closed-loop control of type 1 diabetes," *J. Diabetes Sci. Technol.*, vol. 3, no. 1, pp. 44–55, 2009, doi: 10.1177/193229680900300106.
 - [82] M. E. Spira and A. Hai, "Multi-electrode array technologies for neuroscience and cardiology," *Nature Nanotechnology*, vol. 8, no. 2, pp. 83–94, 2013, doi: 10.1038/nnano.2012.265.
 - [83] R. Kim, S. Joo, H. Jung, N. Hong, and Y. Nam, "Recent trends in microelectrode array technology for in vitro neural interface platform," *Biomed. Eng. Lett.*, vol. 4, no. 2, pp. 129–141, 2014, doi: 10.1007/s13534-014-0130-6.
 - [84] A. Pirog, Y. Bornat, R. Perrier, *et al.*, "Multimed: An integrated, multi-application platform for the real-time recording and sub-millisecond processing of biosignals," *Sensors (Switzerland)*, vol. 18, no. 7, p. 2099, Jun. 2018, doi: 10.3390/s18072099.
 - [85] G. Marion, "An Introduction to Mathematical Modelling."
 - [86] C. Dalla Man, R. A. Rizza, and C. Cobelli, "Meal Simulation of Glucose-Insulin System," *Ieee Trans. Biomed. Eng.*, vol. 54, no. 10, pp. 1–33, 2007.

- [87] C. S. Nunemaker, D. H. Wasserman, O. P. McGuinness, I. R. Sweet, J. C. Teague, and L. S. Satin, "Insulin secretion in the conscious mouse is biphasic and pulsatile," *Am. J. Physiol. - Endocrinol. Metab.*, vol. 290, no. 3, pp. E523–E529, Mar. 2006, doi: 10.1152/ajpendo.00392.2005.
- [88] A. Hill, "The possible effects of the aggregation of the molecules of haemoglobin on its dissociation curves," *J Physiol*, vol. 40, pp. 4–7, 1910, Accessed: Mar. 23, 2020. [Online]. Available: <https://ci.nii.ac.jp/naid/10020096935/>.
- [89] I. J. Stamper and X. Wang, "Mathematical modeling of insulin secretion and the role of glucose-dependent mobilization, docking, priming and fusion of insulin granules," *J. Theor. Biol.*, vol. 318, pp. 210–225, 2013, doi: 10.1016/j.jtbi.2012.11.002.
- [90] F. Preisach, "Über die magnetische Nachwirkung," *Zeitschrift für Phys.*, vol. 94, no. 5–6, pp. 277–302, May 1935, doi: 10.1007/BF01349418.
- [91] A. Pirog, Y. Bornat, R. Perrier, *et al.*, "Multimed: An integrated, multi-application platform for the real-time recording and sub-millisecond processing of biosignals," *Sensors (Switzerland)*, vol. 18, no. 7, pp. 1–25, 2018, doi: 10.3390/s18072099.
- [92] V. Janičić, V. Ilić, N. Pjevalica, and M. Nikolić, "An approach to modeling the hysteresis in ferromagnetic by adaptation of Preisach model," *2014 22nd Telecommun. Forum, TELFOR 2014 - Proc. Pap.*, no. November, pp. 761–764, 2015, doi: 10.1109/TELFOR.2014.7034518.
- [93] R. N. Bergman, D. T. Finegood, and M. Ader, "Assessment of insulin sensitivity in vivo," *Endocr. Rev.*, vol. 6, no. 1, pp. 45–86, 1985, doi: 10.1210/edrv-6-1-45.
- [94] R. Hovorka, F. Shojaei-Moradie, P. V. Carroll, *et al.*, "Partitioning glucose distribution/transport, disposal, and endogenous production during IVGTT," *Am. J. Physiol. - Endocrinol. Metab.*, vol. 282, no. 5 45-5, pp. 992–1007, 2002, doi: 10.1152/ajpendo.00304.2001.
- [95] R. O. Foster, J. S. Soeldner, M. H. Tan, and J. R. Guyton, "Short ten glucose homeostasis in man: A systems dynamics model," *J. Dyn. Syst. Meas. Control. Trans. ASME*, vol. 95, no. 3, pp. 308–314, Sep. 1973, doi: 10.1115/1.3426720.
- [96] R. Basu, C. D. Man, M. Campioni, *et al.*, "Effects of age and sex on postprandial glucose metabolism differences in glucose turnover, insulin secretion, insulin action, and hepatic insulin extraction," *Diabetes*, vol. 55, no. 7, pp. 2001–2014, 2006, doi: 10.2337/db05-1692.
- [97] C. Dalla Man, D. M. Raimondo, R. A. Rizza, and C. Cobelli, "GIM, simulation software of meal glucose-insulin model," *J. Diabetes Sci. Technol.*, vol. 1, no. 3, pp. 323–330, 2007.
- [98] C. Dalla Man, F. Micheletto, D. Lv, M. Breton, B. Kovatchev, and C. Cobelli, "The UVA/PADOVA type 1 diabetes simulator: New features," *J. Diabetes Sci. Technol.*, vol. 8, no. 1, pp. 26–34, 2014, doi: 10.1177/1932296813514502.
- [99] R. Visentin, C. Dalla Man, B. Kovatchev, and C. Cobelli, "The university of virginia/padova type 1 diabetes simulator matches the glucose traces of a clinical trial," *Diabetes Technol. Ther.*, vol. 16, no. 7, pp. 428–434, 2014, doi: 10.1089/dia.2013.0377.
- [100] K. F. Man, K. S. Tang, and S. Kwong, "Genetic algorithms: Concepts and applications," *IEEE Trans. Ind. Electron.*, vol. 43, no. 5, pp. 519–534, 1996, doi: 10.1109/41.538609.
- [101] Goldberg D. E., "Genetic Algorithms in Search," *Optim. Mach. Learn.*, 1989, Accessed:

- Nov. 30, 2020. [Online]. Available: <http://ci.nii.ac.jp/naid/10000038763/en/>.
- [102] A. R. Conn, N. I. M. Gould, and P. L. Toint, "Globally convergent augmented Lagrangian algorithm for optimization with general constraints and simple bounds," *SIAM J. Numer. Anal.*, vol. 28, no. 2, pp. 545–572, 1991, doi: 10.1137/0728030.
 - [103] L. Olçomendy, A. Pirog, Y. B. Bornat, *et al.*, "Tuning of an artificial pancreas controller: an in silico methodology based on clinically-relevant criteria," in *42nd Annual International Conference of the IEEE Engineering in Medicine and Biology Society (EMBC)*, 2020, [Online]. Available: <https://hal.archives-ouvertes.fr/hal-02908200>.
 - [104] R. Oza-Frank, Y. J. Cheng, K. M. V. Narayan, and E. W. Gregg, "Trends in nutrient intake among adults with diabetes in the United States: 1988-2004," *J. Am. Diet. Assoc.*, vol. 109, no. 7, pp. 1173–1178, 2009, doi: 10.1016/j.jada.2009.04.007.
 - [105] R. Vrolix and R. P. Mensink, "Variability of the glycemic response to single food products in healthy subjects," *Contemp. Clin. Trials*, vol. 31, no. 1, pp. 5–11, 2010, doi: 10.1016/j.cct.2009.08.001.
 - [106] R. J. Koenig, C. M. Peterson, R. L. Jones, C. Saudek, M. Lehrman, and A. Cerami, "Correlation of Glucose Regulation and Hemoglobin A_{1c} in Diabetes Mellitus," *N. Engl. J. Med.*, vol. 295, no. 8, pp. 417–420, Aug. 1976, doi: 10.1056/nejm197608192950804.
 - [107] D. M. Nathan, M. B. Davidson, R. A. DeFronzo, *et al.*, "Impaired fasting glucose and impaired glucose tolerance: Implications for care," *Diabetes Care*, vol. 30, no. 3, pp. 753–759, 2007, doi: 10.2337/dc07-9920.
 - [108] B. P. Kovatchev, W. L. Clarke, M. Breton, K. Brayman, and A. McCall, "Quantifying temporal glucose variability in diabetes via continuous glucose monitoring: Mathematical methods and clinical application," *Diabetes Technol. Ther.*, vol. 7, no. 6, pp. 849–862, 2005, doi: 10.1089/dia.2005.7.849.
 - [109] B. P. Kovatchev, D. J. Cox, L. A. Gonder-Frederick, and W. Clarke, "Symmetrization of the blood glucose measurement scale and its applications," *Diabetes Care*, vol. 20, no. 11, pp. 1655–1658, 1997, doi: 10.2337/diacare.20.11.1655.
 - [110] D. Rodbard, "Continuous Glucose Monitoring: A Review of Successes, Challenges, and Opportunities," *Diabetes Technol. Ther.*, vol. 18, no. S2, pp. S23–S213, 2016, doi: 10.1089/dia.2015.0417.
 - [111] G. Agiostratidou, H. Anhalt, D. Ball, *et al.*, "Standardizing clinically meaningful outcome measures beyond HbA_{1c} for type 1 diabetes: A consensus report of the American Association of Clinical Endocrinologists, the American Association of Diabetes Educators, the American Diabetes Association, the Endo," *Diabetes Care*, vol. 40, no. 12, pp. 1622–1630, 2017, doi: 10.2337/dc17-1624.
 - [112] J. R. Petrie, A. L. Peters, R. M. Bergenstal, R. W. Holl, G. A. Fleming, and L. Heinemann, "Improving the clinical value and utility of CGM systems: issues and recommendations: A joint statement of the European Association for the Study of Diabetes and the American Diabetes Association Diabetes Technology Working Group," *Diabetologia*, vol. 60, no. 12, pp. 2319–2328, 2017, doi: 10.1007/s00125-017-4463-4.
 - [113] T. Danne, R. Nimri, T. Battelino, *et al.*, "International consensus on use of continuous glucose monitoring," *Diabetes Care*, vol. 40, no. 12, pp. 1631–1640, 2017, doi: 10.2337/dc17-1600.
 - [114] T. Battelino, T. Danne, R. M. Bergenstal, *et al.*, "Clinical targets for continuous glucose

- monitoring data interpretation: Recommendations from the international consensus on time in range,” *Diabetes Care*, vol. 42, no. 8, pp. 1593–1603, 2019, doi: 10.2337/dci19-0028.
- [115] A. Pirog, “An embedded system for the multiparametric analysis of biological signals: application to the pancreatic biosensor of insulin demand To cite this version: Thèse de Doctorat de l’ Université de Bordeaux Par Antoine Pirog An embedded system for the multi,” 2018.
 - [116] J. Fuchs and R. Hovorka, “Closed-loop control in insulin pumps for type-1 diabetes mellitus: safety and efficacy,” *Expert Review of Medical Devices*, pp. 1–14, 2020, doi: 10.1080/17434440.2020.1784724.
 - [117] A. Caicedo, “Paracrine and autocrine interactions in the human islet: More than meets the eye,” *Seminars in Cell and Developmental Biology*, vol. 24, no. 1. Elsevier Ltd, pp. 11–21, 2013, doi: 10.1016/j.semcdb.2012.09.007.
 - [118] S. Soylu and K. Danisman, “Comparison of PID based Control Algorithms for Daily Blood Glucose Control,” *Proc. 2nd World Congr. Electr. Eng. Comput. Syst. Sci.*, pp. 1–8, 2016, doi: 10.11159/eee16.130.
 - [119] S. Laxminarayan, J. Reifman, and G. M. Steil, “Use of a food and drug administration-approved type 1 diabetes mellitus simulator to evaluate and optimize a proportional-integral-derivative controller,” *J. Diabetes Sci. Technol.*, vol. 6, no. 6, pp. 1401–1412, 2012, doi: 10.1177/193229681200600621.
 - [120] R. M. Bergenstal, W. V. Tamborlane, A. Ahmann, *et al.*, “Effectiveness of Sensor-Augmented Insulin-Pump Therapy in Type 1 Diabetes,” *N. Engl. J. Med.*, vol. 363, no. 4, pp. 311–320, Jul. 2010, doi: 10.1056/NEJMoa1002853.
 - [121] A. S. Brazeau, H. Mircescu, K. Desjardins, *et al.*, “Carbohydrate counting accuracy and blood glucose variability in adults with type 1 diabetes,” *Diabetes Res. Clin. Pract.*, vol. 99, no. 1, pp. 19–23, Jan. 2013, doi: 10.1016/j.diabres.2012.10.024.
 - [122] P. Herrero, J. Bondia, N. Oliver, and P. Georgiou, “A coordinated control strategy for insulin and glucagon delivery in type 1 diabetes,” *Comput. Methods Biomech. Biomed. Engin.*, vol. 20, no. 13, pp. 1474–1482, 2017, doi: 10.1080/10255842.2017.1378352.
 - [123] R. Visentin, C. Dalla Man, Y. C. Kudva, A. Basu, and C. Cobelli, “Circadian variability of insulin sensitivity: Physiological input for in silico artificial pancreas,” *Diabetes Technol. Ther.*, vol. 17, no. 1, pp. 1–7, 2015, doi: 10.1089/dia.2014.0192.
 - [124] R. Visentin, C. D. Man, and C. Cobelli, “One-Day Bayesian Cloning of Type 1 Diabetes Subjects: Toward a Single-Day UVA/Padova Type 1 Diabetes Simulator,” *IEEE Trans. Biomed. Eng.*, vol. 63, no. 11, pp. 2416–2424, 2016, doi: 10.1109/TBME.2016.2535241.
 - [125] R. Visentin, E. Campos-Náñez, M. Schiavon, *et al.*, “The UVA/Padova Type 1 Diabetes Simulator Goes From Single Meal to Single Day,” *J. Diabetes Sci. Technol.*, vol. 12, no. 2, pp. 273–281, 2018, doi: 10.1177/1932296818757747.
 - [126] S. N. Scott, L. Anderson, J. P. Morton, A. J. M. Wagenmakers, and M. C. Riddell, “Carbohydrate restriction in type 1 diabetes: A realistic therapy for improved glycaemic control and athletic performance?,” *Nutrients*, vol. 11, no. 5. MDPI AG, May 01, 2019, doi: 10.3390/nu11051022.
 - [127] A. J. Ahola, V. Mikkilä, S. Mäkimattila, C. Forsblom, R. Freese, and P. H. Groop, “Energy and nutrient intakes and adherence to dietary guidelines among Finnish adults

- with type 1 diabetes,” *Ann. Med.*, vol. 44, no. 1, pp. 73–81, Feb. 2012, doi: 10.3109/07853890.2010.530682.
- [128] M. Lodefalk and J. Åman, “Food habits, energy and nutrient intake in adolescents with Type 1 diabetes mellitus,” *Diabet. Med.*, vol. 23, no. 11, pp. 1225–1232, Nov. 2006, doi: 10.1111/j.1464-5491.2006.01971.x.
- [129] S. Särnbladn, U. Ekelund, and J. Åman, “Physical activity and energy intake in adolescent girls with Type 1 diabetes,” *Diabet. Med.*, vol. 22, no. 7, pp. 893–899, Jul. 2005, doi: 10.1111/j.1464-5491.2005.01544.x.
- [130] H. R. Gilbertson, K. Reed, S. Clark, K. L. Francis, and F. J. Cameron, “An audit of the dietary intake of Australian children with type 1 diabetes,” *Nutr. Diabetes*, vol. 8, no. 1, p. 10, Dec. 2018, doi: 10.1038/s41387-018-0021-5.
- [131] A. Saad, C. D. Man, D. K. Nandy, *et al.*, “Diurnal Pattern to Insulin Secretion and Insulin Action in Healthy Individuals,” 2012, doi: 10.2337/db11-1478.
- [132] L. Hinshaw, C. D. Man, D. K. Nandy, *et al.*, “Diurnal pattern of insulin action in type 1 diabetes implications for a closed-Loop system,” *Diabetes*, vol. 62, no. 7, pp. 2223–2229, 2013, doi: 10.2337/db12-1759.
- [133] C. Toffanin, H. Zisser, F. J. Doyle, and E. Dassau, “Dynamic insulin on board: Incorporation of circadian insulin sensitivity variation,” *J. Diabetes Sci. Technol.*, vol. 7, no. 4, pp. 928–940, 2013, doi: 10.1177/193229681300700415.
- [134] P. Rorsman and F. M. Ashcroft, “Pancreatic β -cell electrical activity and insulin secretion: Of mice and men,” *Physiol. Rev.*, vol. 98, no. 1, pp. 117–214, 2018, doi: 10.1152/physrev.00008.2017.
- [135] C. Dalla Man, F. Micheletto, M. Sathananthan, A. Vella, and C. Cobelli, “Model-Based Quantification of Glucagon-Like Peptide-1-Induced Potentiation of Insulin Secretion in Response to a Mixed Meal Challenge,” *Diabetes Technol. Ther.*, vol. 18, no. 1, pp. 39–46, 2016, doi: 10.1089/dia.2015.0146.
- [136] M. Schiavon, C. D. Man, Y. C. Kudva, A. Basu, and C. Cobelli, “In Silico Optimization of Basal Insulin Infusion Rate during Exercise: Implication for Artificial Pancreas,” 2013. Accessed: Apr. 11, 2020. [Online]. Available: www.jdst.org.
- [137] A. L. Golbeck, C. R. Ahlers-Schmidt, A. M. Paschal, and S. E. Dismuke, “A definition and operational framework for health numeracy,” *American Journal of Preventive Medicine*, vol. 29, no. 4, Elsevier Inc., pp. 375–376, Nov. 01, 2005, doi: 10.1016/j.amepre.2005.06.012.
- [138] S. Suh and J. H. Kim, “Glycemic Variability: How Do We Measure It and Why Is It Important?,” *Diabetes Metab J*, vol. 39, pp. 273–282, 2015, doi: 10.4093/dmj.2015.39.4.273.